BIOCHEMICAL ACTIONS AND DEGRADATIONS OF ATRIAL NATRIURETIC PEPTIDE IN RAT TISSUES

Elizabeth Louise Rugg

A Thesis Submitted for the Degree of PhD
at the
University of St Andrews

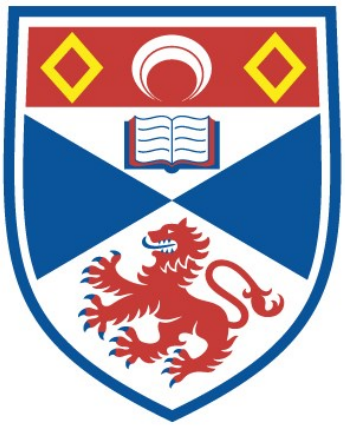

1989

BIOCHEMICAL ACTIONS AND DEGRADATION OF ATRIAL NATRIURETIC PEPTIDE IN RAT TISSUES

A thesis submitted to the University of St. Andrews for the degree of Doctor of Philosophy

by

ELIZABETH LOUISE RUGG

Department of Biology and Pre-clinical Medicine

January 1989

University of St. Andrews

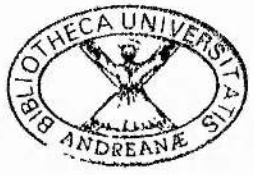

DECLARATION

a) I, Elizabeth Louise Rugg, hereby certify that this thesis has been composed by myself, that it is a record of my own work, and that it has not been accepted in partial or complete fulfilment of any other degree or professional qualification.

Signed Date 31.1.89

b) I was admitted to the Faculty of Science of the University of St. Andrews under Ordinance General No. 12 in October 1984, and as a candidate for the degree of Ph.D. in October 1984.

Signed Date 31.1.89

c) We hereby certify that the candidate has fulfilled the conditions of the Resolution and Regulations appropriate to the degree of Ph.D.

Signatures of Supervisors Date 31.1.89

COPYRIGHT

ACKNOWLEDGMENTS

I should like first of all to thank my supervisors, Drs Jim Aiton and Gordon Cramb, for their constant support, encouragement, and friendship. Second, I thank the technical staff of the Department of Biology and Pre-clinical Medicine (previously Physiology) for all their help. I must also thank my colleagues for their support and friendship, especially Roz Banks, Chris Cutler, Pat Ogden, Nick Simmons and Dave Tivey.

I am also very grateful to Dr Pavel Hamet and colleagues, of the Clinical Research Institute, Montreal, for allowing me to visit their laboratory in September 1987, and for their gift of cyclic GMP antibody, without which several of the experiments reported in this thesis could not have been performed.

Finally, I should like to thank my husband, Mick, without whose support this thesis would not have been completed.

LIST OF CONTENTS

ABSTRACT

Atrial natriuretic peptide (ANP) has previously been shown to increase intracellular cGMP levels in isolated rat ventricular myocytes. Using purified rat cardiac sarcolemmal membranes, a series of experiments was performed to investigate the mechanisms by which this occurs. A second series of experiments was carried out to investigate the nature of ANP degradation by preparations isolated from rat heart, lung and kidney.

In rat cardiac sarcolemmal membranes, ANP produced a 1.8-fold stimulation of manganese-dependent guanylate cyclase activity, with a Km of around 1nM. This activity was attenuated by the presence of 1 mM ATP in the incubation. In the presence of magnesium, guanylate cyclase activity was reduced 20- to 40-fold, but was augmented by ATP. Similar results were obtained in the presence of ANP-PNP, a non-hydrolysable analogue of ATP.

[^{125}I]-ANP binding studies indicated the presence of two receptor/affinity states, with K_D's of less than 10 pM, and around 1 nM for the high and low affinity sites respectively. More than 90% of these receptors were of the low affinity form. Similar results were obtained with bovine adrenal cortex membranes, but with MDCK cell membranes, only high affinity binding sites could be detected.

These experiments indicate that rat cardiac sarcolemmal membranes possess ANP receptors, at least a proportion of which are coupled to guanylate cyclase.

Incubation of [^{125}I]-ANP with isolated rat ventricular myocytes, or with a cytosolic fraction prepared from these cells, resulted in its

rapid degradation. The proteolytic activity appeared to be due to the action of a soluble metallopeptidase. Incubation of [^{125}I]-ANP with a cytosolic fraction prepared from rat kidney and lung indicated that similar degradative activity could be isolated from these tissues.

LIST OF ABBREVIATIONS

ACN	Acetonitrile
ADP	Adenosine 5'-diphosphate
AMP	Adenosine 5'-monophosphate
AMP-PNP	Adenylylimidodiphosphate
ANF	Atrial natriuretic factor
ANP	Atrial natriuretic peptide
ATP	Adenosine 5'-triphosphate
AUFS	Absorbance units full scale
B_{max}	Maximum Binding
BAC	Bovine adrenal cortex
BPFC	Bradykinin potentiating factor C
BNP	Brain natriuretic peptide
cGMP	Guanosine 3':5'-cyclic monophosphate
CO	Cardiac output
cpm	Counts per minute
CNS	Central nervous system
DTT	Dithiothreitol
E-64	Expoxy succinyl-leucyl-agmatine
EC_{50}	Concentration required for half maximal stimulation
EDRF	Endothelial derived relaxant factor
EDTA	Ethylenediamine-tetraacetic acid
GFR	Glomerular filtration rate
GMP	Guanosine 5'-monophosphate
GTP	Guanosine 5'-triphosphate

HEPES	N-2-Hydroxyethylpiperazine-N'-ethanesulfonic acid
HPLC	High performance liquid chromatography
IBMX	Isobutylmethylxanthine
IC_{50}	Concentration required for half maximal inhibition
K_D	Dissociation constant
Km	Michaelis constant
KRBG	Krebs Ringer bicarbonate buffer
KRHG	Krebs Ringer HEPES buffer
MAP	Mean arterial pressure
MDCK	Madin Darby canine kidney
MEM	Modified Eagle Medium
Mr	Apparent molecular weight
NSB	Non-specific binding
PCMB	p-chloromercuric benzoate
PBS	Phosphate buffered saline
PMSF	Phenylmethylsulphonyl fluoride
rpm	Revolutions per minute
ScGMP-TME	2'-O-Monosuccinyl guanosine 3':5'-cyclic monophosphate
SDS	Sodium dodecyl sulphate
S.E.M.	Standard error of the mean
TEA	Triethanolamine
TPR	Total peripheral resistance

CHAPTER 1

1.1 Historical Perspectives

In recent years much evidence has accumulated to suggest that mammalian atria play an important role in body fluid homeostasis. Henry et al. (1956) showed that mechanical distension of the atria, in the absence of volume expansion, elicited an increase in diuresis and natriuresis, whilst Goetz et al. (1970) demonstrated that acute extracellular fluid volume expansion had no effect on urine flow when atrial distension was prevented.

Early studies on the morphology of the mammalian heart revealed the presence, in atrial but not ventricular cells, of electron dense granules which were closely associated with the Golgi complex (Kirsh, 1956; Jamieson & Palade, 1964). The degree of granulation varied according to the salt and water status of the animal, a progressive decrease in granularity being observed with increasing sodium and water loading (Marie et al., 1976; De Bold, 1979). When injected into rats, extracts of atrial muscle were shown to produce powerful natriuretic and diuretic responses, and the term "atrial natriuretic factor" (ANF) was used to describe the substance(s) responsible for this effect (De Bold et al., 1981). Using cell fractionation studies, it was soon established that the natriuretic activity was closely associated the presence of the electron dense granules (De Bold, 1982a; Garcia et al., 1982). It was observed that natriuretic activity was not destroyed by boiling (Trippodo et al., 1982; Grammer et al., 1983) and that recovery was better from acid extracts than from physiological buffers (De Bold, 1982b; De Bold & Flynn et al., 1983).

Together with earlier experiments which had shown that the electron dense granules were able to incorporate [^{3}H]-leucine (Huet & Cantin, 1974; De Bold & Bencosme, 1975), these observations strongly suggested that ANF was proteinaceous in nature.

Since these early studies much work has been carried out on the biochemistry and physiology of ANF, both *in vitro* and *in vivo*. In the remainder of this chapter I shall summarise the current information concerning the synthesis and structure of ANF, its physiological and pharmacological effects, and the role of cGMP in the action of ANF.

1.2 Nomenclature

ANF is now known to be a peptide and therefore I shall use the term ANP (atrial natriuretic peptide) to refer to this substance. Alterations to the length of this peptide are denoted by subscripts and alterations to the amino acid composition are indicated in brackets. For example
$ANP_{5-27}(Tyr^8)$ refers to the amino acid sequence from Ser^5 to Arg^{27} in which Phe^8 has been replaced by Tyr.

1.3 Structure of ANF and Related Peptides

Early attempts to determine the structure of rat ANP resulted in a variety of different peptides, ranging in length from 19 to 35 amino acid residues (Flynn *et al.*, 1983; Atlas *et al.*, 1984; Currie *et al.*, 1984a; Geller *et al.*, 1984; Misono *et al.*, 1984ab; Napier *et al.*, 1984; Seidah et al., 1984). All the sequences identified shared the same 18 amino acid core containing two cysteine residues linked by a disulphide bridge, and were apparently truncated versions of the same peptide. Similar sequences were isolated from human atria and differed

only in the presence of a methionine residue in place of an isoleucine (Kangawa & Matsuo, 1984; Thibault et al., 1984a). Larger molecular weight peptides, which could be converted into the low molecular forms by treatment with trypsin and kallikrein, were also isolated (Currie et al., 1984b). The low molecular weight forms appeared to be derived from the carboxyl-termini of the higher molecular weight molecules.

Using olgionucleotide probes derived from known amino acid sequences of rat ANP, cDNA libraries were screened for the peptide (Maki et al., 1984; Yamanaka et al., 1984). The ANP precursor was determined by the identification of the sequence encoding ANP and by following the N-terminus of this sequence until an area could be identified as being similar to a classic signal polypeptide sequence (Perlman & Halverson 1983). Prepro-ANP was found to consist of 152-amino acids of which the first 24 constituted the signal sequence (Maki et al., 1984). Pro-ANP is composed of the following 126 amino acids of which the final 28 residues make up ANP (fig 1.1). Part of the amino-terminal sequence of pro-ANP has substantial homology with the cardiodilatin peptides isolated from pig atria and shown to possess vaso-relaxant activity (Forssmann et al., 1983; 1984). It is possible that the cardiodilatins are part of a similar atrial peptide in the pig. The final two arginine residues that are encoded for at the C-terminus have never been identified on any ANP fragment as yet isolated, and therefore presumably are cleaved very rapidly from the primary translation product.

Human prepro-ANP has been identified by similar techniques and found to consist of 151 amino acids of which the first 25 residues are the signal peptide (Oikawa et al., 1984). Human prepro-ANP is 80%

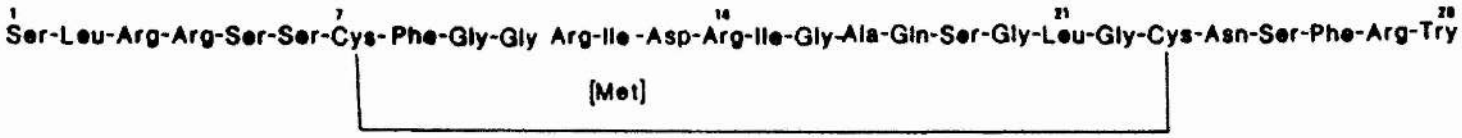

Rat Atrial Natriuretic Peptide (human)

Figure 1.1

Amino Acid Sequence of Rat and Human Atrial Natriuretic Peptide (ANP)

homologous with the rat peptide, the greatest similarity occuring at the carboxyl-terminus. The final 28 amino acids, which constitute ANP, are identical except for the replacement in the human peptide of the isoleucine residue at position 12 in rat ANP with a methionine residue(fig. 1.1).

The cDNA sequences were used in turn to screen genomic DNA libraries for the gene encoding ANP, and the human (Greenberg et al., 1984; Nemer et al., 1984), mouse (Seidman et al., 1984) rat (Argentin et al., 1985), and bovine genes (Vlasuk et al.,1986) have been characterized. The gene is highly conserved between species and is present as a single copy per haploid genome (Seidman et al., 1984; Argentin et al., 1985). The intron-exon structure in all cases consists of 3 exons and two introns. The first exon encodes the AUG initiator codon, the signal peptide, and first 16 amino acids of pro-ANP, in addition to an untranslated 5' sequence. The second exon encodes the sequence up to and including Arg^{125}, and the remaing exon contains codons for the final amino acid (human) or last three amino acids (rat, mouse, and bovine), as well as the stop codon and the 3' untranslated sequences (fig. 1.2).

1.4 ANP Gene Expression

1.4.1 Expression of ANP Gene in the Heart

The measurement of ANP mRNA in atrial tissue has been used to assess ANP gene expression under a number of conditions. ANP mRNA levels were substantially lowered (approximately 30% of control levels) in rats deprived of water or fed on a low sodium diet, whereas there was no effect on transcipt levels in rats on high sodium diets (Tagayanagi et

Figure 1.2

Structure of the Atrial Natriuretic Peptide Gene

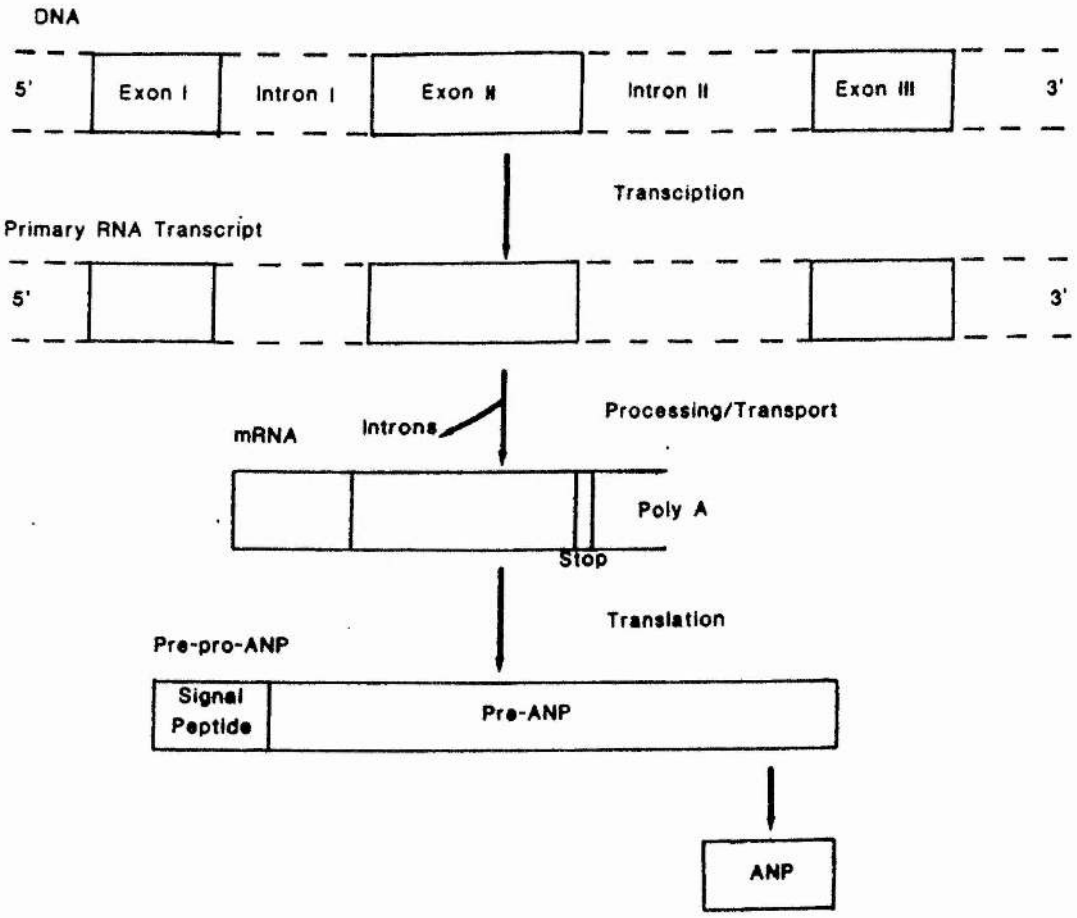

al., 1985). Volume overload produces a small (less than 2-fold) increase in expression (Nemer et al., 1987; Lattion et al., 1986)

The second intron of the rat and human gene contains a consensus sequence for a potential glucocorticoid receptor-binding site (Greenberg et al., 1984; Argentin et al., 1985), raising the possiblity that expression of the ANP gene may be regulated by glucocorticoids. This is supported by the observation that glucorticoids produce a 2- to 3-fold increase in ANP atrial mRNA levels in the rat (Gardener et al., 1986a; Nemer et al., 1987)

1.4.2 Expression of the ANP Gene in Other Tissues

Although secretory vesicles containing ANP have only been found in the atria, cDNA probes have identified ANP transcripts in rat ventricular muscle (Gardener et al., 1986b; Takayanagi et al., 1987a), albeit at concentrations 100- to 250-fold less than those found in atrial tissue. It should be noted however that when the relative volumes of atrial to ventricular tissue are taken into account, the absolute level of ANP mRNA is only around 5-fold less in the ventricles. Although the levels of ANP detected in ventricular muscle are some 1,000- to 20,000-fold less than in atria (Nemer et al., 1986; Takayanagi et al., 1987a), it is possible that the ventricles make a significant contribution to plasma levels of ANP by continual secretion of the peptide into the blood stream.

The levels of ANP, and ANP mRNA in the ventricles are altered in some diseased states and under certain experimental conditions. The levels of ANP are about 3-fold higher in the ventricles of spontaneously hypertensive rats compared to controls (Takayanagi et al., 1987a).

Volume over-load and glucocorticoid administration appear to preferentially increase ANP mRNA in rat ventricles, producing 4- to 11-fold increases in ventricular levels compared to 1.5- to 3 3-fold increases in the atria (Lattion et al., 1986; Nemer et al., 1987). In the cardiomyopathic hampster electron dense granules, similar to those found in atria, have been identified, and found to contain immunoreactive ANP (Cantin et al., 1987; Ding et al., 1987).

Transcripts of ANF have also been detected in the lung, anterior pituitary, and the aortic arch (Gardner et al., 1986b).

1.5 Secretion and Processing of ANP

The exact nature of the peptide secreted into the blood stream has yet to be conclusively determined. Cultures of atrial and ventricular cardiomyocytes, isolated from newborn rats, secrete only 10 to 20 % of ANP as the C-terminal form, the rest being pro-ANP (Glembotski & Gibson, 1985; Bloch et al., 1985). In contrast, the eluate from the perfused rat heart contains only the short form of ANF (Currie et al., 1984c; Lang et al., 1985).

In humans, three forms of ANP have been identified in the atria. Alpha-human ANP (a-hANP) is comprised of the 28 amino acids from the carboxy-terminal of the 126 amino acid prohormone gamma-hANP. Beta-hANP is an antiparallel dimer of alpha-hANP, formed by intermolecular disulphide bridges (Kangawa & Matsuo, 1984; Nakao et al., 1984; Needleman et al.,1985). The dimeric form of ANP has only been identified in humans. Alpha-hANP is the major form of the peptide found circulating in the blood (Miyata et al., 1987; Sugawara et al., 1985), although significant levels of beta-hANP have been detected in

the blood of some subjects (Miyata et al., 1987). It has recently been reported that beta-hANP is converted to alpha-hANP in the human circulation, and that whilst the natriuretic and diuretic activites of administered beta-hANP have a slower onset, the peptide is more potent and has a longer duration of activity (Itoh, et al., 1988).

1.6 ANP in Other Tissues

Immunoreactive ANP has been identified in the lung (Gardner et al., 1986b), and biologically active ANP has been shown to be released from perfused rat lung (Gutkowska & Sirois, 1988).

Immunoreactive ANP has also been identified in the aortic arch (Gardner et al., 1987), the pituitary gland (Samson, 1985), and several areas of the brain. The highest levels in the brain are found in the hypothalamus, septum, and midbrain, with smaller amounts in the cerebral cortex, olfactory bulb, thalamus, pons-medulla, and hippocampus (Jacobowitz et al., 1985). A peptide has recently been isolated from porcine brain which elicits natriuretic and diuretic responses similar to those observed with ANP (Sudoh et al., 1988). This peptide has been termed BNP (brain natriuretic peptide) and consits of 26 amino acid residues which share 60% homology with ANP. BNP may be the major natriuretic peptide in the CNS.

1.7 Physiological Effects

ANP has been shown to have direct actions on a number of different tissues both in vivo and in vitro. These actions include the relaxation of preconstricted smooth muscle, alterations in renal haemodynamics, inhibition of sodium reabsorption in the collecting tubule of the kidney, and inhibition both of renin and aldosterone

release. These effects are discussed in more detail below.

1.7.1 Vascular Effects of ANP

The observation that atrial extracts relaxed preconstricted smooth muscle (Deth et al., 1982; Currie et al., 1983), and the subsequent confirmation that both extracted ANP (Garcia et al., 1984a) and synthesised ANP (Atlas et al., 1984; Garcia et al., 1984b; Cohen & Shenk, 1985) acted similarly, suggested that vaso-relaxation may be responsible for some of the hypotensive actions of ANP. In general, vaso-relaxation is independent of the constrictor, and ANP effectively antagonizes the actions of noradrenaline, histamine, carbachol, and angiotensin II. However, variable responses have been reported to KCl induced vasoconstriction (Garcia et al., 1984a; Rapoport et al 1985; Bratveit et al., 1987). The reasons for this discrepancy in the action of ANF on KCl-induced vasocontriction are not clear, but may be due to differences in the mechanisms by which these compounds alter intracellular Ca^{2+}. Noradrenaline and angiotensin II act both by a receptor-mediated stimulation of Ca^{2+} influx and by the release Ca^{2+} from intracellular stores (Deth & Van Breemen, 1977; Van Breemen et al., 1982). ANP has been shown to inhibit agonist-stimulated Ca^{2+} influx and intracellular Ca^{2+} release, but has no effect on KCl stimulated Ca^{2+} influx (Chiu et al., 1986; Meisheri et al, 1986).

The degree of ANP-induced vaso-relaxation is dependent on both the analogue of ANP used, and the origin of the tissue under investigation. In general, ANP is a more effective vaso-relaxant in arterial than in venous preparations, with the degree of relaxation correlating with the number of receptors in the tissue (Cohen & Schenck 1985). The extension or truncation of the amino-terminal has

little or no effect on the vaso-relaxant properties of the peptide (Misono et al., 1984b; Garcia et al., 1985), and deletion of the Tyr^{28} from the carboxyl-terminal is also without effect. However, removal of Phe^{26}-Arg^{27}-Tyr^{28} residues produces a peptide which is 70- to 1000-fold less potent at relaxing preconstricted smooth muscle (Sugiyama et al.,1984; Garcia et al., 1985; Wakitani et al., 1985; Bratveit et al., 1987; Budzik et al., 1987).

The mechanism of action of ANP as a vaso-relaxant is thought to be mediated by increasing intracellullar cGMP. ANP induced relaxation has been shown to be associated with the formation of cGMP (Rapoport et al., 1985; 1986) and ANP has been shown to increase cGMP in several smooth muscle preparations (see section 2.3). A recent study however has dissociated the vaso-relaxant effects of various analogues of ANP on preconstricted rabbit aorta from the ability of these analogues to raise intracellular cGMP levels in cultured rabbit vascular smooth muscle cells (VSMC; Budzik et al. 1987). In this study, $ANP_{5-27}(Tyr^{8})$ was unable to increase cGMP in VSCM cultures but was able to antagonise the actions of histamine on the aorta preparation. Conversely, ANP_{7-22} and $ANP_{7-22}(Lys^{11})$ stimulated cGMP to the same extent as ANP_{5-28}, but were 1000-fold less effective than ANP_{5-28} as vaso-relaxants. This study therefore calls into question the role of cGMP as the mediator of ANP's vaso-relaxant action. It should however be noted that the effects of ANP on intracellular cGMP and preconstricted smooth muscle were measured in two different systems. Thus the dissociations reported by Budzik et al. (1987) may be due to differences between their two preparations. In addition, cGMP levels in VSMC cells were measured following prolonged incubations (120 min) of peptides with the cells. It is therefore possible that the

differences in the ability of the various peptides to increase intracellular cGMP in these cells may be a result of differential internalisation and/or degradation.

The effects of other vaso-relaxants, such as acetylcholine, histamine, bradykinin and the nitro-vasodilators are also mediated by increases in intracellular cGMP. Acetylcholine, histamine, and bradykinin exert their effect by the release of endothelial-derived relaxant factor (EDRF) and require the presence of an endothelium (for review see Rapoport & Murad, 1983; Furchgott, 1984). The nitro-vasodilators act by the formation of nitric oxide, which in turn increases intracellular cGMP. There is increasing evidence that EDRF is in fact nitric oxide (Palmer et al., 1987), and hence all these compounds act through a common mechanism. In contrast, ANP does not require the presence of an intact endothelium (Winquist et al., 1984) and is not inhibited by methylene blue, a powerful inhibitor of nitric oxide mediated cGMP accumulation (Rapoport et al., 1985; Bratveit et al., 1987). ANP has been shown to increase intracellular cGMP by stimulation of particulate guanylate cyclase (Winquist et al., 1984; Waldman et al., 1984), whereas methylene blue only inhibits the actions of soluble guanylate cyclase. Vaso-relaxation can therefore occur by the action of two classes of vasodilator, which act through different mechanisms to increase intracellular cGMP.

Whilst the studies on isolated vascular preparations are in general consistent with ANF being a potent vasodilator, the evidence in vivo is far from conclusive. Although some studies have reported that administration of ANP results in a decrease in total peripheral resistance (TPR; Ackermann et al., 1894; Fujioko et al., 1985; Volpe

et al., 1986), others have reported no change or even an increase (Koike et al., 1984; Lappe et al., 1985). Some of these variations may be accounted for by different experimental protocols, which make it difficult to directly compare studies. The most consistent observations are with respect to the effects of ANP on mean arterial pressure (MAP) and cardiac output (CO). Administration of ANP (atrial extract or various analogues of ANF) in general causes a reduction in MAP. The reported decreases in MAP in these studies ranged from 0 to 25%. The largest reductions were observed in studies on hypertensive animals (see table 1 in Pegram et al., 1986).

1.7.2 Effects of ANP in the Kidney

The observation by De Bold et al. (1981) that injection of rat atrial extracts into the the rat produces a profound natriuretic and diuretic response has prompted many investigations into the mechanism by which this occurs. The renal response both to atrial extracts and synthetic ANP is rapid (1-2 min) and short lived (less than 20 min) (De Bold et al., 1981; Ackermann et al., 1984; Burnett et al., 1984), and results in increases in potassium, calcium, magnesium and phosphate excretion as well as sodium and water excretion (Keeler and Azzarolo 1983; Burnett et al., 1984). ANP increases glomerular filtration rate (GFR; Atlas et al 1984; Burnett et al., 1984; Camargo et al., 1984; Cogan 1986) and reduces inner medullary hypertonicity (Borstein et al. 1983; Sosa et al., 1986).

In the isolated perfused rat kidney, in the absence of vasoconstriction, ANP increases GFR and produces a small increase in renal vascular resistance. In contrast, in the presence of vasoconstricting agents, ANP produces a net renal vasodilation

(Camargo et al 1984). The effects of ANP on GFR appear to be due to the differential effects of the peptide on the renal vasculature. ANP dilates the arcuate and interlobular arteries, and the afferent arterioles of the glomerulus, but constricts the efferent arterioles of the glomerulus (Camargo et al. 1984; Maack & Kleinert 1986). The net result of this is an increase in the glomerular capillary hydraulic pressure, and hence an increase in GFR. The increase in renal resistance observed in the isolated perfused kidney is presumably due to the absence of any constricting agents in the preparation, and thus the only effect of ANP is as a vasoconstrictor in the efferent arteriole. Although it has been claimed that these changes are sufficient to account for the observed natriuresis (Huang et al., 1985), the glomerular effects only account for a 2- to 3-fold increase in solute and fluid in the distal tubule (Huang et al., 1985). Administration of ANP commonly results in a 10- to 50-fold increase in natriuresis (Burnett et al.,1984; Maack et al., 1984), and therefore other tubular mechanisms must be involved. Partial clamping of the renal artery, which abolishes renal haemodynamic effects, also abolishes the natriuretic actions of ANP (Sosa et al., 1986). This suggests that ANP-induced natriuresis results mainly from the effects of ANP on the renal vasculature, rather than from direct tubular action. Further evidence in support of the importance of the haemodynamic effects of ANP is given by the observation that doses of ANP which do not increase GFR are sufficient to induce a redistribution of renal blood flow from the superficial to the juxtamedullary nephrons (Salazar et al., 1986).

Micropuncture studies and isolated perfused tubule experiments have failed to show any effect of ANP on sodium transport in the area of

the nephron from the proximal convoluted tubule to the cortical collecting duct (Baum & Toto 1986; Cogan, 1986 Huang et al 1985; Kondo et al., 1986). Studies on cells isolated from the inner medullary collecting duct indicate that ANP reduces sodium entry into these cells by a mechanism which does not involve a direct effect on Na^+/K^+-ATPase (Zeidel et al., 1986). Further experiments suggest that the mechanism by which this occurs most probably involves the inhibition of a sodium channel or a Na^+/H^+ exchanger in the luminal membrane (Zeidel, 1988).

1.7.3 Effects of ANP on Renin Release

The constant infusion of ANP results in a rapid decrease in renin secretion in the normal dog (Maack et al., 1984; Burnett et al., 1984). However, a recent study in the rat failed to show any ANP-stimulated alterations in plasma renin concentrations (Hirata et al., 1987a). Since renin release would be expected to increase as a result of the natriuretic and diurectic responses elicited in these experiments, the absence of a rise in plasma renin concentration in the rat indicates that ANP is also supressing renin release in this preparation.

Decreases in renin release may result from an increase in the concentration of sodium reaching the macula densa, or an increase in the hydrostatic pressure at the juxtaglomerular cells lining the afferent arteriole. Since ANP does not lower renin secretion in the non-filtering kidney, it is likely that ANP inhibition of renin release is through a mechanism involving the macula densa (Opgenorth et al., 1986).

1.7.4 Effects of ANP on Aldosterone

As early as 1959 it was noted that stretching the right atria of the dog resulted in decreased aldosterone secretion (Anderson et al, 1959). Subsequent experiments suggested the possibility that this procedure resulted in the release of an inhibitor of aldosterone secretion (Gann & Travis 1964). Since the discovery of ANP much attention has been paid to the role of this peptide as an antagonist of aldosterone secretion. Several reports have shown that ANP and related peptides inhibit basal aldosterone production by adrenal zona glomerulosa cells, and antagonise stimulation by angiotensin II, dibutyryl cAMP and potassium (Atarashi et al., 1984; Chartier et al., 1984; Goodfriend et al., 1984). Although the effects of ANP on stimulated aldosterone secretion are well established, there are reports in which ANP failed to lower basal levels of secretion (eg. Naruse et al., 1987).

In vivo studies have shown that infusion of ANP into both the dog and the rat results in a fall in the plasma aldosterone levels (Maack et al., 1984; Aguilera 1987; Hirata et al., 1987a). Although this may in part be due to the decrease in renin secretion, ANP has been shown to decrease plasma aldosterone in the rat, in the absence of decreases in plasma renin and in the presence of an ACE inhibitor (Hirata et al., 1987a). It therefore appears likely that ANP has a direct effect on aldosterone production by the adrenal cortex. The exact point at which ANP acts to inhibit aldosterone production is not known, however it appears to be at a point prior to mitochondrial uptake and the metabolism of cholesterol (Goodfriend et al., 1984).

ANP appears to have no effect on glucocorticoid production in the rat

or the dog (Atarashi et al., 1984, Maack et al., 1984), but it has been reported to inhibit production by the bovine adrenal gland (De Lean et al 1984a) and by adrenal tissue obtained from patients with Cushing's syndrome (Naruse et al., 1987).

1.8 Summary

ANP produces natriuresis, diuresis and vaso-relaxation under a variety of experimental conditions, both in vivo and in vitro. The major source of ANP in the body is from secretory granules located in the atria, but ANP transcripts have been identified in several other tissues, and these may make significant contributions to overall levels. The inter-relationships between the different effects elicited by ANP are complex; which of these effects are caused by the primary action of ANP, and which are secondary in nature, remains to be conclusively established.

CHAPTER 2

2.1 Guanylate Cyclase and Receptors

In a number of different tissues and preparations, ANP has been shown to increase intracellular cGMP production and stimulate guanylate cyclase activity. In addition, ANP receptors, identified by direct binding studies and autoradiography, have been shown to be widely distributed in mammalian tissues (for review see Atlas, 1986; Genest & Cantin, 1988). The following chapter reviews some of information currently available concerning guanylate cyclase activity and its relationship to the ANP receptor.

2.1 Guanylate Cyclase Activity

Guanylate cyclase is an enzyme which catalizes the formation of cyclic guanosine 3',5'-monophosphate (cGMP) from GTP. Its presence has been identified in almost all cell types examined and its activity can be attributed to at least two isoenzymes, a soluble (cytosolic) and a particulate form. The soluble and particulate isoenzymes coexist in most cells, although the distribution varies from tissue to tissue. Soluble guanylate cyclase is the predominant form in the adult liver (Kimura & Murad, 1975a) and platelets (Bohme *et al.*, 1974), whilst the major form is particulate in regenerating and fetal liver (Kimura & Murad 1975b), intestinal mucosa (De Jonge, 1975) and retinal rod outer segments (Fleischman & Denisevich, 1979; Gordis *et al.*, 1973; Krisanan *et al*, 1978). In the sea urchin sperm (Gray & Drummond, 1976), C_6 rat glioma cells, and B103 rat neuroblastoma cells (Sinacore *et al.*, 1983), guanylate cyclase activity appears to be exclusively due to the particulate isoenzymes.

Soluble guanylate cyclase has been purified to apparent homogeneity and appears to exist as a haem-containing heterodimer (Gezer et al., 1981b; Gerzer et al., 1981c) with an apparent molecular weight of 150,000 (Garber 1979; Lewicki et al., 1980; Gerzer et al., 1981a). This form of the enzyme is stimulated by the nitro-vasodilators such as azides, nitrite, nitroglycerin, and nitroprusside and by the vaso-relaxant, endothelial-derived relaxant factor (EDRF). Further details on the distribution and mechanism of action of soluble guanylate cyclase can be found in the review by Waldman & Murad (1987).

Based on it solubilization characteristics, particulate guanylate cyclase activity can be subdivided (Waldman & Murad, 1987). One form is readily solubilized by detergents, such as Triton X-100, and is a glycoprotein with an estimated molecular weight of 300,000 to 400,000 (Limbird et al., 1975; Goldberg & Haddox, 1977). It has been highly purified from lung (Waldman et al., 1985; Kuno et al., 1986), and SDS polyacrylamide gel electrophoresis yields an apparent molecular weight of 130,000. It is possible that this enzyme exists as a dimer in the cell membrane.

A portion of the particulate guanylate cyclase activity in the microvillus brush border of the intestinal mucosa is resistant to solubilization by a variety of agents including salt, EDTA, detergents, and 1M urea (Waldman et al., 1986). This solubilization-resistant form of the enzyme is associated with microtubular and/or filamentous structures in the cell, and appears to be a different isoenzyme (Waldman et al., 1986).

Particulate guanylate cyclase activity is not stimulated by nitric oxide (Tremblay et al., 1985), and until recently the heat-stable

enterotoxin from E. Coli (ST) was the only known biological activator (Field et al., 1978). ST stimulates only the solubilization-resistant form of guanylate cyclase activity found in intestinal smooth muscle preparations (Waldman et al., 1986). Recently, ANP has been identified as a potent stimulator of particulate guanylate cyclase activity in many tissues, including lung (Kuno et al., 1986), adrenal cortex (Waldman et al., 1984; Tremblay et al., 1986; Takayanagi et al., 1987b), liver (Waldman et al., 1984; Kurose et al., 1987), kidney (Waldman et al., 1984), testes (Marala & Sharma, 1988), and several cultured cell lines (Leitman et al., 1986). Several of these studies have reported ANP stimulation of guanylate cyclase activity in detergent-solubilized membranes, which must necessarily preclude the presence of the solubilization-resistant form. The specificity of ANP for the two forms of particulate guanylate cyclase remains to be established, although it is known that ANP does not stimulate soluble guanylate cyclase activity (Waldman et al., 1984; Winquist et al., 1984).

Particulate guanylate cyclase activity has been co-purified with the ANP binding sites from solubilized plasma membranes of lung and bovine adrenal cortex (Kuno et al., 1986; Takayanagi et al., 1987b). This has led to the suggestion that an ANP receptor is an integral part of the particulate guanylate cyclase molecule. This possibility will be discussed in more detail later in this chapter (sections 2.4.2 and 2.4.3)

2.3 ANP Stimulation of Intracellular cGMP Production

ANP has been shown to increase intracellular cGMP levels in whole cell preparations and established cell lines derived from kidney (Tremblay

et al., 1985; Waldman et al., 1984; Takeda et al., 1986; Inui et al., 1985; Leitman et al., 1988), vascular smooth muscle (Rapoport et al., 1986; Hirata et al., 1984; Hamet et al., 1986, Cohen & Schenk, 1985), endothelia (Leitman et al., 1988), lung (Waldman et al., 1984; Leitman et al., 1988), and mammary gland and testis (Leitman et al., 1988).

ANP-induced vaso-relaxation is thought to be mediated through increases in intracellular cGMP (see section 1.6.1), and the effect of ANP on cGMP production has been examined in a number of cultured smooth muscle cell lines. ANP increases intracellular cGMP levels in bovine aortic smooth muscle cells (BASM; Scarborough et al., 1986; Leitman et al., 1988), A10 vascular smooth muscle cells (A10 VSMC; Nambi et al., 1986; Napier et al., 1986; Neuser & Bellemann, 1986), and primary cultures of rat thoracic smooth muscle cells (Roubert et al., 1987). The concentration of ANP required to produce half maximal increases in intracellular cGMP (EC_{50}) ranged from 1 to 200 nM (Scarborough et al., 1986; Nambi et al.,1986; Roubert et al., 1987). ANP has also been shown to raise intracellular cGMP levels in cultured bovine aortic endothelial cells (BAE), with an EC_{50} of 0.3 nM (Leitman & Murad 1986; Leitman et al., 1988), and in preparations of human coronary artery (Rapoport et al., 1986). Although the EC_{50} values for ANP show a large degree of variation, they are in keeping with the reported levels of ANP required to produce vaso-relaxation in pre-contracted vascular preparations (Budzik et al., 1987; Cohen & Schenk, 1985; Schiller et al., 1987).

ANP-induced elevation of intracellular cGMP concentrations has been reported for several renal preparations. ANP augments cGMP levels in the glomerulus (Ballerman et al., 1985; Tremblay et al., 1985; Takeda

et al., 1986), the cortical collecting duct (Tremblay et al., 1985; Takeda et al., 1986), the distal convoluted tubule (Takeda et al., 1986), and the thick loop of Henle (Tremblay et al., 1985). No effect of ANP has been demonstrated in the proximal tubule (Tremblay et al., 1985; Takeda et al., 1986). Several studies have demonstrated effects of ANP on cGMP levels in cultured cells derived from kidney. Increases in cGMP levels have been reported in MDCK cells (Leitman et al., 1988), LLC-PK_1 cells (Inui et al., 1985), primary cultures of rat glomerular mesangial cells (Ballerman et al., 1985), and cortical collecting tubules (Naray-Fejes-Toth et al., 1988). The concentrations of ANP required to produce half maximum effect (EC_{50}) are 1 and 10 nM for the cortical collecting tubules and LLC-PK_1 cells respectively.

ANP has also been shown to elevate cGMP levels in rat and rabbit ventricular myocytes (Aiton & Cramb, 1985; Cramb et al., 1987), rat leydig cells (Vlasuk et al., 1988; Leitman et al., 1988), cultures of human lung fibroblasts, rat mammary epithelial cells, and bovine kidney (Leitman et al., 1988) and osteoblasts (Fletcher et al., 1986).

2.4 Localization and Purification of ANP Receptors

2.4.1 The Kidney

Autoradiographical studies in the kidney, using [^{125}I]-ANP, have shown labelling of a number of different regions. The majority of labelling is associated with the glomeruli (Bianchi et al., 1985; Koseki et al.,1986a; Carrier et al., 1985; Murphy et al., 1985; Mantyh et al., 1986), but binding sites have been identified on the outer medullary vasa recta (Bianchi et al., 1987), the inner medullary collecting duct, (Bianchi et al., 1987; Koseki et al., 1986a; Mantyh et al.,

1986), the renal artery (Bianchi et al., 1985; Koseki et al.,1986a; Mantyh et al., 1986), and the renal pelvis (Koseki et al., 1986a).

Using ligand binding techniques, high affinity [^{125}I]-ANP binding sites have been demonstrated in renal cortical membranes derived from rat (Napier et al., 1984; Hori et al., 1985; Maack et al., 1987), rabbit (Napier et al., 1984), dog (De Lean et al., 1985), and man (Ishikawa et al., 1987). Similar binding sites have also been identified in intact cells and membranes prepared from the cultured kidney epithelia, LLC-PK$_1$ (Napier et al., 1984; Inui et al., 1985). The estimates of [^{125}I]-ANP affinity and number of binding sites in these preparations show a wide degree of variation, with values for the K_D ranging from 50 to 1000 pM, and B_{MAX} from 15 to 500 fmol/mg protein. The dose response curves for [^{125}I]-ANP binding to rat and rabbit kidney cortex were biphasic, suggesting the presence of high and low affinity receptors with K_D's of 50 and 500 pM (Napier et al., 1984).

Direct binding studies in rat glomerular membranes have identified the presence of a single population of high affinity binding sites, with a K_D of 27 pM (Carrier et al., 1985). Similar studies in isolated rat glomeruli also resulted in the identification of a single class of binding sites. In this preparation, however, they were of lower affinity, with a K_D of 220 pM (Ballermann et al., 1985). More recently, both high and low affinity binding sites have been detected in purified glomerular membranes, with K_D's of 5pM and 2.5nM respectively (Hamada et al., 1987). The discrepancies between these studies may, in part, be accounted for by differences in the concentration of [^{125}I]-ANP used. In particular, Carrier et al. (1985)

used a very low concentration of radioligand (4.4pM) which would almost certainly result in the failure to detect lower affinity binding sites.

Cultures of mesangial and epithelial cells isolated from normal rat glomeruli have indicated that the [^{125}I]-ANP binding sites are confined to the mesangial cells (Ballermann et al., 1985). This study also showed that the number and affinity of [^{125}I]-ANP binding sites on rat glomeruli can be altered by changes in the salt status of the animal. Glomeruli isolated from rats fed on a high salt diet have approximately four times less binding sites compared to those on a low salt diet (426 vs 116 fmol/mg protein), and this is accompanied by a two-fold reduction in the dissociation constant, which decreases from 940 to 380pM.

Purified membrane preparations of glomeruli and inner medullary collecting ducts from rat kidney have been photoaffinity labelled with [^{125}I]-ANP, and subjected to SDS electrophoresis under reducing conditions. In this study, autoradiographs revealed the specific labeling of a single band in both preparations, with an apparent molecular weight of 65 kDa (Koseki et al., 1986b). A similar cross-linking study on a glomerular membrane preparation which had been shown to possess high and low affinity ANP receptors, resulted in the labelling of two bands at 75 kDa and 140 kDa (Hamada et al., 1987).

2.4.2 The Lung

Autoradiographic studies have shown that ANP binding sites are widely distributed in the rat lung. Binding sites have been localized on the endothelial and smooth muscle cells of the arteries, arterioles, veins

and venules, as well as the endothelial cells of the alveoli (Bianchi et al., 1985). Direct binding studies have identified ANP receptors in membranes prepared from rat (Kuno et al., 1986), rabbit (Olins et al., 1986), and bovine (Ishido et al., 1986; Shimonaka et al., 1987) lung. The K_D for [^{125}I]-ANP binding to rat and rabbit lung membranes was 280 and 320 pM respectively, with the Bmax being 120 and 170 fmol/mg protein respectively for the two species.

Rat lung ANP receptors have been purified to apparent homogeneity by a combination of affinity and ion exchange chromatography (Kuno et al., 1986). SDS polyacrylamide gel electrophoresis of the purified preparation, under both reducing and non-reducing conditions, resulted in a single 120 kDa band. [^{125}I]-ANP binding co-purified with guanylate cyclase activity, suggesting that they are part of the same molecule.

Shimonaka et al., (1987) have affinity-purified ANP receptors from bovine lung and this too resulted in the labelling of a 140 kDa band, as identified by SDS polyacrylamide gel electrophoresis. In contrast to the previous study, this was totally converted to a 70 kDa band in the presence of reducing agents.

The differences in the sub-unit composition of the ANP receptor indicated by these two studies may arise from differences in the purification procedures. Kuno et al. (1986) noted that they also found 60 to 70 kDa labelled fragments when they carried out SDS electrophoresis on crude membrane preparations, although these disappeared after purification on a GTP affinity column. This procedure selects for molecules which possess GTP binding sites (and presumably guanylate cyclase activity), and therefore ANP receptors

which are not associated with guanylate cyclase activity will not be retained. It appears from studies on purified ANP receptors isolated from bovine adrenal cortex that the 62 kDa fragment results from ANP receptors not associated with guanylate cyclase activity (Takayanagi et al., 1987b). This is discussed in more detail below.

2.4.3 Adrenal Cortex

[^{125}I]-ANP binding sites have been localized by autoradiography in the zona glomerulosa of rat (Bianchi et al., 1985; Murphy et al., 1985; Mantyh et al., 1986), guinea pig, and man (Mantyh et al., 1986). High affinity binding sites are also present on endothelial and smooth muscle cells of the adrenal cortical arterioles, veins, and venules, the endothelium of the zona glomerulosa capillaries, and in small numbers on the catecholamine storing cells of the adrenal medulla (Bianchi et al., 1985).

Direct binding of [^{125}I]-ANP to bovine zona glomerulosa membranes has identified two binding sites, with K_D's for ANP of 50pM and 5nM (De Lean et al., 1984b). Similar results have been obtained from [^{125}I]-ANP binding studies in solubilized bovine adrenal cortex (BAC) membranes (Meloche et al., 1986a).

[^{125}I]-ANP has been cross-linked to its receptor/binding sites in BAC membranes, and estimations of receptor size have been made by SDS polyacrylamide gel electrophoresis. Several studies have reported the labelling of a single band under reducing conditions, with an apparent molecular weight of 130 kDa (Meloche et al., 1986a; Misono et al., 1985; Koseki et al., 1986b). In contrast, Shinjo et al. (1986) reported the labelling of a 140 kDa band, which totally dissociated

into 70 kDa fragments in the presence of reducing agents. Takayanagi et al. (1987b) have identified two ANP binding sites in BAC membranes, and purified them to apparent homogeneity. Both sites have apparent molecular weights of 135 kDa under non reducing conditions, and have similar affinities for ANP (approximately 60 pM). One of these sites is associated with guanylate cyclase activity whilst the other is not. The band which possesses guanylate cyclase activity is not affected by reducing agents, whilst the other can be reduced to a 62 kDa fragment.

Meloche et al. (1986b) also observed a 68 kDa band in affinity-labelled BAC membranes, but subsequently reported that this band only appeared if the membranes were acid washed and heated at 100^{o}C (Meloche et al., 1986a). Meloche et al. concluded that the low molecular band was due to partial hydrolysis under stringent conditions, and subsequently omitted this step from their purification procedure. A recent report, however, has indicated that a membrane-bound acidic metalloendopeptidase on BAC membranes is responsible for the cleavage of the 140 kDa band into two disulphide-linked 70 kDa fragments (Misono, 1988). It is therefore possible that the action of this peptidase is responsible for the differences in labelling patterns discussed above.

2.4.4 Vascular Receptors

ANP binding sites have been identified in a number of vascular preparations including rabbit aorta (Napier et al., 1984), rat mesenteric and renal arteries (Schiffrin et al., 1985), cultured vascular smooth muscle cells from rat (Hirata et al., 1984) and bovine (Schenk et al., 1985) aorta, A10 smooth muscle cells (Napier et al., 1986), and cultured bovine aortic endothelial cells (Leitman et al.,

1986). Binding in all cases appears to be to a single class of high affinity receptors, although the reported K_D values vary from 50pM to 1nM. Cross-linking studies indicate that the majority of these binding sites have a Mr of 60 to 70 kDa under reducing conditions (Leitman et al., 1988).

2.4.5 Other Tissues

ANP binding sites/receptors have been identified in many other tissues including various regions of the brain (Quiron et al., 1986; Quiron, 1988), the placenta (Sen, 1986), the ciliary process of the eye (Bianchi et al., 1986), and platelets (Schifrin, et al., 1986; for review see Genest & Cantin 1988).

2.5 Structure-Activity Relationships

Modification of the ANP molecule, particularly by carboxyl terminal deletions or disruption of its ring structure, has marked effects on the potency of the peptide to elicit physiological responses (see section 1.6.1). The effects of such alterations on the ability of the peptide to displace [^{125}I]-ANP have been studied in a number of tissues and can be summarised as follows: Deletion of amino acids from the amino terminal results in a gradual reduction in the affinity of the peptide. ANP_{3-28} is equipotent or almost equipotent to ANP_{1-28}, whereas ANP_{5-28} is 3- to 10-fold less potent. ANP_{7-28} is the least potent of the amino-terminal deleted peptides, having an affinity some 20-fold less than the 28 amino acid peptide, ANP_{1-28} (Schiffrin et al., 1985; De Lean et al., 1985; Olins et al., 1986). Deletion of Tyr^{126} from the carboxyl-terminal has little effect on binding affinity (Schiffrin et al., 1985; Carrier et al., 1985; De Lean et

al., 1985). Removal of the tripeptide, Phe^{26}-Arg^{27}-Tyr^{28}, usually results in a 10- to 100-fold reduction in affinity (Schiffrin et al., 1985; Olins et al., 1986), although as much as an 8000-fold reduction in affinity has been reported for the inhibition of [^{125}I]-ANP binding to bovine adrenal cells (De Lean et al., 1985).

A similar profile of activity is observed for the stimulation of intracellular cGMP production, albeit at concentrations some 10- to 1000-fold higher than those observed in the direct binding studies; the order of potency being ANP_{1-28} > ANP_{5-28}> ANP_{5-25} (Leitman & Murad 1986; Nambi et al., 1986; Rapoport et al., 1986; Roubert et al., 1987).

There are however some analogues of ANP which show divergence between their affinity for ANP binding sites and their ability to increase intracellular cGMP. Scarborough et al. (1986) showed that while ANP_{4-28} and ANP_{4-25} were equipotent at displacing radio-labelled ANP, the latter was more than 100-fold less effective than the former at augmenting intracellular cGMP accumulation in BASM cells. Similarly, Leitman and Murad (1986) reported a 6-fold difference in potency between ANP_{3-28} and ANP_{5-25} to displace of [^{125}I]-ANP from cultured bovine endothelial cells, whilst there was more than a 100-fold difference in their ability to increase cGMP in these cells.

A ring-deleted analogue of ANP, ANP_{4-23} (des-Gln^{18}-Gly^{22})-NH_2, has been shown to compete effectively with [^{125}I]-ANP for the majority of binding sites in whole rat kidney and kidney cortex, with only an 8-fold reduction in affinity relative to ANP_{1-28} (Maack et al., 1987). Ring-deleted ANP is however without effect on glomerular filtration rate, sodium and water excretion or vascular resistance in the

isolated perfused rat kidney (Maack et al., 1987). Nor does it relax preconstricted blood vessels or inhibit aldosterone secretion (Lewicki et al., 1988). In contrast, an increase in immunoreactive native ANP is observed when ring deleted ANP is injected into anaesthetized rats, with a corresponding increase in sodium excretion (Maack et al., 1987). These authors concluded that the majority of ANP receptors in the kidney are "biologically silent", and postulated that these receptors act as clearance binding sites; the increase in plasma ANP in the intact preparation being a direct consequence of these binding sites being occupied by ring-deleted ANP. These receptors have been termed C-ANP receptors, and will bind many truncated analogues of ANP with high affinity. The "biologically active" binding sites are refered to as B-ANP receptors, and bind only ANP_{1-28} with high affinity (Maack et al., 1987).

At a molecular level, the 60 to 70 kDa receptor species, as identified by SDS-polyacrylamide electrophoresis under reducing conditions, appears to be the C-ANP receptor, since truncated and ring-deleted analogues of ANP bind to this species with high affinity (Takayanagi et al., 1987b; Lewicki et al., 1988). The 120-140 kDa receptor species, identified under similar conditions, and which is associated with guanylate cyclase activity, has a much lower affinity for truncated ANP analogues compared to ANP_{1-28} (Takayanagi et al., 1987b), and is likely to be the B-ANP receptor (Lewicki et al., 1988).

2.6 Summary

The evidence to date strongly suggests that most cells possess at least two types of ANP receptors. One receptor is intimately associated with the guanylate cyclase enzyme, has a M_r of 120 to 140

kDa under reducing conditions and appears to be responsible for the vaso-relaxant properties of ANP. The second ANP receptor has a M_r of 60 to 70 kDa under reducing conditions, and it has been postulated that this receptor is responsible for the clearance of ANP from the blood stream. No second messenger system has been identified for this receptor.

2.7 Reasons for Experiments

ANP has been shown to increase intracellular cGMP levels in intact rat ventricular myocytes (Aiton & Cramb, 1985). Because ANP is rapidly degraded when incubated with ventricular myocytes (see chapter 9), further investigations into the mechanism of action of ANP were performed in purified rat cardiac sarcolemmal membranes isolated from ventricular muscle. Guanylate cyclase activity and [^{125}I]-ANP binding sites were measured in this preparation and the results compared with similar studies conducted on membranes isolated from bovine adrenal cortex.

[^{125}I]-ANP binding sites have also been identified on intact MDCK (Madin Darby canine kidney) cells (Aiton et al., 1987) and these were further investigated in membrane preparations.

CHAPTER 3

3.1 Materials

ANP (rat alpha ANP_{1-28}) was purchased from Sigma, Poole, Dorset. GTP and adenosine phophates were obtained from BCL, Lewes, Sussex. HPLC grade solvents and salts were supplied by BDH, Poole, Dorset. [^{125}I]-ANP (rat alpha ANP_{1-28}; specific activity 2200 Ci/mmol) and [^{125}I]-Na (specific activity 17 Ci/mg; pH 8-10) were obtained from Du Pont (U.K.) Ltd., Stevenage, Herts. JOKLIKS was purchased from Flow Laboratories, Rickmansworth, Herts. All other culture media were obtained from Gibco, Paisley, Renfrewshire. All other biochemicals were obtained from Sigma, Poole, Dorset. All general reagents were of analytical grade supplied by BDH (Poole, Dorset).

The antibody to cGMP was a gift from Dr. P Hamet (Clinical Research Institute, Montreal, Canada). SQ 20881 was a gift from E.R. Squibb & Sons, Hounslow, Middlesex. Ramipril was a gift from Hoechst U.K. Ltd., Pharmaceuticals Division, Hounslow, Middlesex.

Rats (Wistar) were obtained from the University of St.Andrews stocks. Animals were maintained under a 24 hr day/night cycle and allowed free access to food.

3.2 Membrane Preparation

3.2.1 Sarcolemmal Membranes

Sarcolemmal membranes were prepared as described by Cramb & Dow (1983). Briefly, following decapitation, the hearts were removed from six, 8 to 12 week-old male Wistar rats (200 to 250g) and placed immediately into ice cold JOKLIKS medium (see appendix I). The

ventricles were excised, washed in JOKLIKS and weighed. They were then placed in 50 ml 1mM $NaHCO_3$, pH 8.0 containing 1 mM PMSF and 0.5 mM DTT, minced with scissors, and homogenised using a Polytron (model PTA 10S, Kinematica, Switzerland) at setting 4 for 30 sec. The resulting homogenate was diluted with 300ml of 1 mM $NaHCO_3$, pH 8.0, containing 0.6 M KCl, 50 mM $Na_4P_2O_7$, 5 mM $MgCl_2$, 1 mM PMSF and 0.5 mM DTT, and then stirred for 45 min on ice. The homogenate was filtered though 8 layers of muslin and centrifuged at 25,000 x g for 30min (Beckman J21, Type JA.20 fixed angle rotor). The pellet was resuspended in 80 ml of 1 mM $NaHCO_3$, pH 8.0, containing 25 mM $Na_4P_2O_7$, 2.5 mM $MgCl_2$, 1 mM PMSF and 0.5 mM DTT, and then recentrifuged at 25,000 x g for 30 min. The resulting pellet was resuspended in 8 ml of 5 mM HEPES, pH 7.4, containing 0.5 mM DTT and diluted to 20 ml with 67% (wt/v) sucrose, 5 mM HEPES, 0.5 mM DTT to give a final concentration of 40 % sucrose. Two discontinuous sucrose gradients were formed consisting of a 4 ml cushion of 60 % sucrose, followed by 10 ml of the membrane suspension, 10 ml of 35 % sucrose, 10 ml of 30% sucrose and finally 2 ml of 5 mM HEPES, pH 7.4, 0.5 mM DTT. All sucrose solutions contained 5 mM HEPES, 0.5 mM DTT. The gradients were centrifuged at 100,000 x g for 2 hr (Beckman L2-65B, SW28 rotor). The bands formed at the 0/30% (Fraction A), and 30/35% (Fraction B) interfaces were collected, diluted with 40 ml of 5 mM HEPES, pH 7.4, containing 0.5 mM DTT, and centrifuged 25,000 x g for 40 min (Beckman J21, Type JA.20 fixed angle rotor). The pellets were resuspended in 5 mM HEPES, pH 7.4, 250 mM sucrose, and 0.5 mM DTT, at a protein concentration of 0.5 to 1 mg/ml. The membranes were stored at -20^{o}C and were diluted to give a final protein concentration of 5 to 20 μg/ml in all assays.

3.2.2 Bovine Adrenal Cortical (BAC) Membranes

Bovine adrenal cortical membranes were prepared by a modification of the methods described by Glossmann et al., (1974) and Meloche et al., (1986a). Briefly, adrenal glands were obtained within 20 min of death and sliced into ice-cold phosphate buffered saline (PBS) containing 1 mM EDTA, 0.1 mM PMSF, and 1 μM aprotinin. The outer 1 to 2 mm of cortex were dissected, washed with fresh buffer and placed in 20 mM $NaHCO_3$, containing 10 mM EDTA, 0.1 mM PMSF, 1 μM aprotinin, 10 μM leupeptin and 1 μM pepstatin, at a concentration of 10 g of tissue (wet weight) to 5 ml of buffer. The tissue was roughly chopped in a blender and then homogenized, first with a Polytron homogenizer at setting 4 for 10 to 20 sec, and then with 3 x 5 strokes of a motor driven glass/teflon homogenizer (300 rpm) with cooling between bursts. The resulting homogenate was filtered through a 250 μm net and the filtrate centrifuged at 1000 x g for 10min. The supernatant was recentrifuged at 25,000 x g for 45 min and the pellet resuspended in 250 mM sucrose, 10 mM Tris-HCl, pH 7.2, 1 mM EDTA. This suspension was layered on to the top of a discontinuous sucrose gradient, consisting of 31.5%, 38.5% , 42.5% and 60 % (w/w) sucrose layers, and centrifuged at 100,000 x g for 2 hr in a Beckmann SW28 rotor. The bands which formed at the interfaces were collected and diluted with 10 mM Tris-HCl, pH 7.2, containing 1 mM EDTA, 0.1 μM pepstatin, and 1 μM leupeptin, and recentrifuged at 25,000 x g for 45 min. The final pellet was resuspended in the same buffer containing 250 mM sucrose, and 5 mM $MgCl_2$ and stored frozen at -20°C.

3.2.3 MDCK cell Membranes

MDCK cells (strains I and II) were grown in plastic Roux flasks in Minimum Essential Medium with Earles' salts (MEME; see appendix I), supplemented with non-essential amino acids, 2 mM glutamine, 100 μg/ml kanamycin, 5% (v/v) donor horse serum and 5% (v/v) fetal calf serum in an 95% air/5% CO_2 atmosphere. After 4 days growth, the cells from 2 x 175 ml flasks were washed with 3 x 100 ml of ice cold Krebs buffer, pH 7.4 (see appendix I for composition). The cell were detached by scraping into 100 ml of the same solution and pelleted by centrifugation at 2000 x g for 10 min. The pellets were resuspended in 2 to 5 ml of 50 mM Tris pH 7.4 at 4°C and homogenised using a polytron homogenizer at setting 4 for 30 sec. The homogenate was centrifuged at 25,000 x g for 15 min and the resulting pellet washed once with the same buffer. The final pellet was resuspended in 1ml of 50 mM Tris pH 7.4 (4°C) and stored at -20°C until used.

3.3 Measurement of Guanylate Cyclase Activity

3.3.1 Guanylate Cyclase Assay

Guanylate cyclase activity was measured in rat cardiac sarcolemmal membranes and bovine adrenal cortical membranes as follows. Membranes were usually incubated with 50 mM triethanolamine, pH 7.4, 1 mM GTP, 3 mM $MnCl_2$, 2 mM IBMX, 10 mM theophylline, 0.1 mg/ml creatine phosphokinase, and 5 mM creatine phosphate for 20 min at 37°C in a final assay volume of 100 μl. Variations in this protocol such as the addition of ANP or its truncated analogues, the replacement of Mn^{2+} with Mg^{2+}, or the inclusion of various adenosine phosphates are described in the appropriate figure legends. The preparation of the

reagents and their storage are described in appendix II. Incubations were started by the addition either of membranes or GTP depending on the type of experiment. The final protein concentration was 5 to 20 µg/ml for both membrane preparations. Incubations were terminated by the addition of 1 ml of 30 mM EDTA at 100°C, and the solution was assayed for cGMP by radioimmunoassay. Occasionally a precipitate formed upon the addition of EDTA. This was removed by centrifugation at 1,000 x g for 15 min in a refrigerated centrifuge (Fissons Coolspin) and did not affect the subsequent assay for cGMP. To ensure that none of the reagents interfered with the subsequent measurement of cGMP, blanks were included in all experiments. These tubes contained all the reagents and membranes present in the assay tubes but were not incubated (i.e. zero time points).

3.3.2 Radioimmunoassay for cGMP

cGMP was determined by radioimmunoassay as described by Richman et al., 1980. Duplicate 100 µl of samples or unknown, standard, or buffer were placed in 3.5 ml polypropylene tubes (Sterilin RT30) followed by 100 µl of [^{125}I]-ScGMP-TME (10,000 to 15,000 cpm) and 250 µl . The [^{125}I]-ScGMP-TME and the cGMP antibody were prepared in 50mM sodium acetate buffer, pH 4,75 containig 0.5% BSA (see appendix II). The reagents were allowed to equilibrate by incubation overnight (15 to 24 hr), at 4°C. The antibody was precipitated by the addition of 2 ml of 95% ethanol. The tubes were mixed thoroughly and allowed to stand for 30 min at room temperature. The precipitate was pelleted by centrifugation at 1,500 x g for 30 min at 4°C (Fissons Coolspin), and the supernatant removed by aspiration. The pellet was counted for radioactivity in a Prias gamma counter (Packard Instrument Company,

Illinois, USA).

For each experiment, a standard curve was constructed in the range 30 to 10,000 fmol cGMP. The nonspecific binding, defined as the radioactivity bound in the presence of an excess of cGMP (20 nmol), was subtracted from all values. The results were expressed as the counts bound in the absence of competing cGMP (Co) divided by the counts bound in the presence of cGMP (Cs). A plot of Co/Cs against the cGMP concentration was usually linear over the concentration range 30 to 1000 fmol (fig. 3.1). The exact range of linearity was defined as the range of the pairs of values yielding a correlation coefficient (Pearson r) greater than 0.900. The unknown values were treated in the same manner, and the amount of cGMP in each sample was calculated from the regression equation for the standard curve.

3.3.3 Preparation of [^{125}I]-Tyrosine Methyl Ester Succinyl-cGMP

Succinyl-cyclic GMP tyrosine methyl ester (ScGMP-TME) was labelled with [^{125}I] according to the method described by Richman et al. (1980). 20 μl of ScGMP-TME (2 μg) and 10 μl of [^{125}I]-Na (approx. 1 mCi) were placed in a 1.5 ml microfuge tube, and the reaction initiated by the addition of 20 μl chloramine-T (1 mg/ml in 50 mM potassium phosphate, pH 7.4). After exactly 45 seconds the reaction was terminated by the addition of 50 μl of potassium metabisulphite (1 mg/ml in 50 mM potassium phosphate, pH 7.4). 200 μl of 2.5 mM sodium iodide was then added to reduce the specific activity of the unreacted [^{125}I] and to dilute the ionic strenth to less than 250 mM.

The reaction mix was layered on to the top of the QAE-25 sephadex column which had been pre-equilibrated with 0.05 M ammonium formate pH

Figure 3.1

Measurement of cGMP by Radio-immunoassay

(a) A representative standard curve for the assay of cGMP. Each point is the mean ± SEM of triplicate determinations. (b) A plot of radioactivity bound against cGMP concentration.

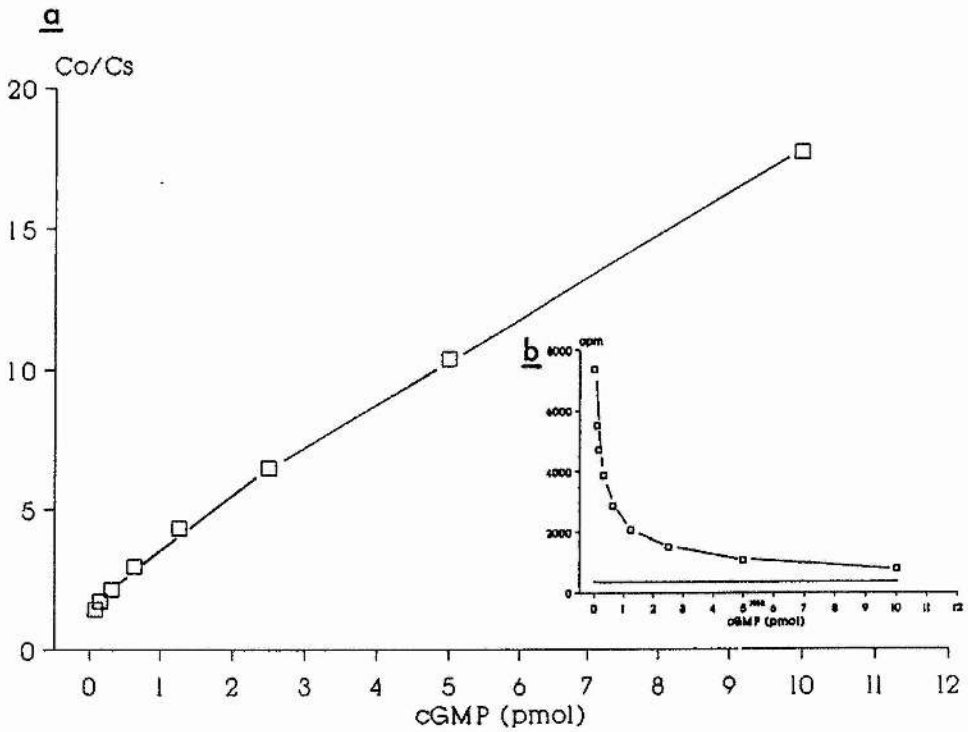

6.0 at 4°C (for details of preparation see appendix II). The solution was allowed to run into the column and the top was then washed with approximately 300 µl of 250 mM ammonium formate, pH 6.0. The [^{125}I]-Sc-cGMP was eluted with 250 mM ammonium formate pH 6.0, at a flow rate of 1 ml/min at 4°C. 1 or 2 ml fractions were collected and from these 5 µl aliquots were counted for radioactivity. Fractions corresponding to peaks in radioactivity were diluted to give 15,000cpm/100µl and assayed for their binding to the cGMP antibody. The fractions containing the highest binding were combined and stored in 100µl aliquots at -70°C.

The results of a typical preparation of [^{125}I]-ScGMP-TME are shown in figure 3.2. Of the three main radioactive peaks eluted from the column, antibody binding was mainly associated with peak C (table 3.1). Fractions from this were combined to provide [^{125}I]-ScGMP-TME for subsequent cGMP assays. Peak A, which showed no antibody binding and eluted close to the void volume of the column, is likely to be free [^{125}I].

3.4. [^{125}I]-ANP Radioreceptor Assay

3.4.1 Cardiac Sarcolemmal Membranes.

Membranes were incubated for 40 min at 37°C with [^{125}I]-ANP (40 to 100 pM) in the presence of varying concentrations of unlabelled ANP and buffer containing 50 mM Tris-HCl, pH 7.4, 100 mM NaCl, 0.1 mM EDTA, 5 mM $MgCl_2$, 1 µM leupeptin, 0.1 µM pepstatin and 1 mg/ml BSA. The final incubation volume was 200 µl. Incubations were terminated by the addition of 2 ml of ice cold wash buffer containing 50 mM Tris-HCl, pH 7.4, and 100 mM NaCl. Bound [^{125}I]-ANP was separated from free

Figure 3.2

Purification of [^{125}I]-ScGMP-TME

Profile of radioactivity eluted from a QAE-25 Sephadex column. The fractions marked by * were assayed for cGMP antibody binding. The shaded area represents the fractions which were combined to give [^{125}I]-ScGMP-TME for use in the cGMP assay. The percentage radioactivity recovered from each peak was 15.8, 6.7, and 77.4, for peaks A, B and C respectively.

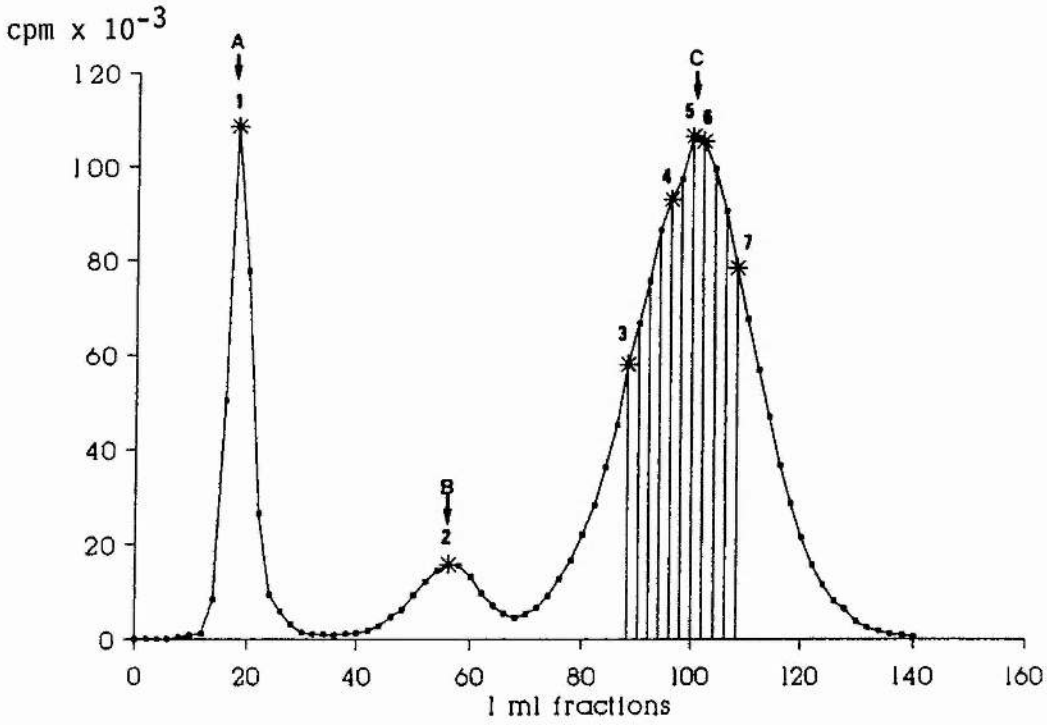

Table 3.1

Radioactivity Bound to cGMP Antibody

Aliquots were removed from the fractions indicated on fig. 3.2 and diluted with 50 mM sodium acetate buffer (pH 4.75), containing 0.5% BSA buffer to give approximately 12,000 cpm/ 100 μl. These were incubated with cGMP antibody in the absence (Co) and presence (C_{NSB}) of 20 nmol cGMP overnight, at 4^{o}C as described in section 3.3.2.

Sample No.	Total cpm	cpm Co	cpm C_{NSB}	% cpm Bound
1	11743	269	632	-3.09
2	15589	799	638	1.03
3	12853	3728	356	26.2
4	12765	3850	339	27.5
5	12168	3749	782	24.4
6	10140	2880	356	24.9
7	13588	3879	753	23.0

by rapid filtration through Whatman GF/F filters followed by washing with 10ml of the same buffer. To reduce background binding the filters were pre-soaked in 0.3% polyethyleneimine for 60 min prior to use (Brunks et al., 1983). The total filtration time including washes was less than 30 sec.

3.4.2 Bovine Adrenal Cortical (BAC) Membranes

The binding assay was carried out as decribed for sarcolemmal membranes. The final membrane concentration was 0.2 to 1.0 mg per ml

3.4.3 MDCK Cell Membranes

The binding assay was carried out as decribed for sarcolemmal membranes except that the incubations were performed at 20°C for 30 min, in 50 mM Tris , pH 7.4 at 20°C, 5 mM $MgCl_2$, 1 μM aprotinin, 500 μM PMSF, 1 mg/ml bacitracin and 1 mg/ml BSA. The final protein concentration was 30 to 300 μg/ml.

3.5. Assessment of [^{125}]-ANP Degradation by High Performance Liquid Chromatography (HPLC)

3.5.1 Sample Preparation

[^{125}I]-ANP was incubated for 40 min at 37°C with rat cardiac sarcolemmal membranes in a final incubation volume of 200 μl, as described previously. The incubation was terminated by the addition of 2 ml of 50 mM Tris, pH 7.4 at 4°C and the samples were partially purified prior to HPLC analysis by passage through preparative C_{18} ODS silica columns (3 ml Tech Elut columns, cat. no. LSP 9515). Briefly, the columns were fitted to a Baker SPE 21 fitration manifold, and washed with 2 x 3 ml of 100% acetonitrile (ACN). The columns were

conditioned with 1 x 3 ml of the sample buffer and samples were added before the column dried. The columns were washed with 3 ml of 15% ACN, containing 0.1% trifluoroacetic acid (TFA) and air-dried for 5 min. The samples were eluted with 2 x 200 μl of 60% ACN, 0.1% TFA, and dried under nitrogen on a Technic sample concentrator at 37^{o}C. The samples were resuspended in 150 μl of 15% ACN, 0.1% TFA and stored at -20^{o}C until analysed.

3.5.2 HPLC Analysis

Assessment of [^{125}I]-ANP degradation was performed on a Gilson HPLC system equipped with Gilson Model 302 dual pumps with 5 ml pump heads, a Gilson model 802 manometer module and mixing chamber, a Rheodyne 7125 injector valve with a 100 μl injection loop, and a Gilson UV holochrome detector fitted with an 11 μl flow cell. The system was fitted with a 150 x 4.6 i.d. C_{18} Spherisorb column (ODS2- SB5-401). Gradient control and peak analysis were carried out on an Apple IIe computer, linked to a Gilson Model 620 Data Master and a NEC PC8023BE-N printer.

[^{125}I]-ANP was eluted from the column with a linear gradient of 15% to 60% (ACN) in 0.1% (TFA), at a flow rate of 1 ml/min and a slope of 0.9 %/min, followed by a gradient of 60 to 100% ACN, at a similar flow rate with a slope of 4 %/min. 60 x 1 ml fractions were collected using a Gilson 205 fraction collector and measured for radioactivity.

3.6 Protein Assay.

Protein concentrations were determined using the Bio-Rad protein assay (Cat. No. 500-0002), which is based on the assay described by Bradford (1976). The principle of the assay is that the absorbance maximum for

Coomassie Brilliant Blue G-200 shifts from 465 nm to 595 nm when protein binding occurrs (Reisner et al., 1975). Briefly, the protein standards, samples, or buffer, were diluted to 800 µl with distilled H_2O and to this was added 200 ul of undiluted Dye Reagent Concentrate (filtered before use). The reagents were mixed thoroughly, avoiding excess frothing and allowed to stand at room temperature for 5 min. The absorbance was then measured at 595 nm in a Phillips P4 8620 spectrophotometer. BSA was used as a standard and the assay was linear over the range 1 to 10 µg of protein (fig 3.3). The sample protein concentration was determined from the regression line for the standard curve. Blanks, containing sample buffer only, were included in each assay, and were normally less than 5 % of the total absorbance.

Figure 3.3

Measurement of Protein Using the Bio-Rad Protein Assay Kit

A typical standard curve for the Bio-Rad protein assay. Each point represents a single determination of absorbance measured at 595 nm. Bovine serum albumin was used as the standard.

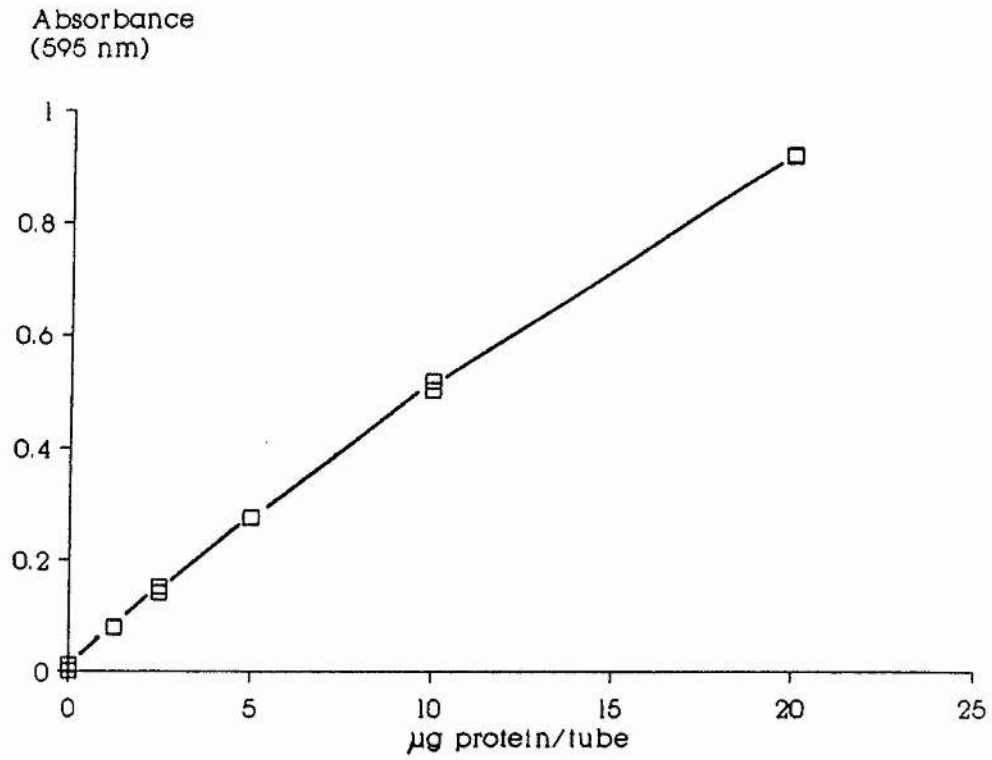

CHAPTER 4

4 Results of Guanylate Cyclase Experiments

4.1.1 Preliminary Experiments in Rat Sarcolemmal Membranes

The effects of incubation time and membrane concentration on guanylate cyclase activity were investigated in purified rat cardiac sarcolemmal membranes. Manganese-dependent guanylate cyclase activity was measured in the presence and absence of ANP, over a range of membrane concentrations (fig. 4.1). At protein concentrations up to 20 μg/ml, both basal and ANP-stimulated guanylate cyclase activity increased linearly with increasing protein. Above this concentration the rate of cGMP production declined.

The relationship between incubation time and Mn^{2+}-dependent guanylate cyclase activity was also examined in these membranes. The rate of cGMP production was constant for at least 20 min, both in the presence and absence of ANP (fig. 4.2), although the absolute rate varied between preparations (table 4.1). Incubations longer then 20 min resulted in a decline in the rate of guanylate cyclase activity.

As a result of these experiments guanylate cyclase activity in rat cardiac sarcolemmal membranes was routinely measured with protein concentrations of less than 20 μg/ml, over a 20 min incubation period.

4.1.2 Comparison of Guanylate Cyclase Activity in Fractions A and B

The purification of cardiac sarcolemmal membranes by sucrose gradient centrifugations resulted in two bands of material, both of which were enriched in plasma membrane markers (Cramb & Dow, 1983). Fraction A was recovered from the 0/30% sucrose interface, and fraction B from

Figure 4.1

The Effect of Protein Concentration on Guanylate Cyclase Activity in Rat Cardiac Sarcolemmal Membranes

Samples containing increasing concentrations of protein were incubated for 20 min at 37°C, in the absence (△—△) and presence (□—□) of 10^{-6}M ANP. Each point represents the mean ± SEM for 3 determinations of guanylate cyclase activity, each of which was measured in duplicate for cGMP.

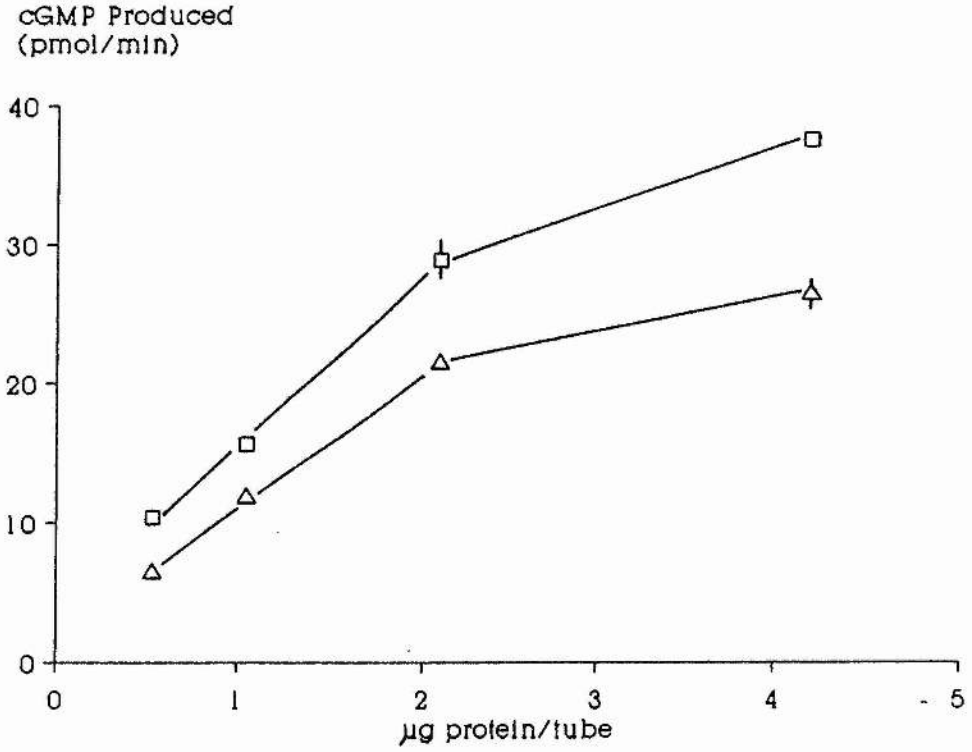

Figure 4.2

Time Course for Guanylate Cyclase Activity in Rat Cardiac Sarcolemmal Membranes

A representative time course for guanylate cyclase activity in the absence (△—△) and presence (□—□) of 10^{-6} M ANP. Each point represents the mean ± SEM for duplicate determinations of guanylate cyclase activity, followed by duplicate determinations of cGMP.

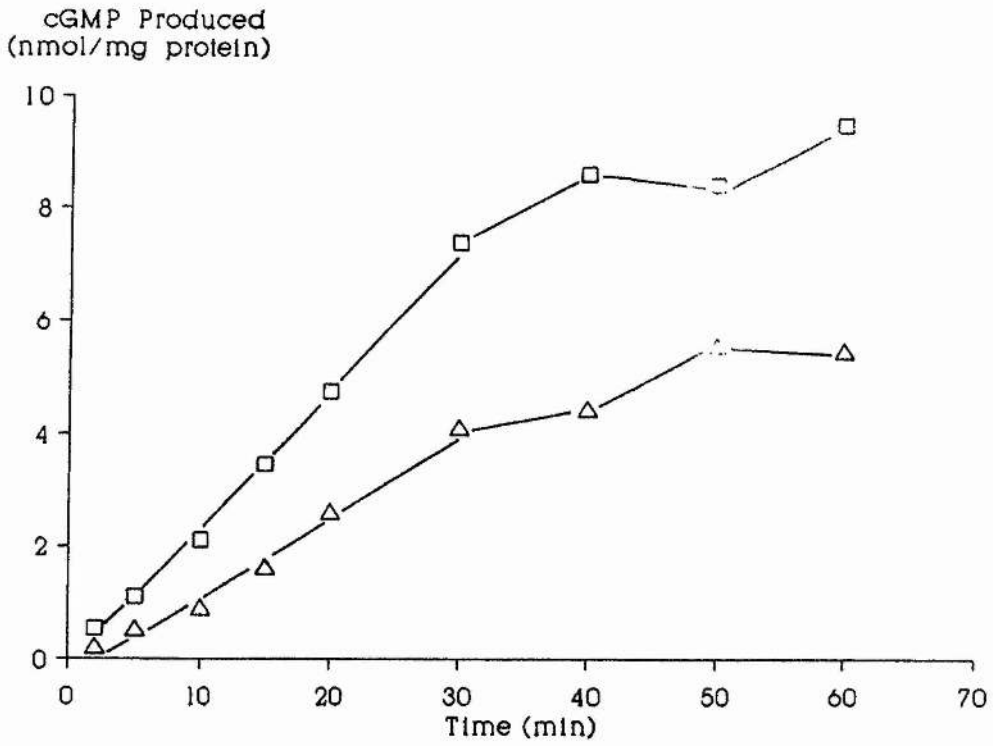

Table 4.1

Comparison of the Initial Rates of Guanylate Cyclase Activity

Rate of cGMP production was measured over the first 20 min. The mean guanylate cyclase activity was 112 ± 20.5 and 204 ± 38.7 pmol/min per mg protein for basal and ANP-stimulated activity respectively. The p values were calculated from the Pearson correlation coefficient (two-tailed probabilities).

Prep.	Condition	GC.Act. pmols/ mg/min	Corr. Coeff.	No. Obs.	p<
1	Basal	117	0.979	8	0.01
1	10^{-6} M ANP	250	0.973	8	0.01
2	Basal	129	0.984	9	0.01
2	10^{-6} M ANP	235	0.997	9	0.01
3	Basal	89	1.000	9	0.01
3	10^{-6} M ANP	127	0.995	9	0.01

the 30/35% interface. Basal and ANP-stimulated guanylate cyclase activities were measured in both fractions and the results compared. The rate of cGMP production by fraction A varied 3-fold for both basal and ANP-stimulated guanylate cyclase activity, ranging from 68.4 to 228 pmol/min per mg protein, and 101 to 359 pmol/min per mg protein respectively. The variability between preparations was larger for fraction B, ranging from 32.5 to 325 pmol/min per mg protein, and 73.3 to 756 pmol/min per mg protein, for basal and ANP-stimulated guanylate cyclase activity respectively. ANP significantly increased the rate of cGMP production in both fractions, with no difference being observed between the absolute levels of either basal, or ANP-stimulated guanylate cyclase activity for the two fractions (table 4.2). A significant difference was observed in the percentage stimulation of basal activity, with 1μM ANP producing a 1.80-fold increase in activity in fraction B, whilst the same concentration produced a significantly smaller increase (1.45-fold) in fraction A (table 4.2). As ANP reliably produced a greater increase in guanylate cyclase activity in fraction B, only this fraction was used for subsequent experiments.

4.1.3 The Effect of Manganese and Magnesium

The effect of manganese and magnesium on guanylate cyclase activity was examined in rat cardiac sarcolemmal membranes. Increasing concentrations of Mn^{2+} resulted in a biphasic response for both basal and ANP-stimulated guanylate cyclase activity (fig 4.3a). In the presence of 1 mM GTP, the rate of cGMP production increased in a dose-dependent manner until around 1 mM Mn^{2+}, above which concentration no further increases in activity were observed. At Mn^{2+} concentrations

Table 4.2

Comparison of Guanylate Cyclase Activity in Fraction A and B Recovered from the Sucrose Gradient Purification of Rat Cardiac Sarcolemmal Membranes

Significant differences between basal and ANP-stimulated levels were tested for using a two-tailed *t* test (paired). * $p < 0.05$, *** $p < 0.001$. Significant differences between manganese-dependent guanylate cyclase activity in fractions A and B were tested for using a two-tailed *t* test (unpaired). # = $p < 0.001$.

Fraction (No.Obs.)		Guanylate Cyclase Activity (pmol cGMP/min /mg protein)		
		Basal	10^{-6}M ANP	ANP/Basal
A (9)	Mn^{2+}	114 ± 18	205 ± 29*	1.45 ± 0.10
B (20)	Mn^{2+}	129 ± 17	241 ± 42***	1.80 ± 0.10#
B (9)	Mg^{2+}	3.21+1.34	11.8+3.40*	3.68

greater than 4 mM guanylate cyclase activity declined. The Km was estimated for values of manganese up to 4 mM, and found to be 50.8 ± 0.7 and 22.8 ± 7.9 μM, with Hill coefficients of 5.41 ± 0.02 and 6.35 ± 0.50, for basal and ANP-stimulated guanylate cyclase activity respectively. In addition the stimulation of guanylate cyclase activity by ANP was markedly reduced at concentrations of Mn^{2+} above 4mM.

The replacement of manganese with magnesium resulted in a substantial reduction of guanylate cyclase activity, with basal and ANP-stimulated activity being 3 to 5% of that observed in the presence of Mn^{2+} (table 4.2). Dose response curves were constructed to examine the effect of magnesium concentration on guanylate cyclase activity. The amounts of cGMP produced in these experiments were very small and although the results were qualitatively similar to those observed with manganese, detailed analysis was not possible (fig. 4.3b)

4.1.4 Effect of GTP on Guanylate Cyclase Activity

The effect of GTP concentration on Mn^{2+}-dependent guanylate cyclase activity was examined in the absence and presence of 1 μM ANP (fig 4.4). With Mn^{2+} concentrations of 3 mM, the rate of cGMP production increased in a dose-dependent manner with increasing concentrations of GTP. Analysis of the data by 'Enzfitter' (allosteric kinetics; see appendix III) gave Km values of 43 ± 16 and 130 ± 60 μM for basal and ANP-stimulated guanylate cyclase activity respectively. The Hill coefficients were 1.79 ± 0.12 and 2.27 ± 0.15 for the two conditions.

4.1.5 Dose Response Curves for ANP, ANP_{5-28}, and ANP_{5-25}

The effects of ANP, ANP_{5-28}, and ANP_{5-25}, on guanylate cyclase

Figure 4.3

The Effect of Manganese and Magnesium on Guanylate Cyclase Activity

Rat cardiac sarcolemmal membranes were incubated for 20 min, at 37°C with increasing concentrations on (a) $MnCl_2$, or (b) $MgCl_2$, in the absence (△—△) and presence (□—□) of 10^{-6} M ANP. Each point is the mean ± SEM of 2 separate experiments in which guanylate cyclase activity was measured in duplicate, followed by duplicate determinations of cGMP.

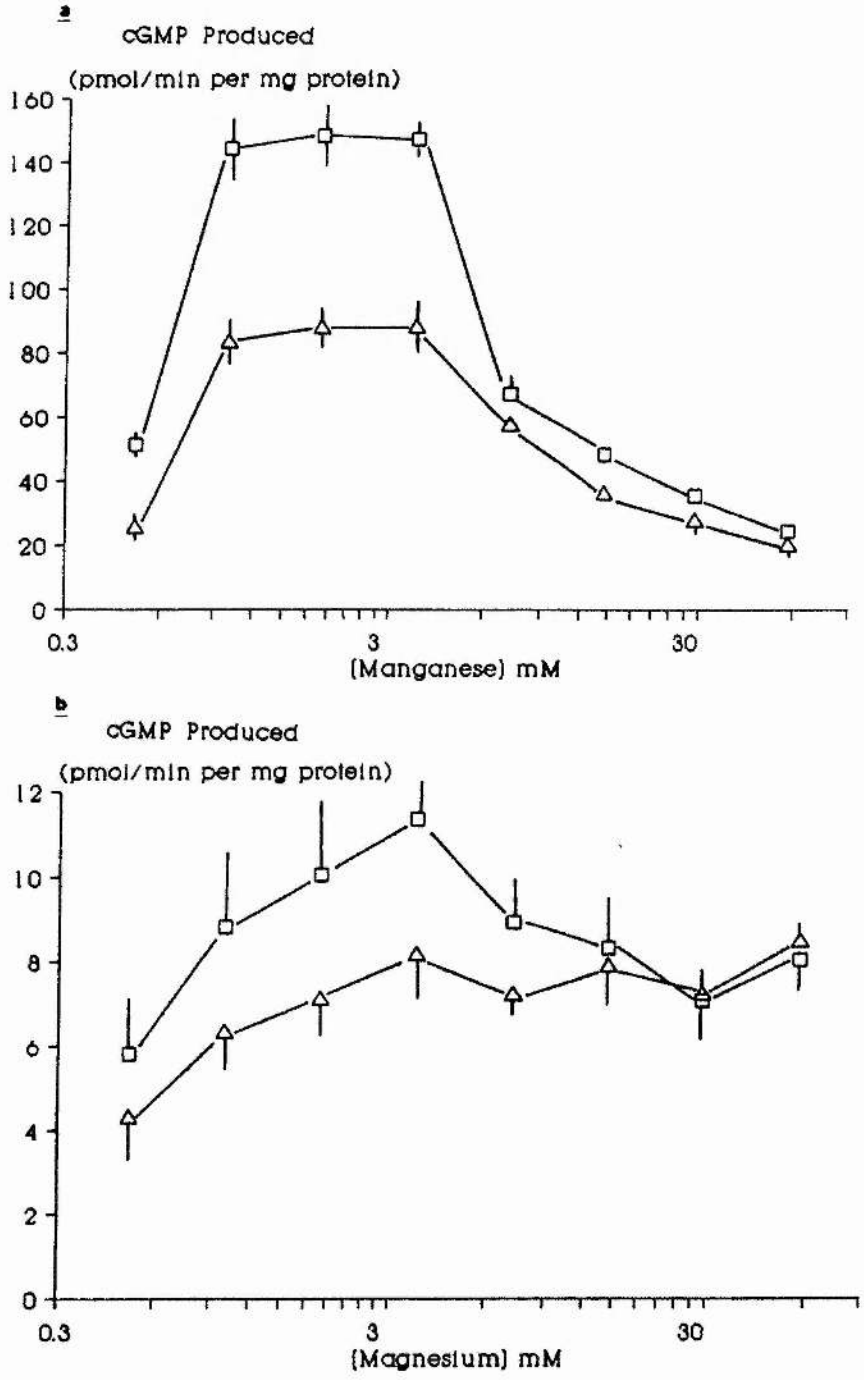

Figure 4.4

Dose Response Curve for GTP Stimulation of Guanylate Cyclase Activity

Rat cardiac sarcolemmal membranes were incubated for 20 min at 37°C, with increasing concentrations of GTP, in the absence (△—△) and presence (□—□) of 10^{-6} M ANP. Each point is the mean ± SEM of duplicate determinations of guanylate cyclase activity, in which cGMP was measured in duplicate.

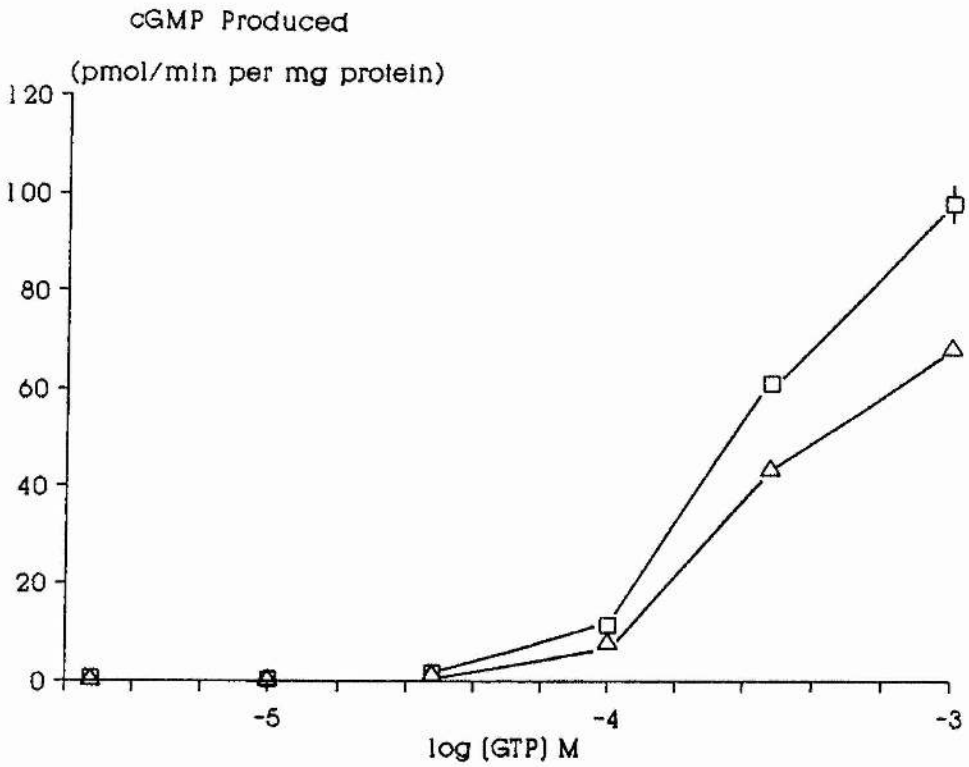

activity in rat cardiac sarcolemmal membranes were examined. Mn^{2+}-dependent guanylate cyclase activity was measured in the presence of increasing concentrations of the peptides (fig. 4.5) and the dose response curves were analysed by Enzfitter (allosteric kinetics). ANP produced the largest stimulation of activity, with an estimated Km of 1.87 $\pm$ 0.43 nM and a Hill Coefficient of 0.468 $\pm$ 0.073. ANP_{5-28} was of similar potency to ANP_{1-28}, with a Km of 0.671 $\pm$ 0.304 nM and a Hill coefficient of 0.766 $\pm$ 0.229. The maximum response to this peptide was however only 50% of that produced by ANP. ANP_{5-25} was the weakest peptide examined and only increased the rate of cGMP production at concentrations of above 100 nM.

4.1.6 Effect of Protease Inhibitors on Guanylate cyclase Activity

The possibility that ANP was degraded during the incubation was examined by the measurement of Mn^{2+}-dependent guanylate cyclase activity in the presence and absence of various protease inhibitors. Detailed dose response curves were constructed for ANP-stimulated guanylate cyclase activity, in the presence and absence of 10 μM phosphoramidon, a specific inhibitor of endopeptidase 24.11 (fig 4.6). The Km values were 0.875 $\pm$ 0.296 nM and 2.43 $\pm$ 1.13 nM with Hill coefficients of 0.269 $\pm$ 0.057 and 0.300 $\pm$ 0.074 for the control and phosphoramidon curves respectively. There were no significant differences between the Km values, the Hill coefficients, or the maximum stimulation for ANP in the two conditions. A number of other inhibitors were also examined for their effect on basal and ANP stimulated guanylate cyclase activity (fig 4.7). None of the inhibitors tested had any effect on basal rates of cGMP production. The inclusion of 0.5 mM PMSF in the incubation medium resulted in a

Figure 4.5

Dose Response Curves for ANP, ANP_{5-28}, and ANP_{5-25} Stimulation of Guanylate Cyclase Activity

Rat cardiac sarcolemmal membranes were incubated for 20 min at 37°C, in the presence of 3 mM $MnCl_2$, and increasing concentrations of ANP (□—□), ANP_{5-28} (△—△), and ANP_{5-25} (○—○). Each point represents the mean ± SEM for 6 (ANP_{1-28}), 3 (ANP_{5-28}), and 1 (ANP_{5-25}) separate experiments in which guanylate cyclase activity was measured in triplicate, followed by duplicate determinations of cGMP. The basal activity was ranged from 32.5 to 325 pmol cGMP/min per mg protein.

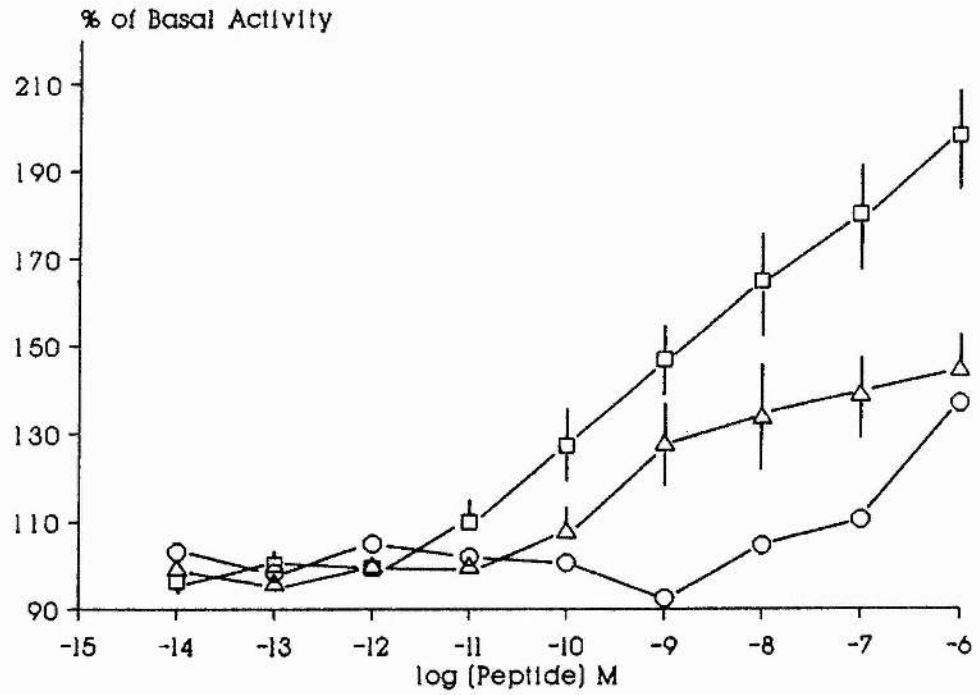

Figure 4.6

Effect of Phosphoramidon on Guanylate Cyclase Activity

Rat cardiac sarcolemmal membranes were incubated for 20 min at 37°C, with increasing concentrations of ANP, in the absence (△——△), and presence (□—□) of 10^{-5} M phosphoramidon. Each point represents the mean ± SEM of 2 separate experiments in which guanylate cyclase activity was measured in triplicate, followed by duplicate determinations of cGMP. The basal activity was 40.6 and 103.6 pmol cGMP/min per mg protein for the two preparations.

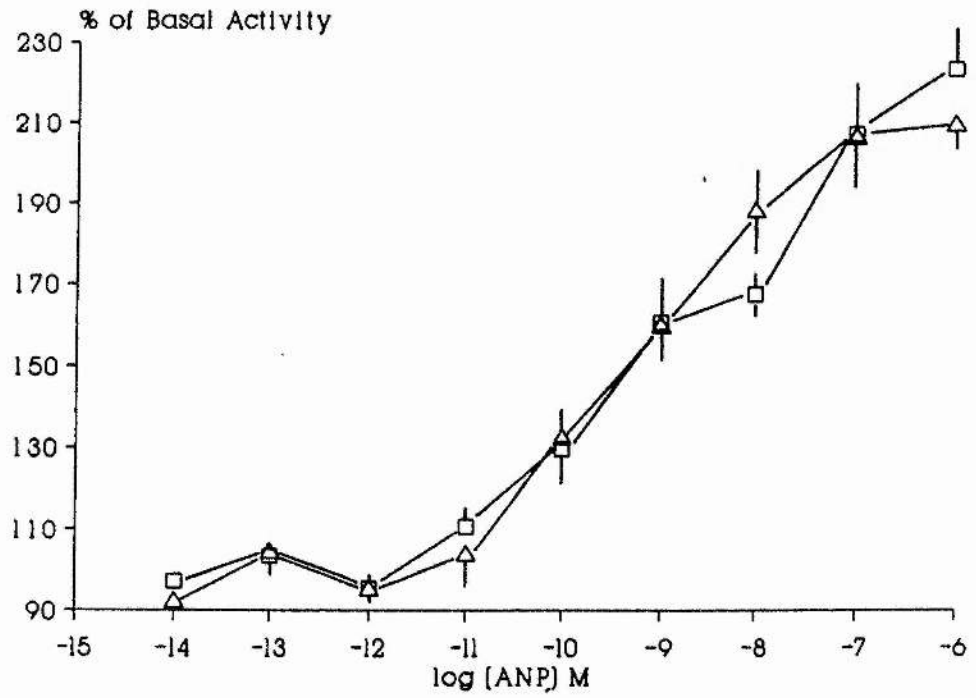

Figure 4.7

The Effect of Various Peptides and Protease Inhibitors on Guanylate Cyclase Activity

Rat cardiac sarcolemmal membranes were incubated for 20 min at 37°C, in the absence or presence of various protease inhibitors at the concentration indicated. Guanylate cyclase activities were determined in the absence (☐) or presence of 10^{-9} M (▩) or 10^{-7}M ANP (▩). Assays were carried out in duplicate followed by duplicate determinations of cGMP. Significant differences from controls are indicated by * = $p < 0.05$, and ** = $p < 0.01$ as determined a two-tailed Student's *t*-test (unpaired solution).

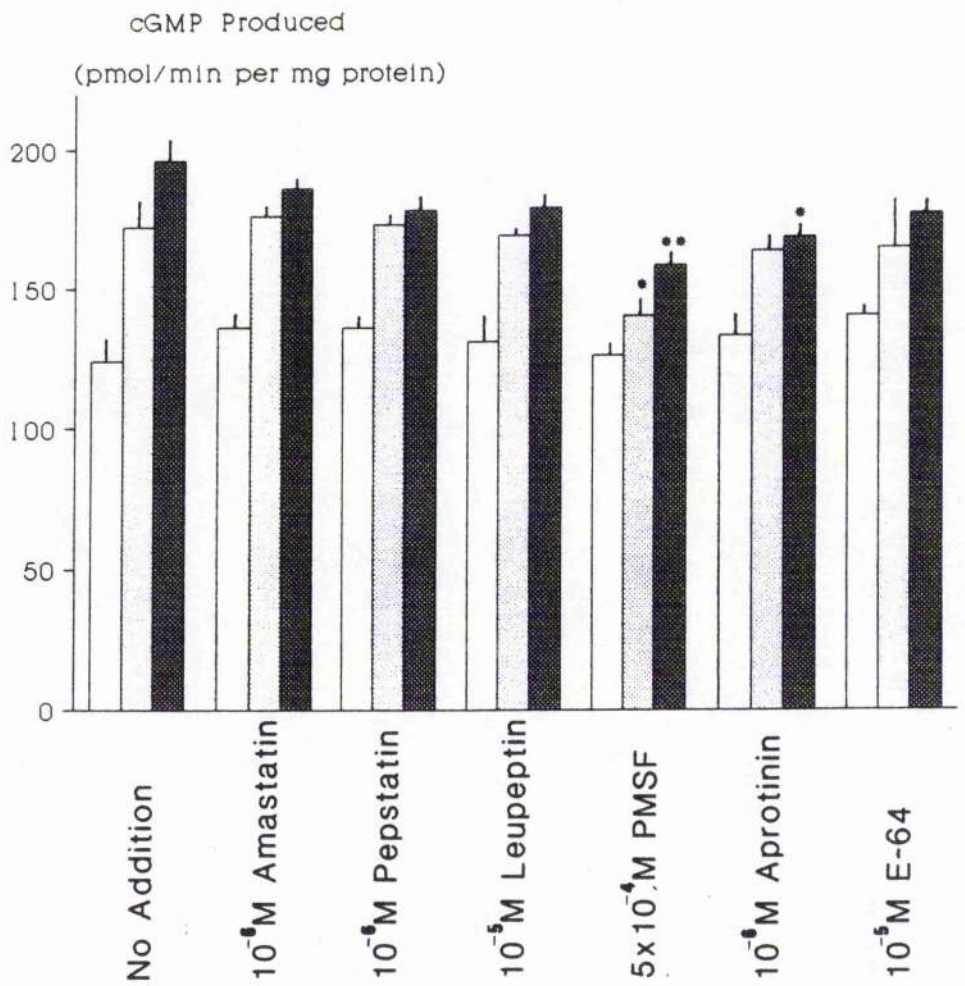
cGMP Produced
(pmol/min per mg protein)
200
150
100
50
0
No Addition
10⁻⁶M Amastatin
10⁻⁶M Pepstatin
10⁻⁵M Leupeptin
5x10⁻⁴M PMSF
10⁻⁶M Aprotinin
10⁻⁵M E-64

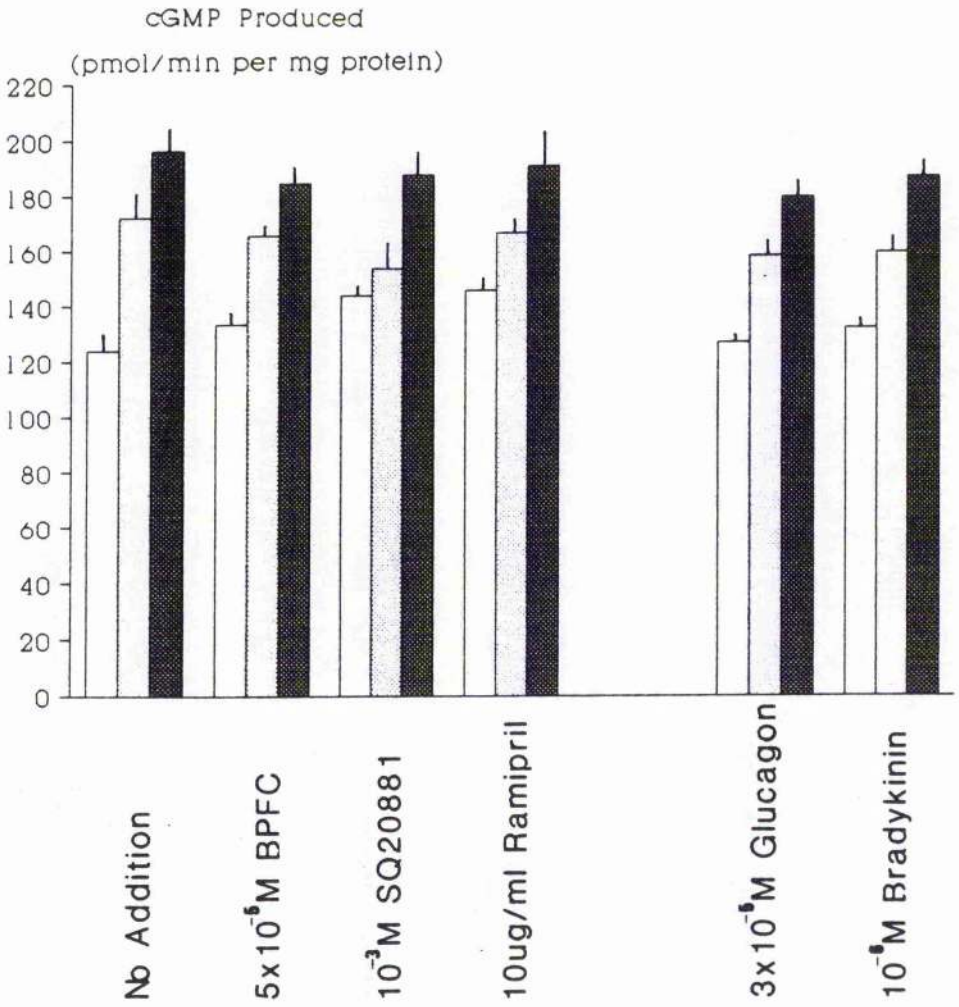
cGMP Produced
(pmol/min per mg protein)
220
200
180
160
140
120
100
80
60
40
20
0
No Addition
5x10⁻⁵M BPFC
10⁻³M SQ20881
10ug/ml Ramipril
3x10⁻⁵M Glucagon
10⁻⁶M Bradykinin

decrease in guanylate cyclase activity in the presence of both 1 nM and 100 nM ANP. Aprotinin also produced a small decrease in guanylate cyclase activity in the presence of 100 nM ANP.

The effect of glucagon and bradykinin, on manganese-dependent guanylate cyclase activity was also examined. Neither of these peptides had any effect on basal or ANP-stimulated cGMP production by rat cardiac sarcolemmal membranes (fig. 4.7).

4.1.7 Effect of Adenosine Phosphates on Guanylate Cyclase Activity

The effect of various adenosine phosphates on Mn^{2+}-dependent guanylate cyclase activity was examined. ADP and AMP, at millimolar concentrations, had no effect on either basal or ANP-stimulated guanylate cyclase activity (fig 4.8). ATP and a non-hydrolysable analogue, AMP-PNP, attenuated cGMP production in both conditions. Dose response curves were constructed for ATP in the presence and absence of 1 μM ANP. The reduction of guanylate cyclase activity was dose dependent, with half maximal inhibition occurring at 2×10^{-3} M for both basal and ANP-stimulated activity (fig 4.9).

The effect of 1 mM ATP on manganese-dependent guanylate cyclase activity was examined over an extended time course (fig. 4.10). As observed in earlier experiments, the rate of cGMP production in the absence of ATP was linear for the first 20 min, for both basal and ANP-stimulated guanylate cyclase activity, while longer incubations resulted in an attenuation of the activity. When ATP was included in the incubation medium the initial rate of cGMP production was slightly reduced, but this lower activity was maintained for the duration of the time-course. Thus, in the presence of ATP, basal and ANP-

Figure 4.8

Effect of Adenosine Phosphates on Mn^{2+}- Dependent Guanylate Cyclase Activity

Rat cardiac sarcolemmal membranes were incubated for 20 min at 37°C, in the absence (□) or presence (▨) of 10^{-6} M ANP, and in the presence of 1 mM adenosine phosphates as indicated. The results are the mean ± SEM of at least 3 separate experiments in which guanylate cyclase was measured in triplicate followed by duplicate determinations of cGMP. Significant differences from controls are indicated by * = $p < 0.05$, ** = $p < 0.01$ and ** = $p < 0.001$ as determined by a two-tailed Student's *t*-test (paired solution).

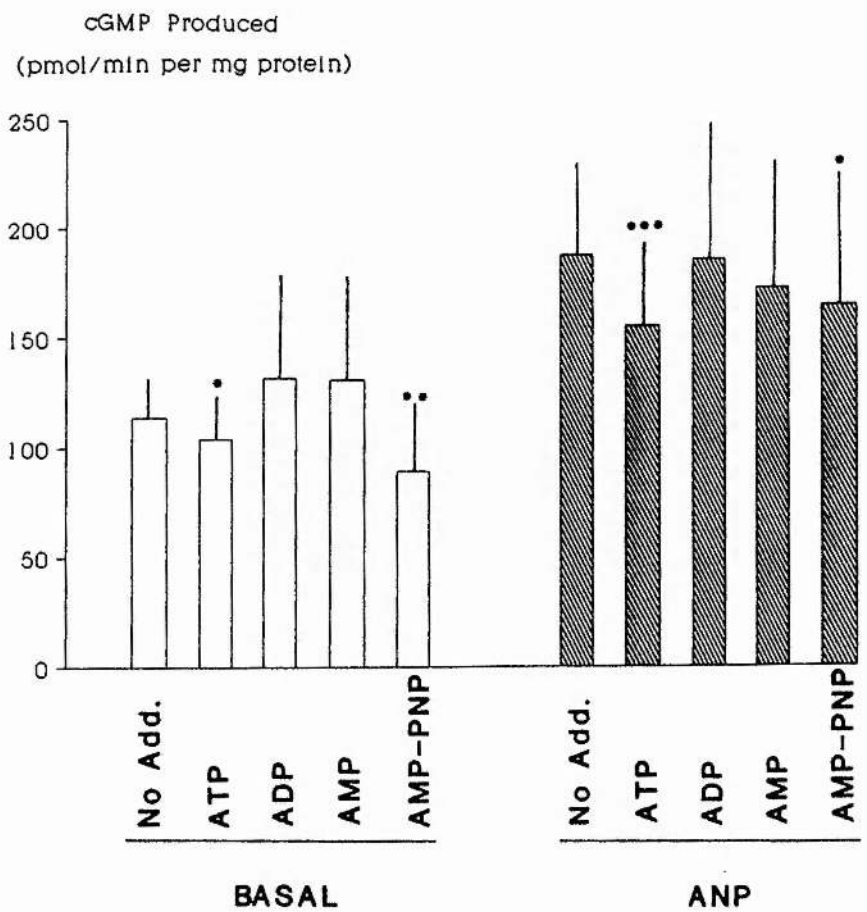

Figure 4.9

Dose Response Curve for the Effect of ATP on Mn^{2+}-Dependent Guanylate Cyclase Activity

Rat cardiac sarcolemmal membranes were incubated for 20 min at 37°C, with increasing concentrations of ATP, in the absence (△——△) or presence of 10^{-6} M ANP (□——□). Mn^{2+} was kept at a concentration 1 mM in excess of the combined GTP and ATP concentrations. The results are the mean ± SEM of 3 separate experiments in which guanylate cyclase was measured in triplicate, followed by duplicate determinations of cGMP.

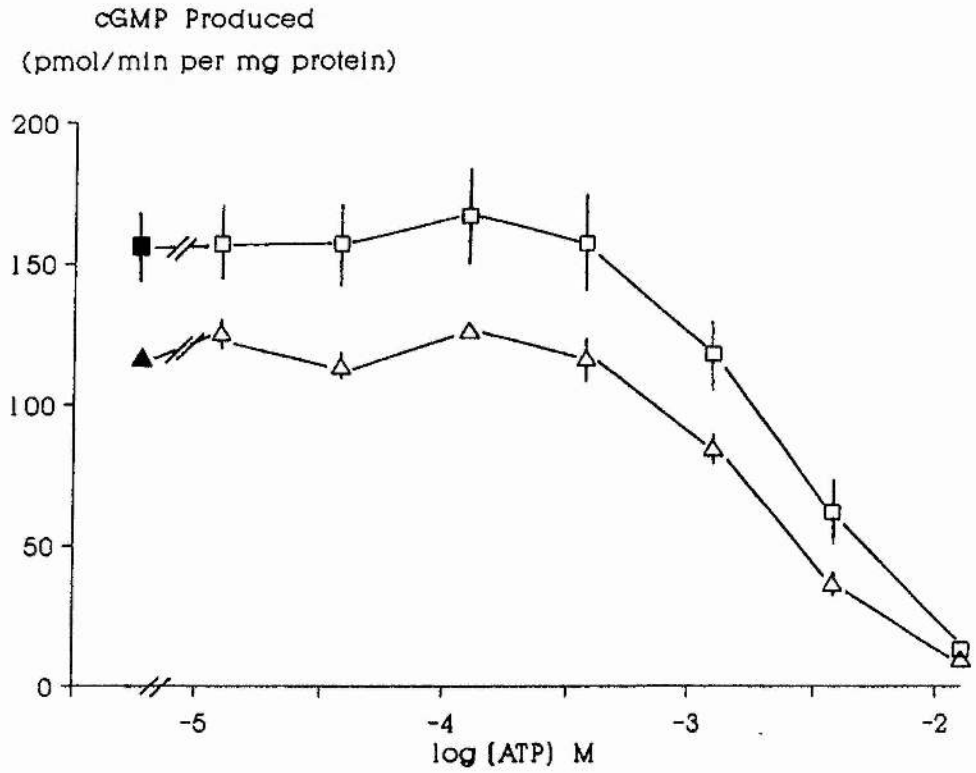

Figure 4.10

The Effect of ATP on the Rate of cGMP Production

Rat cardiac sarcolemmal membranes were incubated for 20 min at 37°C, in the absence (△—△) and presence (□—□) of 10^{-3} M ATP, (a) in the absence and (b)in the presence of 10^{-6} M ANP. The Mn^{2+} concentration was $3x10^{-3}$ M. Each point represents the mean of duplicate determinations of guanylate cyclase activity, which had been assayed in duplicate for cGMP.

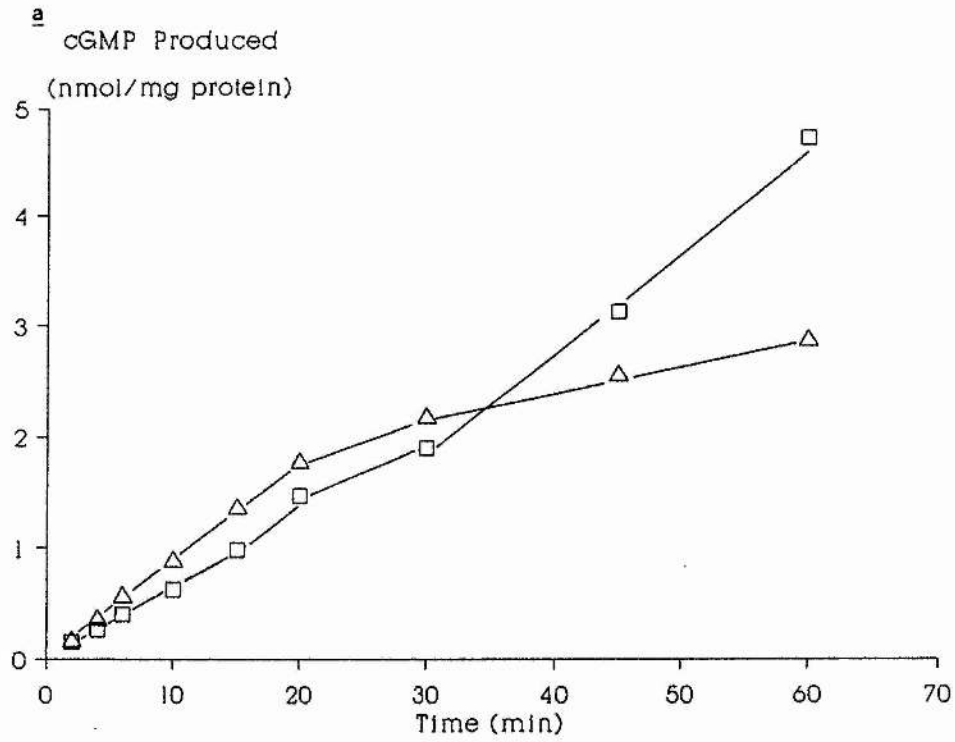
a
cGMP Produced
(nmol/mg protein)
5
4
3
2
1
0
0
10
20
30
40
50
60
70
Time (min)

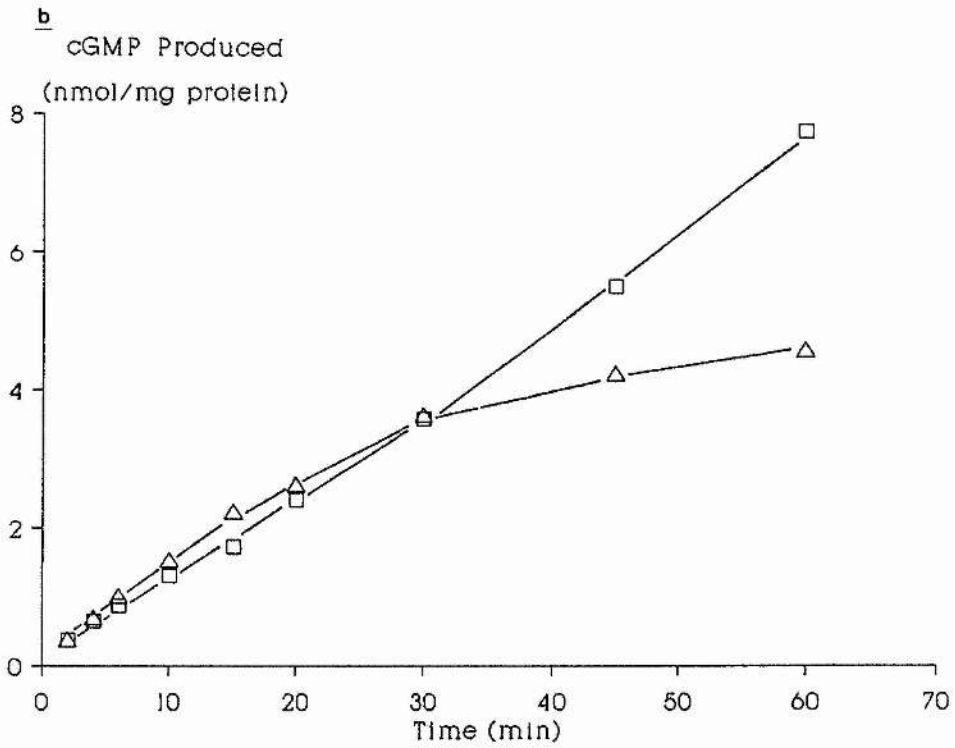
b
cGMP Produced
(nmol/mg protein)
8
6
4
2
0
0
10
20
30
40
50
60
70
Time (min)

stimulated guanylate cyclase activities were constant for at least 60 minutes.

The effects of various adenosine phosphates were also examined on magnesium-dependent guanylate cyclase activity. ADP and AMP, both at 1 mM, had no effect on the rate of cGMP production in either the absence or presence of 1 μM ANP (fig 4.11), although both 1 mM ATP and 1 mM AMP-PNP produced significant increases in basal and ANP-stimulated guanylate cyclase activities. The dose response curves for the effect of ATP on Mg^{2+}-dependent guanylate cyclase activity, both in the presence and absence of ANP, were biphasic (fig 4.12). Concentrations of ATP up to 1mM augmented both basal and ANP-stimulated guanylate cyclase activity with further increases in ATP resulting in a decline in activity under both conditions. A dose response curve was constructed for ANP stimulation of Mg^{2+}-dependent guanylate cyclase activity in the presence of 1mM ATP (fig 4.13). The Km for ANP under these conditions was 2.31 $\pm$ 0.36 nM with a Hill coefficient of 1.22 $\pm$ 0.28.

4.1.8 Guanylate Cyclase Activity in BAC Membranes

Basal and ANP-stimulated, Mn^{2+}-dependent, guanylate cyclase activity was measured in BAC membranes. In these membranes ANP produced a 2.7-fold increase in guanylate cyclase from 267 $\pm$ 39 for basal activity to 728 $\pm$ 54 pmol/min per mg protein for ANP-stimulated activity. The Km for ANP was 0.691 $\pm$ 0.161 nM and the Hill coefficient, of 0.754 $\pm$ 0.026 (fig. 4.14).

Figure 4.11

Effect of Adenosine Phosphates on Mg^{2+}- Dependent Guanylate Cyclase Activity

Rat cardiac sarcolemmal membranes were incubated for 20 min at 37°C, in the absence (□) or presence (▨) of 10^{-6} M ANP, and in the presence of 10^{-3} M adenosine phosphate as indicated. The values are the mean ± SEM of at least 3 separate experiments in which guanylate cyclase was measured in triplicate followed by duplicate determinations of cGMP. Significant differences are indicated by * = $p< 0.05$, ** = $p< 0.01$ and ** = $p< 0.001$ as determined by a two-tailed Student's *t*-test (paired solution).

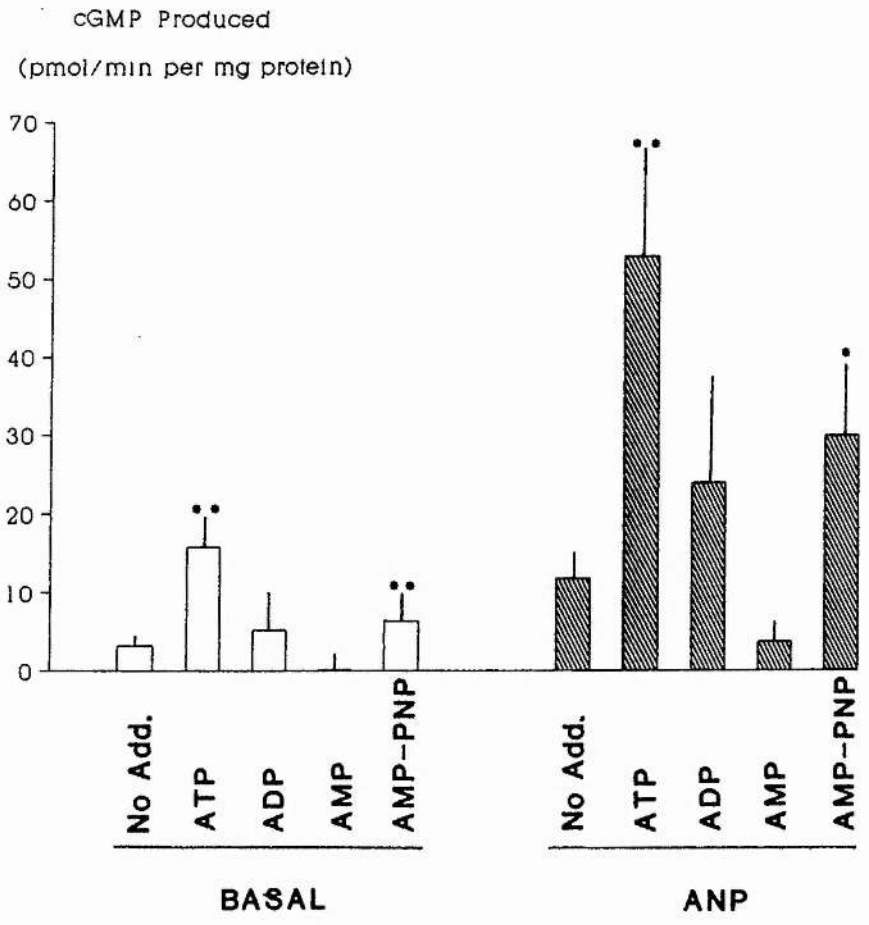

Figure 4.12

Dose Response Curve for the Effect of ATP on Mg^{2+}-Dependent Guanylate Cyclase Activity

Rat cardiac sarcolemmal membranes were incubated for 20 min at 37°C, with increasing concentrations of ATP, in the absence (△——△) or presence of 10^{-6} M ANP (□——□). Mg^{2+} was kept at a concentration 10^{-3} M in excess of the combined GTP and ATP concentrations. The results are the mean ± SEM of 3 separate experiments in which guanylate cyclase was measured in triplicate, followed by duplicate determinations of cGMP.

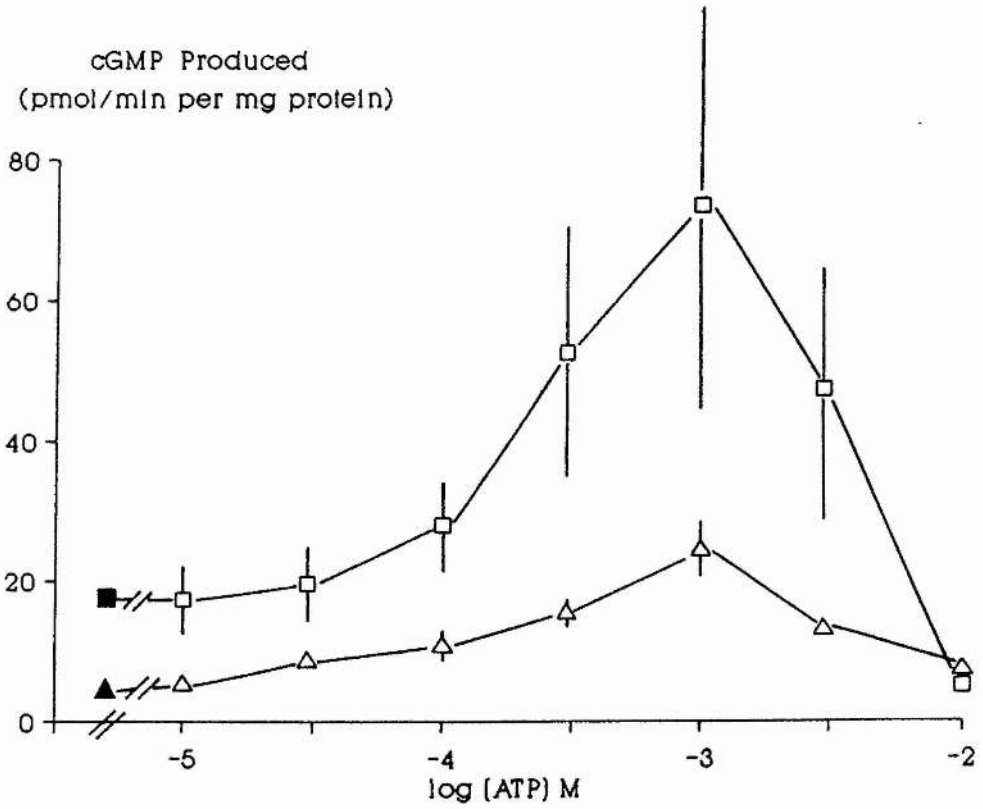

Figure 4.13

Dose Response Curve for ANP in the presence of ATP and Mg^{2+}

Rat cardiac sarcolemmal membranes were incubated for 20 min at 37°C, in the presence of 2mM Mg^{2+}, 1 mM ATP, and increasing concentrations of ANP. Each point is the mean ± SEM of triplicate determinations of guanylate cyclase activity which were assayed in duplicate for cGMP.

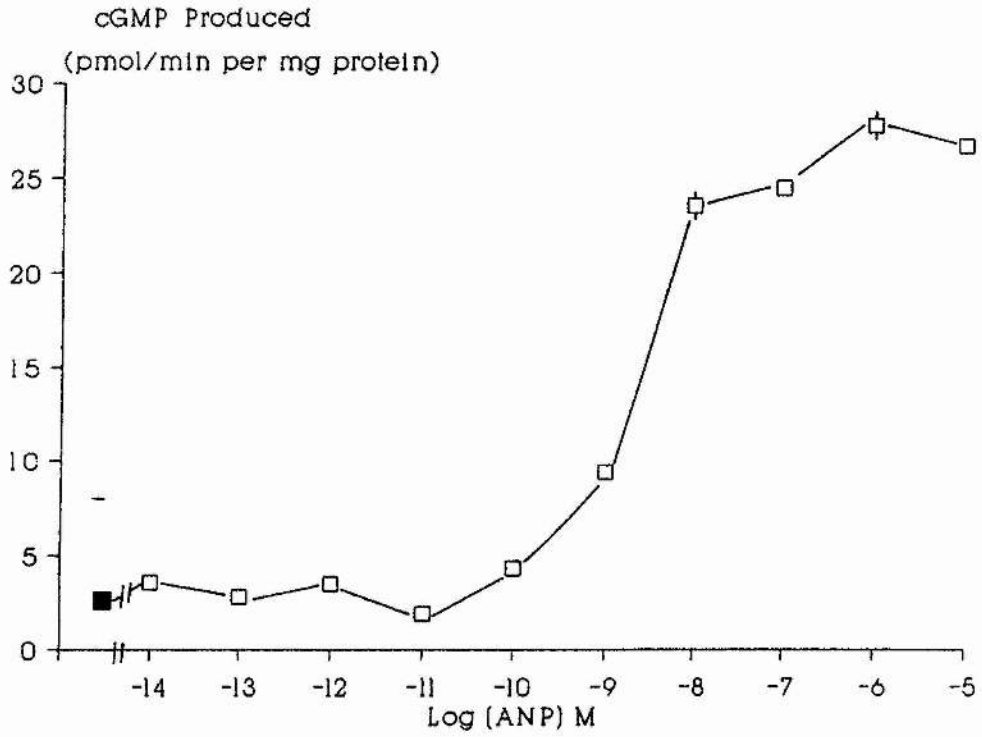

Figure 4.14

Dose Response Curve for ANP Stimulation of Guanylate Cyclase activity in BAC Membranes

A representive dose response curve for ANP stimulation of guanylate cyclase activity in BAC membranes, measured in the presence of $3x10^{-3}$ M Mn^{2+}. The results are the means $\pm$ SEM of triplicate determinations of guanylate cyclase activity in which cGMP was measured in duplicate.

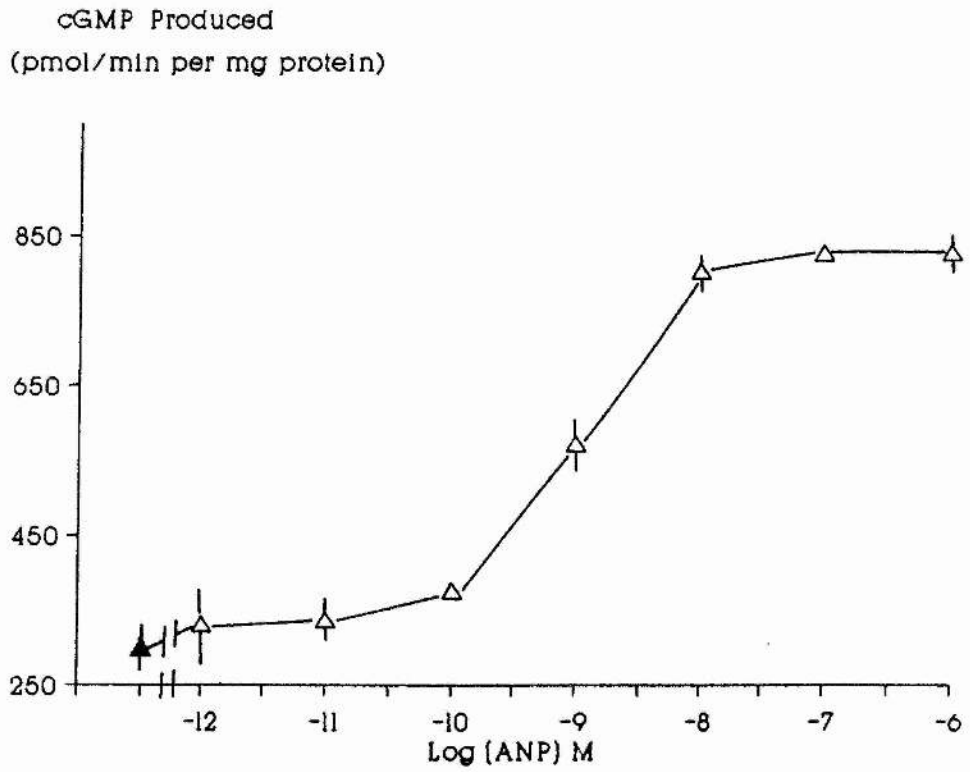

4.2 DISCUSSION

4.2.1 Guanylate Cyclase Activity in Rat Cardiac Sarcolemmal Membranes

These results demonstrate basal and ANP-stimulated guanylate cyclase activity in purified sarcolemmal membranes isolated from rat ventricular muscle. The findings are in agreement with previous reports, which have demonstrated basal guanylate cyclase activity in particulate fractions isolated from the heart ventricles of several species, including rat (Kimura & Murad, 1974; Sulakhe et al., 1976a), rabbit, hamster, guinea pig and mouse (Sulakhe et al., 1976a). The present results are also in agreement with previous studies demonstrating ANP-stimulated increases in intracellular cGMP levels in isolated rat and rabbit ventricular myocytes (Aiton & Cramb, 1985; Cramb et al., 1987).

In rat cardiac sarcolemmal membranes, Mn^{2+} supported 20- to 40-fold higher levels of both basal and ANP-stimulated guanylate cyclase activity than did Mg^{2+}. Similar differences in the levels of basal guanylate cyclase activity have been reported for rat liver plasma membranes (Kimura & Murad, 1975a), for a particulate fraction from rabbit heart ventricles (Sulakhe et al., 1976a), and for basal and ANP-stimulated guanylate cyclase activity in BAC membranes (Tremblay et al., 1986). The dose response curve for GTP, in the presence of excess of Mn^{2+}, indicated positive co-operativity and/or multiple binding sites, with the addition of ANP increasing the maximum velocity of the enzyme but having little effect on the K_m or the slope of the dose response curve. Similar kinetics have been described for basal particulate guanylate cyclase activity in the rat (Kimura & Murad, 1974) and rabbit (Sulakhe et al., 1976b) heart, and for basal

and ANP-stimulated activity in bovine adrenal cortex (Tremblay et al., 1986). Likewise, the Hill coefficient calculated from the stimulatory portion of the manganese dose response curves, both in the absence and presence of ANP, suggested that this cation was exerting positive co-operative effects. In contrast, Mn^{2+} concentrations in excess of 4 mM produced a marked reduction in guanylate cyclase activity. These results are in agreement with reports on the effects of Mn^{2+} ion concentration on basal guanylate cyclase activity in rat (Kimura & Murad 1974) and rabbit (Sulakhe et al., 1976a) heart membranes.

Differences in ANP-stimulated guanylate cyclase activity were observed between fraction A and fraction B. Both these fractions are enriched in membrane enzyme markers, but electron micrographs indicate that the membranes in fraction A have a tendency to 'stick together', forming liposomal-like structures (Cramb & Dow 1983). It is possible that whilst these structures do not affect basal guanylate cyclase activity, they do limit the access of ANP to its receptor, and hence reduce ANP-stimulated activity.

Half-maximal stimulation of guanylate cyclase activity was produced by 1 nM ANP. Similar concentrations of ANP have been reported to produce half-maximal stimulation of guanylate cyclase activity in BAC membranes (Tremblay et al., 1986), and to produce half-maximal elevation of intracellular cGMP levels in cortical collecting tubules (Naray-Fejes-Toth et al., 1988) and LLC-PK_1 cells (Inui et al., 1985). The dose response curve for ANP stimulation of guanylate cyclase activity was shallow in nature, with a Hill coefficient of less than 1, indicating negative co-operativity.

There have been a number of reports documenting the ability of various

truncated analogues of ANP to relax preconstricted smooth muscle, and in all cases ANP_{5-28} was less potent that ANP (Thibault et al., 1984b; Garcia et al., 1985; Olins et al., 1986). Physiological studies have shown that ANP_{5-28} is effective at producing natriuresis and diuresis in rat but not in dog, indicating species variation in the response to these two peptides (Wakitani et al., 1985). This is supported by the observation that while ANP_{5-28} is 10-fold less potent than ANP at producing a half-maximal increase in intracellular cGMP in rat and human cell lines, it is 1000-fold less potent in bovine and canine cells (Leitman & Murad, 1986). In the present experiments, the concentrations of ANP and ANP_{5-28} required to produce half-maximal stimulation of guanylate cyclase activity in rat cardiac sarcolemmal membranes were not significantly different. There was however a significant difference between the maximum responses elicited by these two peptides, with ANP_{5-28} producing less than 50% of the response produced by ANP.

In agreement with a previous report on the effect of ANP_{5-25} on guanylate cyclase activity, this peptide was more than 1000-fold weaker than ANP in stimulating guanylate cyclase activity in rat cardiac sarcolemmal membranes (Leitman & Murad 1986).

4.2.2 Degradation of ANP

Endopeptidase 24.11 has been implicated in the breakdown of ANP by pig kidney membranes (Stephenson & Kenny, 1987a). Phosphoramidon, a specific inhibitor of this peptidase, had no effect on the kinetics of the ANP dose response curves.

Of the other protease inhibitors tested, only the serine protease

inhibitors, PMSF and aprotinin, had any effect on guanylate cyclase activity. Both these compounds produced a small decrease in ANP-stimulated activity. It has previously been shown that treatment of rat liver plasma membranes with various proteases, including several serine proteases, results in an increase of guanylate cyclase activity (Lancombe & Hanoune, 1979). This increase in activity appears to be due to the direct action of the protease on guanylate cyclase, as stimulation occurs even after solubilization of the enzyme. The decrease in activity observed in the presence of PMSF and aprotinin in rat cardiac sarcolemmal membranes (fig. 4.7) raises the possibility that proteolysis is involved in the regulation of ANP-stimulated guanylate cyclase activity in this preparation.

4.2.3 Effect of Adenosine Phosphates

ATP has previously been shown to decrease Mn^{2+}-dependent guanylate cyclase activity in rat and rabbit heart membranes (Kimura & Murad 1974; Sulakhe et al., 1976b). The results reported here support these findings and show that similar decreases in guanylate cyclase activity are observed in purified rat cardiac sarcolemmal membranes, both in the presence and absence of ANP. The effect of ATP on Mg^{2+}-dependent guanylate cyclase activity is more complicated, producing biphasic dose response curves. 1mM ATP, a concentration similar to that found inside the cell, produces a marked stimulation of guanylate cyclase activity. Similar observations have been reported for basal and ANP-stimulated guanylate cyclase activities in rat liver membranes (Kurose et al., 1987). It is likely that the attenuation of guanylate cyclase activity observed at high concentrations of ATP is a result of the direct competition between ATP and GTP, whereas the augmentation

of Mg^{2+}-dependent guanylate cyclase, observed with lower ATP levels, suggests a possible allosteric role for nucleotide. This is supported by the observation that 1 mM AMP-PNP, a non-hydrolysable analogue of ATP, also increases Mg^{2+}-dependent guanylate cyclase. Interestingly, the dose response curve for ANP measured in the presence of magnesium and ATP displays normal Michaelis Menten kinetics, with a Hill coefficient of 1. It is not known if this is a result of magnesium, ATP, or a combination of the two, since ANP dose response curves for Mg^{2+}-dependent guanylate cyclase in the absence of ATP have not been determined.

Further evidence in support of an allosteric role for ATP comes from the measurement of Mn^{2+}-dependent guanylate cyclase activity over an extended time-course. Although 1 mM ATP produces a small decrease Mn^{2+}-dependent guanylate cyclase activity, the rate of cGMP production is maintained for at least 60 min, whereas in the absence of ATP, the cGMP production decreases after about 30 min. This effect is observed both in the presence and absence of ANP, suggesting that modulation of cGMP production by ATP is occurring through the guanylate cyclase entity, rather than through the ANP receptor.

4.2.4 Guanylate Cyclase Activity in BAC Membranes

Guanylate cyclase activity was measured in purified membranes from bovine adrenal cortex (BAC) and compared to that in the cardiac sarcolemmal membrane preparation. The concentration of ANP required to produce half-maximal stimulation in BAC membranes was the same as for heart membranes, and similar to that previously reported for BAC membranes (Tremblay *et al.*, 1986). The dose response curves for ANP were significantly steeper than those observed with rat cardiac

sarcolemmal membranes, suggesting that the kinetics of cGMP production by BAC membranes are closer to normal Michaelis-Menten kinetics than are those observed with the cardiac preparation. BAC membranes were stored in buffer containing 5 mM Mg^{2+}, whereas the cardiac membranes were stored in the absence any divalent cation. Although after dilution the concentration of Mg^{2+} in the guanylate cyclase assay was less than 0.1mM, this may have been high enough to modulate guanylate cyclase activity.

4.3 Summary

These results are consistent with earlier reports indicating basal guanylate cyclase activity in rat cardiac sarcolemmal membranes, and provide evidence of ANP-stimulated guanylate cyclase activity in the same preparation. In addition, these results support the hypothesis that ATP modulates both basal and ANP-stimulated guanylate cyclase activity.

CHAPTER 5

5 Results of Receptor-Binding Experiments

5.1. Binding to Rat Cardiac Sarcolemmal Membranes

Incubation of [^{125}I]-ANP with rat cardiac sarcolemmal membranes at 37^{o}C resulted in a time-dependent increase in radioactivity (fig 5.1). Specific binding, defined as that binding not displaced by 10^{-6}M ANP, reached a steady state within 40 min, with a $t_{1/2}$ of 10 min. The displacement of [^{125}I]-ANP by unlabelled ANP was measured in a number of separate preparations (fig 5.2), and the concentrations of ANP required to produce a 50% inhibition of binding (IC_{50}) were determined by indirect Hill plots. The potency of ANP displacement of [^{125}I]-ANP varied 130-fold, ranging from 1.65×10^{-10} M to 2.17×10^{-8} M, with a mean of $5.16 \pm 3.38 \times 10^{-9}$M. The Hill coefficients ranged from -0.130 to -0.504 (table 5.1), indicating the presence of complex binding phenomena or technical artifacts. The [^{125}I]-ANP displaced was expressed as a percentage of the total [^{125}I]-ANP present in the incubation and the results of the individual experiments combined (fig 5.3a). Scatchard analysis of these data resulted in a biphasic plot, which could be resolved into two straight lines (fig. 5.3b). The estimates of the IC_{50} for ANP were 1.41×10^{-12} M and 9.25×10^{-9} M, for the high and low affinity binding sites respectively. Since analysis of the data by Hill plots and Scatchard plots suggested the presence of two ANP binding sites in the cardiac sarcolemmal membrane preparation, the results of the individual dose response curves were analysed using Enzfit (ligand-binding two-site solution; see appendix III). IC_{50} values for the low affinity site were in good agreement with those obtained by Hill and Scatchard plots, ranging from $1.14 \times$

Figure 5.1

Time Course for the Binding of [^{125}I]-ANP to Rat Cardiac Sarcolemmal Membranes

[^{125}I]-ANP (100pM) was incubated with rat cardiac sarcolemmal membranes (11.3 µg protein/ml) at 37°C, in the absence △——△ (Total) and presence □——□ (NSB) of 10^{-6}M ANP. At the times indicated, 200µl aliquots were removed and filtered through Whatman GF/F filters as described in the materials and methods. The specific binding (✳——✳) was calculated by subtracting the NSB from the total binding. Each point represents duplicate determinations from a single preparation.

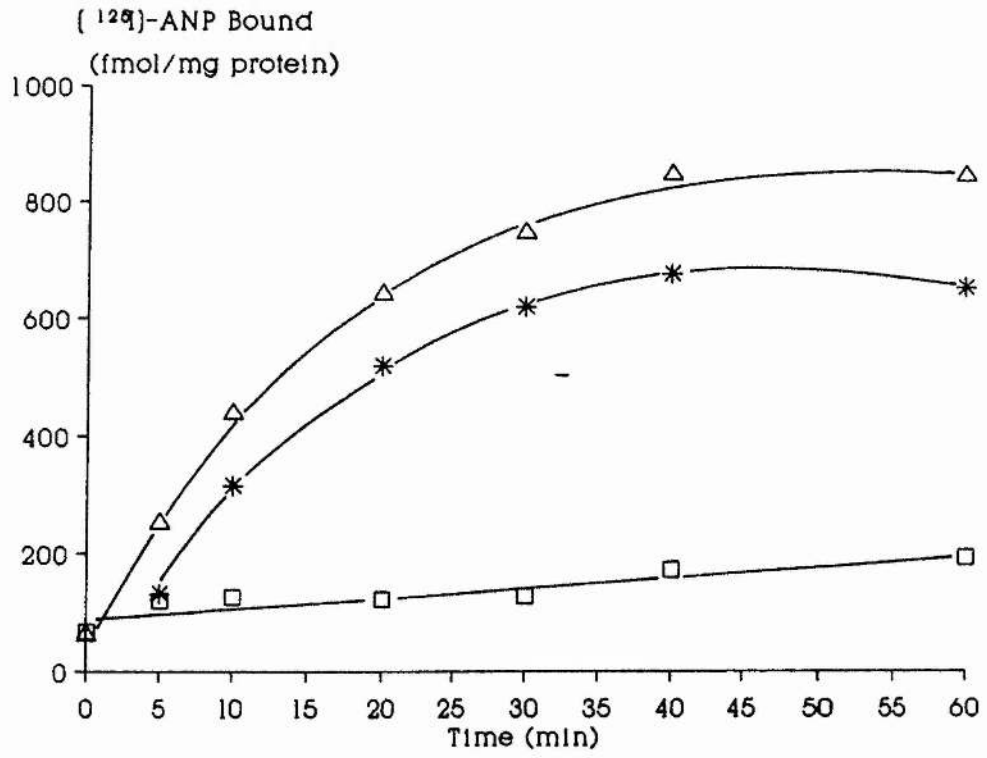

Figure 5.2

Inhibition of [^{125}I]-ANP binding in Rat Cardiac Sarcolemmal Membranes by ANP

Dose response curves for ANP displacement of [^{125}I]-ANP binding to rat cardiac sarcolemmal membranes (2 to 15 µg protein/ml). The results shown are for individual experiments performed on separate membrane preparations, in the presence of [^{125}I]-ANP at (a) 81.6 pM, (b) 88.6 pM, (c) 60.6 pM, (d) 90.0 pM, (e) 70.9 pM, and (f) 43.3 pM. Each point is the mean of at least 2 determinations which varied by less than 10%

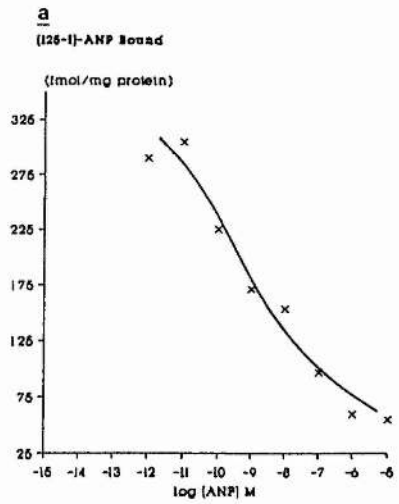
a
[125-I]-ANP Bound
(fmol/mg protein)
325
275
225
175
125
75
25
-15 -14 -13 -12 -11 -10 -9 -8 -7 -6 -5
log [ANP] M

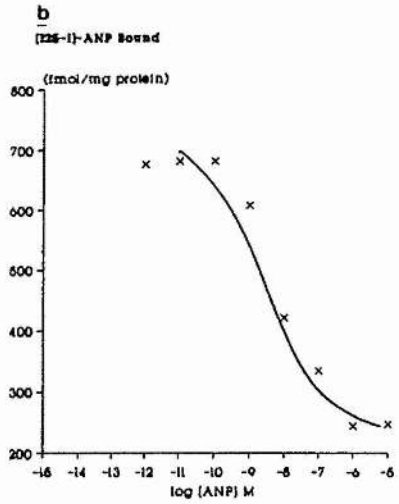
b
[125-I]-ANP Bound
(fmol/mg protein)
800
700
600
500
400
300
200
-15 -14 -13 -12 -11 -10 -9 -8 -7 -6 -5
log [ANP] M

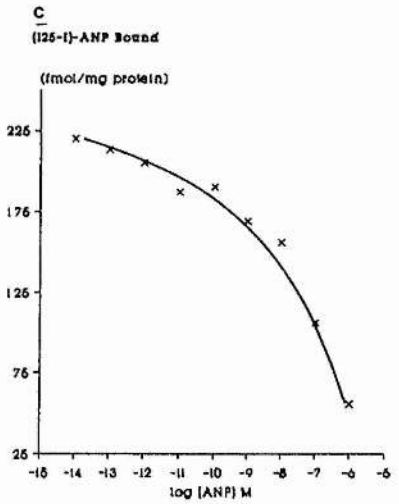
c
[125-I]-ANP Bound
(fmol/mg protein)
225
175
125
75
25
-15 -14 -13 -12 -11 -10 -9 -8 -7 -6 -5
log [ANP] M

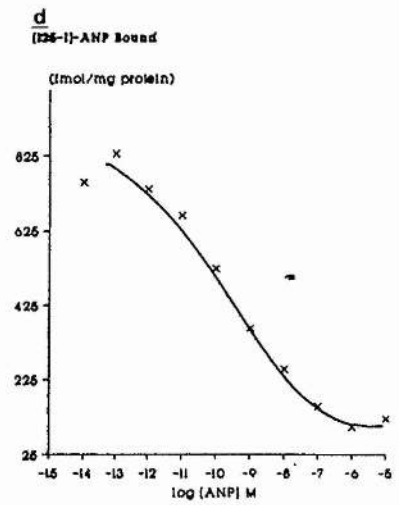
d
[125-I]-ANP Bound
(fmol/mg protein)
825
625
425
225
25
-15 -14 -13 -12 -11 -10 -9 -8 -7 -6 -5
log [ANP] M

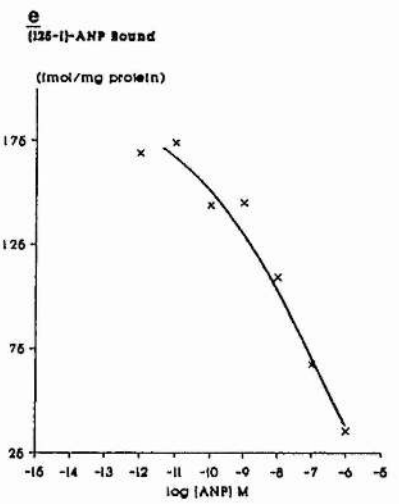
e
[125-I]-ANP Bound
(fmol/mg protein)
175
125
75
25
-15 -14 -13 -12 -11 -10 -9 -8 -7 -6 -5
log [ANP] M

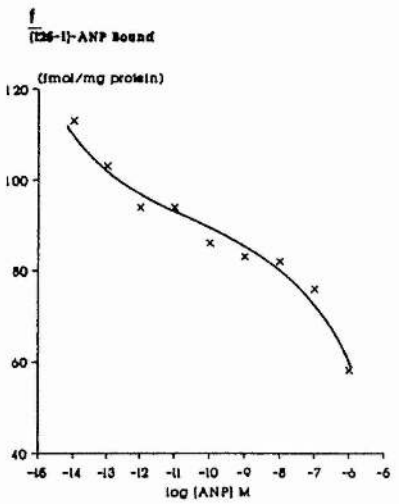
f
[125-I]-ANP Bound
(fmol/mg protein)
120
100
80
60
40
-15 -14 -13 -12 -11 -10 -9 -8 -7 -6 -5
log [ANP] M

Table 5.1

Results of Hill Plots of the ANP Displacement Curves

Expt. No.	Slope	Corr. Coeff.	IC_{50} (pM)	$[^{125}I]$-ANP (pM)
1	-0.130	-0.971	165	43.29
2	-0.287	-0.962	21700	60.6
3	-0.367	-0.967	5047	70.93
4	-0.416	-0.986	1752	81.6
5*	-0.420	-0.990	1648	88.6
6	-0.504	-0.996	628	90.9

* Membranes were prepared in the absence of DTT.

Figure 5.3

Mean Dose Response Curve for ANP Displacement of [^{125}I]-ANP from Rat Cardiac Sarcolemmal Membranes

(a) The results of experiments shown in fig. 5.2 were corrected for NSB, and expressed as the percentage inhibition of [^{125}I]-ANP binding. Each point represents the mean $\pm$ S.E.M. (b) A Scatchard plot of the data from (a).

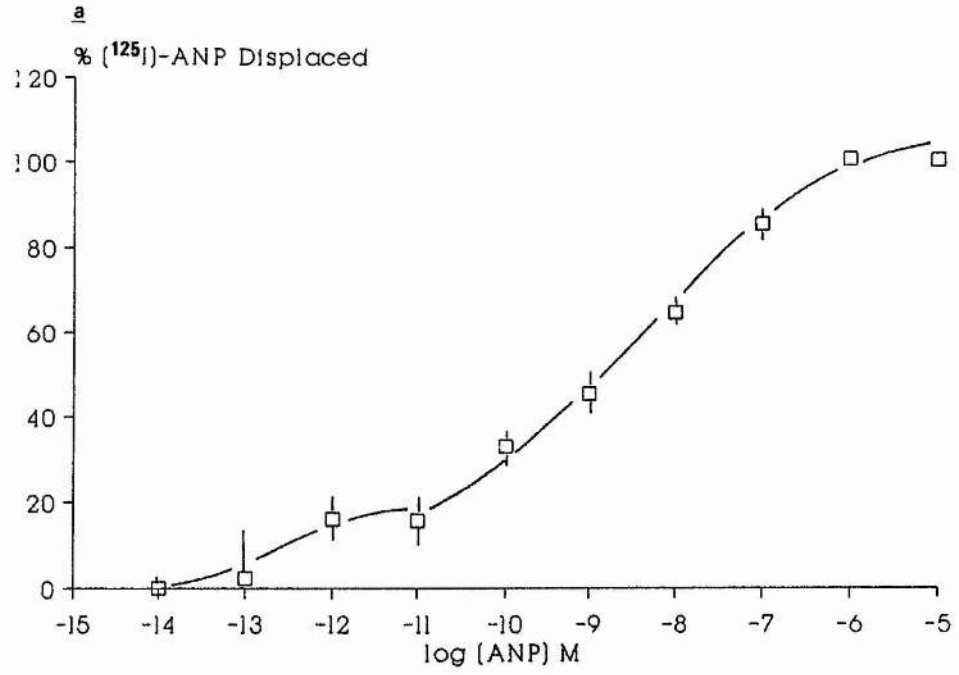
a
% [125I]-ANP Displaced
120
100
80
60
40
20
0
-15
-14
-13
-12
-11
-10
-9
-8
-7
-6
-5
log [ANP] M

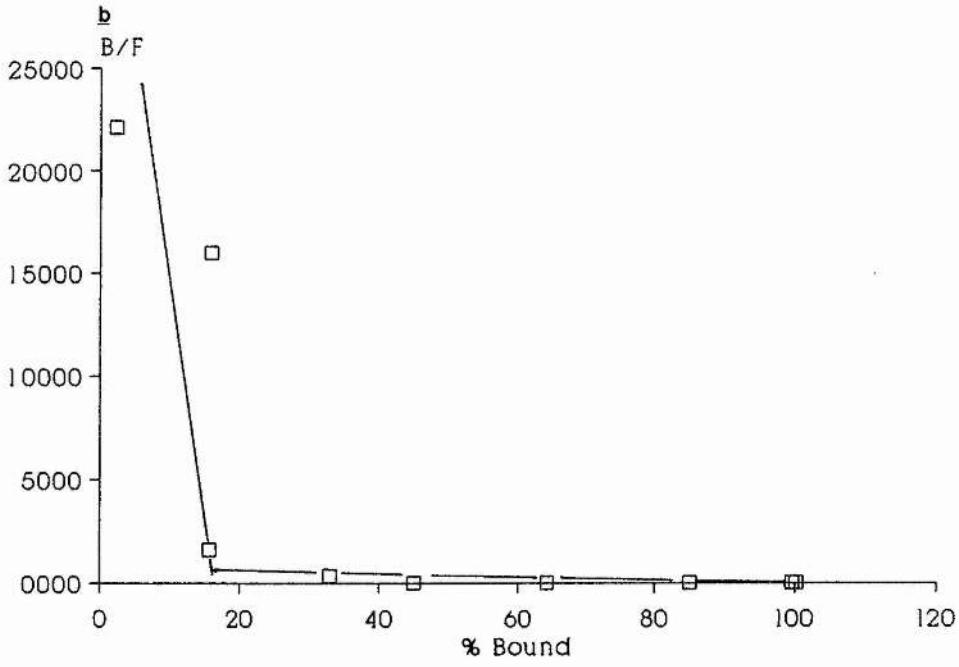
b
B/F
25000
20000
15000
10000
5000
0000
0
20
40
60
80
100
120
% Bound

10^{-10} M to 1.61 x 10^{-8} M with a mean of 3.93 + 2.50 x10^{-9} M. High affinity binding sites could not be detected in two of the dose response curves, and in the rest the estimates for these sites varied 280-fold, ranging from 5.96 x 10^{-14} M to 1.67 x 10^{-11} M, with a mean of 6.11 + 3.90 x 10-^{12} M (table 5.2). The mean of these results was of a similar magnitude to that determined by Scatchard analysis.

The failure to detect high affinity binding sites in two of the experiments may have been related to the concentration of [^{125}I]-ANP present in the incubation. A plot of total [^{125}I]-ANP concentration against the amount of [^{125}I]-ANP displaced by 1 pM ANP yields a straight line, indicative of a negative relationship between the two variables (fig 5.4). The only exception to this general finding were data obtained from sarcolemmal membranes which had been prepared in the absence of dithiotheritol (DTT). Extrapolation of the line illustrated in fig. 5.4 indicates that at a concentration of 30 pM [^{125}I]-ANP, 50% of the radioactivity can be displaced by 1pM ANP. This result is not consistent with ANP and [^{125}I]-ANP possessing the same affinity for the binding site.

To assess the affinity and total number of [^{125}I]-ANP binding sites in purified rat sarcolemmal membranes a saturation binding curve was constructed (fig. 5.5a). Although the maximum concentration of [^{125}I]-ANP (700 pM) was not enough to saturate all the binding sites, a Scatchard plot of the data indicated the presence of two or more affinity states/binding sites in this preparation (fig 5.5b). The K_D's were estimated as 5.59 pM and 0.98 nM, and the B_{max} values were 10.55 and 980 fmol/mg protein, for the high and low affinity sites respectively. Analysis of the data by Enzfit, (ligand binding two-site

Table 5.2

Results of Enzfit Analysis of ANP Displacement Curves

The K_D for ANP were determined using the Cheng Prusoff equation. The dissociation constants for [^{125}I]-ANP were 10.9 pM and 1.23 nM for the high and low affinity sites respectively.

Expt.	Site I (pM)		Site II(nM)		^{125}I]-ANP
No.	IC_{50}	K_D	IC_{50}	K_D	(pM)
1	0.060	0.012	0.114	0.110	43.3
2	0.410	0.063	2.630	2.51	60.6
3	16.7	2.130	16.10	15.2	70.9
4	7.27	0.857	0.904	0.848	81.6
5*	-	-	3.730	3.48	88.6
6	-	-	0.131	0.122	90.9
Mean	6.11	0.765	3.930	3.66	
± S.E.M	± 3.9	± 0.494	± 2.500	± 2.40	

* Membranes were prepared in the absence of DTT

Figure 5.4

Relationship Between Radioactivity Displaced and Concentration of [^{125}I]-ANP

A comparison of the percentage radioactivity displaced by 10^{-12} M ANP, and the total concentration of [^{125}I]-ANP. The data are the individual values from fig. 5.3. Membranes were prepared in the presence (□) or absence (*) of DTT.

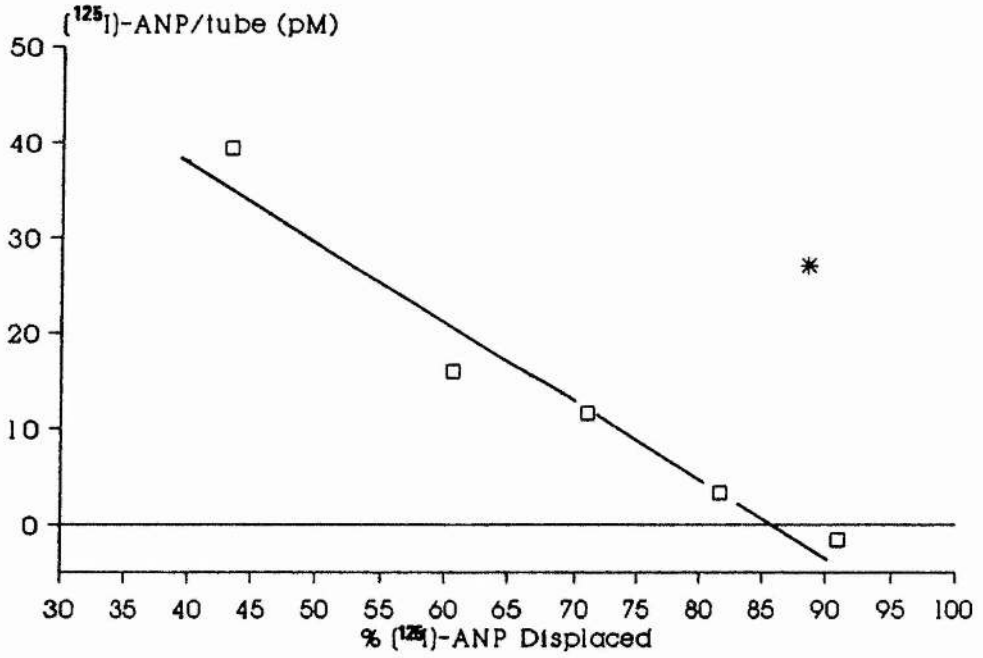

Figure 5.5

Saturation Curve for [^{125}I]-ANP Binding to Rat Cardiac Sarcolemmal Membranes

(a) Rat cardiac sarcolemmal membranes were incubated for 40 min at 37^{o}C, with increasing concentrations of [^{125}I]-ANP in the absence △—△(total binding) and presence □—□(NSB) of 10^{-6}M ANP. Specific binding, ∗—∗, is the total binding minus the NSB. The results are the mean ± S.E.M. for triplicate determinations from a single membrane preparation. (b) Scatchard plot of the data shown in (a)

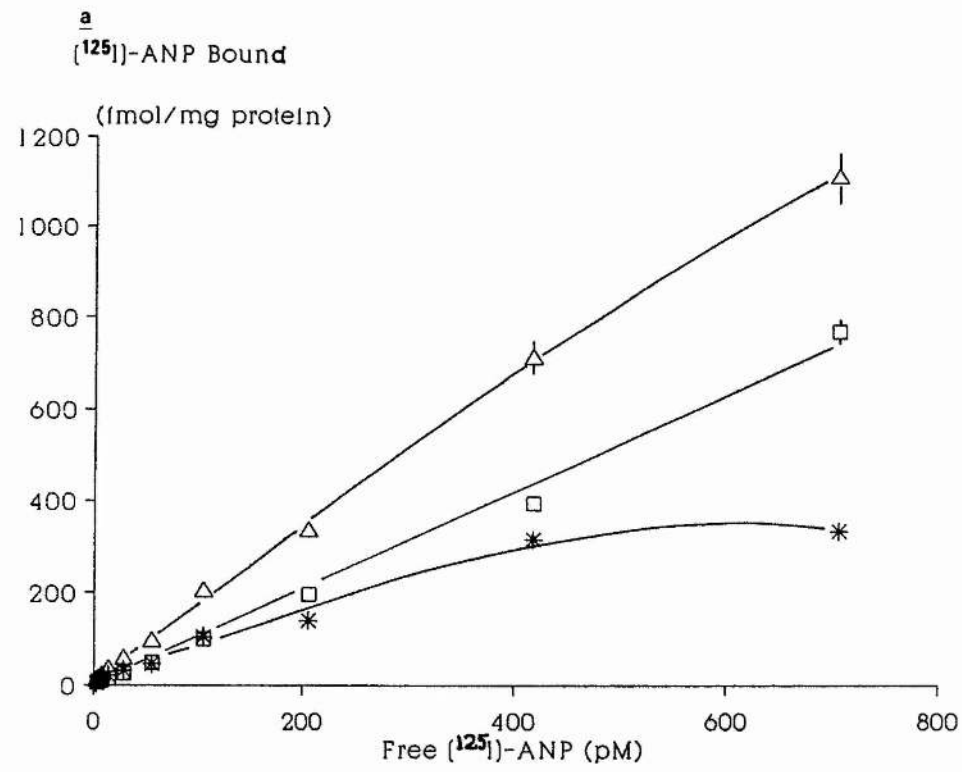
a
[125I]-ANP Bound
(fmol/mg protein)
1200
1000
800
600
400
200
0
0
200
400
600
800
Free [125I]-ANP (pM)

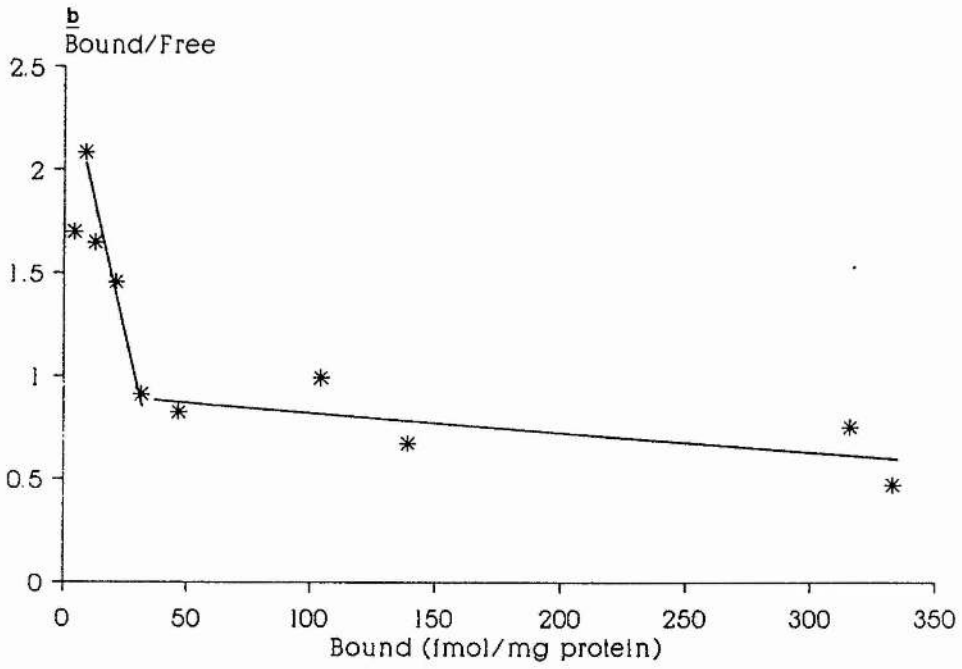
b
Bound/Free
2.5
2
1.5
1
0.5
0
0
50
100
150
200
250
300
350
Bound (fmol/mg protein)

solution) gave similar results, with a K_D of 10.9 pM and a B_{max} 15.3 fmols/mg protein for the high affinity site, and a K_D of 1.23 nM and B_{max} of 944 fmols/mg protein for the low affinity site. These results are very close to the IC_{50} values obtained from ANP displacement curves.

The possibility that degradation of [^{125}I]-ANP was responsible for the complex binding curves was examined. Endopeptidase 24.11 has been shown to degrade [^{125}I]-ANP in pig kidney membranes (Stephenson & Kenny 1987a). Therefore ANP displacement curves were constructed in the presence and absence of 10 μM phosphoramidon, a specific inhibitor of this enzyme. Phosphoramidon had no effect on the displacement of [^{125}I]-ANP by unlabelled ANP (fig. 5.6).

To exclude the possibility that degradation by unspecified peptidases was occurring, and to confirm the results of the previous experiment, HPLC analysis was performed on the samples. Membranes were incubated with [^{125}I]-ANP for 40 min at 37^{o}C, in the presence and absence of unlabelled ANP (1 μM) and phosphoramidon (10 μM). After 40 min the samples were extracted on Sep-Pak C_{18} cartridges and analysed by reverse phase HPLC. The profiles of the recovered radioactivity were compared with those obtained from [^{125}I]-ANP standards which had either been extracted or applied directly to the HPLC column. The distribution of radioactivity in the standards was the same whether or not they had been extracted, with more than 90% of the radioactivity eluting in a single peak at 51.23% ACN (figs. 5.7a and 5.7b). Following incubation of the radioligand with sarcolemmal membranes in the absence of unlabelled ANP, the amount of radioactivity recovered was reduced to 75%, with two small peaks of radioactivity eluting at

Figure 5.6

The effect of Phosphoramidon on [^{125}I]-ANP Binding to Rat Cardiac Sarcolemmal Membranes

[^{125}I]-ANP was incubated with rat cardiac sarcolemmal membranes for 40 min at 37^{o}C, in the presence of ANP at the concentration indicated. The results are expressed as the percentage of [^{125}I]-ANP bound in the presence of 10^{-5} M phosphoramidon compared with that bound in its absence. Values are the means $\pm$ the S.E.M. from 3 separate membrane preparations.

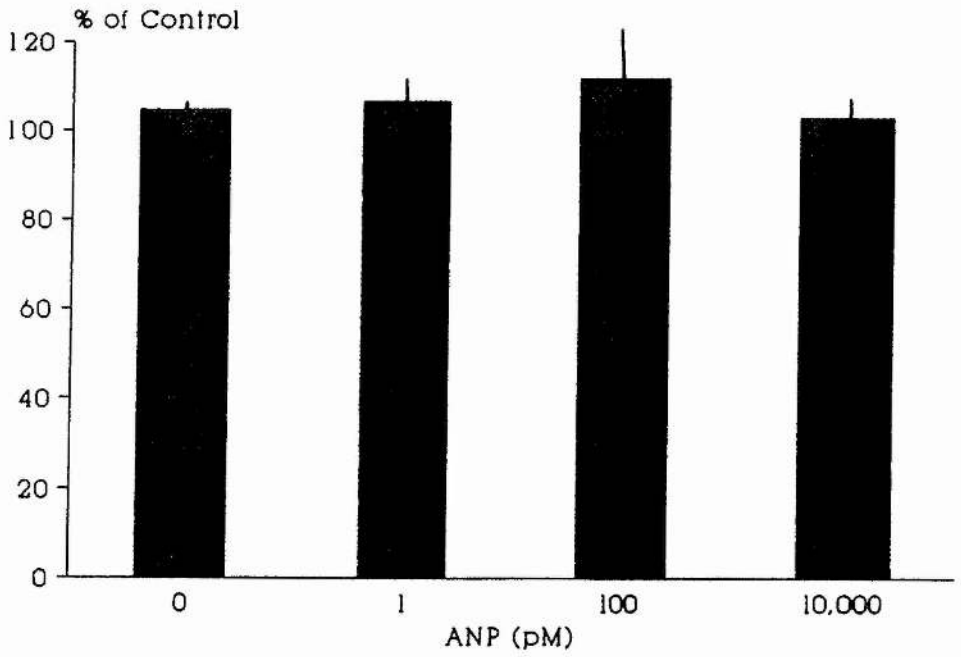

Figure 5.7

HPLC Analysis of [^{125}I]-ANP

Profile of the distribution of radioactivity following reverse phase HPLC analysis of [^{125}I]-ANP. (a) standard; (b) extracted standard. [^{125}I]-ANP incubated with cardiac sarcolemmal membranes for 40 min at 37^{o}C, (c) in the absence, and (d) in the presence of 10^{-6} M ANP, or (e) 10^{-5} M phosphoramidon, or (f) 10^{-6} M ANP and 10^{-5} M phosphoramidon. Arrows indicate, (1) the position of native [^{125}I]-ANP, and (2) and (3), the positions of radiolabelled breakdown products.

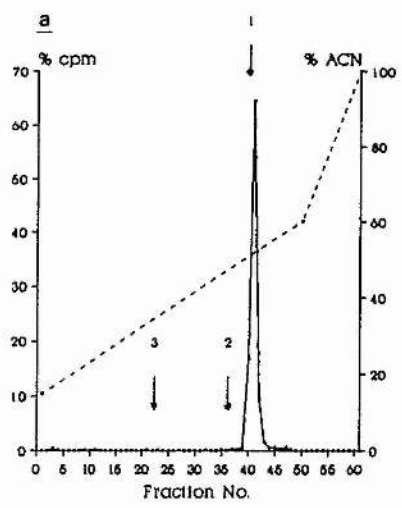
a
% cpm
% ACN
Fraction No.

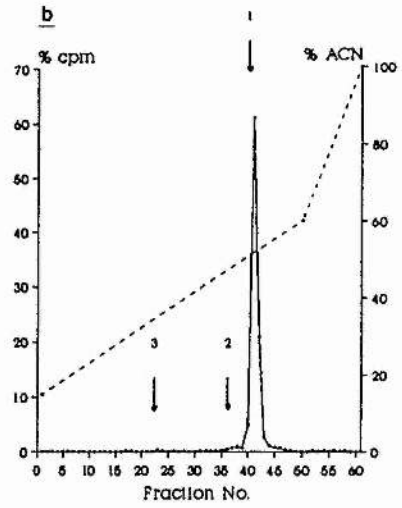
b
% cpm
% ACN
Fraction No.

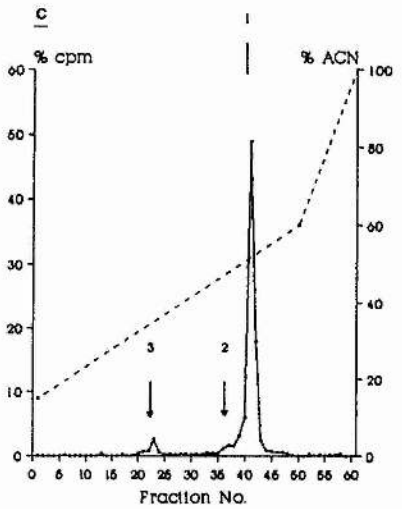
c
% cpm
% ACN
Fraction No.

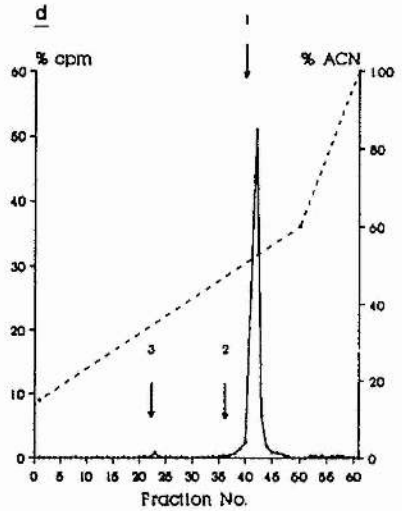
d
% cpm
% ACN
Fraction No.

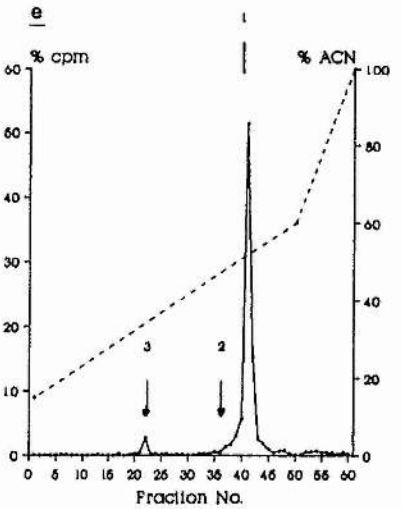
e
% cpm
% ACN
Fraction No.

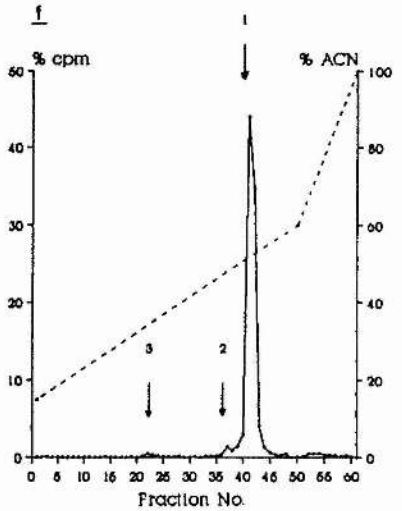
f
% cpm
% ACN
Fraction No.

48.9% and 34.4% ACN (fig. 5.7c). The addition of 1 μM ANP increased the radioactivity in the major peak to 85% of the total counts, with a corresponding reduction in the two smaller peaks (fig. 5.7d). The inclusion of phosphoramidon in the incubation had no effect on the amount or distribution of the radioactivity recovered (figs. 5.7e and 5.7f and table 5.3).

5.1.2. [^{125}I]-ANP Binding to Membranes Isolated from Bovine Adrenal Cortex

The incubation of [^{125}I]-ANP with membranes isolated from bovine adrenal cortex resulted in a time-dependent increase in radioactivity with a $t_{1/2}$ for specific binding of 5.3 min at 20°C (fig. 5.8). The effect of increasing concentrations of [^{125}I]-ANP was examined in these membranes (fig. 5.9a). As with binding to cardiac sarcolemmal membranes, the highest concentration of [^{125}I]-ANP available was not enough to fully saturate the binding sites. Nonetheless, a Scatchard plot of the data indicated the presence of two binding sites (fig. 5.9b), with K_D of 11.3 pM and 0.972 nM, and B_{MAX} of 8.59 fmol/mg protein and 2.32 pmol/mg protein, for the high and low affinity sites respectively. The data were also analysed by Enzfitter (ligand binding, two-site solution). The K_D's were estimated as 26.1 pM and 1.78 nM, with B_{MAX} of 25.1 fmol/mg protein and 3.56 pmol/mg protein for the high and low affinity sites respectively.

5.1.3 [^{125}I]-ANP Binding to Membranes Isolated from MDCK cells

Experiments were carried out on crude membranes isolated from two strains of MDCK cells (Madin Darby canine kidney cells). The

Table 5.3

Distribution of Radioactivity Following the Incubation of [^{125}I]-ANP with Cardiac Sarcolemmal Membranes

The distribution of radioactivity following the incubation of [^{125}I]-ANP with purified rat cardiac sarcolemmal membranes. The results are expressed as a percentage of the total radioactivity recovered from the HPLC. See text for details of extracted (Ex.) and non-extracted (Non-Ex.) standards.

	Control		Phosphoramidon			
	Buffer	ANP	Buffer	ANP	Standards	
% ACN		10^{-6}M		10^{-6}M	Ex.	Non-Ex.
34.3	5.30	1.57	4.40	1.20	0.48	0.34
48.8	4.40	2.39	4.34	2.16	1.36	0.96
51.2	75.4	85.7	77.3	85.5	89.4	89.3
Total	85.1	89.7	86.0	88.9	91.26	89.3

Figure 5.8

Time Course for the Binding of [^{125}I]-ANP to BAC Membranes

[^{125}I]-ANP (100pM) was incubated with BAC membranes (118 μg protein/ml) at 37^{o}C, in the absence △——△(Total) and presence □——□(NSB) of 10^{-6}M ANP. The specific binding (*——*) was calculated by subtracting the NSB from the total binding. Each point represents duplicate determinations from a single preparation.

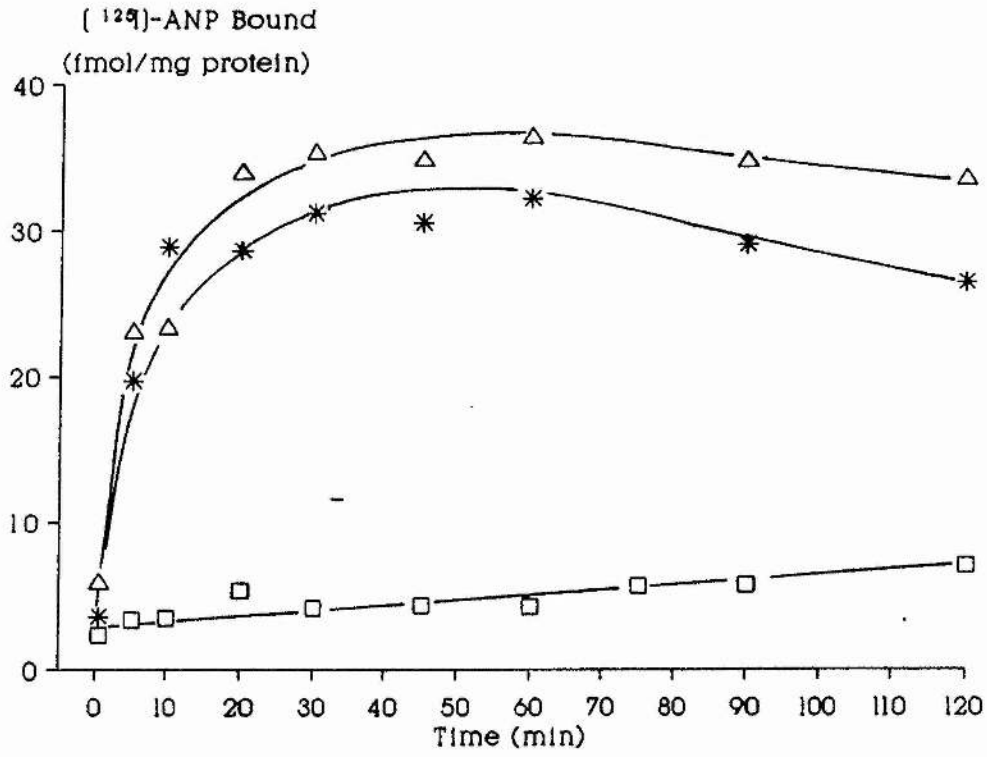

Figure 5.9

Saturation Curve for [^{125}I]-ANP Binding to BAC Membranes

(a) BAC membranes were incubated for 40 min at 37^{o}C, with increasing concentrations of [^{125}I]-ANP in the absence △—△(total binding) and presence □—□(NSB) of 10^{-6}M ANP. Specific binding, ✱—✱, is the total binding minus the NSB. The results are the mean ± S.E.M. for triplicate determinations from a single membrane preparation.

(b) Scatchard plot of the data shown in (a)

a

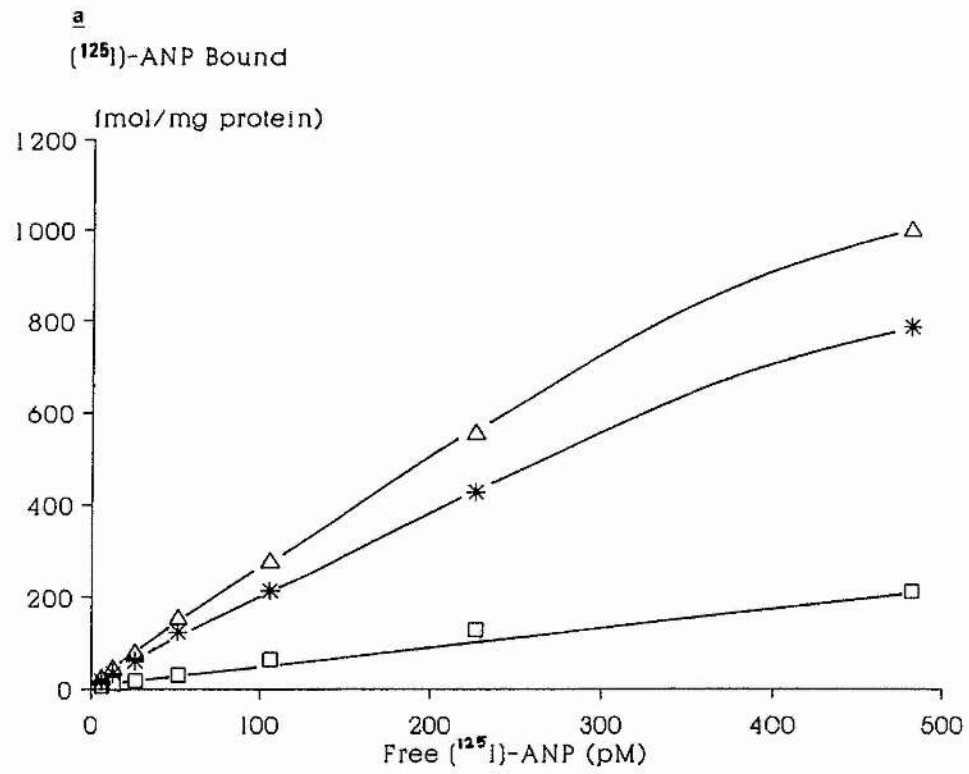
([125]I)-ANP Bound
(fmol/mg protein)
1200
1000
800
600
400
200
0
0
100
200
300
400
500
Free ([125]I)-ANP (pM)

b

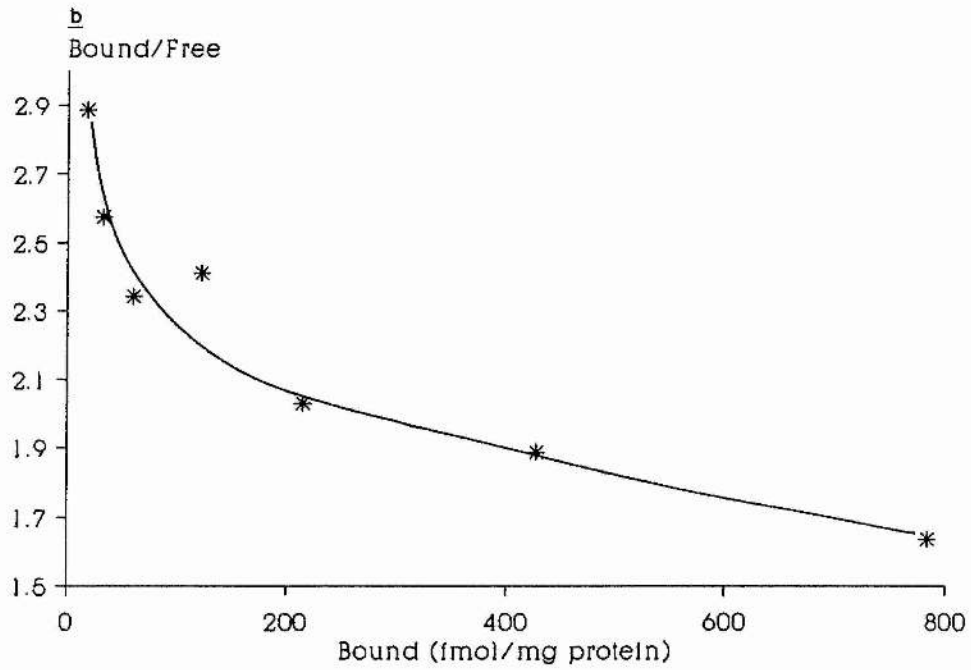
Bound/Free
2.9
2.7
2.5
2.3
2.1
1.9
1.7
1.5
0
200
400
600
800
Bound (fmol/mg protein)

association of [^{125}I]-ANP to crude membranes prepared from MDCK cells (strain I) was time-dependent, with a $t_{1/2}$ of 14.58 $\pm$ 2.75 min at 20^{o}C min (fig. 5.10). A saturation curve for [^{125}I]-ANP binding to these membranes was constructed, and Scatchard analysis of this curve indicated a single population of high affinity binding sites (fig 5.11). Further analysis of the data using Enzfit, (ligand binding one-site solution) gave a K_D of 41.3 pM and a B_{max} of 339 fmol/mg protein. Dose response curves were constructed for the displacement of [^{125}I]-ANP by unlabelled ANP (fig. 5.12). The [^{125}I]-ANP displaced was expressed a percentage of the total [^{125}I]-ANP present in the incubation and the results of the individual experiments combined (fig. 5.13). Scatchard analysis of the results again indicated a single class of binding sites with an IC_{50} of 30.5 pM (fig. 5.13b). Analysis the data from the individual dose response curves by Enzfitter (ligand binding one-site solution) yielded an IC_{50} 15.5 $\pm$ 1.8 pM. When the IC_{50} was corrected for the amount of [^{125}I]-ANP present in the incubation (Cheng & Prusoff, 1973; see appendix III), a K_D of 8.18 pM was obtained for ANP. However, Hill plots (indirect) of the same data had slopes ranging from -0.397 to -1.302, suggesting the presence of more complex interactions in these experiments (table 5.4).

Similar displacement experiments were performed on membranes prepared from strain II MDCK cells. No specific binding of [^{125}-I]-ANP could be demonstrated with these membranes (fig. 5.14).

Figure 5.10

Time Course for the Binding of [^{125}I]-ANP to MDCK (strain I) Membranes

[^{125}I]-ANP (30 pM) was incubated with MDCK (strain 1) membranes (34 µg protein/ml) at 37°C, in the absence △——△(Total) and presence □——□(NSB) of 1 µM ANP. The specific binding (*——*) was calculated by subtracting the NSB from the total binding. Each point represents duplicate determinations from a single preparation.

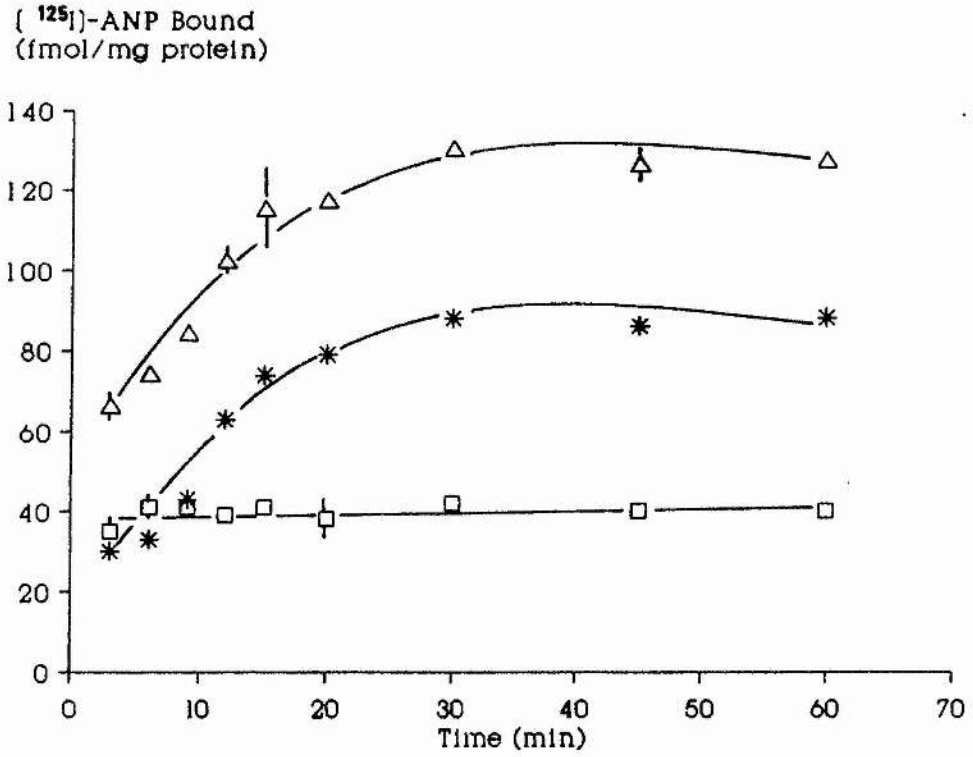

Figure 5.11

Saturation Curve for [^{125}I]-ANP Binding to MDCK (Strain I) Membranes

MDCK (strain I) membranes were incubated for 30 min at 20°C, with increasing concentrations of [^{125}I]-ANP in the absence △—△ (total binding) and presence □—□ (NSB) of 10^{-6} M ANP. Specific binding, *——*, was calculated by subtracting the NSB from the total binding. The results are the mean ± S.E.M. for triplicate determinations from a single membrane preparation.

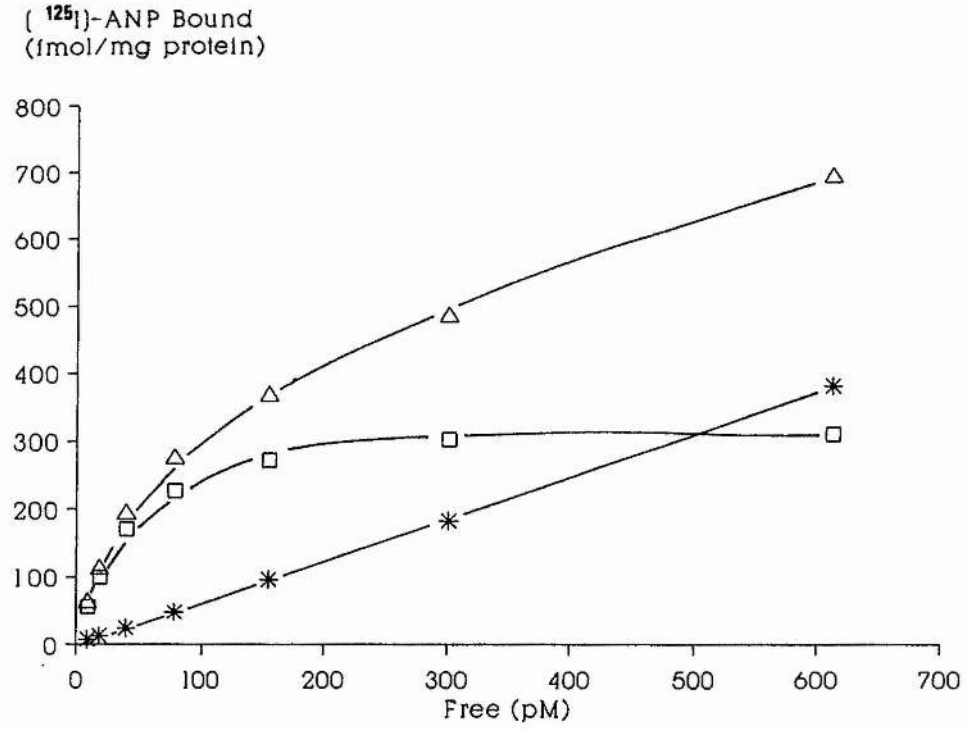
(125I)-ANP Bound
(fmol/mg protein)
800
700
600
500
400
300
200
100
0
0
100
200
300
400
500
600
700
Free (pM)

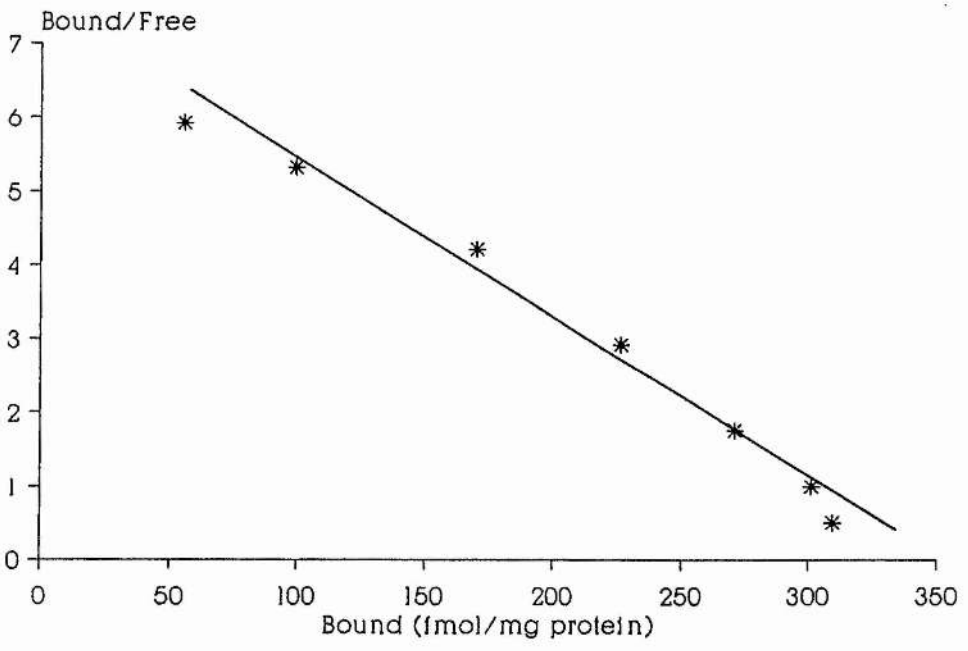
Bound/Free
7
6
5
4
3
2
1
0
0
50
100
150
200
250
300
350
Bound (fmol/mg protein)

Figure 5.12

ANP Displacement of [^{125}I]-ANP Binding to MDCK (Strain I) Membranes

[^{125}I]-ANP (37pM) was incubated with MDCK (Strain I) membranes(10 to 40 μg protein/ml) for 30 min at 20°C, in the presence of increasing concentrations of unlabelled ANP. The results shown are for 4 separate experiments performed on separate membrane preparations. Each point is the mean of at least 2 determinations, which varied by less than 10%.

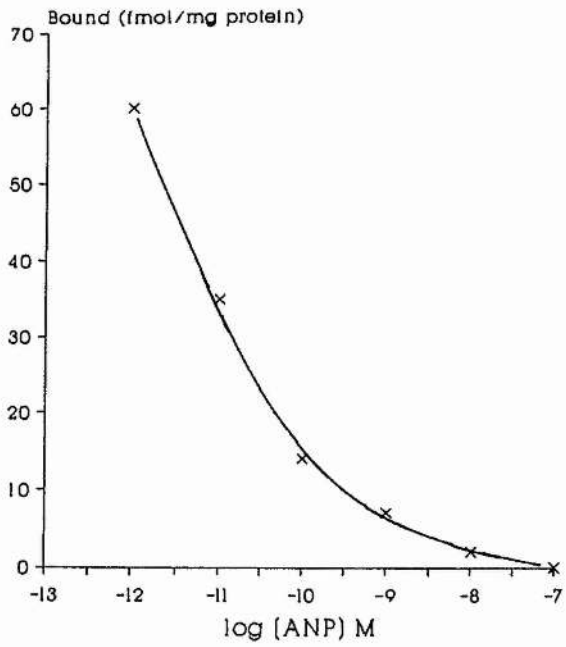
Bound (fmol/mg protein)
70
60
50
40
30
20
10
0
-13
-12
-11
-10
-9
-8
-7
log [ANP] M

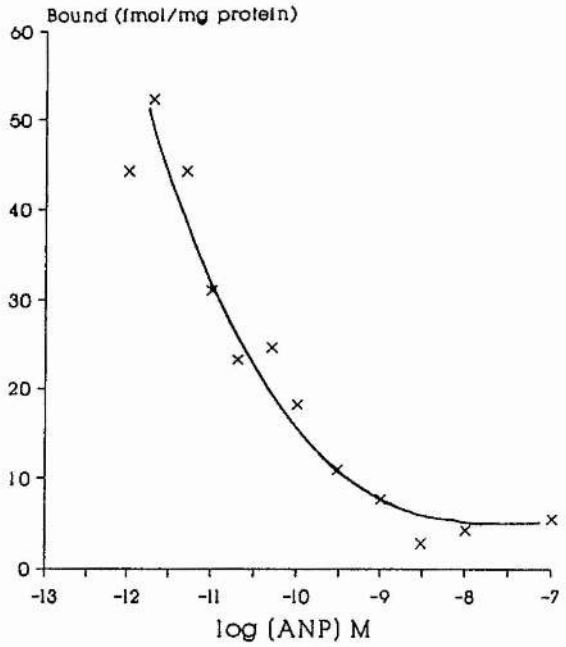
Bound (fmol/mg protein)
60
50
40
30
20
10
0
-13
-12
-11
-10
-9
-8
-7
log [ANP] M

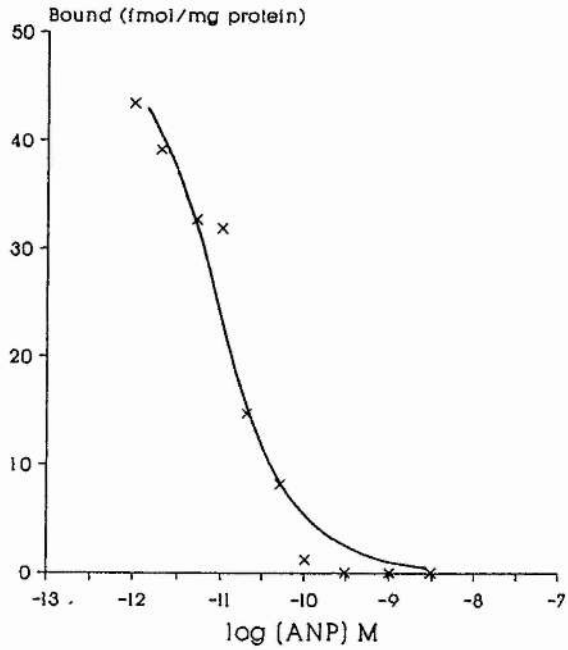
Bound (fmol/mg protein)
50
40
30
20
10
0
-13
-12
-11
-10
-9
-8
-7
log [ANP] M

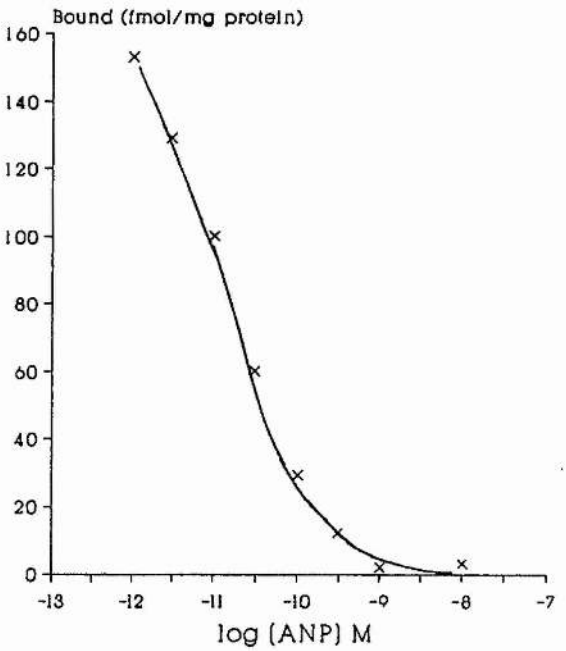
Bound (fmol/mg protein)
160
140
120
100
80
60
40
20
0
-13
-12
-11
-10
-9
-8
-7
log [ANP] M

Figure 5.13

Mean Dose Response Curve for ANP Displacement of [^{125}I]-ANP from MDCK (Strain I) Membranes

(a) The results of experiments shown in fig. 34 were corrected for NSB, and expressed as the percentage inhibition of [^{125}I]-ANP binding. Each point represents the mean ± S.E.M. (b) A Scatchard plot of the data shown in (a).

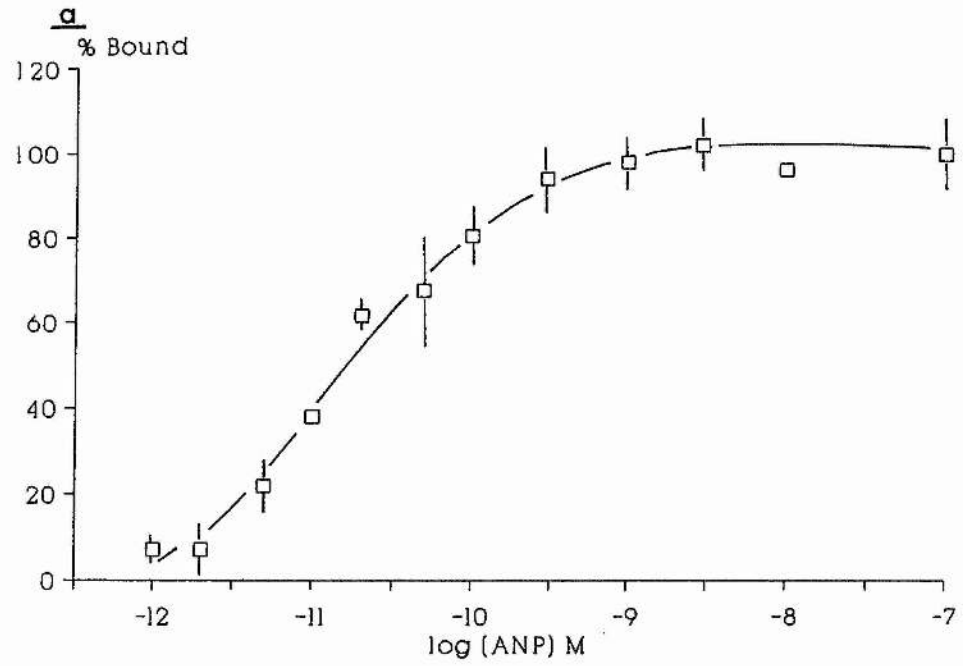
a
% Bound
120
100
80
60
40
20
0
-12
-11
-10
-9
-8
-7
log (ANP) M

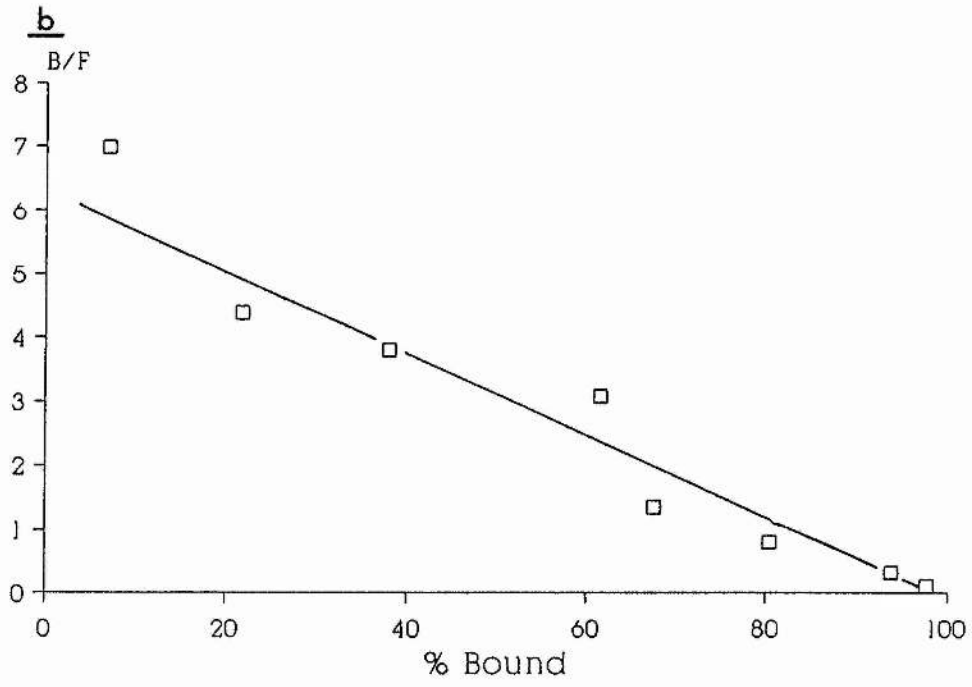
b
B/F
8
7
6
5
4
3
2
1
0
0
20
40
60
80
100
% Bound

Table 5.4

Results from the Hill Plots of the ANP Displacement Curves

Expt. No.	Slope Coeff.	Corr. (pM)	IC_{50}	$[^{125}I]$-ANP (pM)
1	-0.525	-0.994	17.8	37
2	-0.397	-0.900	24.6	37
3	-1.302	-0.976	10.8	37
4	-0.902	-0.992	12.7	37
Mean			16.5	
± S.E.M.			± 3.1	

Figure 5.14

ANP Displacement of [^{125}I]-ANP binding to MDCK (Strain II) Membranes

[^{125}I]-ANP (37pM) was incubated with MDCK (Strain II) membranes (10 to 40 µg protein/ml) for 30 min at 20°C, in the presence of increasing concentrations of unlabelled ANP. The results shown are for 2 separate experiments performed on separate membrane preparations. Each point is the mean of duplicate determinations, which varied by less than 10%.

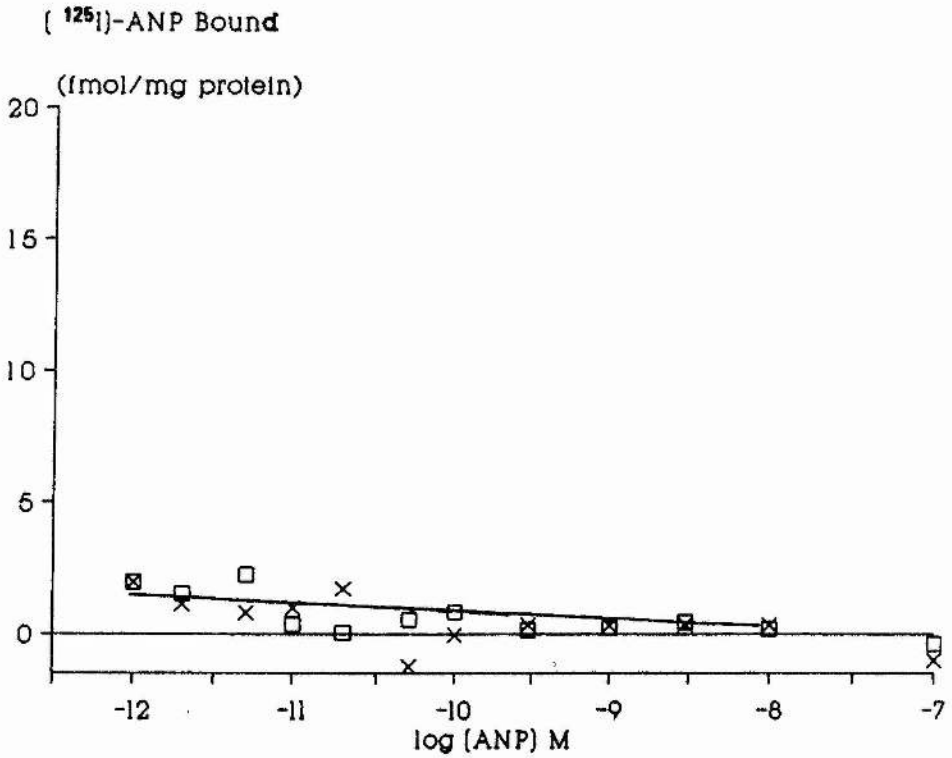

5.2 Discussion of [^{125}I]-ANP binding experiments

5.2.1 Analysis of Data From Ligand Binding Experiments

There are two general approaches which can be taken to analyse ligand binding data: (i) the transformation of the data to a linear form, and (ii) the statistical fitting of raw data to a mathematical model.

The most commonly used transformations are Scatchard plots (Scatchard, 1949) and Hill plots (Hill, 1913; Adair, 1925; see appendix III). The premise behind both these transformations is that the ligand interacts with a single population of binding sites via a simple reversible bimolecular reaction which obeys the Law of Mass Action (Limbird, 1986). When this is the case then Scatchard plots of the data are straight lines, with a slope equal to - $1/K_D$, and the x intercept equal to the maximum number of binding sites in the preparation. Similarly, a Hill plot of the same data will also be a straight line, with a slope (Hill coefficient) of 1 and an x intercept equal to the K_D. Curvilinear Scatchard plots and Hill coefficients of greater or less than 1 indicate complex binding phenomena or technical artifacts. For example, a Hill coefficient of less than 1 suggests either negative co-operativity (ie. the affinity of the receptor decreases with increasing occupancy), multiple receptor populations, or multiple affinity states of a single receptor. In contrast, a Hill coefficient of greater than 1 suggests either positive co-operativity (i.e. the affinity of the receptor increases with increasing occupancy; Limbird, 1986), or the possibility that the reaction has not reached equilibrium (Motulsky & Mahan, 1984).

Curved Scatchard plots can arise for similar reasons, with upward

concave plots indicating negative co-operativity, multiple binding sites or multiple affinities of the same binding site. In situations where evidence exists to suggest the presence of two binding sites, it is possible to resolve the Scatchard plots into two straight lines, from which can be estimated the affinities and relative proportions of the two binding sites (Barnett et al., 1978; Rugg et al., 1978). This analysis is based on the assumption that the ligand interacts independently with the two binding sites via a simple bimolecular reaction. When the affinities of the two binding sites differ by 100-fold or more, such that the high affinity site is almost saturated before binding to the low affinity site is detectable, then the resolution of Scatchard plots into two straight lines will provide an accurate estimation of the IC_{50} or K_D of the ligand (Nahorski, 1981). This however, is predicated on one of the following assumptions being valid: i) the radioligand must not distinguish between the two binding sites i.e. it must have the same affinity for both sites, or ii) if the radioligand does have different affinities for the two sites, these affinities must be the same as those for the displacing ligand.

Curve-fitting routines provide a more flexible approach to the assessment of ligand binding data. The models of receptor binding on which the computer programmes are based are analogous to those of the Scatchard and Hill analyses described above. For example, 'Allfit' is based on the Hill equation (De Lean et al., 1978), whilst 'Ligand' is derived from the 'sum of hyperbolas' model of complex receptor binding (Feldman, 1972; Munson & Robard, 1980). These computer-assisted forms of analysis provide a more objective approach than line-fitting by eye when multiple binding sites or complex interactions are present.

With any form of analysis it is important to ensure that the model to which the data is being fitted correctly describes the system under investigation. For this reason, it is useful to analyse ligand binding data by a number of different methods. The more agreement there is between the different methods, the more reliable are the conclusions that can be drawn concerning the data. This approach has been applied to the ligand binding experiments described in this chapter, with the data being first assessed by Scatchard and Hill plots, and subsequently by curve fitting of the data to a one- or two-site model for receptor binding, using Enzfitter (see appendix III).

5.2.2. Binding Experiments in Rat Cardiac Sarcolemmal Membranes and BAC Membranes

Hill plots (indirect) of the data from ANP displacement experimemts with rat cardiac sarcolemmal membranes and BAC membranes had low Hill coefficients. Scatchard plots of the same data were upwardly concave. Although these results suggest multiple ANP binding sites and/or affinity states in these preparations, similar plots would result from technical artifacts in the experiments. Potential causes of upwardly concave Scatchard plots include i) inappropriate definition of non-specific binding, ii) the aggregation of ligand at higher concentrations to form a dimer or multimer possessing a lower affinity for the receptor, and iii) a difference in affinity of the ligand and radioligand for the receptor (Limbird, 1986).

Non-specific binding (NSB) is an estimation of binding not associated with physiological binding sites (receptors). This binding results from the adsorption of radiolabel to the filter, the interaction of label with non-receptor sites in the membrane (such as partition

between the lipid bilayer and the incubation medium) and the presence of radiolabel which has merely become trapped, possibly in vesicles in the membranes. Since binding due to these processes would not be expected to saturate, NBS should increase linearly as a function of radiolabelled ligand. In the present experiments the amount of [^{125}I]-ANP displacement by 1 μM ANP was directly proportional to the concentration of radioligand (figs. 5.5, 5.9, 5.11). In addition, no further displacement of radioactivity was observed when 10 μM ANP was included in the incubation. These results suggest that the counts bound in the presence of 1 μM ANP are a reasonable assessment of NSB. Therefore it is unlikely that innaccurate measurement of NSB contributes to the curvilinear Scatchard plots.

A dimeric form of ANP (beta-hANP), which consists of two antiparallel ANP molecules linked by intermolecular disulphide bridges, has been identified in human atria (Kangawa & Matsuo, 1984; Oikawa et al., 1984). In addition it has been reported that a free thiol group in BSA can participate in the opening and rejoining of alpha-hANP to form a BSA-ANP conjugate (Miyata et al., 1987). Reactions of this kind have not been reported for rat ANP, although there is no obvious reason why they should not occur. It is possible that the 5-10% of radioactivity which was not recovered following HPLC analysis of [^{125}I]-ANP was in fact high molecular weight complexes of the peptide. Since such complexes, if they are present, would only account for a small proportion of the total radioactivity, it is unlikely that this is the cause of the non-linear Scatchard plots and low Hill coefficients.

Misinterpretation of binding data, because of differing affinities between the labelled and unlabelled ligand, would only arise if the

calculation of the results were based on the combined concentration of these two species (Taylor 1975). In the experiments described here no prior assumptions were made as to the relative affinities of ANP and [^{125}I]-ANP for binding sites in any of the membranes investigated.

Other artifactual reasons for non-linear Scatchard plots, and Hill coefficients differing from 1, include the measurement of binding prior to reaching equilibrium, and degradation of the ligand to a less active form during the incubation (Limbird, 1986). Both these artifacts would give rise to downward concave curves and Hill coefficients greater than 1, and therefore can be excluded as contributing to the effects seen in sarcolemmal and BAC membranes. It is therefore likely that the curved Scatchard plots and the low Hill coefficients resulting from the ligand binding experiments carried out in these membranes reflect the nature of the ANP receptor(s) in these preparations, rather than technical difficulties with the assays.

The presence of two ANP receptors has been well documented in several tissues (Meloche et al.,1986a; Napier et al.,1984; Hamada et al., 1987), and therefore the results were analysed assuming this to be the case in cardiac sarcolemmal and BAC membranes. IC_{50} values calculated for ANP binding to high and low affinity sites in these preparations are similar to those previously reported for BAC membranes (Meloche et al., 1986a), rat and rabbit kidney cortex membranes (Napier et al., 1984), and purified rat glomerular membranes (Hamada et al., 1987). There was considerable variation in the affinity of ANP for these binding sites between different preparations of rat cardiac sarcolemmal membranes (tables 5.1 and 5.2), and in two preparations only a single site could be detected. Some of the variation may be

accounted for by the differences in the amount of radiolabel present in the experiments, and this may explain the failure to detect high affinity binding sites in two of the preparations. As less than 5% of the [^{125}I]-ANP binding sites in the sarcolemmal membranes are of high affinity, these sites can only be measured when the radiolabel is at a concentration such that it does not bind to the low affinity sites. The concentrations of [^{125}I]-ANP present in the two experiments where only single binding sites could be measured were 88.6 and 90.9 pM. It is likely that at these concentrations significant amounts of radiolabel binds to the low affinity, high capacity sites and results in a masking of the presence of the high affinity, low capacity binding sites.

The concentration of radiolabel must also be taken into account when estimating the K_D's for ANP for the IC_{50} values determined from displacement experimemts. This is normally achieved by application of the Cheng Prusoff equation (Cheng & Prusoff,1973; see appendix III). This correction factor is based on the assumption that the radiolabelled ligand interacts with both populations of binding sites with a single affinity (Cheng & Prusoff, 1973; Limbird, 1986). Scatchard analysis of saturation binding data indicates that [^{125}I]-ANP has different affinities for the two binding sites, and in addition it is likely that these affinites differ from those for ANP (fig. 5.4).

Although the assumptions of the Cheng Prusoff equation are violated, it is possible to assess the effect of the radioligand concentration on apparent affinity of ANP for its binding sites by the use of the K_D values calculated from the [^{125}I]-ANP saturation binding experiment.

Assuming the K_D of [^{125}I]-ANP to be 10.9 pM and 1.23 nM for the high and low affinity sites respectively, the K_D of ANP for the two sites can be calculated (table 5.2). The concentration of [^{125}I]-ANP was less then 100 pM in all the displacement experiments, and therefore it had little effect on the apparent affinity of ANP for the low affinity site. In contrast, these concentrations of radiolabel have a marked effect on the estimation of the affinity of ANP for the high affinity sites, with the calculated K_D values being 5- to 9-fold lower than the IC_{50} values.

It is not possible from any of these experiments to determine whether the two binding sites are actually due to distinct receptors, or if they are a result of the same receptor with two distinct affinity states. In addition, it is possible that the complex binding curves described here and elsewhere are a result of negative co-operativity. Kinetic studies on the dissociation rate of radiolabel, in the presence and absence of an excess of unlabelled ligand, are required before this possibility can be excluded (De Meyts et al., 1976).

5.2.3 [^{125}I]-ANP Binding to Membranes Isolated from MDCK cells

The results of the experiments carried out with MDCK cell (strain I) membranes indicate the presence of a single population of binding sites, which possess an affinity for ANP similar to that observed for the high affinity site in rat cardiac sarcolemmal and BAC membranes. Similar studies with MDCK (strain II) cell membranes failed to detect any specific ANP binding site. These results confirm earlier studies from this laboratory, which have identified [^{125}I]-ANP binding sites in intact MDCK (Strain I) cells but not in strain II cells (Aiton et al., 1987).

MDCK cells are established cell lines which display many features characteristic of renal epithelia (Misfeldt et al., 1976; Cereijido et al., 1978). Two strains of these cells have been described which differ in morphological, biochemical, and physiological characteristics. Strain I cells form monolayers with characteristics similar to collecting duct cells. They have a high electrical resistance, and a low basal short circuit current, which can be stimulated by adrenaline, prostaglandin E_1, and arginine vasopressin. In contrast, strain II cells form low resistance monolayers, with a short circuit current which is insensitive to any of these hormones. Strain II cells possess the proximal tubule enzyme markers alkaline phosphatase and gamma-glutamyl transpeptidase, whereas strain I cells do not. In addition, the specific activity of $(Na^+ + K^+)$-ATPase is two-fold higher in strain II than strain I cells (Richardson et al., 1981). Other differences between the two strains include the existence of beta adrenergic receptors and VIP receptors on strain I, which are absent from strain II (Rugg & Simmons, 1984; Rugg & Simmons 1986).

A recent report by Leitman et al. (1988) failed to detect ANP binding sites in intact MDCK cells, and it is therefore likely that the cells used in that study were equivalent to the strain II cells described here. ANP receptors have been identified on rat inner medullary collecting ducts (Koseki et al., 1986ab), and thus the present results are consistent with the observation that strain I cells have characteristics similar to these cells. Furthermore the lack of binding sites on strain II cells supports the evidence that these cells are of proximal origin.

5.2.4 Summary

The results of [^{125}I]-ANP binding studies carried out in purified rat cardiac sarcolemmal and BAC membranes are consistent with the existence of high and low affinity ANP receptors and/or affinity states. In contrast, similar studies with MDCK (strain I) cell membranes indicate the presence of a single receptor in this preparation, with an affinity similar to the high affinity site observed in cardiac and adrenal preparations.

CHAPTER 6

6 General Discussion of Guanylate Cyclase and Ligand Binding Experiments

ANP stimulates guanylate cyclase activity in rat cardiac sarcolemmal membranes with a potency similar to or slightly higher than that described for other preparations, including rat kidney membranes (Waldman et al., 1984) and bovine adrenal cortex membranes (Tremblay et al., 1986). The results of [^{125}I]-ANP binding experiments in the sarcolemmal membranes are consistent with the presence of two binding sites, with affinities for ANP of around 10 pM and 1 nM respectively.

Similar high and low affinity binding sites have been described for other preparations (De Lean et al., 1984b; Hamada et al., 1987; Resink et al., 1988)). Maack et al. (1987) have identified two ANP receptors in the rat kidney, one of which possesses biological activity (B-ANP receptors), while the other is apparently devoid of biological activity (C-ANP receptors). Likewise, several biochemical studies have identified two different ANP receptors, one of which is coupled to guanylate cyclase (see section 2.4). The ANP receptor coupled to guanylate cyclase ($M_r \simeq 130$ kDa) has been termed the ANP-1 receptor and the uncoupled site ($M_r \simeq 66$ kDa) the ANP-2 receptor (Murad et al., 1988). Based on i) the correlation between the incidence of C-ANP receptors and ANF-2 receptors, and ii) the fact that B-ANP receptors mediate increases in intracellular cGMP, whereas C-ANP receptors do not, it has been proposed that the B-ANP receptor is the 130 kDa site and the C-ANP receptor is the 66 kDa site (Lewicki et al., 1988). This awaits confirmation. More than 95% of the ANP binding sites in most

cells and tissues appear to be of the C-ANF (or ANP-2) receptor type (Maack et al., 1987; Leitman & Murad, 1987), and this may explain the linear Scatchard plots obtained with many preparations.

A comparison of the ANP dose response curves for the stimulation of guanylate cyclase activity and the displacement of [^{125}I]-ANP in rat cardiac sarcolemmal membranes (figs. 4.5 and 5.3) makes it tempting to speculate that the high affinity sites in this preparation are the C-ANP (ANF-1) receptors, and the low affinity sites are the B-ANP (ANF-2) receptors. If this is the case then the majority of binding sites in this preparation are of the biologically active type. Evidence against this hypothesis comes from ligand binding studies on purified ANF-1 and ANF-2 receptors from bovine adrenal cortex, which indicate that the two types of receptor have equal affinities for ANP (K_D = 54 to 69 pM; Takayanagi et al., 1987b). It should be noted, however, that Takayanagi et al. found that after co-purification of guanylate cyclase with ANP binding sites, the enzyme could no longer be stimulated by ANP. A similar loss in ANP-stimulated guanylate cyclase activity has been observed after the purification of guanylate cyclase activity from rat lung (Kuno et al., 1986). It is therefore possible that affinities of ANP for its receptors may be different in purified preparations, compared to membrane preparations. Investigation of the subunit composition of the ANP receptors in rat cardiac sarcolemmal membranes is required before firm conclusions can be drawn. In addition, studies with the ring-deleted analogue of ANP, C-ANP$_{4-23}$ may also help to identify the predominant ANP receptor in rat cardiac sarcolemmal membranes. If the low affinity sites are the biologically active ANP receptors, then C-ANP$_{4-23}$ should not displace [^{125}I]-ANP from these sites (see section 2.5).

Ligand binding experiments with MDCK (strain I) cells indicated the presence of a single population of binding sites with an affinity for ANP similar to that of the high affinity binding sites in rat cardiac sarcolemmal membranes. No guanylate cyclase activity could be detected in this preparation. These results are consistent with the hypothesis that the high affinity binding sites are devoid of biological activity, and it is predicted that C-ANP$_{4-23}$ will displace [^{125}I]-ANP from all the sites in this preparation.

As noted previously, Leitman et al., (1988) failed to identify any [^{125}I]-ANP binding sites on MDCK cells from their laboratory, although ANP did increase intracellular cGMP in these cells. If the cells used in their experiments are the same as MDCK (strain II) cells, it is possible that strain II cells possess a small number of B-ANP receptors and ANP should stimulate guanylate cyclase activity in these cells.

CHAPTER 7

7 Degradation of [^{125}I]-ANP

7.1 Introduction

The majority of investigations into the mechanism of action of ANP have been concerned with the synthesis and release of this peptide, its receptor binding, and its ability to stimulate guanylate cyclase activity. Little attention has been paid to its inactivation however, although ANP has a half-life in the blood of only 1 to 3 minutes (Luft et al., 1986; Yandle et al., 1986; Murthy et al., 1986ab).

A number of peptide hormones, such as angiotensin, glucagon, and LHRH are believed to be inactivated at the brush border of the renal proximal tubule, which is rich in membrane bound peptidases (Carone et al., 1982; Kenny & Maroux, 1982). In the lung, angiotensin I converting enzyme is responsible for the both the activation and inactivation of peptides. This enzyme both hydrolyses angiotensin I to form the potent vasoconstrictor angiotensin II, and degrades the hypotensive agent, bradykinin (Linehan et al., 1986; Ferreira et al., 1967).

ANP may be degraded by mechanisms similar to those described above. Moreover, the rate of its degradation may be as important as its rate of synthesis in the regulation of plasma levels of this hormone. This chapter reviews the possible mechanisms by which the degradation of ANP may occur.

7.2 Classification of Proteases and Peptidases

7.2.1. Introduction

On the basis of their mechanisms of action, mammalian proteases can be divided into two main groups, the endopeptidases (or proteinases) and the exopeptidases. Endopeptidases attack bonds within protein or peptide chains, and are generally either classified according to the reactive groups at their catalytic site (the serine, cysteine, or aspartic proteinases) or in terms of metal co-factor requirements (the metalloproteases). Exopeptidases cleave peptide bonds at the ends of the peptide/protein molecule and can be classified according to their site (terminus) of attack, preferred substrate and/or size of fragment liberated (fig. 7.1). These groups are further subdivided according to the actions of various inhibitors and their pH specificity. Comprehensive reviews of proteinase activity and inhibitors include monographs by Barrett & McDonald (1980), McDondald & Barrett (1986) and Barrett & Salvesen (1986). A summary of protease activity and protease inhibitors relevant to this thesis is given below.

7.2.2 Serine Proteinases

Serine proteinases are the largest group of proteolytic enzymes, and can be subdivided into chymotrypsin-like proteinases and subtilisin-like proteinases. Whilst the subtilisin-like proteinases are found only in bacteria, the chymotrypsin-like proteinases are ubiquitous to the plant and animal kingdom. The wide variety of serine proteinases found in mammals include enzymes involved in blood coagulation, complement activation, digestion, hormone generation or degradation, fibrinolysis, phagocytosis, and protein turnover.

Figure 7.1

Classification of Proteases

The subdivision of proteases according to their site of action.

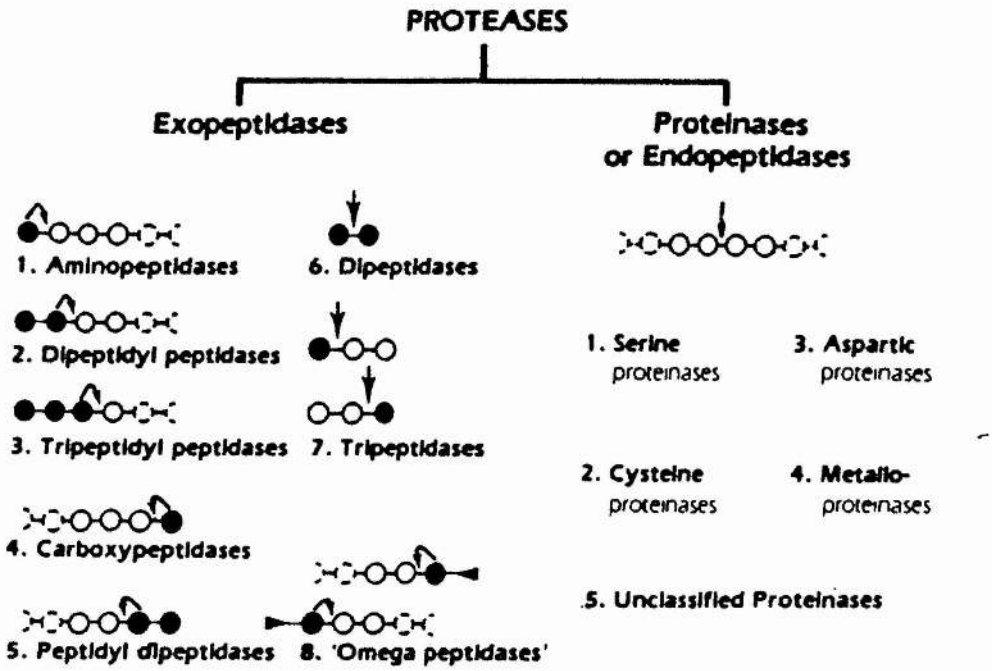

Serine proteinases contain, at their active site, serine and histidine residues, and many specific inhibitors of this class of enzyme act by interaction with these amino acids.

Phenylmethylsulphonyl fluoride (PMSF) is a member of a group of such inhibitors which acts by the formation of a sulphonyl enzyme derivative which is resistant to hydrolysis. PMSF has a broad specificity and inactivates a number of enzymes including tryptases, elastases, and blood coagulation proteinases.

Aprotinin is another broad spectrum serine proteinase inhibitor, which was first identified in bovine lymph nodes and found to inactivate kallikrein. It has subsequently been identified in several other bovine tissues and found to inhibit a number of other enzymes, including trypsin, chymotrypsin, and plasmin. Aprotinin acts by the formation of a stable complex with the active site of the proteinase (Huber & Bode, 1978; Blow et al., 1972). Since aprotinin is a large molecule (Mol. Wt 6200) its ability to form this complex is directly related to the 'goodness of fit' between the inhibitor and the active site of the enzyme. For instance, aprotinin has a high affinity for trypsin with only minimal conformational changes of the two structures being required to form a stable complex (Huber & Bode, 1978). In contrast, the relatively low affinity of this inhibitor for chymotrypsin is caused by the 'poor fit' of the enzyme with the active site in aprotinin (Blow et al., 1972).

Leupeptin is a peptide aldehyde of microbial origin, and is a potent inhibitor of serine proteinases which possess 'trypsin-like' activity (Umezawa, 1976). Thus it is a potent inhibitor of trypsin, plasmin, and kallikrein, but only poorly inhibits chymotrypsin and thrombin

(Aoyagi et al., 1969). Leupeptin is also a potent inhibitor of some cysteine proteinases as discussed below.

7.2.3 Cysteine proteinases

Cysteine proteinases have at their catalytic site cysteine and histidine imidazole residues. This group of proteinases contain enzymes such as papain, many of the cathepsins and the family of calcium dependent proteinases, known as the calpains.

Many inhibitors of these enzymes act by alkylation of the cysteine sulphydryl group, and one such group of compounds are the epoxysuccinyl peptides. Epoxysuccinyl-leucyl-agmatine (E-64), which was the first member of this family to be discovered, rapidly inactivates papain, cathepsin B, cathepsin L, ficin, and calpain. It is not a universal inhibitor of cysteine proteinases, having little effect on proteolysis by streptoccal cysteine proteinase, and no effect on clostripain activity. E-64 does not inhibit any of the serine or aspartic proteinases, or any metalloproteases yet tested (Barrett et al., 1982).

A variety of other reagents such as N-ethylmaleimide, iodo- and bromoacetates and p-chloromercuric benzoate (PCMB) inhibit cysteine proteinase activity by a mechanism similar to E-64 (Means & Feeney, 1971). These reagents are not as specific as the epoxysuccinyl peptides and will also react with low molecular weight thiol compounds and cysteine proteinases.

Leupeptin inhibits several cysteine proteinases, including papain, cathespin B (Umezawa, 1982), and calpains I and II (Sasaki, et al., 1984). It is a member of a class of enzyme inhibitors referred to as

transition-state analogue inhibitors, which act by mimicking the geometry of the transition state for the enzyme catalysed reaction (see Rich, 1986).

7.2.4 Aspartic proteinases

Pepsin and cathepsin D are the two major members of this class of proteinases. The mechanism by which they act is not fully understood, but it is known to involve two aspartate residues at the active site (Tang *et al.*, 1973). Pepstatins are a group of potent inhibitors of this class of proteinases and studies using X-ray crystallography indicate that these inhibitors act by binding to the active site of these enzymes (Bott *et al.*, 1982; James et al., 1982).

7.2.5 Metalloproteases

This is a diverse group of proteases, whose catalytic activity is dependent on the presence of a metal ion, usually zinc, at the active site. Included in this group of proteases are thermolysin, mammalian collagenase, almost all of the membrane-bound endopeptidases and the majority of the exopeptidases. Inhibitors of this class of protease usually act by chelating the metal ion associated with the enzyme.

Metal ion chelators such as 1,10-phenanthroline and EDTA (ethylenediamine-tetraacetic acid) are both good inhibitors of metalloprotease activity. However, whilst 1,10-phenanthroline is specific for this class of proteases, EDTA will also inhibit calcium-dependent serine proteases.

Phosphoramidon is a member of a phosphorus containing group of inhibitors specific for neutral metalloendopeptidases, in particular

the bacterial protease thermolysin. The only mammalian protease known to be inhibited by phosphoramidon is endopeptidase 24.11.

Amastatin is a peptide inhibitor derived from a species of streptomyces and is an inhibitor of some of the metallo-exopeptidases. It is specific for amino peptidases, inhibiting the actions of aminopeptidase A, leucine aminopeptidase, tyrosine aminopeptidase, tripeptidyl-, and tetrapeptidyl-aminopeptidases. It has no effect on the activity of aminopeptidase B, trypsin, chymotrypsin, elastase, papain, pepsin or thermolysin.

7.2.6 Unclassified Proteinase Inhibitors

Bacitracin is the name given to a number of polypeptide antibiotics produced by certain strains of Bacillus subtilis and Bacillus licheniformis. Of this group of antimicrobial agents the most common is Bacitracin A, which contains four D-aminoacids, including ornithine, which is not normally present in proteins. Bacitracin A exerts its antibiotic action by inhibiting the dephosphorylation of lipid pyrophosphate to lipid phosphate and so impairing cell wall synthesis (Bowman and Rand, 1980). The mechanism by which it inhibits proteolysis is unknown but, as it is a polypeptide, it may well involve binding to the catalytic site. It is a potent inhibitor of glucagon degradation (Desbuquois et al., 1974).

7.3.1 The Removal of ANP from the Circulation

There are two different mechanisms by which peptide and protein hormones may be removed from the circulation, namely receptor-mediated endocytosis and degradation. Receptor-mediated endocytosis involves the binding of the hormone to its receptor followed by the

internalisation of the hormone-receptor complex, resulting in the 'down regulation' of the receptor. This process has been demonstrated to occur following ANP binding to cultured vascular smooth muscle cells (Hirata et al., 1985; Napier et al., 1986), and there is increasing evidence to suggest that this process is important in the regulation of ANP levels. As described earlier, there are at least two types of ANP receptor, one coupled to guanylate cyclase, the other not (section 2.4). It has been postulated that the receptor which is not associated with guanylate cyclase activity acts as a 'clearance' receptor, thereby modulating ANP levels in the blood (Maack et al., 1987). This view is supported by the observation that this receptor type appears to be more susceptable to down regulation than the guanylate cyclase coupled form (Hirata et al., 1987b).

Degradation of ANP by the action of various non-specific endogenous tissue proteases may also account for the loss of this peptide from the circulation. It is not known to what exent degradation contributes to the regulation of plasma ANP levels, but there have been several reports suggesting an inherent instability of ANP when incubated with various biological preparations.

In the remainder of this chapter I shall outline the major findings concerning the degradation of ANP.

7.3.2 Degradation of ANP in the Blood

The importance of the blood in the inactivation of ANP was first investigated by Veress et al., (1985), who reported that the pre-incubation of ANP with whole blood or plasma resulted in the attenuation of the renal response in the bioassay rat. Although no

identification was made of the protease(s) responsible, plasma kallikrein was precluded by the observation that the effect was abolished when the platelets and leucocytes were removed from the plasma. [Plasma kallikrein is located in the plasma per se (Kluft, 1978).] A subsequent investigation has shown that incubation of ANP with plasma results in the conversion of the 28 amino acid ANP_{1-28} to the 24 amino acid ANP_{5-28} (Murthy et al., 1986b). In both of these reports degradation is relatively slow ($t_{1/2}$, 60min) and unlikely to account for the rapid disappearance of both radiolabelled ANP and immunoreactive ANP from the bloodstream (Murthy et al., 1986ab). It is therefore unlikely that blood components play a major role in the degradation of ANP in the body.

7.3.3. Degradation of ANP in the Kidney

Incubation of ANP with rat kidney cortex membranes results in rapid degradation of the peptide. The initial cleavage site has been identified as occurring at the Cys^7-Phe^8 bond (Koehn et al., 1987). Degradation could be inhibited by the inclusion of EDTA and 1,10-phenanthroline in the incubation, thus suggesting that a metalloendoprotease may be responsible. Stephenson & Kenny (1987a) carried out similar experiments using pig kidney microvilli membranes and also identified this bond as a potential cleavage site. They obtained similar degradation profiles when ANP was incubated with endopeptidase-24.11, and suggested that this enzyme was primarily responsible for the breakdown of ANP by kidney membranes. The importance of endopeptidase-24.11 in the degradation of ANP is discussed in more detail in section 7.4.3.

7.3.4 Degradation of ANP in the Lung

The lung is important for the degradation of several peptides, including angiotensin I and bradykinin (Bakhle, 1968; Yang *et al.*, 1971). Since the majority of ANP released from the heart first passes through the pulmonary circulation, any degradation by the lung will be of primary importance to the final levels of peptide circulating in the systemic system. Hydrolysis of ANP has been shown to occur during the perfusion of the rat lung *in vitro* (Numan *et al.*, 1986). Using *in situ* perfused rabbit lungs, Turrin & Gillis (1986) showed that 67% of radiolabelled ANP was removed from the circulation during a single passage through the lung. The radioactivity could be recovered from the preparation by perfusion with unlabelled ANP, suggesting that the radiolabel was binding to a specific receptor. Since no analysis was made of the recovered radioactivity it is not known if degradation of radiolabelled ANP had occurred.

7.3.5. Degradation of ANP in the Mesenteric Artery

Studies of the fate of [^{125}I]-ANP in the isolated perfused mesenteric artery have shown that less than 40% of the ligand is intact after 15 min at 37^{o}C (Murthy et al., 1986b). The degradation profile of this peptide, as assessed by reverse phase HPLC, is similar to that obtained from *in vivo* studies and thus suggests a similar mechanism of breakdown. It is not known if degradation involves receptor binding or if it is caused by the action of a protease(s).

7.3.6. Summary

The incubation of ANP with kidney, lung, mesenteric artery and plasma *in vitro* results in degradation of the peptide. The extent to which

these tissues are responsible for degradation *in vivo* is not known, but it is unlikely that plasma is a major contributor because of its slow action. It is also unclear whether the enzymes responsible for degradation are of intracellular or extracellular origin.

7.4 Degradation of ANP by Purified Proteases

7.4.1 Tissue Kallikrein

The name tissue kallikrein refers to a group of very closely related serine proteases found in the pancreas and salivary glands, and excreted in the urine. These enzymes are highly active in the hydrolsis of the peptide bond on the carboxyl side of the sequence Phe-(or Leu)-Arg-X, and are capable of cleaving prorenin to renin (Sealey *et al.*, 1978) and proinsulin to insulin (Ole-Moi Yoi *et al.*, 1979).

Incubation of ANP (synthetic and partially purified) with pancreatic kallikrein results in a marked reduction in the natriuretic and diuretic responses to these peptides (Thibault *et al.*, 1984c; Briggs *et al.*, 1984). Furthermore, the simultaneous infusion of aprotinin, a serine protease inhibitor, with ANP results in the potentiation of the renal responses in the rat. Since the kidney is a major source of kallikrein activity, it is possible that renal kallikrein is, at least in part responsible for the inactivation of ANP *in vivo*.

7.4.2 Other Serine Proteases

Other serine proteases, namely trypsin, chymotrypsin, and elastase have been shown to reduce the diuretic and natriuretic activity of ANP

(Briggs et al., 1984). It is unlikely that trypsin and chymotrypsin are present in sufficient quantities in tissues which come in contact with ANP to cause degradation in vivo. Elastase (tissue) is present in mammalian aorta and is secreted by cultures of rabbit aortic smooth muscle cells (Barrett and McDonald, 1980). It therefore may be responsible for some of the degradation observed in vivo.

7.4.3 Endopeptidase-24.11

Endopeptidase-24.11, a membrane bound ectoenzyme, was first purified from rabbit kidney (Kerr and Kenny 1974), and shown to be most abundant in the brush border of the proximal tubules (Booth & Kenny, 1974). It has since been found in the kidneys of other species, including the pig (Kerr & Kenny 1974), rat, mouse (Kenny et al., 1981), and man (Abbs & Kenny 1983). It has also been identified in a variety of other organs and tissues including pig intestine, lymph nodes, chondrocytes, pituitary and brain synaptic membranes (Matas et al., 1983; Gee et al., 1985). An enzyme with similar characteristics has been found in bovine pituitary (Almenoff et al., 1981; Orlowski & Wilks, 1981).

Endopeptidase-24.11 cleaves bonds on the amino side of hydrophobic amino acid residues (Kerr & Kenny 1974). The efficiency of this hydrolysis is greatly influenced by the nature of the residues on the amino side of the cleaved bond, preferring arginine or small neutral amino acids for the two residues adjacent to the cleavage position (Orlowski & Wilks 1981; Almenoff & Orlowski 1983; Matsas et al., 1984). This enzyme is the only mammalian representive of a class of Zn^{2+}-containing metalloendopeptidases for which phosphoramidon is a potent specific inhibitor (Suda et al., 1973; Kenny, 1977). The

contribution of this enzyme to ANP degradation in preparations containing other peptidases can be assessed by measuring activity in the presence and absence of this inhibitor. Endopeptidase-24.11 has been shown to contribute to the hydrolysis of substance P, bradykinin, oxytocin and angiotensins I, II and III by pig kidney microvillar membranes (Stephenson and Kenny 1987b), and to the degradation of [Leu]enkephalin and substance P by caudate synaptic membranes (Matsas et al., 1983). Endopeptidase-24.11 is identical to the enzyme enkephalinase (Almenoff et al., 1981; Fulcher et al., 1982; Matsas et al., 1983).

Incubation of ANP with purified endopeptidase 24.11 or pig kidney microvillar membranes results in the rapid hydrolysis of the peptide within the disulphide linked ring, and a slower hydrolysis of Ser^{25}-Phe^{26} bond, yielding the C-terminal fragment Phe-Arg-Tyr (Stephenson and Kenny 1987a). Cleavage occurs at three points within the loop (Cys^{7}-Phe^{8}, Arg^{14}-Ile^{15} and Gly^{16}-Ala^{17}), although the initial point of attack has not been identified. Other studies using rat and rabbit kidney brush border membranes have identified the Cys^{7}-Phe^{8} bond as the primary site of ANP hydrolysis in these preparations (Koehn et al., 1987; Olins et al., 1987). These membranes are known to contain a large number of peptidases but, as phosphoramidon was not used to assess the contribution of endopeptidase-24.11 to this hydrolysis, it remains to be established if this enzyme is responsible.

The widespread distribution of endopeptidase-24.11, and its apparent specificity for the Cys^{7}-Phe^{8} bond of ANP, strongly suggest an important role in the metabolism of ANP. Approximately 30% of ANP isolated from human coronary sinus plasma was found to be in the

'ring-open' form (Cys^7-Phe^8 cleaved ANP; Yandle et al., 1987), and it is possible that endopeptidase 24.11 or a similar enzyme is responsible for this hydrolysis. It is known that the integrity of the disulphide bond is essential for the biological activity of ANP (Chartier et al., 1984, Misono et al., 1984b), from which may be surmised that hydrolysis at any point within the ring would also cause inactivation. This however has not been demonstrated and the possibility that 'ring open-ANP' possesses activity cannot be excluded. The slower hydrolysis of ANP at Ser^{25}-Phe^{26} identified by Stephenson & Kenny (1987a) may also be of biological importance, as removal of the tripeptide Phe^{26}-Arg^{27}-Tyr^{28} from the C-terminal results in a 70- to 150-fold reduction in vaso-relaxant and diuretic potency (Sugiyama et al., 1984; Garcia et al., 1985).

7.5 Reasons for Experiments

Receptors for [^{125}I]-ANP have been identified in purified sarcolemmal membranes prepared from rat ventricular muscle, and ANP has been shown to stimulate guanylate cyclase activity in this preparation. Incubation of ANP with intact rat and rabbit ventricular myocytes, in the presence of a phosphodiesterase inhibitor, results in an increase in intracellular cyclic GMP (Aiton & Cramb, 1985; Cramb et al., 1987), but attempts to measure specific binding of radiolabelled ANP in these intact preparations were unsuccessful. As described earlier, rapid degradation of ANP has been demonstrated in many preparations, both in vivo and in vitro, and this could explain the failure to measure [^{125}I]-ANP binding to these cells.

In the following chapter I will present evidence to show that [^{125}I]-ANP is rapidly degraded when incubated with rat and rabbit ventricular

myocytes and that part of this degradative activity is associated with a soluble extract isolated from cell homogenates. I will also present results which show that similar degradative activity can be isolated from a soluble fraction prepared from rat kidney and lung.

CHAPTER 8

8.1 Materials

Collagenase (Type I) was obtained from Lorne laboratories, Reading, Berks. Heparin (5000 units/ml) was supplied by The Boots Company, Nottingham, Notts. All other reagents were supplied as described in section 3.1.

Rats (Wistar) and rabbits (New Zealand White) were obtained from the University of St. Andrews stocks. Animals were kept under a 24 hr day/night cycle and allowed free access to food.

8.2 Methods

8.2.1.i Isolation of Rat Ventricular Myocytes

Rat ventricular myocytes were prepared from 8-12 week- old male Wistar rats (200-250g) by a modification of the method described by Powell et al., (1980). The rats were injected with heparin (2500 IU, ip.) 30 min before sacrifice. Following decapitation, the heart was rapidly removed, with the minimum amount of handling, and washed with ice cold KRBG (Ca^{2+} free). The aorta was cannulated, secured with cotton thread (fig. 8.1), and perfused retrogradely (Langendorff technique) at 37^{o}C with KRBG (Ca^{2+} free) at a rate of approximately 1ml/min. The first 15 to 25 ml of perfusate, which removed most of the blood cells, was discarded and the eluate then was recirculated for a further 1 to 2 minutes and the total perfusate volume adjusted to 100ml. Calcium was then added to the perfusate to a final concentration of 20μM, and perfusion continued for a further 3 to 5 minutes. If, during this initial perfusion period, the flow rate declined or the heart

Figure 8.1

Perfusion Apparatus

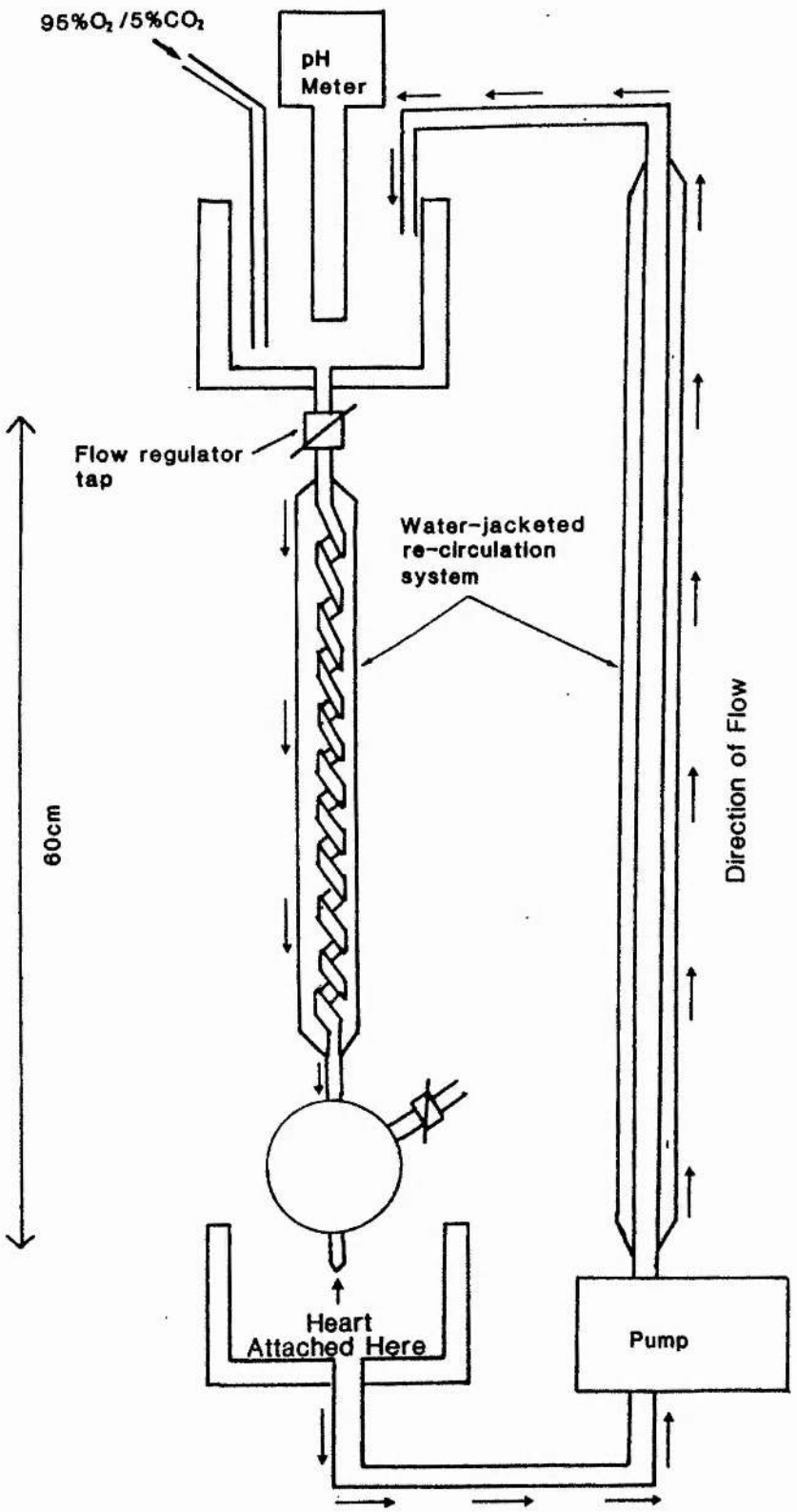

developed white patches, indicative of ischaemia and necrosis, the preparation was discarded. Finally, collagenase was dissolved in 10 mls of perfusate and added to the reservoir. The perfusion was continued for a further 20 to 30 minutes during which time the pH was maintained in the range of 7.1-7.8 by regulating the rate of gassing with 95% O_2/5% CO_2. During this time the flow rate was monitored and in a typical preparation it would gradually slow and then begin to increase, at which point the heart was removed from the perfusion apparatus. The exact time that this occurred varied from preparation to preparation. The atria were discarded and the ventricles were chopped into small pieces. These were placed together with 130mg BSA Fraction V (essentially fatty acid free) in a teflon beaker containing 50ml of perfusate. Digestion was continued at 37^{o}C for a further 10 to 20 minutes. During this period the dispersion of the myocytes was aided by gentle trituration with a wide bore pipette. The appearance of single cells was monitored by light microscopy. Trypsin and DNAse were added at a final concentration of 0.1%, for the final 5 min of digestion, as this prevented the cells aggregating during subsequent purification and incubations.

The digest was filtered through a 118 μm nylon net to remove undigested tissue, and the filtrate centrifuged at 60 x g for 1 min at room temperature in a bench top centrifuge (MSE). The pellet was resuspended in 10 to 15 ml of KRBG (20 μM Ca^{2+}, 0.1% BSA), 5 to 8 ml were layered onto the top of 4% BSA in KRBG (20 μM Ca^{2+}) and centrifuged at 60 x g for 1 min. The resulting pellets were resupended in 5ml of the same buffer and the previous step repeated. The final pellet was resuspened in 5 to 10 ml of KRHG (20μM Ca^{2+}, 1% BSA). An aliquot of the cell suspension was diluted with isoton and

cell number estimated on a Coulter Counter (Model ZM) attached to a Coulter Channelizer (Model 250). (See appendix IV).

The percentage rods (intact cells) to rounds (damaged cells) was estimated using a haemocytometer. The cell number was normally adjusted to between 10^5 and 10^6 cells/ml with KRHG, 20 uM Ca^{2+}, 1% BSA and the cells were gassed with 100% O_2 and kept at 37°C until required.

8.2.1.ii Isolation of Rabbit Ventricular Myocytes

Ventricular myocytes were isolated from 6- to 10-week old New Zealand White rabbits (1.5-2.5 kg) as described in the preceding section, except for the following modifications. The rabbits were given 5000 IU of heparin intravenously, 30 min prior to death. The final perfusion volume was 200 ml and the final digestion of the ventricles, in the teflon beaker, was performed in 75ml of perfusate. The amounts of collagenase and BSA were adjusted as appropriate to keep the concentrations at the same levels as described for the rat.

8.2.1.iii Results and Discussion

The rat hearts produced an average of 3.44×10^6 cells per preparation, whilst the rabbit hearts, which were approximately four times larger by weight, averaged approximately twice as many cells (7.55×10^6). Examination of these cell suspensions by light microscopy revealed that they were composed of 'rod' and 'round' shaped cells. The rods were intact myocytes and the rounds were damaged cells, formed because their cell membranes were 'leaky' to Ca^{2+}, causing them to contract (Powell et al., 1978). The average yield of rods (intact cells) was 70 % and 30% for rat and rabbit

respectively. The average cell volume differed between the two species, being 20774 μm^3 and 17464 μm^3 for rat and rabbit respectively. These results are summarised in table 8.1. It is not clear if the difference in size between the rat and rabbit myocytes represents a true difference or merely reflects the different proportion of rods and rounds in the preparations. The rounds must by necessity have a smaller volume than the rods, since a change in shape from a cylinder to a sphere, in the absence of a change in surface area, results in a smaller volume. In addition, as Coulter counter estimates of cell volume are based on the assumption that the cells are spheroid, this will lead to an under-estimation of cell volume when rods are present (Nash et al., 1979). A correlation of cell volume with % rods sugggests a linear relationship between these two variables (Fig. 8.2). Additional values are needed, especially for preparations of rat myocytes containing a low proportion of rods, and rabbit myocytes containing a high proportion of rods, before a definite conclusion concerning the difference in size between the two species can be drawn.

8.2.2 Preparation of Homogenate and Soluble Fraction from Ventricular Myocytes

Myocytes were prepared as described in the previous section and diluted in KRHG, 20 μm Ca^{2+}, 1% BSA to the concentration required in the assay. The cells were homogenised with a Polytron PT10 homogeniser at setting 4 for 30 seconds. This homogenate was either used directly or the soluble fraction was prepared from it by centrifugation at 100,000 x g for 60 min in a Beckman SW 65 rotor. The final supernatant was stored in 1ml aliquots at -20^{o}C until use.

Table 8.1

Summary of Rabbit and Rat Ventricular Myocyte Preparations

	Yield	Volume	
	Cells x 10^6	μm^3	% Rods
Rabbit	7.54±1.44 (11)	17464±563 (12)	30.7±4.7 (8)
Rat	3.44±0.80 (8)	20774±1119 (7)	70.2± .5 (11)

Figure 8.2

Comparison of the Volume of Rat and Rabbit Myocytes with the Number of Rods Present in the Preparation

Values from individual preparations of rat (□), and rabbit (△) ventricular myocytes. The correlation coefficient for the regression equation was 0.697.

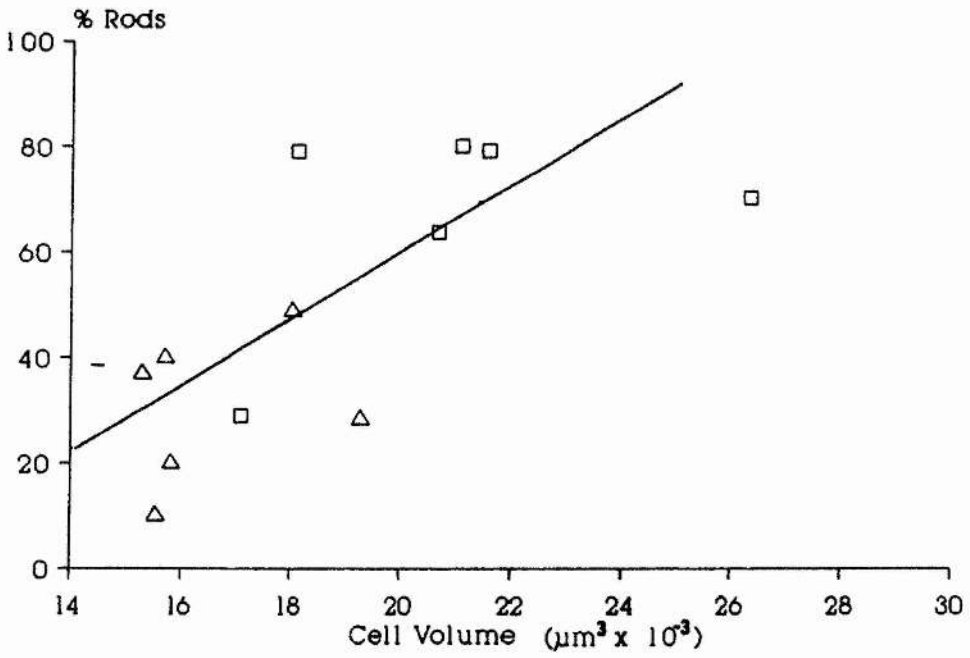

8.2.3 Preparation of Soluble Fraction from Rat Lung and Kidney.

The lungs and kidneys were rapidly removed from freshly killed 8-12 week old male Wistar rats (approx. 250g). The kidneys were dissected into two fractions, the cortex and medulla. The tissues were homogenised in 5-10 vol. 10 mM tris-HCl, pH 7.4, at 4°C with a Polytron PT10 Homogeniser at setting 4 for 3 x 20 sec bursts. The homogenate was centrifuged at 2000 x g for 15min in a Fisons Coolspin and the resulting supernatant was centrifuged at 100,000 x g for 60min using a Beckman SW 65 rotor. The final supernatant was stored in 1ml aliquots at -20°C until use.

8.2.4 Measurement of [^{125}I]ANP Degradation

8.2.4.i Principle of Assay

Proteins and large peptides form insoluble precipitates when mixed with certain acids such as trichloroacetic acid (TCA) and perchlororic acid (PCA). This property has been widely used to deproteinize biological fluids and cell extracts prior to analysis for low molecular weight, acid stable molecules such as glucose and amino acids. It has also been used to determine the extent of degradation of insulin and glucagon following incubation with proteases (Bohley et al., 1971). [^{125}I]-ANP can be completely precipitated by 5% TCA and this has been used to estimate peptide degradation

8.2.4.ii Protocol

[^{125}I]-ANP degradation was measured as the percentage of radiolabel not precipitated by 5% TCA. In a typical experiment with ventricular myocytes, 50 μl of cell suspension (1 to 5 x 10^4 cells/ml), or soluble

fraction isolated from these cells, were incubated for 15 min at 37°C with 25 µl [^{125}I]-ANP (100 or 200 pM), 25 µl buffer (50 mM Tris-HCl, pH 7.4), and peptide or protease inhibitor when indicated. Incubations were terminated by the addition of 100 µl of ice cold 10% bovine serum albumin followed by rapid sampling of 50 µl aliquots into 250 µl 6% TCA. After standing on ice for 15 min, precipitable radioactivity was separated from the non-precipitable by centrifuging for 2 min in a Beckman microfuge. The tip of the microfuge tube containing the pellet was removed and the radioactivity in both the pellet and supernatant were determined in a Packard Gamma Counter.

The percentage [^{125}I]-ANP degraded was defined as:

$$\left[\frac{\text{cpm in supernatant}}{\text{Total cpm}}\right] \times 100 - \text{Background}$$

The background was defined as the percentage radioactivity not precipitated by 5% TCA when [^{125}I-]-ANP was incubated in the absence of cells or cell extract. This ranged from 7 to 13% of the total radioactivity and did not vary with incubation time or temperature. These values of non-precipitable radioactivity are consistent with the HPLC analysis of [^{125}I]-ANP which indicated that approximately 10% of the radioactivity was not associated with the peptide (section 5.1).

The protocol for the measurement of the degradation of [^{125}I]-ANP by the soluble fractions from isolated kidney and lung was as described above, except that the incubation tubes contained 10 to 100 µg of protein from the appropiate fraction.

8.2.5 Degradation of ANP by rat ventricular myocytes

ANP was incubated with the soluble fraction prepared from rat

ventricular myocytes at 37°C as described for degradation of [^{125}I]-ANP above. At various times 100µl aliquots were removed and mixed with 33.3 µl of 0.4% TFA and 60% ACN. An assessment of ANP degradation was made by reverse phase HPLC using the system described in section 3.5.2. Briefly, 100 µl of incubation mixture were injected onto a C_{18} Spherisorb column (ODS2, Capital HPLC Specialists) and ANP and its degradation products were eluted with a linear gradient of 15% to 60% acetonitrile (ACN) in 0.1% trifluoroacetic acid (TFA), at a flow rate of 1ml/min and a slope of 0.9%/min. The elution was monitored at 220nm with a Gilson Holochrome UV monitor attached to a Rikadenki chart recorder. The concentration of ANP was linear with respect to peak area over the range 0.4 to 1.6 nmols (fig. 8.3).

Figure 8.3

A Standard Curve for the determination of ANP Concentration by HPLC

Known amounts of ANP, in the range 0.4 to 1.6 nmol, were analyzed by HPLC. (□), (×) and (✱) indicate determinations carried out on different days.

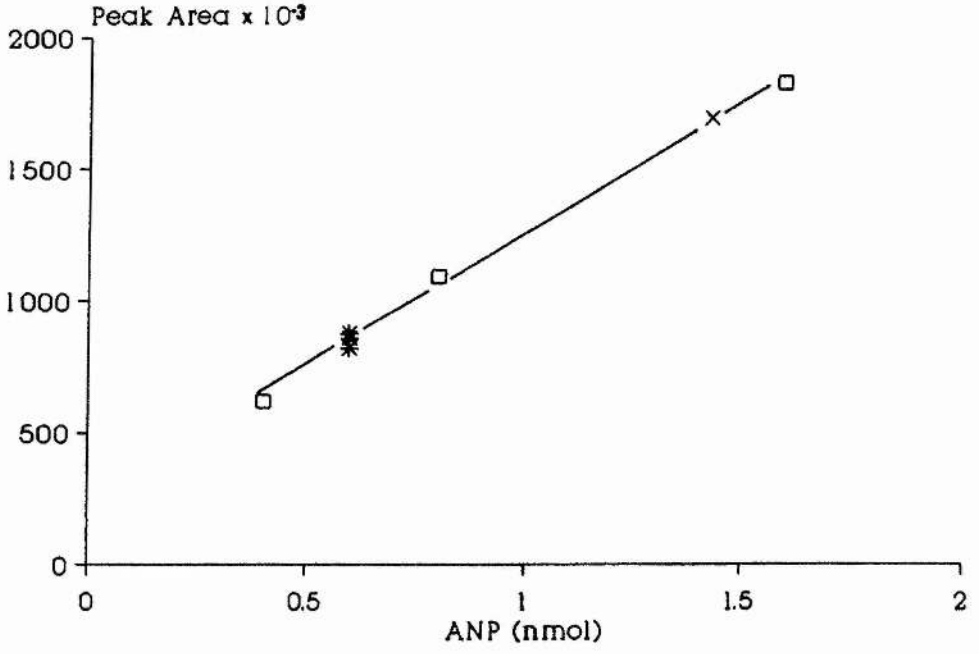

CHAPTER 9

9 Results of Degradation Studies

9.1 Preliminary Experiments with Rabbit Ventricular Myocytes

Incubation of rabbit ventricular myocytes with [^{125}I]-ANP resulted in the rapid degradation of the peptide, as measured by loss of acid precipitable radioactivity. Degradation was temperature sensitive, with significant breakdown occurring even at 4^{o}C (fig. 9.1). The initial rate of degradation was variable between preparations, with the mean rate being 3.38 $\pm$ 1.37 fmol/min per 10^6 cells (table 9.1). One possible source of this variation was the length of time the myocytes were preincubated prior to the measurement of degradative activity. To assess the effect of preincubation time on the rate of degradation, cells were preincubated for 0.5, 10 and 30 min at 37^{o}C, followed by the measurement of degradative activity in the whole preparation and in the 6,500g supernatant (fig 9.2). Approximately 50% of the degradative activity was located in the supernatant immediately following the resuspension of cells. This rose to nearly 70% of the total activity after 30 min. During this time the total degradative activity also slowly increased, suggesting that the factor(s) responsible for the degradation were leaching from the cells into the incubation medium. To assess the potential latent activity in the cells, myocytes were homogenised and degradation rate compared with that of the intact preparation (fig. 9.3). Homogenisation resulted in a 1.65- fold increase in degradation rate in this preparation. Preincubation of the homogenate for 15 minutes at 60^{o}C resulted in almost total loss of degradative activity (fig. 9.4).

Figure 9.1

Degradation of [^{125}I]-ANP by Rabbit Ventricular Myocytes

A representative experiment showing the degradation of [^{125}I]-ANP by rabbit ventricular myocytes, at 4°C (△—△) and 20°C (□—□). Each point is the mean ± SEM of triplicate determinations.

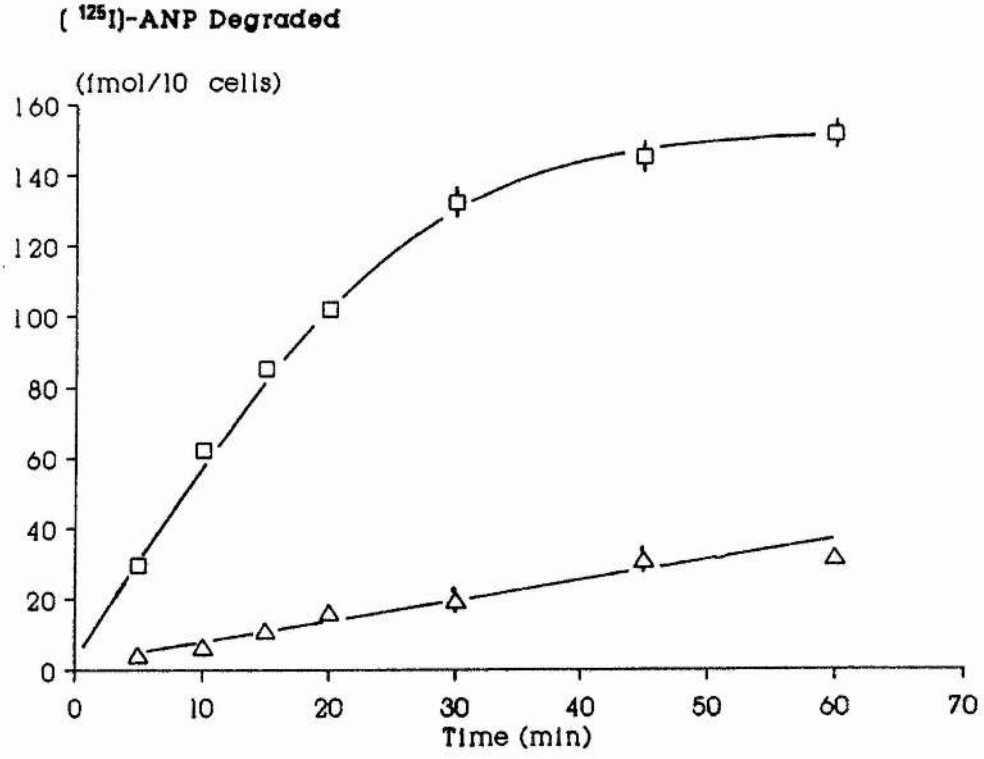

Table 9.1

$[^{125}I]$-ANP Degradation by Rabbit Ventricular Myocytes

Prep. No.	Temp °C	$[^{125}I]$-ANP Degraded fmol/min per 10^6 Cells		
		Cells/ml	Cells	Homogenates
1	4	$5x10^5$	0.567	-
1	20	$5x10^5$	6.033	-
2	20	$5x10^5$	1.377	2.376
3	20	$5x10^5$	2.650	-
4	20	$1.25x10^5$	-	21.04
5	20	$1.8x10^5$	-	3.566

Figure 9.2

Effect of Preincubation Time on [^{125}I]-ANP Degradation by Rabbit Ventricular Myocytes

Rabbit ventricular myocytes were preincubated at 37°C for the times indicated. [^{125}I]-ANP degradation associated with the cell suspension was subsequently measured over 30 min in the total cell suspension (△—△), or the 6,000 x g supernatant (□—□) at 20°C. Each value represents the mean ± SEM for 3 determinations.

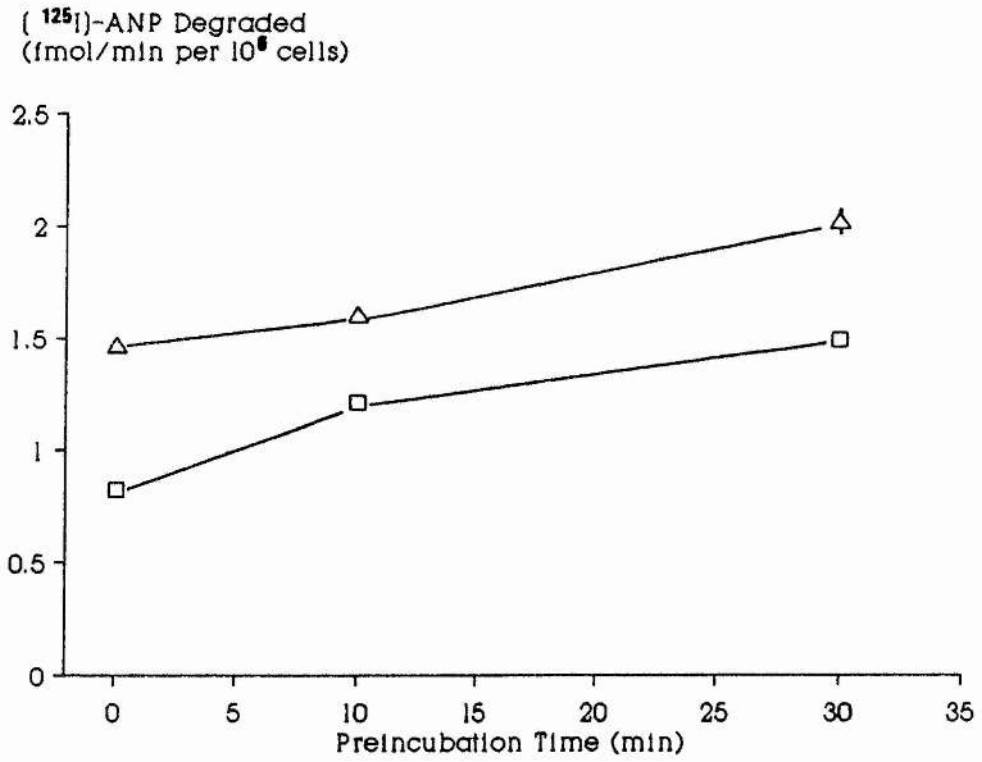

Figure 9.3

The Effect of Homogenization on the Degradation of [^{125}I]-ANP by Rabbit Ventricular Myocytes

The degradation of [^{125}I]-ANP by intact cells (△—△), or homogenates (□—□) of rabbit ventricular myocytes at 20°C. Each value represents the mean ± SEM of triplicate determinations.

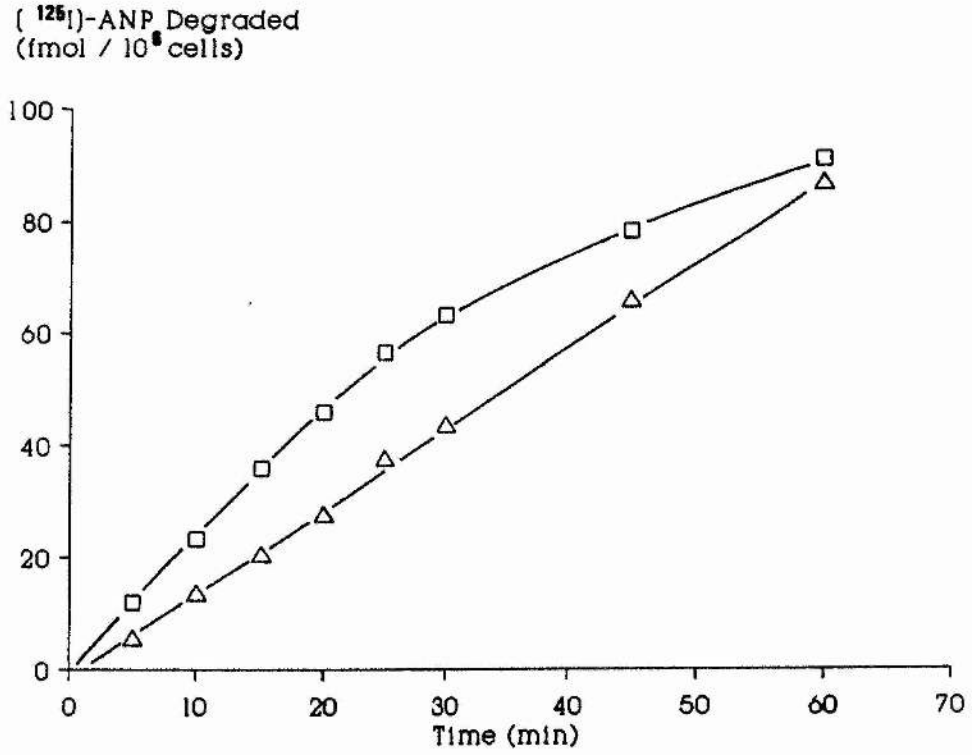

Figure 9.4

The Effect of Heat Treatment on [^{125}I]-ANP Degradation by Rabbit Ventricular Myocytes

Rabbit ventricular myocytes were preincubated for 15 min at 20°C (△—△) or 60°C (□—□) prior to the measurement of [^{125}I]-ANP degradation at 20°C. Each point represents the mean ± SEM for triplicate determinations.

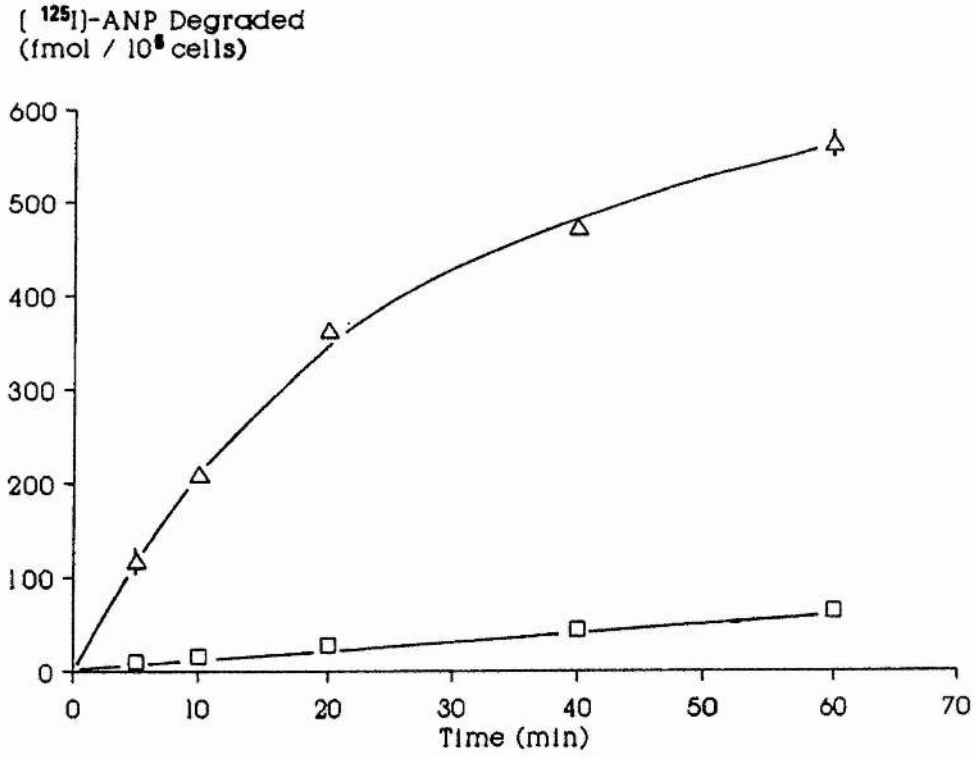

9.2 Experiments with rat ventricular myocytes

Similar degradation was observed during the incubation of [^{125}I]-ANP with rat ventricular myocytes (fig. 9.5). The initial degradation rate, at 20^{o}C, was 6.70 $\pm$ 1.12 fmol/min per 10^6 cells. This increased to 40.13 $\pm$ 10.49 fmol/min per 10^6 cells on homogenization (fig. 9.6). Experiments performed with intact rabbit ventricular myocytes suggested that at least some of this activity was soluble (fig. 9.3). To investigate if this was the case with rat ventricular myocytes, a soluble (cytosolic) fraction was prepared from an homogenate of these cells. The average degradative activity of the total homogenate, at 37^{o}C, was 68.08 $\pm$ 4.99 fmol/min per 10^6 cells. Of this approximately 60% of the degradative activity could be recovered from the supernatant (fig. 9.6).

9.3 Degradation of [^{125}-I]-ANP by the Soluble Fraction from Rat Ventricular Myocytes

The results of the investigations described above suggested that a substantial proportion of degradative activity was located in the soluble fraction isolated from rat ventricular myocytes. To further investigate the nature of this breakdown, several protease and peptidase inhibitors were tested for their effects on degradation (fig. 9.7). Incubation of soluble fraction with the general serine protease inhibitors phenylmethylsulphonyl fluoride (PMSF) and aprotinin, had no effect on activity. Amastatin, an inhibitor of a number of aminopeptidases also failed to inhibit degradation. SQ 20881, a peptidyl dipeptidase A inhibitor, produced a small reduction in degradative activity whilst bradykinin potentiating factor C (BPFC), an inhibitor of the same enzyme, and phosphoramidon, a

Figure 9.5

The Effect of Homogenization on the Degradation of [^{125}I]-ANP by Rat Ventricular Myocytes

The degradation of [^{125}I]-ANP by intact cells (△—△), or homogenates (□—□) of rat ventricular myocytes, measured at 20°C. Each value represents the mean ± SEM of triplicate determinations.

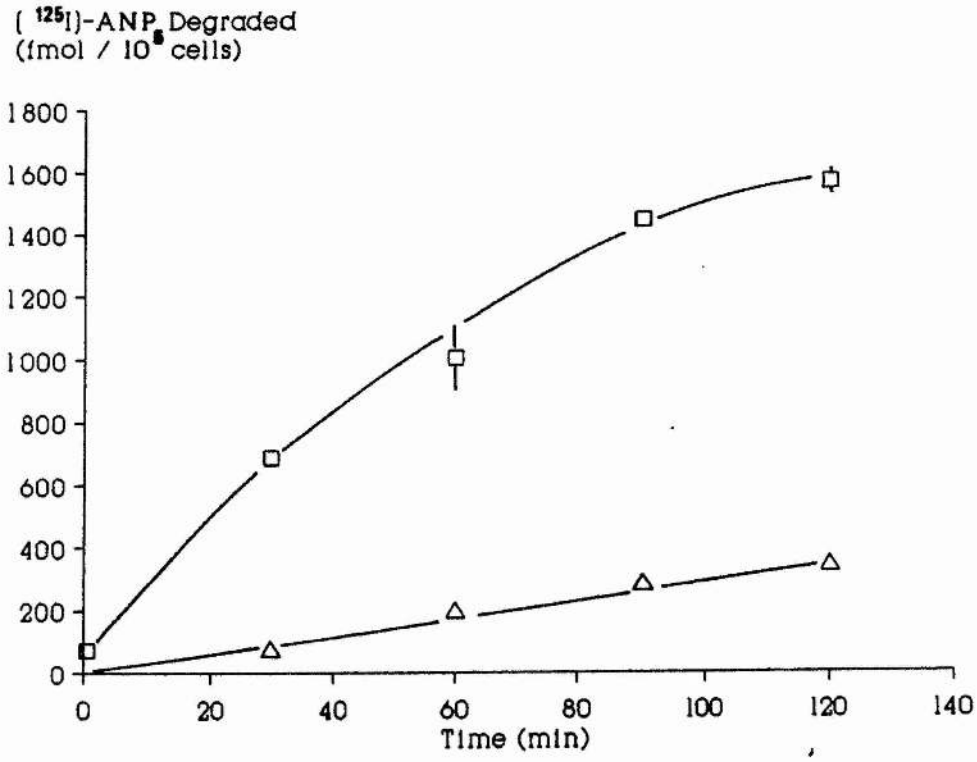

Figure 9.6

The Degradation of [^{125}I]-ANP by Rat Ventricular Myocytes

The degradation of [^{125}I]-ANP was measured in the preparations indicated. Each values is the mean ± SEM for the number of experiments indicated.

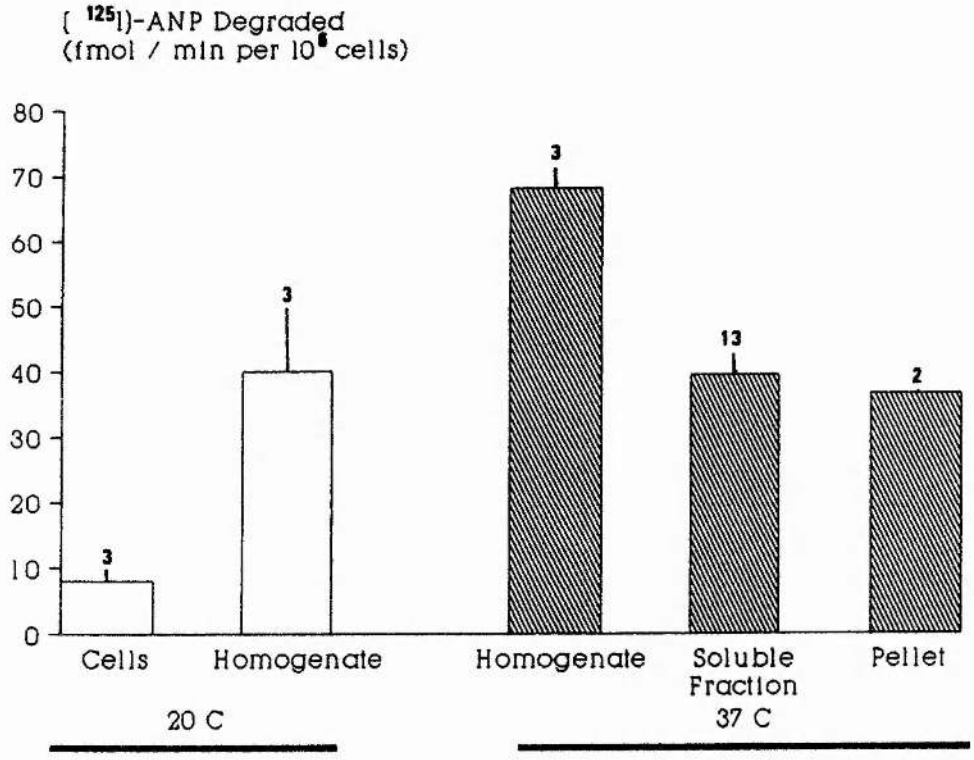

Figure 9.7

The Effect of Various Protease Inhibitors and Peptides on [^{125}I]-ANP Degradation by a Soluble Fraction from Rat Ventricular Myocytes

Degradation was measured over a 15 min incubation period at 37°C in the presence of various protease inhibitors. The soluble fraction was preincubated with EDTA and PCMB at 37°C for 45 min, prior to the measurement of degradation (▨). The results are the mean ± SEM. Significant differences from 100% are indicated by * = $p < 0.05$, ** = $p < 0.01$ and *** = $p < 0.001$ as determined using a two-tailed Student's *t*-test (unpaired solution).

% ([125]I)-ANP Degradation
120
100
80
60
40
20
0
45 min Preincubation
10⁻⁴M Casein
5x10⁻⁴M PMSF
10⁻⁴M Aprotinin
10⁻⁴M Amastatin
10⁻⁴M E-64
10⁻⁴M Phosphoramidon
10⁻⁴M 1,10 Phenanthroline
1mg/ml Bacitracin
10⁻³M EDTA
10⁻⁴M PCMB

% ([125]I)-ANP Degradation
120
100
80
60
40
20
0
10⁻⁶M ANP
3x10⁻⁶M Glucagon
10⁻⁴M Bradykinin
10⁻³M SQ20881
10⁻⁴M BPFC

specific inhibitor of endopeptidase 24.11, were without effect. The general metallo-proteinase inhibitors, 1,10-phenanthroline and EDTA, produced an almost total inhibition of degradation, as did the cysteine protease inhibitor, PCMB. EDTA and PCMB were only effective after a 45 min preincubation at 37°C. Epoxysuccinyl-leucyl-agmatine (E-64), an irreversible inhibitor of some cysteine proteinases also failed to reduce degradation. The most effective protease inhibitor tested was the bacterial antibiotic bacitracin, which totally inhibited degradation.

ANP, glucagon, and bradykinin were found to inhibit [^{125}I]-ANP degradation and the effect of these peptides was examined in more detail. ANP inhibited the degradation of [^{125}I]-ANP in a dose-dependent manner (fig. 9.8), with half-maximal inhibition occurring at $3.31 \pm 0.68 \times 10^{-7}$M (see table 9.2). Similar dose response curves were obtained for the inhibitory actions of glucagon and bradykinin (fig. 9.8), although these peptides were less potent than ANP, with half-maximal inhibition occurring at $6.95 \pm 1.88 \times 10^{-6}$M and $3.12 \pm 0.36 \times 10^{-5}$M respectively.

The effect of pH on degradative activity of the soluble fraction isolated from rat ventricular myocytes was also examined. The degradative activity was optimum at alkaline pH's, with a 30-fold stimulation of activity occurring as the pH was increased from 6.5 to 8.5 (fig. 9.9a). In order to assess whether changes in pH in the physiological range could increase degradative activity, [^{125} I]-ANP was incubated with the soluble fraction at pH 6.1 for 15 min. The pH was then increased to 7.5 and incubation continued for a further 15 min. This small alteration in pH resulted in almost a doubling of the

Figure 9.8

Dose Response Curves for the Inhibition of [^{125}I]-ANP Degradation by ANP, Glucagon, and Bradykinin

Degradation of [^{125}I]-ANP by a soluble fraction isolated from rat ventricular myocytes was measured over a 15 min incubation period at 37°C in the presence of increasing concentrations of ANP (□—□), glucagon (△—△), or bradykinin (◇—◇). The results are the mean ± SEM from at least 3 separate experiments.

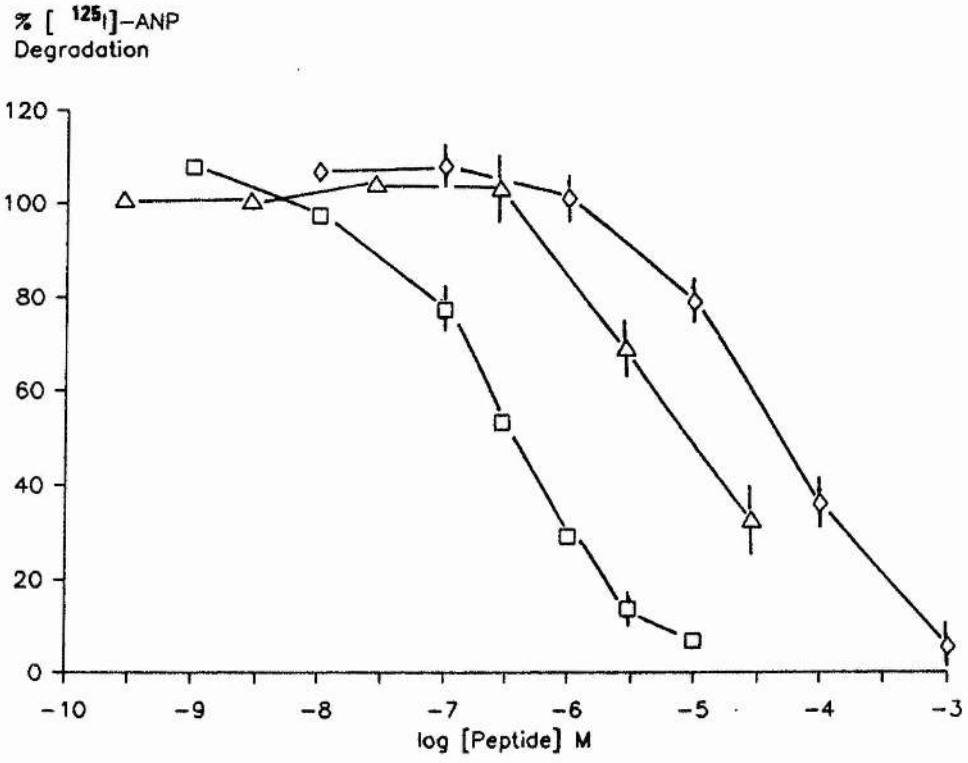

Figure 9.9

The Effect of pH on [^{125}I]-ANP Degradation by a Soluble Fraction Isolated from Rat Ventricular Myocytes

(a) [^{125}I]-ANP was incubated for 15 min at 37^{o}C with soluble fraction at the pH indicated. Each value is the mean ± SEM for 2 separate experiments in which degadation rate was determined in triplicate. (b) Time course of [^{125}I]-ANP degradation at pH 6.1 and 7.5; degradative activity was monitored either at pH 6.1 for all time points (△—△), or initially at pH 6.1 and then, after adjustment at pH 7.5 (□—□), as indicated by the arrow.

a

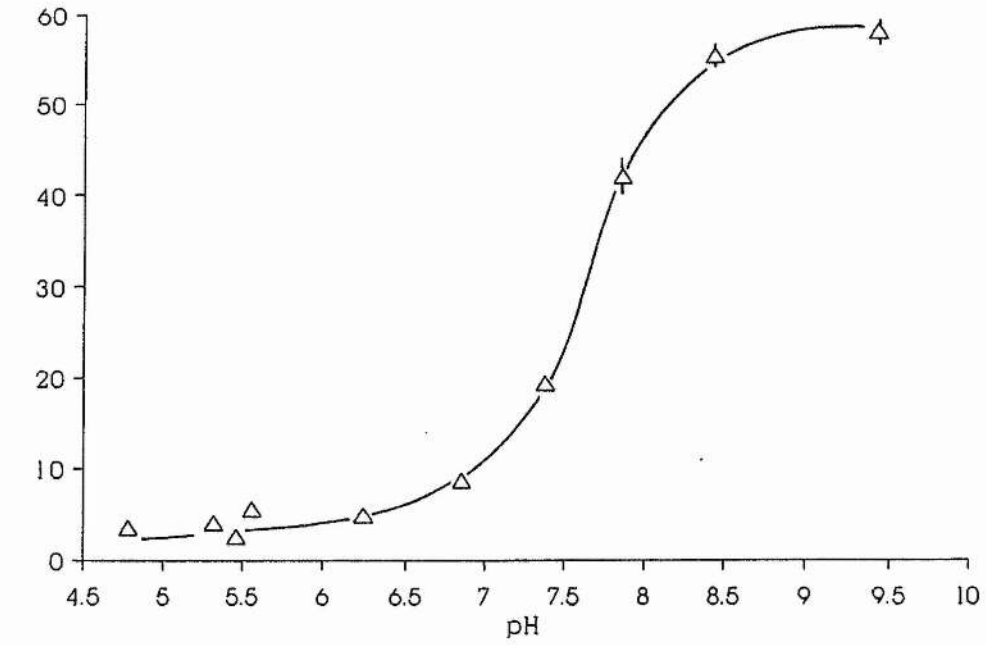
(125I)-ANP Degraded
(fmol/min/10^6 cells)
60
50
40
30
20
10
0
4.5
5
5.5
6
6.5
7
7.5
8
8.5
9
9.5
10
pH

b

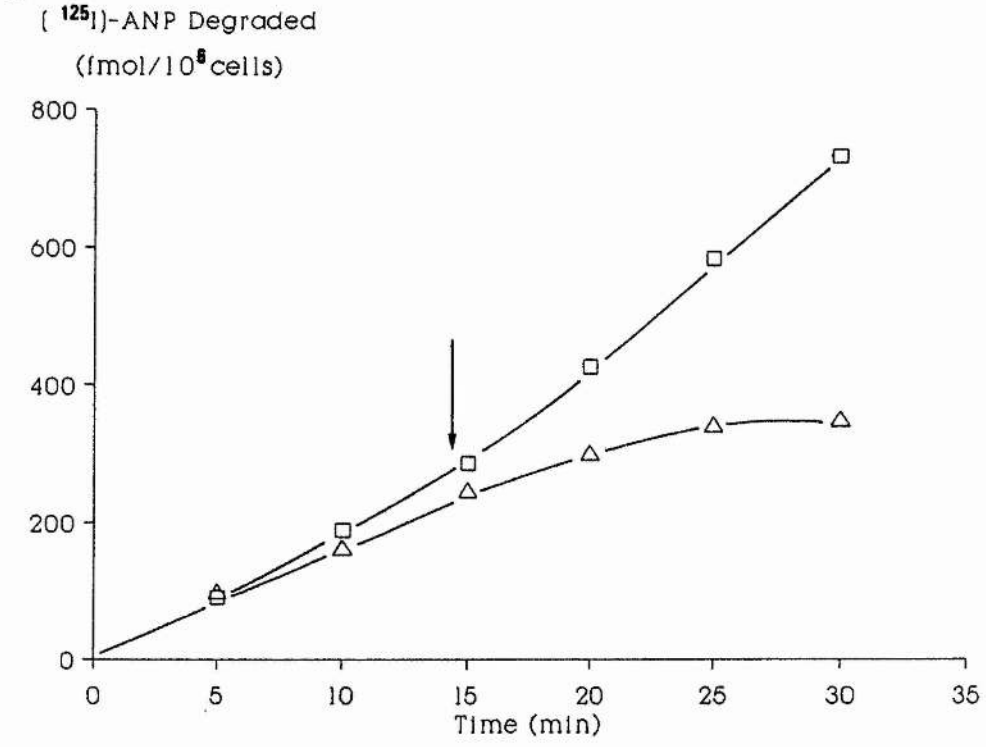
(125I)-ANP Degraded
(fmol/10^6 cells)
800
600
400
200
0
0
5
10
15
20
25
30
35
Time (min)

Table 9.2

Concentrations of ANP, Glucagon, and Bradykinin Required to Produce 50% Inhibition of Binding

The mean concentrations of ANP required to produce half maximal inhibiton of [^{125}I]-ANP degradation by the soluble fraction from lung, kidney cortex, kidney medulla, and ventricular myocytes, were compared using a two-tailed *t*-test (unpaired). * ($p<0.05$), and ** ($p<0.01$) indicates values which were signficantly different from those obtained from the kidney cortex preparation. Similar comparisons were made for glucagon. # ($p< 0.05$), and ## ($p<0.01$) indicates values which were significantly different from those obtained from the lung preparation.

	IC_{50}		
	ANP	Glucagon	Bradykinin
Lung	0.557±0.072*(3)	1.99±0.64 (4)	13.6±3.1 (3)
Kidney Cortex	1.04±0.13 (3)	6.74±1.73# (3)	20.3±5.4 (3)
Kidney Medulla	0.463±0.075*(3)	9.89±1.52##(4)	26.6±9.5 (3)
Vent.Myocytes	0.331±0.068**(3)	6.95±1.88 (3)	31.2±3.6 (3)

degradation rate, from 16.1 fmol/min per 10^6 cells to 29.7 fmol/min per 10^6 cells (fig. 9.9b).

9.4 HPLC Analysis of ANP Degradation by Soluble Fraction from Rat Ventricular Myocytes

Reverse phase HPLC was used to examine the degradation of unlabelled ANP by the soluble fraction isolated from rat ventricular myocytes. Degradation of ANP was both rapid and complex, with several products being formed (fig. 9.10). After only 2 min incubation at 37°C, approximately 50% of the ANP was degraded, and by 20 min ANP was undetectable (fig. 9.11). There was a corresponding appearance of two products, which eluted at 19.42% ACN (peak 1) and 22.77% ACN (peak 2). Peak 1 increased steadily with increasing incubation time whilst peak 2, after an initial decline, reached a steady state at a level slightly higher than its initial value. After 5 min incubation a third product eluted with 34.97% ACN (peak 3). This increased slowly to reach a steady state after 40min (fig. 9.12a).

During the course of the incubation two other major products appeared, eluting at 43.52% ACN (peak 4) and 44.99% ACN (peak 5) respectively. These products showed a steady increase over the first 15 to 20min, followed by a slow decline to almost undetectable levels (fig. 12b).

9.5 Degradation of [^{125}-I]-ANP by Soluble fraction Prepared from Rat Lung and Kidney

To investigate the tissue specificity of the proteolytic factor(s) responsible for degrading [^{125}I]-ANP, similar experiments were performed with the soluble fraction isolated from rat kidney cortex, kidney medulla and lung.

Figure 9.10

Profile of ANP Degradation Products

The absorbance profile of the products eluted by HPLC from a C_{18} reverse-phase column, following incubation of ANP with the soluble fraction from rat ventricular myocytes at 37°C for (a) 0 min, (b) 5 min, and (c) 40 min. Absorbance was measured at 220 nm.

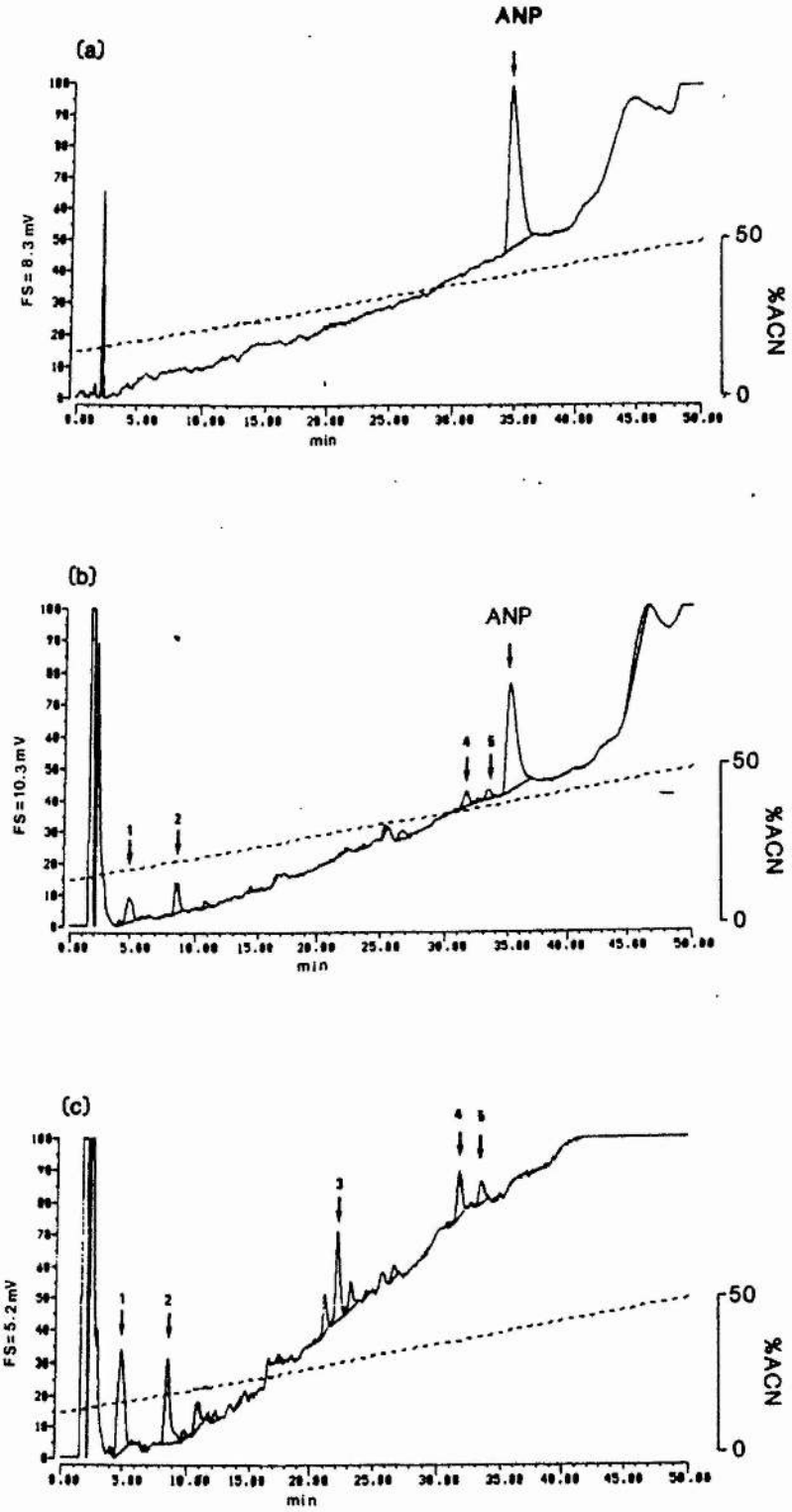
(a)
ANP
FS=8.3mV
50
%ACN
0
min
(b)
ANP
1
2
4
5
FS=10.3mV
50
%ACN
0
min
(c)
1
2
3
4
5
FS=5.2mV
50
%ACN
0
min

Figure 9.11

The Degradation of ANP following Incubation with Soluble Fraction from Rat Ventricular Myocytes

ANP was incubated with soluble fraction at 37°C for the times indicated. ANP levels were monitored by absorbance at 220 nm.

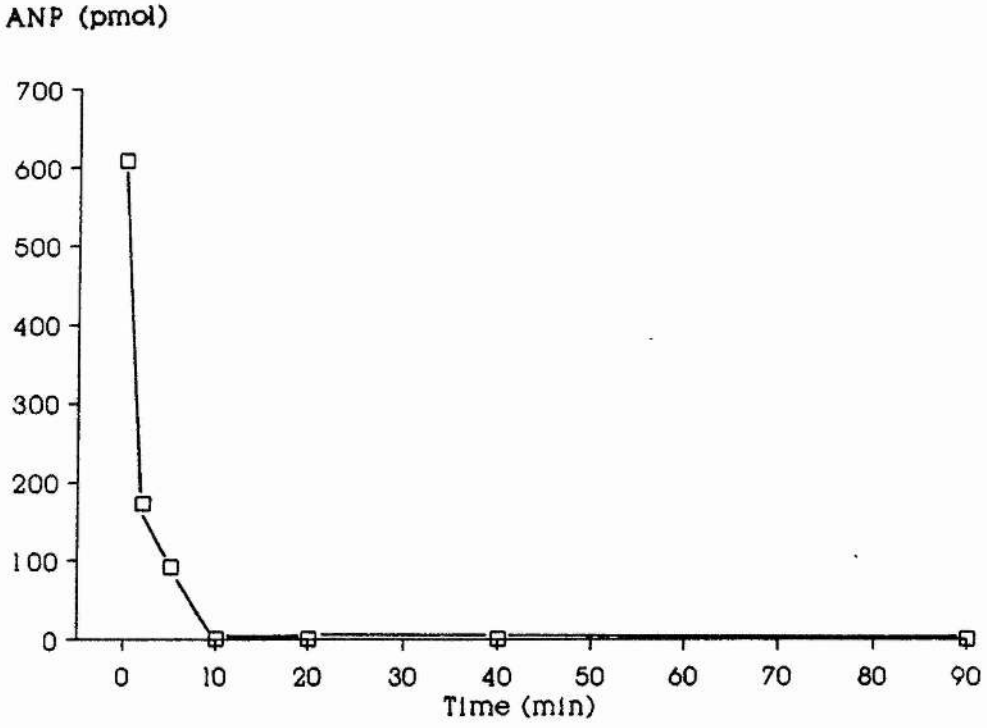

Figure 9.12

Time Course for the Degradation Products of ANP

(a) Peaks 1 (□——□), 2 (x——x), and 3 (△——△). (b) Peaks 4 (◊——◊), and 5 (✱——✱) as indicated in fig. 9.10. A Peak Area of 100,000 is equivalent to 0.01 AU.min.

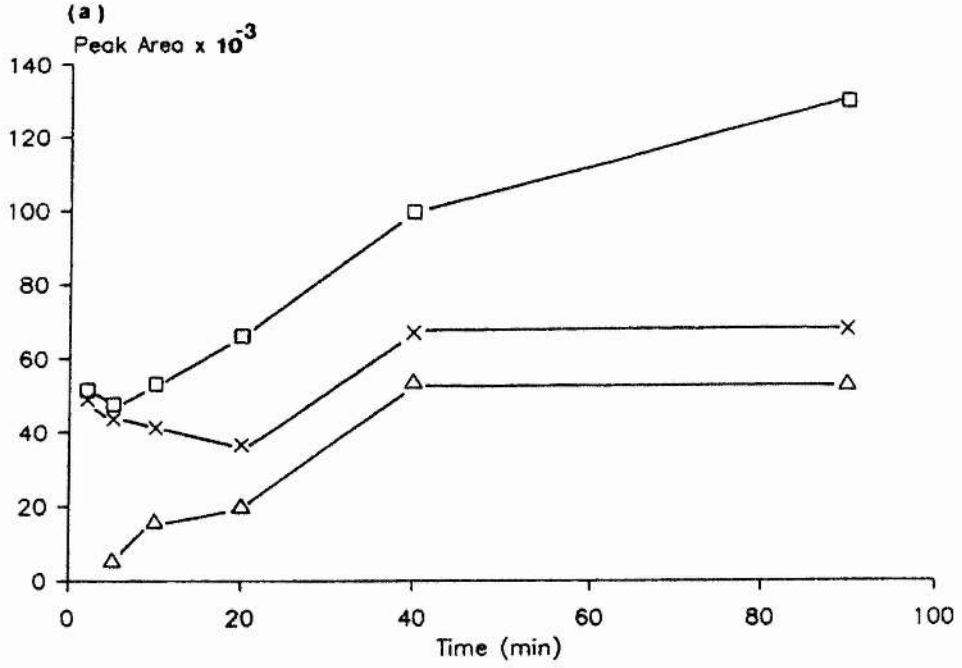

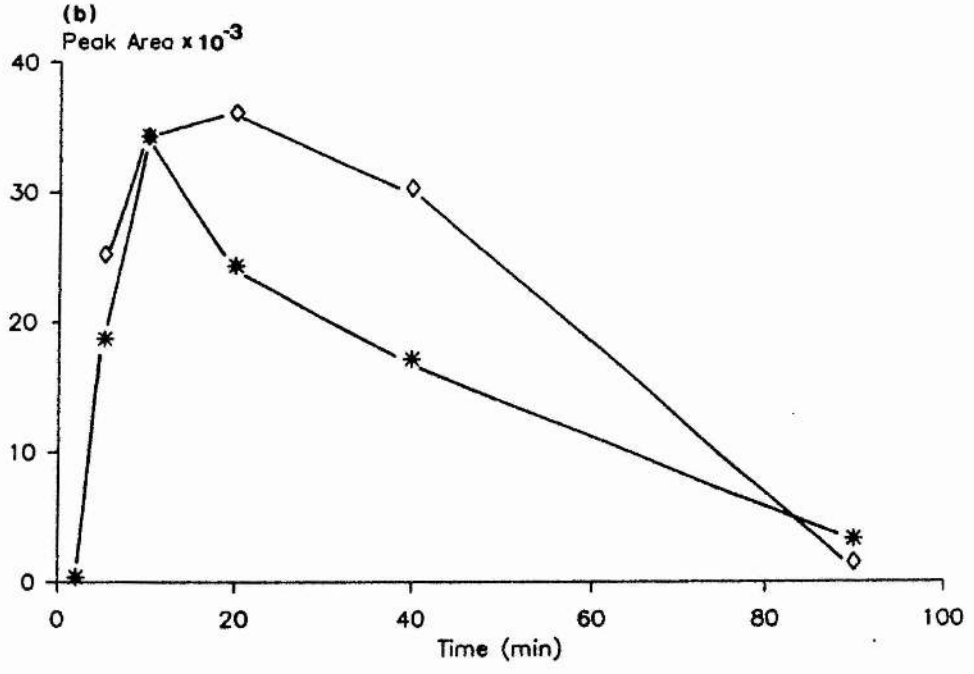

Although [^{125}-I]-ANP was degraded by all preparations, the rate of degradation was significantly lower in the soluble fraction from the lung than from the kidney (table 9.3). There was no difference in the degadation rates of the two kidney preparations (table 9.3). The effects of various protease inhibitors on [^{125}I]-ANP degradation rate were examined. The incubation of [^{125}I]-ANP with soluble fraction prepared from rat kidney cortex, kidney medulla and lung, in the presence of phosphoramidon, E-64, amastatin, and aprotinin, had little or no effect on the rate of degradation by any of the preparations (figs. 9.13, 9.14 and 9.15). Similar incubations in the presence of 1,10-phenanthroline and bacitracin reduced degradation by 70 to 80% in all preparations. PCMB only produced a significant inhibition of degradative activity in the kidney medulla soluble fraction. Likewise, EDTA only inhibited activity in the kidney cortex soluble fraction. There was, however, a tendency for these compounds to decrease degradative activity in all preparations by a small amount.

ANP, glucagon, and bradykinin were all effective at reducing degradation (table 9.3), and the dose response curves to these compounds were examined in more detail (figs. 9.16, 9.17, and 9.18). ANP inhibited degradation in a dose-dependent manner, with half-maximal inhibition occurring at similar concentrations in the kidney medulla and lung preparations, although ANP was slightly less potent at inhibiting degradation in the kidney cortex (table 9.2). Glucagon was equipotent at inhibiting degradation by both kidney preparations, and was significantly more potent at inhibiting degradation by the lung than the kidney. Bradykinin was also most effective at inhibiting degradation by the lung. The order of potency for inhibition of degradation by these three peptides was ANP > glucagon > bradykinin in

all preparations.

Table 9.3

Summary of the Degradation of [^{125}I]-ANP by a Soluble Fraction Prepared from Rat Heart, Lung, and Kidney

Mean basal degradative activities of the soluble fractions isolated from lung, kidney cortex, and kidney medulla were compared using two tailed *t*-test (unpaired). The basal activities of both kidney fractions were significantly higher than that obtained from lung. *** $p < 0.001$

	[^{125}I]-ANP Degraded			
	fmol / min per mg protein			fmol/min 10^6 cells
	Lung	Kidney Cortex	Kidney Medulla	Myocytes
Basal	4.50 (17) ±0.68	11.10 (19)*** ±1.16	14.48 (17)*** ±2.16	41.94 (26) ±2.88
ANP (10^{-5}M)	0.41 (4) ±0.11	2.05 (4) ±0.43	1.23 (4) ±0.34	6.13 (3) ±2.07
Glucagon ($3x10^{-5}$M)	1.25 (6) ±0.37	5.30 (5) ±0.23	4.68 (6) ±0.78	6.20 (4) ±1.19
Bradykinin (10^{-3}M)	1.50 (4) ±0.55	4.83 (4) ±0.61	3.17 (4) ±1.04	21.00 (4) ±2.64

Figure 9.13

The Effect of Various Protease Inhibitors on [^{125}I]-ANP Degradation by a Soluble Fraction from Rat Lung

Degradation was measured over a 15 min incubation period, at 37°C. The soluble fraction was preincubated with EDTA and PCMB at 37°C, for 45 min, prior to the measurement of degradation (▨). The results are the mean ± SEM for the number of experiments indicated (see appendix V). Significant differences from 100% are indicated by ** = $p < 0.01$ as determined using a two-tailed Student's *t*-test (unpaired solution).

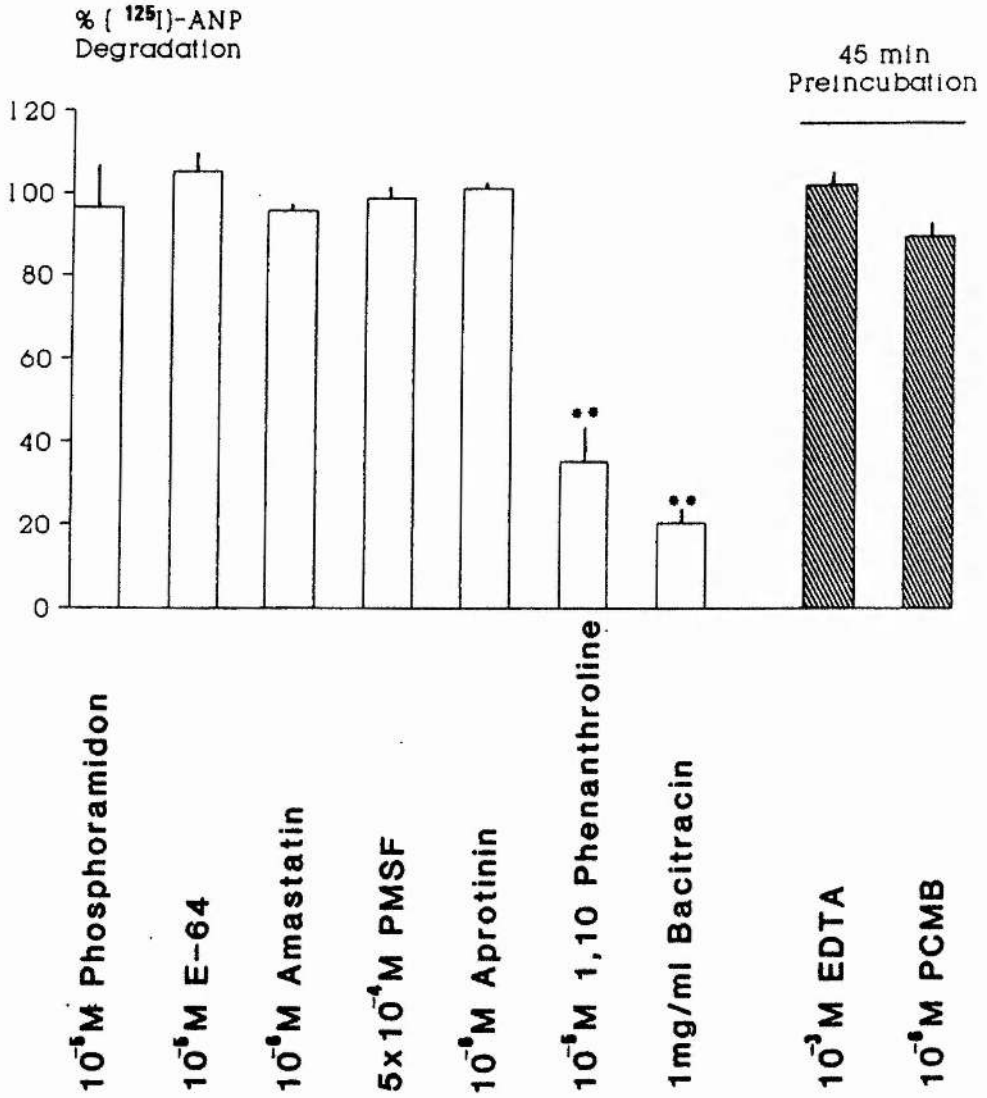

Figure 9.14

The Effect of Various Protease Inhibitors on [^{125}I]-ANP Degradation by a Soluble Fraction from Rat Kidney Cortex

Degradation was measured over a 15 min incubation period, at 37°C. The soluble fraction was preincubated with EDTA and PCMB at 37°C, for 45 min, prior to the measurement of degradation (▨). The results are the mean ± SEM for the number of experiments indicated (see appendix V). Significant differences from 100% are indicated by * = $p < 0.05$, ** = $p < 0.01$ and $p < 0.001$ as determined using a two-tailed Student's *t*-test (unpaired solution).

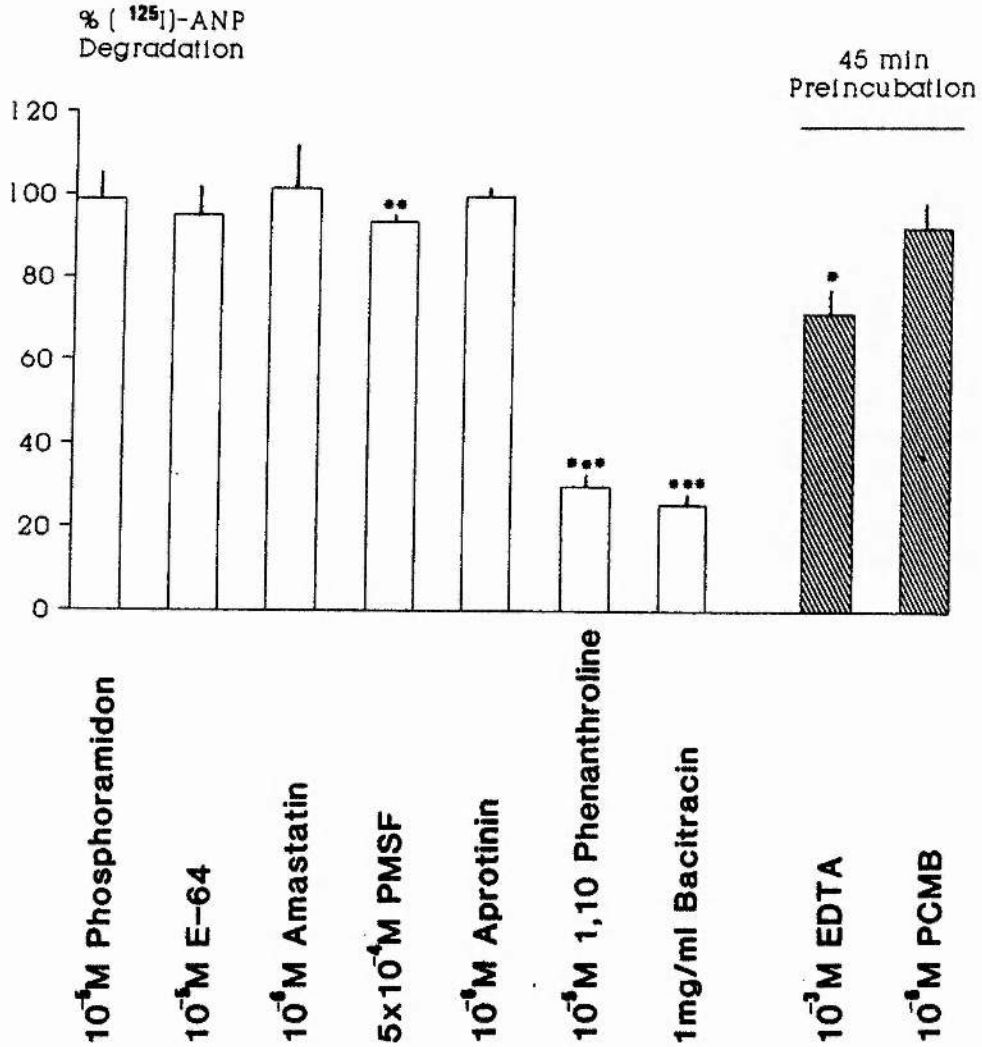

Figure 9.15

The Effect of Various Protease Inhibitors on [^{125}I]-ANP Degradation by a Soluble Fraction from Rat Kidney Medulla

Degradation was measured over a 15 min incubation period at 37°C. The soluble fraction was preincubated with EDTA and PCMB at 37°C for 45 min, prior to the measurement of degradation (▨). The results are the mean ± SEM for the number of experiments indicated (see appendix V). Significant differences from 100% are indicated by * = $p < 0.05$,** = $p < 0.01$ and $p < 0.001$ as determined using a two-tailed Student's *t*-test (unpaired solution).

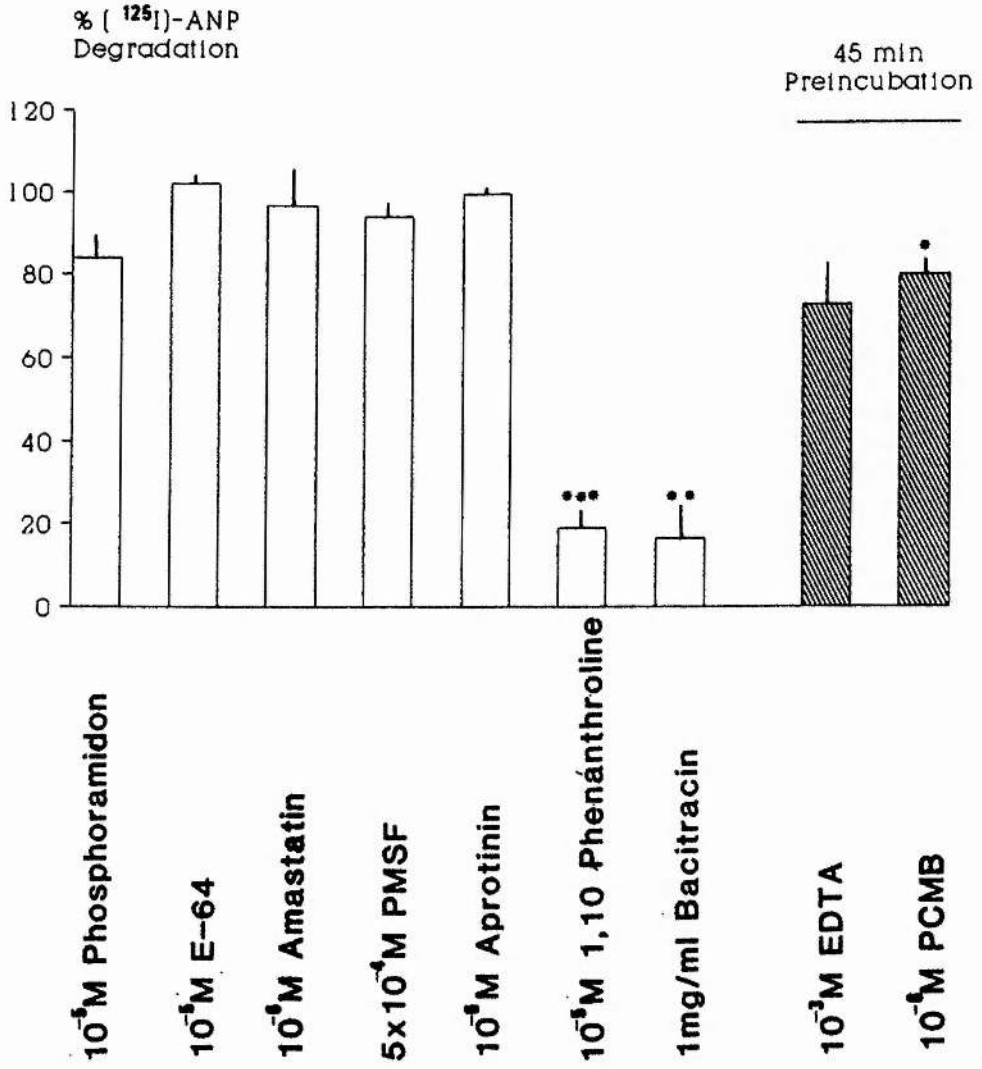

Figure 9.16

Dose Response Curves for the Inhibition of [^{125}I]-ANP Degradation by ANP, Glucagon, and Bradykinin

Degradation of [^{125}I]-ANP by a soluble fraction isolated from rat lung was measured over a 15 min incubation period at 37°C in the presence of increasing concentrations of ANP (□—□), glucagon (△—△), bradykinin (◇—◇). The results are the mean ± SEM for at least 3 separate experiments.

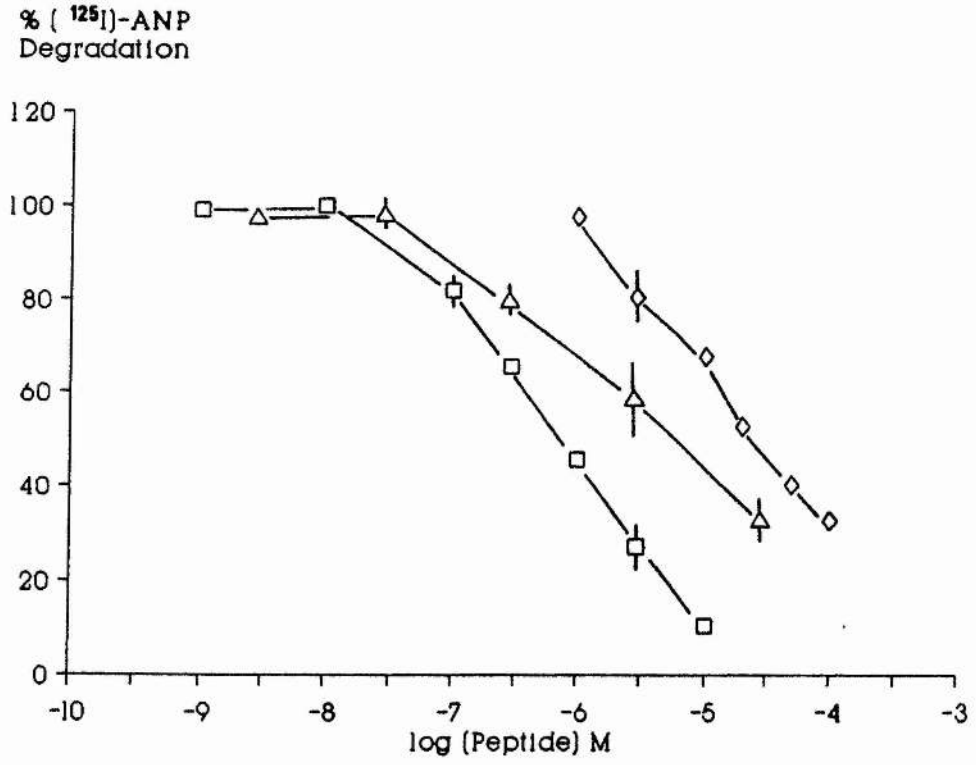

Figure 9.17

Dose Response Curves for the Inhibition of [^{125}I]-ANP Degradation by ANP, Glucagon, and Bradykinin

Degradation of [^{125}I]-ANP by a soluble fraction isolated from rat kidney cortex was measured over a 15 min incubation period at 37°C in the presence of increasing concentrations of ANP (□—□), glucagon (△—△), and bradykinin (◇—◇). The results are the mean ± SEM for at least 3 separate experiments.

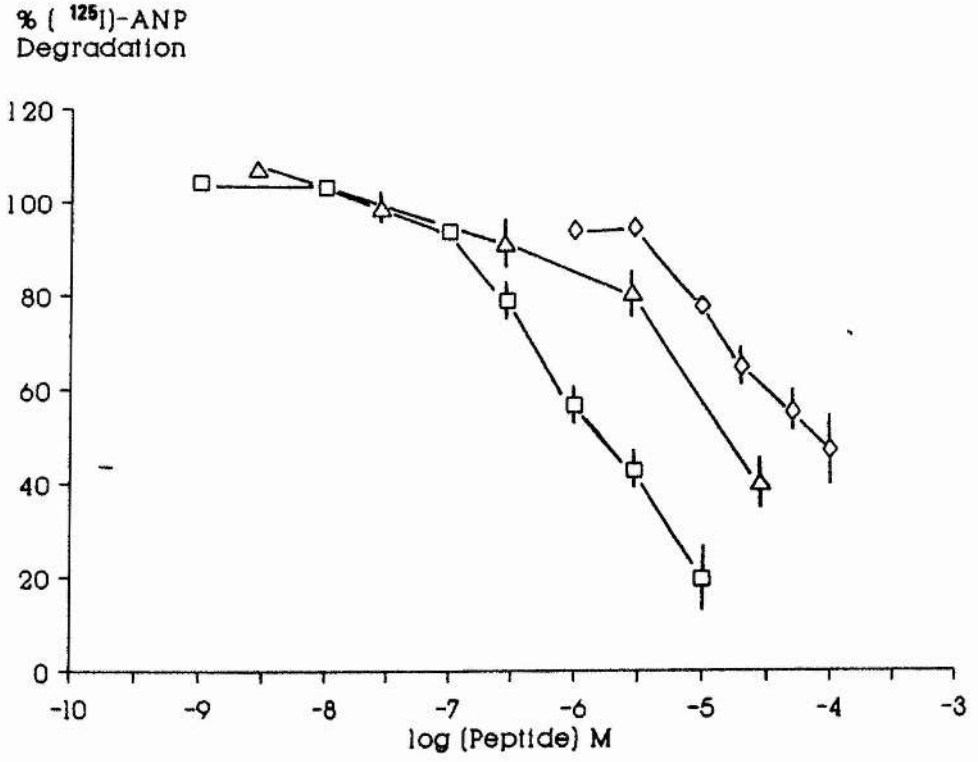

Figure 9.18

Dose Response Curves for the Inhibition of [^{125}I]-ANP Degradation by ANP, Glucagon, and Bradykinin

Degradation of [^{125}I]-ANP by a soluble fraction isolated from rat kidney medulla was measured over a 15 min incubation period at 37°C in the presence of increasing concentrations of ANP (□—□), glucagon (△—△), or bradykinin (◇—◇). The results are the mean ± SEM for at least 3 separate experiments.

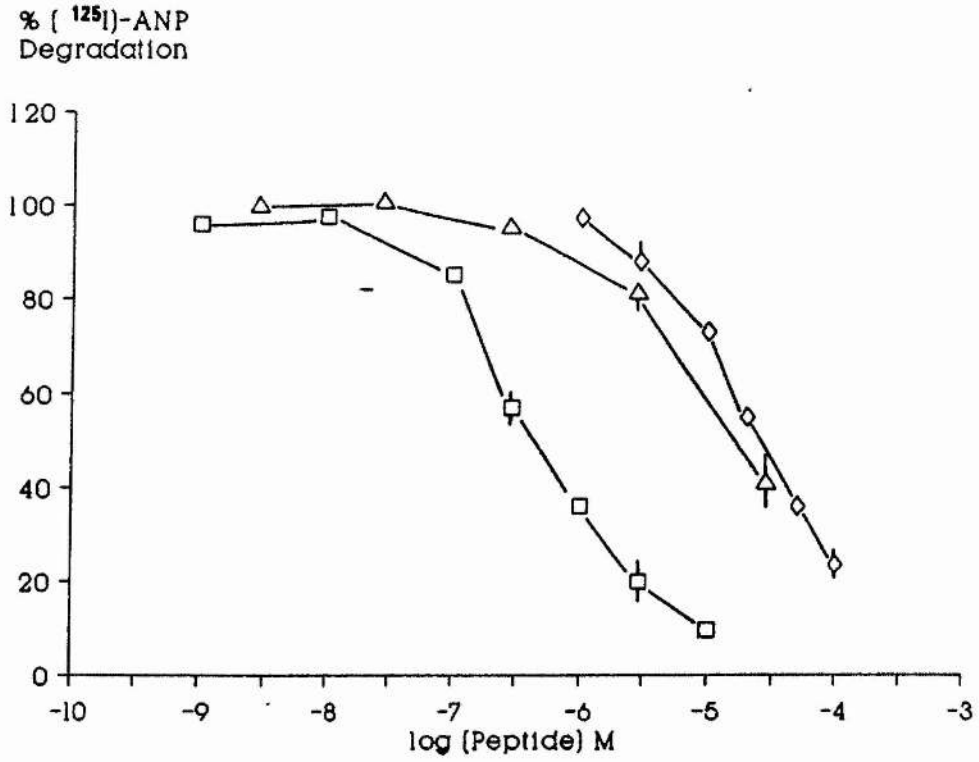

CHAPTER 10

10 Discussion of Degradation Experiments

10.1 Introduction

Following interaction with a membrane receptor, many peptide hormones are degraded by one of two mechanisms. The major pathway is internalization through receptor- mediated endocytosis, followed by degradation in the lysosome (King & Cautrecasas, 1981; Anderson & Kaplan, 1983). Examples of this process are the degradation of insulin by adipocytes (Marshall, 1985ab), and the degradation of epidermal growth factor by human fibroblasts (Wiley et al, 1985). Alternatively, some peptides have been shown to be degraded by membrane-bound proteinases, and this is the case with the hydroylisis of bradykinin,and angiotensins I, II, and III by pig kidney membranes (Stephenson & Kenny, 1987b). Elucidation of the processes by which ANP is degraded is of primary importance to an understanding of the regulation of the levels of this peptide in the body, and ultimately to an understanding of its physiological actions.

There have been several reports on the degradation of ANP during incubation of this peptide with kidney membranes (Napier et al., 1984; Koehn et al., 1987; Stephenson & Kenny, 1987a). Proteolytic activity in these preparations is most likely due to the action of the metalloproteinase, endopeptidase-24.11 (Stephenson & Kenny, 1987a). In addition, the conversion of ANP_{5-27} to ANP_{5-25} by enzymes isolated from bovine atria (Harris & Wilson 1985) and human atria (Sakharov et al., 1988) have also been described. These enzymes appear to be isozymes of pulmonary peptidyl dipeptidase A (EC 3.4.15.1).

10.2 Experiments with Intact and Homogenates of Rat and Rabbit Ventricular Myocytes

These experiments were performed to assess the extent of the degradation which occurs when [^{125}I]-ANP is incubated with isolated ventricular myocytes, and to determine the cellular localization of this degradative activity. The results clearly show that incubation of [^{125}I]-ANP with rat and rabbit ventricular myocytes results in the rapid degradation of the radiolabelled peptide. Degradative activity was increased when the cells were homogenised, suggesting that at least part of the activity was of intracellular origin. Degradative activity was also temperature sensitive, increasing in rate with increasing incubation temperature up to 37^{o}C. However, activity was almost totally abolished by a 15 min pre-incubation at 60^{o}C. These results strongly suggest that the factor(s) responsible for the degradation of radiolabelled ANP is proteinaceous in nature.

After incubating the myocytes for a short period, a significant amount of degradative activity was located in the incubation medium, this suggesting that the factor(s) responsible for degradation was leaching from the cells into the medium. Since homogenisation increased degradative activity, it is likely that the number of damaged cells in the preparation, in combination with the length of time the cells are incubated prior to the assay of [^{125}I]-ANP degradation, will effect the total measurable activity. These variables may account for some of the variation observed in the proteolytic activity of intact myocyte suspensions. Further experiments on the cellular distribution of the degradative activity in homogenates of rat ventricular myocytes, localised more than 60% of this activity to the 100,000 x g

supernatant (cytosolic fraction).

It is therefore concluded that degradative activity, observed when [^{125}I]-ANP is incubated with ventricular myocytes, is due to the action of unspecified protease(s) in the preparation. It is further concluded that at least part of this activity is of intracellular origin, and soluble in nature.

10.3 Experiments with a Soluble Fraction Isolated from Rat Ventricular Myocytes

At least 50% of the proteolytic activity found in homogenates of rat ventricular myocytes was located in the soluble or cytosolic fraction, and is therefore unlikely to be a result of the membrane-bound proteases described in section 10.1. In order to elucidate the nature of this soluble activity, further experiments were carried out. An initial classification of protease activity can be made on the basis of the relative action of a number of protease inhibitors on the preparation (Knight, 1986). This approach was used to assess the protease activity present in the soluble fraction isolated from rat ventricular myocytes. Since 1% BSA was present throughout the incubations, and casein was without effect on the degradative activity, it is unlikely that degradation in this preparation occurs by the action of non-specific proteases.

Incubation of [^{125}I]-ANP with the soluble fraction isolated from rat ventricular myocytes in the presence of EDTA or 1,10 phenanthroline resulted in at least an 80% reduction of degradative activity. Both EDTA and 1,10 phenanthroline are general metalloproteinase inhibitors, which act by chelation of the metal ion at the active site enzyme. The

general serine proteinase inhibitors, phenylmethylsulphonyl fluoride (PMSF) and aprotinin, were without effect. This profile of inhibition, that is, a suppression of activity by EDTA and 1,10 phenatholine, in the absence of an effect with serine proteinase inhibitors, is a good indication of the presence of a metalloproteinase (Powers & Harper 1986). The general cysteine proteinase inhibitor, p-chloromercuric benzoate (PCMB), also inhibited degradation, indicating a requirement of free sulphydryl groups for proteolytic activity (Camargo et al., 1973; Rich, 1986). Both ETDA and PCMB required preincubation with the ventricular cell suspension in order to inhibit activity. This suggest these compounds act as 'slow-binding inhibitors', possibly interacting with the protease with normal Michaelis Menten kinetics, but followed by a slow re-arrangement of the enzyme-inhibitor complex (Knight, 1986)

The lack of inhibition by epoxyl succinyl-leucyl-agmatine (E-64), a specific inhibitor of a number of cysteine proteinases, precludes the presence of papain and cathepsin B, H, and L activity in this preparation (Barrett et al., 1982). Other specific protease inhibitors were tested for their effect on degradative activity. Amastatin, an inhibitor of a number of metallo-exopeptidases, including leucine amino peptidase, tyrosine aminopeptidase, and tripeptidyl- and tetrapeptidyl-aminopeptidases (Powers & Harper, 1986), was also without effect. The contribution of these enzymes to degradation can therefore be discounted. Phosphoramidon, a specific inhibitor of endopeptidase 24.11 (Suda, et al., 1973; Kenny, 1977) also failed to reduce proteolytic activity.

ANP, glucagon and bradykinin were all effective inhibitors of

degradative activity. Comparison of the amino acid composition of ANP and bradykinin reveals the presence of the dipeptide sequences phenylalanine-arginine at the carboxyl-termini of both peptides (fig. 10.1). These amino acids are known to be cleaved by peptidyl dipeptidase A in bradykinin, and are a potential site of hydrolysis in ANP or related peptides (Harris & Wilson, 1985). Removal of these residues from bradykinin is potently inhibited by bradykinin potentiating factor C (BPFC) and SQ 20881 (Erdos 1976). BPFC had no effect on degradation rate, although a small reduction in activity was observed in the presence of SQ 20881. It is possible that peptidyl dipeptidase A, or a similar enzyme, may be responsible for some of the degradation observed, but is unlikely to account for all of the activity. A similar comparison of the amino acid sequences for glucagon and ANP reveals no obvious sequence homology between the two peptides (fig. 10.1). Bacitracin, a potent inhibitor of glucagon degradation in the liver, also suppresses proteolytic activity in the present experiments. This may indicate a common mechanism of inactivation.

Degradation of radiolabelled ANP by ventricular soluble fraction is optimum at pH 9.0, and small changes in pH from 6.1 to 7.5 produce a marked effect on degradative activity. These results raise the possibility that changes in pH in the physiological range may regulate proteolytic activity.

A group of enzymes with similar inhibition profiles have been described and termed metal-dependent cysteine proteinases. These enymes include cytosol insulin-glucagon proteinase, calcium-dependent cysteine proteinase I and II, collagenase-like peptidase, and lens

Ser-Leu-Arg-Arg-Ser-Ser-Cys-Phe-Gly-Gly Arg-Ile-Asp-Arg-Ile-Gly-Ala-Gln-Ser-Gly-Leu-Gly-Cys-Asn-Ser-Phe-Arg-Try

Atrial Natruretic Peptide (rat)

His-Ser-Gln-Gly-Thr-Phe-Thr-Ser-Asp-Tyr-Ser-Lys-Tyr-Leu-Asp-Ser-Arg-Arg-Ala-Gln-Asp-Phe-Val-Gln-Trp-Leu-Met-Asn-Thr

Glucagon

Arg-ProPro-Gly-Phe-Ser-Pro-Phe-Arg

Bradykinin

Figure 10.1

The Amino Acid Sequence of ANP, Glucagon, and Bradykinin

neutral proteinase and brain neutral endopeptidases (Barrett and McDonald, 1980). Calcium-dependent proteinase I utilises casein and albumin as a substrate, and calcium-dependent proteinase II is labile above pH 8.0. It is therefore unlikely that these enzymes are responsible for the degradative activity observed in this preparation. Lens neutral proteinase is also unlikely to account for degradation as this enzyme is only poorly inhibited by 1,10 phenanthroline. Cytosol insulin-glucagon proteinase, in addition to having a similar inhibition profile to the activity in ventricular soluble fraction, also possesses a similar affinity for glucagon . The K_m for degradation of glucagon by this enzyme is 3×10^{-6}M (Duckworth, 1976; Barrett and McDonald, 1980). This value which is very close to that observed for glucagon inhibition of [^{125}I]-ANP degradation by ventricular soluble fraction

Two brain neutral endopeptidases have also been described which have similar characteristics to the preparation described here. These enzymes, endopeptidase A and B, have been purified from a soluble fraction of rabbit brain and appear to play a role in the central nervous system in the hydrolysis of small peptides such as bradykinin, angiotensin I and II and LH-RH (Camargo et al., 1979). The pH optimum for endopeptidase B hydrolysis of bradykinin is 8.5 (Oliveira et al., 1976), close to that observed for degradation of [^{125}I]-ANP by ventricular soluble fraction. This enzyme has however only been shown to hydrolyse Pro-Phe bonds and these are not present in ANP.

Before discussing the results of the HPLC investigation, it is worth considering several points concerning the nature of reversed-phase HPLC (RP-HPLC) separation, and the interpretation of data obtained by

this method. RP-HPLC columns are packed with micro-particulate silica, which has been chemically modified to give a surface coating of hydrophobic hydrocarbon chains. The principle of separation is based on the relative affinities of the substances under investigation for the hydrophobic solid phase and the polar, usually aqueous mobile phase. The alteration of the polarity and hydrophobicity of the mobile phase makes this an extremely useful technique for the analysis of substances of mixed hydrophobic-hydrophillic character, as is the case with peptides. Substances are eluted from RP columns in order of increasing hydrophobicity. Because larger peptides usually possess more hydrophobic groups, peptides will be eluted with increasing size. Some small peptides, however, possess a disproportionate number of hydrophobic residues, and therefore may be retained on the column for much longer than would be predicted by their size. To identify the composition of a peak, it is therefore necessary either to carry out amino acid analysis of that peak or to show that it elutes in the same position as a sample of known composition. An example of the sensitivity of this technique is given by fact that ANP and 'ring-open' ANP can be separated by RP HPLC (Koehn et al., 1987). These peptides have identical amino acid compositions but differ in their secondary stucture, in that the amino acid chain of the 'ring-open' form has been cleaved at the Cys^{7}-Phe^{8} bond.

The identification of several peaks resulting from the incubation of ANP with ventricular soluble fraction indicated that the degradation was complex. Since amino acid analysis was not carried out, and the only peptide of known composition was ANP itself, it is not possible to identify the points at which hydrolysis occurs. It is however possible to draw some conclusions from this investigation. The initial

rate of disappearance of ANP from the incubation medium was 280 pmol/min per 10^6 cells. The rate of degradation measured by acid precipitation of [^{125}I]-ANP was 380 pmol/min per 10^6 cells under similar conditions. These values are in good agreement and indicate that acid precipitation is a reasonable measure of ANP degradation. The initial products of degradation were rapidily eluted from the column, and are characteristic of the elution profile for small peptides or, possibly, single amino acids. This suggests that initial cleavage occurs at one or both of the termini. HPLC analysis of [^{125}I]-ANP degradation by the isolated rat mesenteric artery (in vitro) and during circulation (in vivo) resulted in the rapid appearance of a breakdown product in a similar position to that seen in this preparation (Murthy et al. 1986b). These authors concluded that this peak was the carboxyl-terminal of ANP.

As discussed above, 'ring-open' ANP formed by the cleavage of the Cys^7- Phe^8 bond results in a peptide which elutes just prior to intact ANP. Hydrolysis of this bond has been shown to be the initial cleavage point in kidney cortex membranes (Koehn et al., 1987), possibly via the action of endopeptidase 24.11. (Stephenson & Kenny, 1987a). It is possible that the product eluting in peak 3 may be 'ring-open' ANP. Given the number of products formed during the incubation, and the fact that two of these appear simultaneously during the first two minutes, it is likely that more than one protease is responsible for the proteolytic activity observed in this preparation. Further experiments in the presence and absence of a combination of protease inhibitors, followed by amino acid analysis of the products, are needed to draw firm conclusions as to the nature of degradation in this preparation.

10.4 Degradation of ANP by Soluble Fractions Prepared from Rat Kidney Cortex, Kidney Medulla and Lung

Studies of the distribution of proteolytic activity in the kidney indicate that the majority of this activity is associated with the proximal convoluted tubule (Golder *et al.*, 1970; Maack *et al.*, 1971), the brush border membranes being particularly rich in peptidases (Kenny & Maroux, 1982). In the lung, there are high levels of peptidyl dipeptidase activity, which is responsible for the conversion of angiotensin I to angiotensin II. The majority of information available concerning proteolytic activity in these two tissues is on the action of membrane bound enzymes.

Experiments were performed to assess the degradation of [^{125} I]-ANP by the soluble fractions isolated from rat kidney cortex, kidney medulla, and lung, and to compare this with that observed in the soluble fraction prepared from ventricular myocytes. All preparations possessed proteolytic activity, although the activity isolated from the lung was approximately 3-fold less than from the kidney. Unlike the distribution of membrane-bound enzymes, the degradative activity was approximately the same in soluble fractions isolated from kidney cortex and kidney medulla.

ANP, glucagon and bradykinin inhibited the rate of degradation in all preparations. They showed similar potencies to those observed for inhibition of degradative activity in ventricular soluble fraction, with the exception of ANP which was significantly weaker at inhibiting proteolytic activity in the kidney cortex soluble fraction.

Comparison of the effects of several proteinase inhibitors on the

degradative activity in the various preparations indicate that there are tissue differences. None of the inhibitors examined was as effective at reducing proteolytic activity in these preparations as they were at reducing activity in the soluble fraction from rat ventricular myocytes. In addition, some of the inhibitors showed selectivity between the preparations, suggesting the enzymes responsible for degradative activity were different. In particular, a small (10%), but significant inhibition of the activity of kidney cortex soluble fraction was observed in the presence of PMSF. These results suggest the presence of serine proteinase activity in this preparation.

As is the case for ventricular soluble fraction, further studies, using a combination of inhibitors and the analysis of the degradation products, are required before any conclusions can be drawn about the nature of proteolysis in these preparations.

10.5 Summary

These results show that a soluble protease or proteases, which degrade [^{125}I]-ANP, is present in the high speed supernatant fraction isolated from the heart, kidney and lung of the rat. Inhibition of proteolytic activity by ANP, glucagon and bradykinin is similar in all cases, whereas different inhibition profiles are obtained when various protease inhibitors are included in the incubation. The degradation of radiolabelled ANP by the soluble fraction prepared from heart appears to be primarily caused by the action of a metal-dependent cysteine proteinase, although the possibility of other proteases being present can not be excluded. The proteolytic degradation observed in the preparations isolated from lung and kidney are almost cerainly due to

the actions of more than one enzyme.

CHAPTER 11

11 The Role of ANP in Cardiac Muscle

Experiments described in this thesis demonstrate the presence of [^{125}I]-ANP receptors in purified rat cardiac sarcolemmal membranes, and ANP stimulation of guanylate cyclase activity in the same prepartion. These results extend earlier studies from this laboratory which demonstrated ANP-stimulation of intracellular cGMP levels in isolated rat and rabbit ventricular myocytes (Aiton & Cramb, 1985; Cramb et al., 1987). The concentration of ANP required to produce half-maximal stimulation of guanylate cyclase activity in the purified membrane preparation, is approximately 10-fold less than that required for half-maximal elevation of intracellular cGMP in the intact preparation. This discrepancy is most likely a result of the rapid degradation of ANP which occurrs when the peptide is incubated with ventricular myocytes. Despite this degradation, ANP is able to produce a 5-fold increase in intracellar cGMP in these cells and produce levels of the cyclic nucleotide which are approximately 50% higher than those observed in the presence of carbachol, and nearly 40% of the response to sodium nitroprusside (Cramb et al., 1987).

The role of cGMP as a second messenger for ANP has been questioned because of the discepancy between the levels of the peptide circulating in the blood stream and the concentrations of ANP required to increase cGMP (see section 2.3). However, the concentration of ANP in the heart, as assessed by sampling blood from the coronary sinus (Yandle et al., 1987), is more than sufficient to increase ventricular cGMP. This strongly suggest that the heart ventricles are a target tissue for ANP.

Increases in intracellular cGMP have been correlated with a reduction in the force of contraction of ventricular muscle (George et al., 1970; George et al., 1973; Endoh , 1979; Lincoln & Keely, 1980), and dibutyl cGMP has been shown to antagonize the positive inotropic effect of isoprenaline (Watanabe & Besch, 1975). It appears that cGMP antagonizes agonist-induced positive inotropic effects, with little or no effect on resting tension (Endoh, 1979; Watanabe & Besch, 1975). These results are similar to those observed for ANP-induced relaxation of preconstricted smooth muscle (see section 1.6.1). It is therefore possible that ANP stimulation of intracellular cGMP may also result in a negative inotropic effect on ventricular muscle. This being the case then at least part of the decrease in cardiac output observed in vivo (see section 1.6.1) may be a result of a decrease in stroke volume brought about by the direct action of ANP.

An alternative role for ANP receptors sited on ventricular muscle is that they are part of a feedback mechanism. The existence of ANP and ANP transcripts in ventricular muscle raises the possibility that ANP released from the atria may modulate the expression of the ANP gene in the ventricles.

In conclusion, the results presented in this thesis provide biochemical evidence for the direct action of ANP on ventricular muscle. In addition, they provide evidence of proteases in heart, lung, and kidney which rapidly degrade ANP. Further studies are required to determine the physiological role of ANP in the heart, and the contribution of proteolytic degradation to the nature and time-course of its activity.

REFERENCES

Abbs, M.T. & Kenny, A.J. (1983) Clin. Sci. **65**, 551-559

Ackermann, U., Irizawa, T.G., & Sonnenberg, H. (1984) Can. J. Physiol. Pharmacol. **62**, 819-826

Adair, G.S. (1925) J. Biol. Chem. **63**, 529-545

Aguilera, G. (1987) Endocrinol. **120**, 299-304

Aiton, J.F. & Cramb, G. (1985) J. Physiol. **367**, 101P

Aiton, J.F., Cramb, G. & Rugg, E.L. (1987) J. Physiol. **382**, 148P

Almenoff. J., Wilk, S. & Orlowski, M. (1981) Biochem. Biophys. Res. Commun. **102**, 206-214

Almenoff, J. & Orlowski, M. (1983) Biochemistry **22**, 590-599

Anderson, C.H., McCally, M. & Farrell, G.L. (1959) Am. J. Physiol. **64**, 202-207

Anderson, R.G.W & Kaplan, J. (1983) Mol. Cell. Biol. **1**, 1-52

Aoyagi, T., Miyata, S., Nanto, M., Kojima, F., Matsuzaki, M., Ishizuka, M., Takeuchi, T., & Umezawa, H. (1969) J. Antibiot. **22**, 558-568

Argentin, S. Nemer, M., Drouin, J., Scott, G.K., Kennedy, B.P. & Davies, P.L. (1985) **260**, 4568-4571

Atarashi, K., Mulrow, P.J., Franco-Saenz, R., Snajdar, R., & Rapp, J. (1984) Science **224**, 992-993

Atlas, S.A. (1986) Recent Prog. in Hormone Res. **42**, 207-249

Atlas, S.A., Kleinert, H.D., Camargo, M.J., Januszewicz, A., Sealey, J.E., Laragh, J.H., Schilling, J.W., Lewicki, J.A., Johnson, L.K., Maack, T. (1984) Nature **309**, 717-719

Bakhle, Y.S. (1968). Nature **220**, 919-920

Ballermann, B.J., Hoover, R.L., Karnovsky, M.J. & Brenner, B.M. (1985) J. Clin. Invest. **76**, 2049-2056

Barnett, D.B., Rugg, E.L. & Nahorski, S.R. (1978) Nature **273**, 166-168

Barrett A.J. & McDonald (1980) Mammalian Proteases - Volume 1: Endopeptidases. Academic Press, London.

Barrett, A.J., Kembhavi, A.A., Brown, M.A., Kirschke, H. Knight, C.G., Tamai, M. & Hanada, K. (1982) Biochem. J. **201**, 189-198

Barrett, A.J. & Salvesen, G. (1986) Research Monographs in Cell and Tissue Physiology - Volume 12: Proteinase Inhibitors. Elsevier, Amsterdam.

Baum, M. & Toto, R.D. (1986) Am. J. Physiol. **250**, F66-F69

Bianchi, C., Gutkowska, J., Garcia, R., Thibault, G., Genest, J. & Cantin M. (1985) Histochemistry **82**, 441-452

Bianchi, C., Anand-Srivistava, M.B., De Lean, A., Gutkowska, J., Forthommme, D., Genest., J. & Cantin, M. (1986) Current Eye Research **5**, 283-293

Bianchi, C., Gutkowska, J., Garcia, R., Thibault, G., Genest, J. & Cantin M. (1987) J. Histochem. Cytochem. **35**, 149-153

Bloch, K.D., Scot, J.A., Zisfein, J.B., Fallon, J.T., Margolies, M.N., Seidman, C.E., Matsueda, G.R., Homey, C.J., Graham, R.M., & Seidman, J.G. (1985). Science **230**, 1168-1171.

Blow. D.M., Wright, C.S., Kukla, D., Ruhlmann, A., Steigemann, W. & Huber, R. (1972) J. Mol. Biol. **69**, 137-144

Bohley, P., Kirschke, H., Langner, J., Ansorge, S., Weideranders, B., & Hanson, H. (1971) In J.T. Dingle (Ed.) Tissue Proteinases. North Holland, Amsterdam, pp 187-219

Bohme, E., Jung, R. & Mechler, I. (1974) Methods Enzymol. **38**, 199-202

Booth. A.G. & Kenny, A.J. (1974) Biochem. J. **142**, 575-581

Borenstein, H.B., Cupples, W.A., Sonnenberg, H. & Veress, A.T. (1983) J. Physiol. **344**, 133-140

Bott, R., Subramanian, E. & Davies, D.R. (1982) Biochemistry **21**, 6956-6962

Bowman, W.C. & Rand, M.J. (1980) Text Book of Pharmacology, Blackwell Scientific Publications

Bradford, M. (1976) Anal. Biochem. **72** 248-255

Bratveit, M., Rydningen, H.T. & Helle, K.B. (1987) Acta Physiol. Scand. **130**, 593-599

Briggs, J.P., Marin-grez, M.,Steipe, B., Schubert, G. & Schnermann, J. (1984) Am. J. Physiol. **247**, F480-F484

Brunks, R.F., Lawson-Wendling, K., & Pugsley, T.A. (1983). Anal. Biochem. **132**, 74-81

Budzik, G.P., Firestone, S.L., Bush, E.N., Connolly, P.J., Rockway, T.W., Sarin, V.K. & Holleman, W.H. (1987) **144**, 422-431

Burnett, J.C., Granger, J.P. & Opgenorth, T.J. (1984) Am. J. Physiol. 247, F863-F866

Camargo, A.G.M., Shapanka, R. & Greene, L.J. (1973) Biochemistry **12**, 1838-1844

Camargo, A.G.M., Caldo, H. & Ries, M.L. (1979) J. Biol. Chem. **254**, 5304-5307

Camargo, M.J.F., Kleinert, H.D., Atlas, S.A., Sealey, J.E., Laragh, J.H. & Maack, T. (1984) Am. J. Physiol. **246**, F447-F456

Cantin, M., Ding, J., Thibault, G., Gutkowska, J., Salmi, L., Ballak, M., Garcia, R. & Genest, J. (1987) Mol. Cell. Endocrinol. **52**, 105-113

Carone, F.A., Peterson, D.R. & Flouret, G. (1982) J. Lab. Clin. Med. **100**, 1-14

Carrier, F., Thibault, G., Schiffrin, E.L., Garcia, R., Gutkowska, J., Cantin, M. & Genest, J. (1985) Biochem. Biophys. Res. Commun. **132**, 666-673

Cereijido, M., Robbins, E.S., Dolan, W.J., Rotunno, C.A. & Sabatini, D.D. (1978) J. Cell Biol. **77**, 853-880

Chartier, L., Schiffrin, E. & Thibault, G. (1984) Biochem. Biophys. Res. Commun. **122**, 171-174

Cheng, Y. & Prusoff, W.H. (1973) Biochem. Pharmacol. **22**, 3099-3108

Chiu, P.J.S., Tetzloff, C. & Syhort, E.J. (1986) Eur. J. Pharmacol. **124**, 277-284

Cogan, M.G. (1986) Am. J. Physiol. **250**, F710-F714

Cohen, M.L. & Schenck, K.W. (1985) Eur. J. Pharmacol. **108**, 103-104

Cramb, G. & Dow, J.W. (1983) Biochim. Biophys. Acta **736**, 99-108

Cramb, G., Banks, R., Rugg, E.L. & Aiton, J.F. (1987) Biochem. Biophys. Res. Commun. **148**, 962-970

Currie, M.G., Geller, D.M., Cole, B.R., Boylan, J.G., Yu Sheng, W., Holmberg, S.W. & needleman, P. (1983) Science **221**, 71-73

Currie, M.G., Geller, D.M., Cole, B.R., Siegel, N.R., Fok, K.F., Adams, S.P., Eutbank, S.R., Galluppi, G.R., & Needleman, P. (1984a). Science **223**, 67-69.

Currie, M.G., Geller, D.M., Chao, J. Margolius, H.S. & Needleman, P. (1984b) Biochem. Biophys. Res. Commun. **120**, 461-466

Currie, M.G., Seekin, D., Geller, D.M., Cole, B.R. & Needleman, P. (1984c) Biochem. Biophys. Res. Commun. **124**, 711-717

De Bold, A.J. & Bencosome, S.E. (1975) In P.E.Roy, & P.Harris (Eds.) The cardiac cytoplasm. Vol. 8. University Park Press, Baltimore. pp 129-138

De Bold, A.J. (1979) Proc. Soc. Exp. Biol. Med. **161**, 508-511

De Bold, A.J., Borenstein,H.B., Veress, A.T. & Sonnenberg, H. (1981) Life Sci. **28**, 89-94

De Bold A.J. (1982a)Proc. Soc. Exp. Biol. Med. **179**, 133-138

De Bold A.J. (1982b) Can. J. Physiol. Pharmacol **60**, 324-330

De Bold A.J. & Flynn T.G. (1983) Life Sci. **33**, 297-302

De Lean, A., Munson, P.J. & Rodbard, D. (1978) Am. J. Physiol. **235**, E97-E102

De Lean, A., Racz, K., Gutkowska, J., Nguyen, T.T., Cantin, M. & Genest, J. (1984a) Endocrinol. **115**, 1636-1638

De Lean, A., Gutkowska, J., McNicoll, N., Schiller, P.W., Cantin, M. & Genest, J. (1984b) Life Sci. **35**, 2311-2318

De Lean, A., Vinay, P. & Cantin, M. (1985) FEBS Lett. **193**, 239-242

De Meyts, P., Bianco, A. & Roth, J. (1976) J. Biol. Chem. **251**, 1877-1888

Desbuquois, B., Krug, F. & Cuatrecasa, P. (1974) Biochim, Biophys. Acta **343**, 101-120

Deth, R. & Van Breemen, C. (1977) J. Membr. Biol. **30**, 363-380

De Jonge, H.R. (1975) FEBS Lett. **53**, 237-242

Deth, R.C., Wong, K., Fukozawa, S., Rocco, R., Smart, J.L. & Lynch, C.J., Waward, R. (1982) Fed. Poc. **41**, 983A

Ding, J., Thibault, G., Gutkowska, J., Garcia, R., Karabatsos, T., Jasmin, G., Genest, J. & Cantin, M. (1987) Endocrinol. **121**, 248-257

Duckworth, W.G. (1976) Biochim. Biophys. Acta **437**, 531-542

Endoh, M. (1979) Japan. J. Pharmacol. **29**, 855-864

Erdos, E.G. (1976) Mol. Pharmacol. **25**, 1563-1569

Feldman, H.A. (1972) Anal. Biochem. **48**, 317-338

Ferreira, S.H., and Vane, J.R. (1967) Brit. J. Pharmacol. Chemotherap. **30**, 417-424

Field, M., Graf, L.H., Laird, W.J. & Smith, P.L. (1978) Proc. Natl. Acad. Sci. USA **75**, 2800-2804

Fleischmann, D. & Denisevich, M. (1979) Biochemistry **18**, 5060-5066

Fleischmann, D., Denisevich, M., Raveed, D. & Pannbacker, R. (1980) Biochim. Biophys. Acta **630**, 176-186

Fletcher, A.E., Allan, E.H., Casley, D.J. & Martin, T.J. (1986) FEBS Lett. **208**, 263-268

Flynn, T.G., de Bold, M.L. & de Bold, A.J. (1983) Biochem. Biophys. Res. Commun. **117**, 859-865

Forssmann, W.G., Hock, D., Lottspeich, F. Henschen, A., Kreye, V., Christmann, M., Reinecke, M., Metz, J., Carlquist, M. & Mutt, V. (1983) Anat. Embryol. **168**, 307-313

Forssmann, W.G., Birr, C., Carlquist, M., Christmann, M., Finke, R., Henschen, A., Hock, D., Kirchheim, H., Kreye, V., Lottspeich, F. Metz, J., & Mutt, V. & Reinecke, M., (1984) Cell Tissue Res. **238**, 425-430

Freeman, R.H., Davis, J.O, & Vari, R.C. (1985) Am. J. Physiol. **248**, R495-R500

Fujioka, S., Tamaki, T., Fukui< K., Okahara, T. & Abe, Y. (1985) Eur. Pharmacol. **109**, 301-304

Fulcher, I.S., Matsas, R., Turner, A.J. & Kenny, A.J. (1982) Biochem. J. **203**, 519-522

Furgchott, R.F. (1984). Ann. Rev. Pharmacol. Toxicol. **24**, 175-197.

Gann, D.S., & Travis, R.H., (1964) Am. J. Physiol. **207**, 1095-1101

Garbers, D.L. (1979) J. Biol. Chem. **254**, 240-243

Garcia, R., Thibault, G., Ong, H. & Genest, J. (1982) Experimentia **38**, 1071-1073

Garcia, R., Thibault, G., Cantin, M. & genest, J. (1984a) Am. J. Physiol. **247**, R34-39

Garcia, R., Thibault, G., Nutt, R.F., Cantin, M. & Genest, J. (1984b) Biochem. Biophys. Res. commun. **119**, 685-688

Garcia, R., Thibault, G., Seidah, N.G., Lazure, C., Cantin, M., Genest, J., & Chretien, M. (1985) Biochem. Biophys. Res. Commun. **126**, 178-184

Gardner, D.G., Hane, S., Trachewsky, D., Schenk, D. & Baxter, J.D. (1986a) Biochem. Biophys. Res. Commun. **139**, 1047-1054

Gardner, D.G., Deschepper, C.F., Ganong, W.F., Hane, S., Fiddes, J., Baxter, J.D. & Lewicki, J. (1986b) Proc. Natl. Acad. Sci. **83** 6697-6701

Gardner, D.G., Deschepper, C.F., & Baxter, J.D. (1987). Hypertension **9**, 103-106.

Gee. N.S., Bowes, M.A., Buck, P. & Kenny, A.J. (1985) Biochem. J. **228**, 119-126

Geller, D.M., Currie, M.G., Siegel, N.R., Fok, K.F., Adams, S.P. & Needleman, P. (1984) Biochem. Biophys. Res. Commun. **121**, 802-807

Genest, J., Cantin, M. (1988) Rev. Physiol. Biochem. Pharmacol. **110**, 1-145

George, W.J., Polson, J.B., O'Toole' A.G. & Goldberg, N.D. (1970) Proc. Natl. Acad. Sci. USA 66,398-403

George, W.J., Wilkerson, R.D. & Kadowitz, P.J. (1973) J. Pharmacol. Exp. Therapeu. **184**, 228-235

Gerzer, R., Hofmann, F., Bohme, E., Ivanova, K., Spies, C. & Schultz, G. (1981a) Adv. Cyclic Nucleotide Res. **14**, 255-261

Gerzer, R., Bohme, E., Hofmann, F. & Schultz, G. (1981b) FEBS Lett. **132**, 71-74

Gerzer, R., Hofmann, F. & Schultz, G., (1981c) Eur. J. Biochem.**116**, 479-486

Glembotski, C.C., & Gibson, T.T. (1985). Biochem. Biophys. Res. Commun. **132**, 1008-1017.

Glossmann, H., Baukal, A.J. & Catt, K.J. (1974) J. Biol. Chem. **249**, 825-834

Goetz, K.L., Hremreck, A.S., Slick, G.L. & Starke, H.S. (1970) Am. J. Physiol. **219**, 1417-1423

Goldberg, N.D. & Haddox, M.K. (1977) Ann. Rev. Biochem. **46**, 823-896

Golder, M.P., Mahler, R. & Boyns, A.R. (1970) Biochem. J. **118**, 14P-15P

Goodfriend, T.L., Elliott, M.E., Atlas, S.A. (1984) Life Sci. **35**, 1675-1682

Gordis, C., Virmaux, N., Urban, P.F. & Mandel, P. (1973) FEBS Lett. **30**, 163-166

Grammer, R.T., Fukiemi, H., Inagami, T & Misono, K.S. (1983) Biochem. Biophys. Res. Commun. **116**, 696-703

Gray, J.P. & Drummond, G.E. (1976) Arch. Biochem. Biophys. **172**, 31-38

Greenberg, B.D., Bencen, G.H., Seilhamer, J.J., Lewicki, J.A. & Fiddes, J.C. (1984) Nature **309**, 656-658

Gutkowska, J. & Sirois P. (1988) In B.M. Brenner, & J.H. Laragh (Eds.) Advances in Atrial Peptide Research. Vol. II. Raven Press, New York, pp 165-168

Hamada, M., Burmester, K.A., Graci, K.A., Frohlich, E.D. & Cole, F.E. (1987) Life Sci. **40**, 1731-1737

Hamet, P., Tremblay, J., Pang, S.C., Skuherska, R., Schiffrin, E.L., Garcia, R., Cantin, M., Genest, J., Palmour, R., Ervin, F.R., Martin, S. & Goldwater, R. (1986) Hypertension **4** (suppl. 2), S49-S56

Harris, R.B. & Wison, I.B. (1985) Peptides **6**, 393-396

Henry, J.P., Gauer, O.H. & Reeves, J.L. (1956) Circ. Res. 4, 85-92

Hill, A. V., (1913), Biochem. J. **7**, 471-480

Hirata, Y., Tomita, M., Yoshimi, H. & Ikeda, M. (1984) Biochem. Biophys. Res. Commun. **125**, 562-568

Hirata, Y., Takata, S., Tomita, M. & Takaichi, S. (1985) Biochem. Biophys. Res. Commun. **132**, 976-984

Hirata, Y., Ishui, M., Sugimoto, T., Matsuoka, H., Ishimitsu, T., Atarashi, K., Sugimoto, T., Miyata, A., Kangawa, K. & Matsuo, H. (1987a) Clin. Sc. **72**, 165-170

Hirata, Y., Hirose, S., Takata, S., Takagi, Y. & Matsubara, H. (1987b) Eur. J. Pharmac. **135**, 439-442

Hori, R., Inui, K., Saito, H., Matsukawa, Y., Okumura, K., Nakao, K., Morii, N. & Imura, H. (1985) Biochem. Biophys. Res. Commun. **126**, 773-779

Huang, L.L., Lewicki, J., Johnson, L.K. & Cogan, M.G. (1985) J. Clin. Invest. **75**, 769-773

Huber, R., Bode, W., (1978) Acc. Chem. Res. **11**,114-122

Huet, M. & Cantin, M. (1974) Lab. Invest. **30**, 525-532

Inui, K., Saito, H., Matsukawa, Y., Nakao, K., Morii, N., Imura, H., Shimokura, M., Kiso, Y. & Hori, R. (1985) Biochem. Biophys. Res. Commun. **132**, 253-260

Ishido, M., Fugita, T., Hagiwara, H., Shimonaka, M., Saheki, T., Hirata, Y. & Hirose, S. (1986) Biochem. Biophys. Res. Commun. **140**, 101-106

Ishikawa, Y., Umemura, S., Yasuda, G., Uchino, K., Shindou, T., Minamizawa, K., Toya, Y. & Kaneko, Y. (1987) Biochem. Biophys. Res. Commun. **147**, 135-139

Itoh, H., Nakao, K., Mukoyama, M., Shino, S., Morii, N., Sugawara, A., Yamada, T., Saito, Y., Arai, H., & Imura, H. (1988) In B.M. Brenner, & J.H. Laragh (Eds.) Advances in Atrial Peptide Research. Vol. II. Raven Press, New York, pp 179-183

Jacobowitz, D.M., Skafitsch, G., Keiser, H.R., Eskay, R.L. & Zamir, N. (1985) Neuroendocrinol. **40**, 92-94

Jamieson, J.D. & Palade, G.E. (1964) J. Cell Biol. **23**, 151-172

James, M.N.G., Sielecki, A., Salituro, F., Rich, D.H. & Hofmann, T. (1982) Proc. Nalt. Acad. Sci. USA **79**, 6137-6141

Kangawa, K. & Matsuo, H. (1984) Biochem. Biophys. Res. Commun. **118**, 131-139

Keeler, R. & Azzarolo, A.m. (1983) Can. J. Physiol. Pharmacol. **61**, 996-1002

Kenny, A.J. (1977) in A.J. Barrett (Ed.), Proteinases in Mammalian Cells and Tissues. Elsevier/North-Holland, Amsterdam, pp 393-444

Kenny. A.J., Fulcher, I.S., Ridgwell, K. & Ingram, J. (1981) Acta Biol. Med. Germ. **40**, 1465-1472

Kenny, A.J. & Maroux, S. (1982) Physiol. Rev. **62**, 91-118

Kerr, M.A. & Kenny, A.J. (1974) Biochem. J. **137**, 477-488

Kimura, H. & Murad, F. (1974) J. Biol. Chem. **249**, 6910-6916

Kimura, H. & Murad, F. (1975a) J. Biol. Chem. **250**, 4810-4817

Kimura, H. & Murad, F. (1975b) Proc. Natl. Acad. Sci. USA **72**, 1965-1972

King, A.C., & Cuatrecasas, P. (1981) New Eng. J. Med. **305**, 77-88.

Kirsch, B. (1956) Exp. Med. Surg. **114**, 99-112

Kluft, C. (1978) J. Lab. Clin. Med. **91**, 83-95

Koehn, J.A., Norman, J.A, Jones, B.N., LeSueur, L., Sakane, Y. & Ghai, R.D. (1987) J. Biol. Chem. **262**, 11623-11627

Koike, H., Sada, T., Miyamoto, M., Oizumi, K., Sugiyama, M. & Inagami, T. (1984) Eur. J. Pharmacol. **104**, 391-392

Kondo, Y., Imai, M., Kangawa, K. & Matsuo, H. (1986) Pflugers Arch. **406**, 273-278

Koseki, C., Hayashi, Y., Torikai, S., Furuya, M., Ohnuma, N. & Imai, M. (1986a) Am. J. Physiol. **250**, F210-F216

Koseki, C., Hayashi, Y., Ohnuma, N. & Imai, M. (1986b) Biochem. Biophys. Res. Commun. **136**, 200-207

Knight, C.G. (1986) In Barrett, A.J. & Salvesen, G. Research Monographs in Cell and Tissue Physiology - Volume 12: Proteinase Inhibitors. Elsevier, Amsterdam, pp 23-51

Krishnan, N., Fletcher, R.T., Chader, G.J. & Krishna, G. (1978) Biochim. Biophys. Acta **523**, 508-515

Kuno, T., Andresen, J. W., Kamisaki, Y., Waldman, S.A., Chang, L.Y., Saheki, S., Leitman, D.C., Nakane, M. & Murad, F. (1986) J. Biol. Chem. **261**, 5817-5823

Kurose, H., Inagami, T. & Ui, M. (1987) FEBS Lett. **219**, 375-379

Lancombe, M. & Hanoune, J.(1979) J. Biol. Chem. **254**, 3697-3699

Lang, R.E., Tholken, H., Ganter, D., Luft, F.C., Ruskoaho, H., & Unger, T.H. (1985). Nature **314**, 264-266.

Lappe, R.W., Smits, J.F., Todt, J.A., Debets, J.J. & Wendt, R.L. (1985) Cir. Res. **56**, 606-612

Lattion, A.L., Michel, J.B., Arnauld, E., Corvol, P. & Soubrier, F. (1986) Am. J. Physiol. **251**, H890-H896

Lazure, C.,Chretien, M., Cantin, M. & Genest, J. (1985) Biochem. Biophys. Res. Commun. **125**, 938-946

Leatherbarrow, R.J. (1987) Enzfitter. Elsevier, Amsterdam

Leitman, D.C. & Murad, F. (1986) Biochim. Biophys. Acta **885**, 74-79

Letiman, D.C., & Murad, F.(1987) Endocrinol. Metab. Clin. N. Am. **16**, 79-105

Leitman, D.C., Jeffrey, W.A., Catalano, R.M., Waldman, S.A., Tuan, J.J. & Murad, F. (1988) J. Biol. Chem. **263**, 3720-3728

Lewicki, J.A., Brandwein, H.J., Waldman, S.A. & Murad, F. (1980) J. Cyclic Nucleotide Res. **6**, 283-296

Lewicki, J., Schenk, D., Fuller, F., Porter, G., McEnroe, G., Arfsten, A., Schwartz, K., Kang, L-L., Maack, T. & Scarborough, R. (1988) In B.M. Brenner, & J.H. Laragh (Eds.), Advances in Atrial Peptide Research. Vol. II. Raven Press, New York, pp 31-39

Limbird, L.E. & Lefkowitz, R.J. (1975) Biochim. Biophys. Acta **377**, 186-196

Limbird, L.E. (1986) Cell Surface Receptors: A Short Course on Theory and Methods. Martinus Nijhoff Publishing, Boston.

Lincoln, T.M. & Keely, S.L. (1980) J. Cyclic Nucleo. Res. **6**, 83-91

Linehan, J.H., Dawson, C.A., Richaby, D.A., Bronikowski, T.A., Gillis, C.N., & Pitt, S.R. (1986). In D.L. Yudelivich & G.E. Mann (Eds.) Carrier Mediated Transport of Solutes from Blood to Tissue. Longmans, London, pp 251-264

Luft., F.C. Lang, R.E., Aronoff,G.R., Ruskoaho, H., Toth,M., Ganten, D., Sterzel, R.B. & Unger, T. (1986) J. Pharmacol. Exp, Ther. **236**, 416-418

Maack, T., Mackensie, D.D.S. & Kinter, W.B. (1971) Am.J. Physiol. **221**, 1609-1616

Maack, T., Marion, D.N., Camargo, M.J., Kleinert, H.D., Laragh, J.H., Vaughan, E.D. & Atlas, S.A. (1984) Am J. Med. **77**, 1069-1075

Maack, T. & Kleinert, H.D. (1986) Biochem. Pharmacol **35** 2057-2064

Maack, T., Suzuki, M., Almeida, F.A., Nussenzveig, D., Scarborough, R.M., McEnroe, G.A. & Lewicki, J.A. (1987) Science **238**, 675-678

Maki, M., Takayanagi, R., Misono, K.S., Pandey, K.N., Tibbetts, C. & Inagami, T. (1984) Nature **309**, 722-724

Mantyh, C.R., Brecha, N.C., Soon-Shiong, P. & Mantyh, P.W. (1985) New England J. Med. **312**, 1710

Mantyh, C.R., Kruger, L., Brecha, N.C. & Mantyh, P.W. (1986) Hypertension **8**, 712-721

Marala, R.B. & Sharma, R.K. (1988) Biochem. J. **251**, 301-304

Marie, J.P., Guillemot, H. & Hatt, P.Y. Pathol. Biol. (Paris; 1976) **24**, 549-554

Marshall, S. (1985a). J. Biol. Chem. **260**, 13517-13523

Marshall, S. (1985b). J. Biol. Chem. **260**, 13524-13531

Matsas, R., Fulcher, I.S., Kenny, A.J. & Turner, A.J. (1983) Proc. Natl. Acad. Sci. U.S.A. **80**, 3111-3115

Matas, R., Kenny, A.J. & Turner, A.J. (1984) Biochem. J. **223**, 433-440

McDonald J.K. & Barrett A.J. (1986) Mammalian Proteases - Volume 2: Exopeptidases. Academic Press, London.

Means, G. & Feeney, R. (1971) Chemical Modification of Proteins. Holden-Day, San Francisco

Meisheri, K.D., Taylor, C.J. & Saneii, H. (1986) Am. J. Physiol. **250**, C171-C174

Meloche, S., Ong, H., Cantin, M. & De Lean, A. (1986a) Mol. Pharmacol. **30**, 537-543

Meloche, S., Ong, H., Cantin, M. & De Lean, A. (1986b) J. Biol. Chem. **261**, 1525-1528

Misfelt, D.S., Hamamoto, S.T. & Pitelka, D.R. (1976) Proc. Natl. Acad. Sci. U.S.A. **73**, 1212-1216

Misono, K.S., Fukumi,H., Grammer, R.T. & Inagami, T. (1984a) Biochem. Biophys. Res. Commun.**119**, 524-529

Misono, K.S., Grammer, R.T., Fukumi,H. & Inagami, T. (1984b) Biochem. Biophys. Res. Commun.**123**, 444-451

Misono, K.S., Grammer, R.T., Rigby, J.W. & Inagami, T. (1985) Biochem. Biophys. Res. Commun. **130**, 994-1001

Misono, K.S. (1988) Biochem. Biophys. Res. Commun. **152**, 658-667

Miyata, A., Toshimori, T., Hashiguchi, T., Kangawa, K., & Matsuo, H. (1987) Biochem. Biophys. Res. Commun. **142**, 461-467

Motulshy, H.J. & Mahan, L.C. (1984) Mol. Pharmacol. **25**, 1-9

Munson, P.J. & Robard,D. (1980) Anal. Biochem. **107**, 220-239

Murad, F., Leitman, D.C., Bennett, B.M., Molina. C. & Waldman, S.A. (1988) In B.M. Brenner, & J.H. Laragh (Eds.) Advances in Atrial Natriuretic Research, Vol II. Raven Press, New York. pp 53-60

Murphy, K.M.M., McLaughlin, L.L., Michener, M.L. & Needleman, P. (1985) Eur. J. Pharmacol. **111**, 291-292

Murthy, K.K., Thibault, G., Schiffrin, E.L., Garcia, R., Chartier, L., Genest, J. & Cantin, M. (1986a) Peptides 7, 241-246

Murthy, K.K., Thibault, G., Garcia, R., Gutkowska, J., Genest, J. & Cantin, M. (1986b) Biochem. J. **240**, 461-469

Nahorski, S.R. (1981). In J.W. Lamble (Ed) Towards Understanding Receptors. Elsevier/North Holland, Amsterdam, pp 71-77

Nakao, K., Sugawara, A., Morii, N., Sukamoto, M., Suda, M., Sonedaj, J., Ban, T., Kihara, Y., Yamori, Y., Shimokura, M., Ksio, Y., & Imura, H. (1984) Biochem. Biophys. Res. Commun. **124**, 815-821.

Nambi, P., Whitman, M., Gessner, G., Aiyar, N. & Crooke, S.T. (1986) Proc. Natl. Acad. Sci. USA **83**, 8492-8495

Napier, M.A., Dewey, R.S., Albers-Schonberg, G., Bennet, G.D., Rodkey, J.A., Marsh, E.A., Whinnerey, M., Seymour, A.A. & Blaine, E.H. (1984) Biochem. Biophys. Res. Commun. **120**, 981-988

Napier, M.A., Arcuri, K.E. & Vandlen, R.L. (1986) Arch. Biochem. Biophys. **248**, 516-522

Naray-Fejes-Toth, A., Carretero, O.A. & Fejes-Toth, G. (1988) Hypertension **11**, 392-396

Naruse, M., Obana, K., Naruse, K., Yamaguchi, H., Demura, H., Inagami, T. & Shizume, K. (1987) J. Clin. Endocrinol. & Metabol. **64**, 10-15

Nash, G.B., Tatham, P.E.R., Powell, T., Twist, V.W., Speller, R.D., & Loverock, L.T. (1979). Biochim. Biophys. Acta 587, 99-111.

Needleman, P., Adams, S.P., Cole, B.R., Currie, M.G., Geller, D.M., Michener, M.L., Saper, C.B., Schwartz, D., & Standaert, D.G. (1985). Hypertension, 7, 469-482.

Nemer, M., Chamberland, M., Sirois, D., Argentin, S., Drouin, J., Dixon, R.A.F., Zivin, R.A. & Condra, J.H. (1984) Nature **312**, 654-656

Nemer, M., Lavigne, J.P., Drouin, J. Thibualt, G., Gannon, M., Antakly, T. (1986) Peptides 7, 1147-1152

Nemer, M., Argentin, S., Lavigne, J.P., Chamberland, M. Drouin, J. (1987) J. Cell. Biochem. **11A**, 121

Neuser, D. & Bellemann, P. (1986) FEBS Lett. **209**, 347-351

Numan, N.A., Gillispie, M.N. & Altiere, R.J. (1986) Fed. Proc. **45**, 907

Oikawa, S., Imai, M., Veno, A., Tanak, S., Nogushi, T., Nakazato, H., Kangawa, K., Fukuda, A. & Matsuo, H. (1984) Nature **309**, 724-726

Ole-Moi Yoi, O., Spragg, J. & Austen, K.F. (1979) Proc. Natl. Acad. Sci. USA **76**, 3612-3616

Olins, G.M., Patton, D.R., Tjoeng, F.S. & Blehm, D.J. (1986) Biochem. Biophys. Res. Commun. **140**, 302-307

Olins, G.M., Spear, K.L., Siegel, N.R. & Zurcher-Neely, H. (1987) Biochim. Biophys. Acta **901**, 97-100

Oliverira, B., Martins, A.R. & Camargo, A.G.M. (1976) Biochemistry **15**, 1967-1974

Opgenorth, T.J., Burnett, J.C., Granger, J.P., & Scriven, T.A. (1986) Am. J. Physiol. **250**, F798-F801

Orlowski, M. & Wilks, S. (1981) Biochemistry **20**, 4942-4950

Palmer, R.M.J., Ferrige, A.G., & Moncada, S. (1987). Nature **327**, 524-526

Pegram, B.L., Trippodo, N.C., Natsume, T., Kardon, M.B., Frohlich, E.D., Cole, F.E. & MacPhee, A.A. (1986) Fed. Proc. **45**, 2382-2386

Perlman, D. & Halverson, H.O. (1983) J. Mol. Biol. **167**, 391-409

Powell, T., Terrar, D. A. & Twist, V. M. (1980) J. Physiol. Lond. **302**, 131-153

Powell, T., Steen, E.M., Twist, V.M., & Woolf, N. (1978) J. Mol. Cell Cardiol. 10, 287-292

Powers, J.C. & Harper, J.W. (1986) In Barrett, A.J. & Salvesen, G. Research Monographs in Cell and Tissue Physiology - Volume 12: Proteinase Inhibitors. Elsevier, Amsterdam, pp 219-298

Quiron, R., Dalphe, M. & Dam, T.V. (1986) Proc. Natl. Acad. Sci. USA, **83**, 174-178

Quiron, R. (1988) Trends in Neurosci. **11**, 58-62

Rapoport, R.M. & Murad, F. (1983) J. Cyclic Nucleotide Protein Phosphorylation Res. **9**, 281-296

Rapoport, R.M., Waldman, S.A., Schwartz,K., Winquist, R.J. & Murad, F. (1985) European J. Pharmacol. **115**, 219-229

Rapoport, R. M., Ginsburg, R., Waldman, S.A. & Murad, F. (1986) Eur. J. Pharmacol. **124**, 193-196

Resink., T.J., Scott-Burden, T., Jones, C.R., Baur, U. & Buhler, F.R. (1988) In B.M. Benner, & J.H. Laragh (Eds.), Advances in Atrial Natriuretic Research, Vol II. Raven Press, New York, pp 45-52

Rich, D.H. (1986) In Barrett, A.J. & Salvesen, G. Research Monographs in Cell and Tissue Physiology - Volume 12: Proteinase Inhibitors. Elsevier, Amsterdam, pp 153-173

Richardson, J.C.W., Scelera, V. & Simmons, N.L. (1981) Biochim. Biophys. Acta **673**, 26-36

Richman,R.A., Kofp, G.S., Hamet, P. & Johnson, R.A. (1980) J. Cyclic Nucleo. Res. **6**, 461-468

Reisner, A.H., Nemes, P. & Bucholtz, C. (1975) Anal. Biochem. **64**, 509-516

Roubert, P., Lonchampt, M.O., Chabrier, P.E., Plas, P., Goulin, J. & Braquet, P. (1987) Biochem. Biophys. Res. Commun. **148**, 61-67

Rugg, E.L., Barnett, D.B. & Nahorski, S.R. (1978) Mol. Pharmacol. **14**, 996-1005

Rugg, E.L. & Simmons, N.L. (1984) Quat. J. Expt. Physiol. **69**, 339-353

Rugg, E.L. & Simmons, N.L. (1986) Renal Physiol. **9**, 72

Sakharov, I.Y., Dukhania, E.A., Molokoedova, A.S., Danilov, S.M., Ovchinnikov, M.V., Bespalova, Zh.D. & Titov, M.I (1988) Biochem. Biophys. Res. Commun. **151**, 109-113

Salazar, F.J., Fiksen-Olsen, M.J., Opgenorth, T.J., Granger, J.P., Burnett, J.C. & Romero, J.C. (1986) Am. J. Physiol. **251**, F532-F536

Samsom, W.K. (1985) Endocrinol. **117**, 1279-1281

Sasaki, T., Kikuchi, T., Yumoto, N., Yoshimura, N., and Murachi, T. (1984) J. Biol. Chem. **259**, 12489-12494

Scarborough, R.M., Schenk, D.B. McEnroe, G.A., Arfsten, A., Kang, L-L., Schwartz, K. & Lewicki, J.A. (1986) J. Biol. Chem. **261**, 12960-12964

Scatchard, G., (1949) Ann. N.Y. Acad. Sci. **51**, 660-672

Schenk, D.B., Phelps, M.N., Porter, J.G., Scarbrough, R.M., McEnroe, G.A. & Lewicki, J.A. (1985) J. Biol. Chem. **260**, 14887-14890

Schiffrin, E.L., Chartier, L., Thibault, G., St.-Louis, J., Cantin, M., & Genest, J. (1985) Circ. Res. **56**, 801-807

Schiffrin, E.L., Deslongchamps, M., & Thibault, G. (1986). Hypertension 8(suppl. II), II6-II10

Schiller, P.W., Maziak, L.A., Nguyen, T.M.-D., Godin, J., Garcia, R., DeLean, A. & Cantin, M. (1987) Biochem. Biophys. Res. Commun. **143**, 499-505

Sealey, J. E., Atlas, S.A., Laragh, J.H., Oza, N.B. & Ryan, J.W. (1978) Nature **275**, 144-145

Seidah, N.G., Lazure, C., Chretien, M., Thibault, G. Garcia, R., Cantin, M., Genest, J., Nutt, R.F., Brady, S.F., Lyle, T.A., Paleveda, W.J., Colton, C.D., Ciccarone, T.M., & Veber, D.F. (1984) Proc. Natl. Acad. Sci. U.S.A. **81**, 2640-2644

Seidman, C.E., Bloch, K.D., Klein, K.A., Smith, J. A. & Seidman, J.G. (1984) Science **226**, 1206-1209

Sen. I. (1986) Biochem. Biophys. Res. Commun **135**, 480-486

Shimonaka, M., Saheki, T., Hagiwara, H., Ishido, M., Nogi, A., Fujita, T., Wakita, K., Inada, Y., Kondo, J. & Hirose, S. (1987) J. Biol. Chem. **262**, 5510-5514

Shinjo, M., Hirata, Y., Hagiwara, H., Akiyama, F., Murakami, K., Kojima, S., Shimonaka, M., Inada, Y. & Hirose, S. (1986) Biomed. Res. **7**, 35-38

Sinacore, M.S., Lewicki, J.A., Waldman, S.A & Murad, F. (1983) Fed. Proc. **42**, 1853, 1893

Sosa, R.E., Volpe, M., Marion, D.N., Atlas, S.A., Laragh, J.H., Vaughan, E.D. & Maack, T. (1986) Am. J. Physiol. **250**, F520-F524

Stephenson S.L. & Kenny A.J. (1987a) Biochem. J. **243**, 183-187

Stephenson S.L. & Kenny A.J. (1987b) Biochem. J. **241**, 237-247

Suda, H., Aoyagi, T., Takeuchi, T. & Umezawa, H. (1973) J. Antibiot. **26**, 621-623

Sudoh, T., Kangawa, K., Minamino, N. & Matsuo, H. (1988) Nature **332**, 78-81

Sugawara, A., Nakao, K., Morii, N., Sakamato, M., Suda, M., Shimikura, M., Kiso, Y., Kihara, M., Yamori, Y., Nishimura, K., Soneda, J., Ban, T., & Imura, H. (1985) Biochem. Biophys. Res. Commun. **129**, 439-446

Sugiyama, M., Fukumi, H., Grammer, R.T., Misono, K.S., Yabe, Y., Morisowa,Y. & Inagami, T. (1984) Biochem. Biophys. Res. Commun. **123**, 338-344

Sulakhe, P.V., Sulakhe, S.J., Leung, N., L-K., St. Louis, P.J. & Hickie, R.A. (1976a) Biochem. J. **157**, 705-712

Sulakhe, S.J., Leung, N.L-K., Sulkhe & P.V. (1976b) Biochem. J. **157**, 713-719

Takayanagi, R., Tanaka, I., Maki, M. & Inagami, T., (1985) Life Sci. **36**, 1843-1848

Takayanagani, R., Imada, T. & Inagami, T., (1987a) Biochem. Biophys. Res. Commun. **142**, 483-488

Takayanagani, R., Inagami, T., Snajdar, R.M., Imada, T. Tamura, M. & Misono, K.S. (1987b) J. Biol. Chem. **262**, 12104-12113

Takeda, S. Kusano, E. & Murayama, N. Yasushi, A., Hosoda, S., Sokabe, H. & Kawashima, H. (1986) Biochem. Biophys. Res. Commun. **136**, 947-954

Tang, J., Sepulveda, P., Masciniszyn, J., Chen, K.C.S., Huang, W.Y., Too, N., Liu, D., & Lanier, J.P. (1973) Proc. Natl. Acad. Sci. USA **70**, 3437-3439

Taylor, S.I. (1975) Biochem. J. **14**, 2357-2361

Trippodo, N.C., Macphee, A.A., Cole, F.E. & Blakesly, H.L. (1982) Proc. Soc. Exp. Med. **170**, 502-508

Thibault, G., Carrier, F., Garcia, R., Gutkowska, J., Seidah, N.G., Chretien, M., Cantin, M. & Genest, J. (1984a) Clin. Invest. Med. **7(suppl. 2)**, 59

Thibault, G., Garcia, R., Carrier, F., Seidah, N.G., Lazure, C., Chretien, M., Cantin, M., and Genest, J. (1984b) Biochem. Biophys. Res. Commun. **125**, 938-946

Thibault, G., Garcia, R., Cantin, M. & Chretien, J. (1984c) Can. J. Physiol. Pharmacol. **62**, 645-649

Tremblay, J., Gerzer, R., Vinay, P., Pang, S.C., Beliveau R. & Hamet, P. (1985) FEBS Lett. **181**, 17-22

Tremblay, J., Gerzer, R., Pang, S.C., Cantin, M., Genest, J. & Hamet, P. (1986) FEBS Lett. **194**, 210-214

Turrin, M. & Gillis, C.N. (1986) Biochem. Biophys. Res. Commun. 868-873

Umezawa, H. (1976) Methods in Enzymol. **45**, 678-695.

Umezawa, H. (1982) Ann. Rev. Microbiol. **36**, 75-99.

Van Breemen, C., Aaronson, P.I., Loutzenhiser, R.D. & Meisheri, K.D. (1982) Fed. Proc. **41**, 2891-2897

Veress, A.T., Chong, C.K. & Sonnenberg, H. (1985) Can. J. Physiol. Pharmacol. **63**, 1615-1617

Vlasuk, G.P., Miller, J., Bencer, G.H. & Lewicki, J.A. (1986) Biochem. Biophys. Res Commun **136**, 396-403

Vlasuk, G.P., Arcuri, K.E., Ciccarone, T.M. & Nutt, R.F. (1988), FEBS Lett. **228**, 290-294

Volpe, M., Odell, A., Kleinert, H.D., Muller, F., Camargo, M.J.F., Laragh, J.H., Maack, T., Vaughan, E.D. & Atlas, S.A. (1985) Hypertension **7 (Suppl. I)**, I43-I48

Volpe, M., Sosa, R.E., Muller, F.B., Camargo, M.J., Glorioso, N., Laragh, J.H., Maack, T. & Atlas, S.A. (1986) Am. J. Physiol. **250**, H871-H878

Waldman, S.A., Rapoport, R.M. & Murad, F. (1984) J. Biol. Chem. **259**, 14332-14334

Waldman, S.A., Chang, L.Y. & Murad, F. (1985) Prep. Biochem. **15**, 103-120

Waldman, S.A., Kuno, T., Kamisaki, Y. Chang, l.Y., Gariepy, J., Schoolnik, G. & Murad, F. (1986) Infect. Immun. **51**, 320-326

Waldman, S.A. & Murad, F. (1987) Pharmacol. Rev. **39**, 163-196

Wakitani, K., Oshima, T., Loewy, A.D., Holmberg, S.W., Cole, B.R., Adams, S.P., Fok, K.F., Currie, M.G. & Needleman, P. (1985) Circ. Res. **56**, 621-627

Watanabe, A.M. & Besch, H.R. (1975) Cir. Res. **37**,309-317

Wiley, H.S., Van Nostrand, W., McKinley, D.N., & Cunningham, D.D. (1985). J. Biol. Chem. **260**, 5290-5295

Winquist, R.J., Faison, E.P., Waldman, S.A., Schwartz, K., Murad, F. & Rapoport, R.M. (1984) Proc. Natl. Acad. Sci. USA **81**, 7661-7664

Yamanaka, M., Greenberg, B., Johnson, L., Seilhamer, J., Brewer, M., Freidemann, T., Miller, J., Atlas, S., Laragh, J., Lewicki, J. & Fiddes, J. (1984) Nature **309**, 719-722

Yandle, T.G., Richards, A.M., Nicholls, M.G., Cuneo, R., Espiner, E.A. & Livesey, J.H. (1986) Life Sci. **38**,1827-1833

Yandle, T., Crozier, I., Nicolls, G., Espiner, E., Carne, A. & Brennan, S. (1987) Biochem. Biophys. Res. Commun. **146**, 832-839

Yang, H.Y.T., Erdos, E.G., Levin, Y. (1971) J. Pharmacol. Exp. Therapeu. **117**, 291-300

Zeidel, M.L., Seifter, J.L., Lear, S., Brenner, B.M. & Siva, P. (1986) Am. J. Physiol. **251**, F379-F383

Zeidel, M.L. (1988) In B.M. Brenner, & J.H. Laragh (Eds.), Advances in Atrial Peptide Research. Vol. II. Raven Press, New York, pp 109-119

APPENDICES

Appendix I

I.1 Composition of Culture Media

Ingredients	MEME mg/litre	JOKLIKS mg/litre
L-Arginine HCl	126.4	105.00
L-Cystine disodium salt	28.4	29.60
L-Glutamine	-	294.00
L-Histidine HCl H_2O	41.90	41.90
L-Isoleucine	52.50	52.00
L-Leucine	52.50	52.00
L-Lysine HCl	73.06	72.50
L-Methionine	14.90	15.00
L-Phenylalanine	33.02	32.00
L-Threonine	47.64	48.00
L-Tryptophan	10.20	10.00
L-Tyrosine disodium salt	45.02	46.98
L-Valine	46.9	46.00
D-Ca pantothenate	1.00	1.00
Choline chloride	-	1.00
Folic acid	1.00	1.00
i-Inositol	2.00	2.00
Nicotinamide	1.00	1.00
Pyridoxyl HCl	1.00	1.00
Riboflavin	0.10	0.10
Thiamin HCl	1.00	1.00
$CaCl_2$	264.90	-
KCl	400.00	400.00
$MgSO_4.7H_2O$	200.00	242.40
NaCl	6800.00	6500.00
$NaHCO_3$	-	2000.00
$NaH_2PO_4.2H_2O$	158.30	1500.00
D-Glucose	1000.00	2000.00
Phenol red sodium salt	17.00	10.00
Sodium succinate 6H2O	110.0	-
Succinic acid	75.00	-
Choline bitartrate	1.80	-
Dihydrostreptomycin Sulphate		50.00
Sodium penicillin G	-	75000.00 IU

I.2 Composition of Buffers

Salt	1.KREBS (mM)	2.KRBG (mM)	3.KRHG (mM)	4.PBS (mM)
NaCl	137.0	118.5	118.5	150.0
KCl	5.40	2.58	2.58	-
$CaCl_2$	2.80	-	1.00	-
$MgSO_4$.	1.20	1.19	1.19	-
NaH_2PO_4.	0.30	-	-	1.87
Na_2HPO_4	-	-	-	12.63
KH_2PO_4.	0.30	1.19	1.19	-
Tris base	14.00	-	-	-
$NaHCO_3$	-	14.50	-	-
HEPES	-	-	25.0	-
Glucose	12.0	11.1	11.1	-
Manitol	-	2.00	-	-

I.3 Preparation of Buffers

I.3.1 Materials

All chemicals were of analytical grade supplied by BDH, Poole, Dorset. All solutions were made up in water which had been double distilled followed by purification using a Milli Q Water system (Milli Q H_2O; Millipore, Harrow, Middlesex).

I.3.2 KREBS

The salts were dissolved in Milli Q H_2O and the pH adjusted to 7.4 with 1 M HCl, before making up to volume.

I.3.3 KRBG (Krebs Ringer Bicarbonate Buffer)

The salts were dissolved in Milli Q H_2O and filtered though a 0.45 μm Nylon 66 filters (Anachem, Luton, Beds.) before making up to volume. The buffer was gassed with 95% O_2/5% CO_2 for 20 min prior to use.

I.3.4 KRHG (Krebs Ringer Hepes Buffer)

The salts were dissolved in Milli Q H_2O, the pH adjusted to 7.4 using 1 M NaOH and the solution was filtered though a 0.45 μm Nylon 66 filters before making up to volume. The buffer was gassed with 100% O_2/ for 20 min prior to use.

I.3.5. PBS (Phosphate Buffered Saline)

The salts were dissolved in Milli Q H_2O at the concentration indicated to give PBS at pH7.4

Appendix II

II.1 Guanylate Cyclase Assay and cGMP Assay

II.1.1 Reagents for Guanylate Cyclase Assay

200 mM Theophylline. Stable at room temperature. Heat to redissolve before use.

20 mM Isobutylmethylzanthine (IBMX). Stable at room temperature. Heat to re-dissolve before use.

1 M Triethanolamine (TEA), pH 7.4. Stable at room temperature.

100 mM Phosphocreatine (CP). Store in 19 mg aliquots at -20^{0}C. Dissolve in 0.5 ml distilled H_2O immediately prior to use).

2 mg/ml Creatine phosphokinase (CK). Store in 1 mg aliquots at -20^{0}C. Dissolve in 0.5 ml 1% BSA just prior to use.

50 mM Guanosine 5'-triphosphate (GTP) See below.

60 mM $MnCl_2$. Stable at room temperature.

The following solutions are prepared just prior to use.reagents are mixed

Reaction Mix

Reagent	Volume
Theophylline	1
IBMX	2
TEA	1
H_2O	2
CP	1
CK*	1

* Make sure the solution is cool before addition

GTP/$MnCl_2$

100µl GTP
650µl H_2O
250µl $MnCl_2$ (Add this last)

II.1.2.i Preparation of GTP Stock Solution

Commercially obtained GTP contains significant amounts of cGMP which result in high blank values being obtained from the guanylate cyclase assay. It is therefore necessary to purify GTP prior to use.

II.1.2.ii Purification of GTP

A 0.7 x25 cm column was prepared containing Dowex AG 50-W-X8 and washed with 2 x 20 ml of 0.1 M HCl. Approximately 500 mg GTP was dissolved in 2ml 0.1 M HCl and the solution applied to the column. GTP was eluted with 0.1M HCl and 12 x 1 ml fractions were collected. Aliquots from the fractions were diluted (1:20,000) and the optical density measured at O.D. at 255 nm. The concentration of GTP in the fractions was calculated from the extinction coefficient as follows :

$$A = E \times [M] \times l$$

where A = Absorbance at 255 nm

E = Extinction coefficient = 12,400 at 255 nm

[M] = Molar concentration

l = light path length (cm)

The fractions containing GTP were combined and the pH was adjusted to 7.4 with 1M TEA and NaOH such that the final concentrations of GTP and TEA were 50 mM.

Store in 100µl aliquots at -20°C.

II.2 Measurement of cGMP

II.2.1.Preparation of [^{125}I]-Tyrosine Methyl Ester Succinyl-c GMP ([^{125}I]-ScGMP)

II.2.1.i.Reagents

Succinyl-cyclic GMP tyrosine methyl ester (ScGMP-TME) was dissolved in 0.5 M potassium phosphate, pH 7.4, at a final concentraton of 0.1 mg/ml. It was stored at -20^{o}C in 20 µl aliquots.

[^{125}-I]-Na (Amersham International, radioactive concentration = 100 mCi [^{125}-I]/ml, specific activity 15 mCi [^{125}-I]/µg iodine

QAE- Sephadex (A-25; Sigma) was resuspended 0.1 M ammonium formate, pH 6.0, 2 to 3 days prior to use and stored at 4^{o}C.

0.5 M potassium phosphate, pH 7.4. Make fresh.

0.05 M potassium phosphate, pH 7.4. Make fresh.

1 mg/ml chloramine-T in 0.05M potassium phosphate, pH7.4. Made up just before use.

1 mg/ml potassium metabisulphite in 0.05 M potassium phosphate, pH 7.4. Made up just before use.

0.05 M ammonium formate, pH 6.0. Made freshly.

0.25 M ammonium formate, pH 6.0. Made freshly.

2.5 mM sodium iodide, in Milli-Q water. Prepared immediately prior to use.

II.2.2. Preparation of QAE-25 Column

A 1 x 10 ml plastic pipette was plugged with glass wool and filled with preswollen QAE-25 Sephadex in 0.1M ammonium formate. The column was allowed to equilibrate at 4°C and then washed with at least 125mls of 0.05M ammonium formate, pH 6.0. It was stored at at 4°C until required.

Reagents for cGMP Assay

Buffer: 50 mM sodium acetate, pH 4.75 in 0.5% BSA

Antibody: Undiluted stock stored in 100 μl aliquots at -70°C. The antibody was diluted 1:1000 with acetate buffer. This could be stored for up to 6 months at -20°C. The antibody was finally diluted 1:25 in the same buffer for use in the assay.

Radiolabel: [^{125}I]-cGMP (approx. 15000 cpm/100 μl)

cGMP (2 x 10^{-4}M) was prepared in H_2O and stored at -20°C.

Appendix III

III Analysis of Dose Response Curves

III.1 Indirect Hill Plots:

$$\log \frac{[DR]_I}{[DR] - [DR]_I} = n\log [I] + n\log EC_{50}$$

Where [DR] = amount of binding in the absence of competitor I

$[DR]_I$ = amount of binding in the presence of competitor I

[I] = concentration of competitor

n = Hill coefficient

III.1.2 Scatchard plot:

$$\frac{B}{F} = \frac{-1}{K_D.B} + \frac{Bmax}{K_D}$$

Where B = Bound = concentration of ligand bound to the receptor at equilibrium

Bmax = Maximum number of binding sites

F = Free = concentration of free ligand present in the incubation at equilibrium

K_D = Equilibrium dissociation constant

III.1.3 Cheng Prusoff equation:

$$K_{DI} = \frac{EC_{50}}{1 + \frac{[D^*]}{K_{D*}}}$$

Where K_{DI} = equilibrium dissociation constant for competitor I

$[D^*]$ = concentration of free radioligand

K_{D*} = equilibrium dissociation constant for radioligand.

III.2.1 Enzfitter :

Where possible dose response curves were analysed by Enzfitter, a data analysis package from Elsevier Biosoft (Cambridge, U.K.). This programme uses non-linear regression analysis to provide the best-fit for a given set of data to a specified equation (R.J. Leatherbarrow, 1987). In the present studies Enzfitter was utilized to fit data to the following equations:

III.2.2 Ligand binding 1 site

$$B = \frac{Bmax \times F}{K_D + F}$$

Where B = Bound = concentration of ligand bound to the receptor at equilibrium

Bmax = Maximum number of binding sites

K_D = Equilibrium dissociation constant

F = Free = concentration of free ligand present in the incubation at equilibrium

III.2.3 Ligand binding 2 sites

$$B = \frac{Bmax_1 \times F}{K_{D1} + F} + \frac{Bmax_2 \times F}{K_{D2} + F}$$

Where B = Bound = concentration of ligand bound to the receptor at equilibrium

$Bmax_1$ = Maximum number of site 1 binding sites

$Bmax_2$ = Maximum number of site 2 binding sites

K_{D1} = Equilibrium dissociation constant for site 1

K_{D2} = Equilibrium dissociation constant for site 2

F = Free = concentration of free ligand present in the incubation at equilibrium

III.2.4 Allosteric kinetics (Hill equation)

$$Rate = \frac{Vmax \times [S]^n}{(Km + [S]^n)}$$

Where Vmax = Maximum rate

Km = Michaelis constant

[S] = Substrate concentration

n = Hill coefficient

Appendix IV

Measurement of Cell Volume using a Coulter Counter

The coulter counter estimates the number and volume of cells by measuring the change in electrical resistance caused by the displacement of electrolyte as the cell passes through the electrode aperture. The resulting drop in voltage is directly proportional to the volume of the cell. For the measurement of ventricular myocyte number and cell volume the following settings were employed :

Aperture	=	4
Attenuator	=	256
Window width	=	0/70

Appendix V

Tables containing data from which figures were constructed

Figure 3.1

Measurement of cGMP by Radio-immunoassay

cGMP (fmol/tube)	Mean±SEM cpm	Co/Cs
-	7370±227	1.000
78	5515±50	1.402
156	4695±11	1.698
313	3848±24	2.110
625	2855±77	2.948
1250	2065±10	4.310
2500	1495±27	6.465
5000	1064±24	10.395
10000	772±10	17.674
NSB	355±20	-

Figure 3.3

Measurement of Protein Using the Bio-Rad Protein Assay Kit

BSA (μg/tube)	Absorbance (595nm)	
0	0.000	0.011
1.25	0.079	0.078
2.5	0.140	0.152
5	0.275	0.276
10	0.503	0.518
20	0.920	0.918

Figure 4.1

The Effect of Protein Concentration on Guanylate Cyclase Activity in Rat Cardiac Sarcolemmal Membranes

Protein (μg/tube)	cGMP Produced (fmol/min per tube)	
	Basal	10^{-6}M ANP
0.525	6.46±0.29	10.3±0.2
1.05	11.9±0.3	15.7±0.6
2.1	21.5±0.7	28.9±1.9
4.2	26.4±1.0	37.4±0.2

Figure 4.2

Time Course for Guanylate Cyclase Activity in Rat Cardiac Sarcolemmal Membranes

Time (min)	cGMP (pmol/mg protein)	
	Basal	10^{-6}M ANP
1	268	463
2.3	473	804
5	849	1465
10	1414	2012
15	1661	4529
20.3	2593	5149
25	5453	8093
30	6649	8769

Figure 4.3

The Effect of Manganese and Magnesium on Guanylate Cyclase Activity

[Cat] (mM)	cGMP Produced (pmol/min per mg protein)			
	Mn^{2+}		Mg^{2+}	
	Basal	10^{-6}M ANP	Basal	10^{-6}M ANP
0	0.44±3.51	1.02±1.45	4.09±1.09	5.14±0.23
0.5	25.4±1.16	51.5±3.65	4.29±1.09	5.81±1.36
1	83.1±6.53	144±9.93	6.31±0.86	8.81±1.94
2	87.8±6.24	148±9.02	7.08±0.94	10.04±1.81
4	88.0±9.0	147±5.62	8.13±1.14	11.34±0.95
8	57.4±1.56	6 48.3±2.19	7.86±0.96	8.29±1.32
32	27.5±4.38	35.4±0.58	7.19±0.67	7.05±1.00
64	19.9±3.08	24.5±1.56	8.44±0.50	8.01±0.69

Figure 4.4

Dose Response Curve for GTP Stimulation of Guanylate Cyclase Activity

[GTP] (M)	cGMP Produced (pmol/min per mg protein)	
	Basal	10^{-6}M ANP
$3x10^{-6}$	0.31±0.22	0.53±0.12
10^{-5}	0.28±0.20	0.33±0.17
$3x10^{-5}$	1.33±0.37	1.69±0.04
10^{-4}	7.76±0.40	11.3±0.38
$3x10^{-4}$	43.4±1.19	61.0±1.60
10^{-3}	68.2±1.80	97.7±2.45

Figure 4.5

Dose Response Curves for ANP, ANP_{5-28}, and ANP_{5-25} Stimulation of Guanylate Cyclase Activity

[Peptide] (M)	% of Basal Activity		
	ANP	ANP_{5-28}	ANP_{5-25}
10^{-14}	96.4±2.6	99.2±0.6	103
10^{-13}	100±3.5	95.8±5.4	98
10^{-12}	99.5±2.2	99.8±2.05	105
10^{-11}	110±6.0	99.8±0.7	102
10^{-10}	127±9.4	108±6.9	101
10^{-9}	147±8.4	128±10	93
10^{-8}	165±13	134±13	105
10^{-7}	180±13	139±10	110
10^{-6}	198±13	145±9	137

Figure 4.6

Effect of Phosphoramidon on Guanylate Cyclase Activity

[ANP]	% of Basal Activity	
(M)	Control	Phosphoramidon
10^{-14}	92.0±4.4	97.1±1.7
10^{-13}	104±2.3	103±5.3
10^{-12}	95.0±3.2	95.4±1.75
10^{-11}	104±8.7	111±4.3
10^{-10}	132±6.0	129±4.4
10^{-9}	160±13	161±8.8
10^{-8}	188±12	167±4.9
10^{-7}	206±13	207±14
10^{-6}	209±5.4	223±9.8

Figure 4.7

The Effect of Various Peptides and Protease Inhibitors on Guanylate Cyclase Activity

Inhibitor	(M)	[ANP] (M) 0	10^{-9}M	10^{-7}M
None	-	124±8	172±9	196±8
Amastatin	10^{-6}	136±6	176±4	186±4
Peptstatin	10^{-6}	136±5	173±2	178±6
Lepeptin	10^{-5}	131±9	169±2	179±5
PMSF	$5x10^{-4}$	126±4	140±6	158±5
Aprotinin	10^{-6}	133±8	163±7	168±6
E-64	10^{-5}	140±3	164±20	176±2
BPFC	$5x10^{-5}$	133±4	165±4	184±7
SQ 20881	10^{-3}	143±5	153±10	187±7
Ramipril	10ug/ml	145±4	166±6	190±12
Glucagon	10^{-6}	126±3	157±7	178±7
Bradykinin	$5x10^{-5}$	131±3	158±7	185±3

Figure 4.8 & Figure 4.11

Effect of Adenosine Phosphates on Mn^{2+}- and Mg^{2+}- Dependent Guanylate Cyclase Activity

	Guanylate Cyclase Activity			
	$[Mn^{2+}]$ (3mM)		$[Mg^{2+}]$ (2mM)	
Addition	Basal	ANP	Basal	ANP
None	114±20	187±42	3.2±1.3	11.8±3.4
ATP	104±21	155±39	15.8±4.0	52.9±14.1
ADP	132±48	185±65	5.2±5.0	23.9±13.7
AMP	131±48	172±58	-0.6±2.6	3.7±3.1
AMP-PNP	89±30	164±62	6.3±3.7	29.9±9.1

Figure 4.9

Dose Response Curve for the Effect of ATP on Mn^{2+}-Dependent Guanylate Cyclase Activity

	Mn^{2+}-Dependent Guanylate Cyclase Activity			
[ATP]	(pmol/min per mg protein)		% of Control	
(M)	Basal	10^{-6}M ANP	Basal	10^{-6}M ANP
0	111±4.2	158±14	100	100
10^{-5}	125±0.5	157±15	112±5	99±3
$3x10^{-5}$	113±5	157±15	102±4	99±2
10^{-4}	126±3	167±19	113±4	105±3
$3x10^{-4}$	116±8	157±19	104±9	99±3
10^{-3}	84±5	118±14	76±7	74±3
$3x10^{-3}$	36±4	62±15	33±7	38±7
10^{-2}	9.2±0.4	13±3	8±0	8±1

Figure 4.10

The Effect of ATP on the Rate of cGMP Production

Time (min)	Guanylate Cyclase Activity (pmol cGMP /mg protein)			
	Control		1mM ATP	
	Basal	10^{-6}M ANP	Basal	10^{-6}M ANP
2	164	359	156	363
4	359	674	265	643
6	565	986	402	861
10	881	1520	624	1298
15	1357	2210	982	1719
20	1774	2608	1466	2401
30	2175	3613	1902	3574
45	2553	4202	3126	5481
60	2865	4545	4693	7722

Figure 4.12

Dose Response Curve for the Effect of ATP on Mg^{2+}-Dependent Guanylate Cyclase Activity

[ATP] (M)	Mg^{2+}-Dependent Guanylate Cyclase Activity (pmol/min per mg protein)		% of Control	
	Basal	10^{-6}M ANP	Basal	10^{-6}M ANP
0	4.5±0.5	17.8±4.8	100	100
10^{-5}	5.2±0.1	17.3±6.2	127±27	102±6
$3x10^{-5}$	8.6±1.0	9.6±6.6	199±21	116±10
10^{-4}	10.7±2.4	28.0±7.3	233±30	178±14
$3x10^{-4}$	5.4±2.3	52.5±20	362±83	297±39
10^{-3}	24.4±4.7	73.4±32	572±67	396±74
$3x10^{-3}$	13.0±1.3	47.3±20	303±40	264±37
10^{-2}	7.3±1.3	5.0±0.8	160±10	44.5±22

Figure 4.13

Dose Response Curve for ANP in the presence of ATP and Mg^{2+}

[ANP] (M)	cGMP Produced pmol/min per mg protein
0	2.2 ± 0.6
10^{-14}	3.5 ± 0.4
10^{-13}	2.8 ± 0.1
10^{-12}	3.5 ± 0.1
10^{-11}	1.9 ± 0.2
10^{-10}	4.3 ± 0.2
10^{-9}	9.4 ± 0.3
10^{-8}	23.5 ± 0.6
10^{-7}	24.4 ± 0.4
10^{-6}	27.7 ± 0.6
10^{-5}	26.6 ± 0.5

Figure 4.14

Dose Response Curve for ANP Stimulation of Guanylate Cyclase activity in BAC Membranes

[ANP] (M)	cGMP Produced (pmol/min/mg protein)
0	287 ± 34
10^{-12}	367 ± 59
10^{-11}	335 ± 28
10^{-10}	374 ± 15
10^{-9}	570 ± 38
10^{-8}	800 ± 24
10^{-7}	824 ± 17
10^{-6}	825 ± 25

Figure 5.1

Time Course for the Binding of [^{125}I]-ANP to Rat Cardiac Sarcolemmal Membranes

Time (min)	[^{125}I]-ANP Bound (fmol/mg protein)		
	Total	NSB	Specific
0	62.6	67	-
5	252	120	132
10	439	126	314
20	641	122	519
30	745	127	618
40	845	171	674
60	842	192	650

Figure 5.2 & Figure 5.3

Inhibition of [^{125}I]-ANP binding in Rat Cardiac Sarcolemmal Membranes by ANP

ANP (M)	[^{125}I]-ANP Bound fmol/mg protein						% Inhibition Mean ± SEM
0	187	117	212	725	298	835	
10^{-14}	-	113	220	753	-	-	-0.93 ± 3.87
10^{-13}	-	103	213	-	-	-	2.21 ± 11.8
10^{-12}	169	94	205	732	290	676	16.0 ± 6.17
10^{-11}	174	94	187	666	305	6812	15.7 ± 6.04
10^{-10}	144	86	190	524	226	681	32.8 ± 4.05
10^{-9}	145	83	169	363	172	608	45.1 ± 5.29
10^{-8}	109	82	156	252	154	421	64.3 ± 3.76
10^{-7}	67	76	106	152	97	334	85.0 ± 4.36
10^{-6}	35	58	56	98	60	244	100 ± 0.62
10^{-5}	-	-	-	120	55	2479	9.6 ± 0.77

Figure 5.4

Relationship Between Radioactivity Displaced and Concentration of [^{125}I]-ANP

Preparation	[125I]-ANP (pM)	% Displaced
1	43.29	39.0
2	60.6	15.91
3	70.9	11.6
4	81.6	3.3
5*	88.6	27.0
6	90.9	-1.6

* Membranes prepared in the absence of DTT.

Figure 5.5

Saturation Curve for [^{125}I]-ANP Binding to Rat Cardiac Sarcolemmal Membranes

Free	[^{125}I]-ANP Bound (fmol/mg protein)		
pM	Total	NSB	Specific
2.48	9.53 ± 0.36	5.31 ± 0.54	4.22
4.15	15.1 ± 0.27	6.47 ± 0.27	8.64
7.76	21.6 ± 0.63	8.77 ± 1.35	12.8
14.65	35.1 ± 0.45	13.8 ± 0.81	21.4
29.18	56.7 ± 1.17	24.8 ± 0.63	31.92
56.7	94.7 ± 3.24	47.9 ± 3.33	46.76
105	203 ± 6.56	99.1 ± 2.34	104.3
206	334 ± 7.10	195 ± 6.65	139
418	710 ± 39.6	394 ± 16.9	316
706	1101 ± 70.5	765 ± 25.5	333

Figure 5.6

The effect of Phosphoramidon on [^{125}I]-ANP Binding to Rat Cardiac Sarcolemmal Membranes

ANP	$\frac{\text{cpm bound (control)}}{\text{cpm bound (phosphoramidon)}} \times 100$		
(M)		n	t
0	104.6 ± 1.36	3	3.38
10^{-12}	106.6 ± 4.70	3	1.40
10^{-10}	111.6 ± 12.2	3	0.95
10^{-8}	102.8 ± 4.79	3	0.58

Figure 5.8

Time Course for the Binding of [^{125}I]-ANP to BAC Membranes

Time (min)	[^{125}I]-ANP Bound (fmol/mg protein)		
	Total	NSB	Specific
0.5	5.8	2.3	3.6
5	23.0	3.3	19.7
10	33.3	3.4	28.9
20	33.9	5.3	28.6
30	35.3	4.1	31.1
45	34.8	4.3	30.5
60	36.3	4.2	32.1
90	34.7	5.7	29.0
120	33.4	7.0	26.4

Figure 5.9

Saturation Curve for [^{125}I]-ANP Binding to BAC Membranes

Free [ANP] (pM)	[125I]-ANP Bound (fmol/mg protein)		
	Total	NSB	Specific
6.03	22.6	5.3	17.3
12.7	42.5	9.9	32.7
25.8	78.0	17.6	60.4
51.3	152	28.7	124
105.7	278	63.0	215
226.3	554	127	427
481.3	994	211	783

Figure 5.10

Time Course for the Binding of [^{125}I]-ANP to MDCK (strain I) Membranes

Time (min)	[^{125}]-ANP Bound (fmol/mg protein)		
	Total	NSB	Specific
3	66±5	35±5	30
6	74±2	41±5	33
9	84±1	41±3	43
12	102±5	39±3	63
15	115±11	41±6	74
20	117±2	38±1	79
30	130±2	42±3	88
45	126±4	40±2	86
60	127±2	40±3	88

Figure 5.11

Saturation Curve for [^{125}I]-ANP Binding to MDCK (Strain I) Membranes

[ANP] Free (pM)	[^{125}I]-ANP Bound (fmol/mg protein)		
	Total	NSB	Specific
9.38	62.9	7.5	55.4
18.7	112.5	13.1	99.4
40.4	193.8	23.8	170.0
77.9	275.0	47.9	227.1
155.1	367.8	96.3	271.5
301.4	483.9	182.6	301.3
612.9	689.4	380.1	309.3

Figure 5.12 & Figure 5.13

ANP Displacement of [^{125}I]-ANP Binding to MDCK (Strain I) Membranes

ANP (M)	Specific [^{125}I]-ANP Bound (fmol/mg protein)				% Inhibition Mean ± SEM
	1	2	3	4	
0	58	52	46	171	-
10^{-12}	60	44	43	153	7.0±4.0
$2x10^{-12}$	-	52	39	-	7.1±7.1
$3x10^{-12}$	-	-	-	129	-
$5x10^{-12}$	-	44	33	-	21.9±6.7
10^{-11}	35	31	32	100	38.0±2.7
$2x10^{-11}$	-	23	14	-	61.7±6.1
$3x10^{-11}$	-	-	-	60	-
$5x10^{-11}$	-	25	8	-	67.6±14.7
10^{-10}	14	18	1	29	80.4±6.7
$3x10^{-10}$	-	11	0	12	93.7±8.6
10^{-9}	7	8	0	2	97.7±7.5
$3x10^{-9}$	-	3	0	-	101.6±6.9
10^{-8}	2	4	-	3	95.6±1.7
10^{-7}	0	5	-	0	99.2±9.4

Figure 5.14

ANP Displacement of [^{125}I]-ANP binding to MDCK (Strain II) Membranes

ANP (M)	Total [^{125}I]-ANP Bound (fmol/mg protein)	
0	1.20	0.45
10^{-12}	1.96	1.96
$2x10^{-12}$	1.11	1.52
$5x10^{-12}$	0.79	2.24
10^{-11}	0.98	0.35
$2x10^{-11}$	1.71	0.03
$5x10^{-11}$	-1.26	0.54
10^{-10}	-0.5	0.82
$3x10^{-10}$	0.32	0.13
10^{-9}	0.29	0.22
$3x10^{-9}$	0.35	0.44
10^{-8}	0.32	0.19
10^{-7}	-1.01	-0.38

Figure 8.2

Comparison of the Volume of Rat and Rabbit Myocytes with the Number of Rods Present in the Preparation

Rabbit		Rat	
% Rods	Cell Vol. (μm^3)	% Rods	Cell Vol. (μm^3)
48	18019	64	20704
40	15699	80	21119
37	15277	70	26351
10	15531	79	21590
20	15813	79	18111
28	19268	29	17095

Figure 8.3

Standard Curve for HPLC Determination of ANP

Date	ANP (nmol)	Area (220 nm)	AUFS	Ret. Time (min)
3-12-87	1.43	1689595	0.2	33.73
4-12-87	1.60	1820294	0.05	33.15
4-12-87	0.80	1092462	0.05	33.15
4-12-87	0.40	618888	0.05	33.18
8-12-87	0.60	857806	0.05	35.06
8-12-87	0.60	820262	0.05	34.18
8-12-87	0.60	875563	0.05	33.44

Figure 9.1

Degradation of [^{125}I]-ANP by Rabbit Ventricular Myocytes

Time (min)	[^{125}I]-ANP Degraded fmol/min per 10^6 Cells	
	4°C	20°C
5	3.67±2.68	29.53±0.53
10	5.93±1.33	62.20±1.22
15	10.60±0.92	85.13±1.86
20	15.60±1.50	101.8±1.39
30	19.00±3.06	131.9±3.15
45	30.33±3.01	144.7±4.30
60	31.07±.057	151.0±4.85

Figure 9.2

Effect of Preincubation Time on [^{125}I]-ANP Degradation by Rabbit Ventricular Myocytes

Preinc. (min)	[^{125}I]-ANP Degraded fmol/min per 10^6 cells	
	Cell Suspen.	Supernatant
0.5	1.46±0.03	0.82±0.04
10	1.60±0.03	1.21±0.04
30	2.01±0.04	1.49±0.06

Figure 9.3

The Effect of Homogenization on the Degradation of [^{125}I]-ANP by Rabbit Ventricular Myocytes

Time (min)	[^{125}I]-ANP Degraded fmol/min per 10^6 Cells	
	Cells	Homogenate
5	5.28±1.24	11.84±0.02
10	13.28±0.36	23.24±1.12
15	20.28±0.64	35.80±0.36
20	27.36±0.40	45.84±1.20
25	37.36±0.56	56.48±0.56
30	43.32±0.20	63.08±0.32
45	65.40±0.24	78.08±0.68
60	86.36±1.16	90.76±0.60

Figure 9.4

The Effect of Heat Treatment on [^{125}I]-ANP Degradation by Rabbit Ventricular Myocytes

Time (min)	[^{125}I]-ANP Degraded fmol/10^6 Cells	
	Control	60°C
0	0.03±0.72	1.8±3.1
5	116±14	10.0±1.8
10	208±10	16.2±1.6
20	361±7.3	27.9±3.0
40	470±5.3	44.8±1.9
60	559±13	64.3±1.3

Figure 9.5

The Effect of Homogenization on the Degradation of [^{125}I]-ANP by Rat Ventricular Myocytes

Time (min)	[^{125}I]-ANP Degraded fmol/ 10^6 Cells	
	Cell Suspen.	Homogenate
0.5	-	73±3.4
30	73±11.2	688±11.2
60	194±4.5	1005±127
90	279±22.7	1443±16.6
120	338±12.1	1565±42.9

Figure 9.6

$[^{125}I]$-ANP Degradation by Rat Ventricular Myocytes at 20°C

	$[^{125}I]$-ANP Degraded fmol/min per 10^6 Cells	
Cells/ml	Cells	Homogenates
$2.6x10^5$	7.32	-
$4x10^4$	14.47	-
$4x10^4$	5.93	-
$2.5x10^4$	4.12	22.13
$1.3x10^5$	-	9.80
$3.4x10^4$	-	58.45
Mean±S.E.M	7.96±2.27	40.1±10.5

Figure 9.6

$[^{125}I]$-ANP Degradation by Rat Ventricular Myocytes at 37°C

	$[^{125}I]$-ANP Degraded fmol/min per 10^6 Cells		
Cells/ml	Homogenates	Sol.Fraction	Pellet
$1.3x10^4$	61.68	-	-
$5x15^4$	68.7	54.4	-
$5x10^4$	73.86	48.8	38.0
$5x10^4$	-	55.9	-
$5x10^4$	-	39.0	-
$5x10^4$	-	56.7	-
$5x10^4$	-	27.0	-
$6.5x10^4$	-	26.4	-
$3.3x10^4$	-	38.15	-
$5x10^4$	-	26.3	-
$2.5x10^4$	-	43.9	-
$2.5x10^4$	-	36.5	-
$2.5x10^4$	-	34.5	-
$5x10^4$	-	25.4	35.3
Mean ± S.E.M.	68.1±3.5	39.5±3.2	36.7

Figure 9.7

The Effect of Various Protease Inhibitors and Peptides on [^{125}I]-ANP

Inhibitor	[M]	Degradation % of Control	No.	p<
Casein	10^{-4}	98.0±13.5	5	NS
PMSF	$5x10^{-4}$	99.4±7.0	3	NS
Aprotinin	10^{-6}	102.5±3.6	3	NS
Amastatin	10^{-6}	98.9±3.2	5	NS
E-64	10^{-5}	102.2±3.5	6	NS
Phosphoramidon	10^{-5}	99.7±2.2	5	NS
1,10 Phenanthroline	10^{-5}	7.2±2.6	5	0.001
Bacitracin	1mg/ml	0.89±1.25	3	0.001
EDTA	10^{-3}	15.5±2.95	3	0.01
PCMB	10^{-6}	9.7±3.74	3	0.01
ANP	10^{-5}	6.9±3.97	3	0.01
Glucagon	$3x10^{-5}$	32.3±8.59	4	0.01
Bradykinin	10^{-3}	6.9±5.48	2	0.01
SQ 20881	10^{-3}	83.7±3.1	3	0.05
BPFC	10^{-4}	95.1±1.8	3	NS

Figure 9.8

Dose Response Curves for the Inhibition of [^{125}I]-ANP Degradation by ANP, Glucagon, and Bradykinin

	% of Control Degradation		
Conc (M)	ANP	Glucagon	Bradykinin
$3x10^{-10}$	-	100.5	-
10^{-9}	107.8±0.5	-	-
$3x10^{-9}$	-	100.1±1.3	-
10^{-8}	97.1±0.5	-	106.5
$3x10^{-8}$	-	103.6±1.7	-
10^{-7}	77.2±4.5	-	107.7±4.1
$3x10^{-7}$	53.3±2.2	102.7±8.7	-
10^{-6}	29.1±2.4	-	100.7±4.8
$3x10^{-6}$	13.7±4.0	68.7±7.2	-
10^{-5}	6.9±3.2		78.9±4.0
$3x10^{-5}$	-	32.3±8.6	-
10^{-4}	-	-	36.0±4.8
10^{-3}	-	-	5.5±3.9

Figure 9.9a

The Effect of pH on [^{125}I]-ANP Degradation by a Soluble Fraction Isolated from Rat Ventricular Myocytes

pH	[^{125}I]-ANP Degraded fmol/min/10^6 cells
4.78	3.39 ± 0.65
5.32	3.91 ± 0.35
5.56	5.37 ± 0.24
5.46	2.40 ± 0.67
6.24	4.74 ± 0.85
6.85	8.49 ± 1.18
7.38	19.17 ± 0.45
7.86	41.77 ± 2.09
8.43	55.16 ± 1.45
9.42	57.55 ± 1.58

Figure 9.9b

Time min	[^{125}I]-ANP Degraded fmol/10^6 cells	
	pH 6.1	pH 6.1
5	97.1 ± 10.9	90.2 ± 4.3
10	161 ± 14.7	188 ± 7.3
		pH 7.5
15	245 ± 9.0	285 ± 16.3
20	299 ± 14.3	425 ± 10.4
25	339 ± 6.0	582 ± 14.8
30	347 ± 17.7	730 ± 6.3

Figure 9.11

The Degradation of ANP following Incubation with Soluble Fraction from Rat Ventricular Myocytes

Time (min)	Peak Area (x 10^{-3})	ANP (nmol)
0	858	0.609
2	424	0.175
5	344	0.95
10	N.D.	-
20	N.D.	-
40	N.D.	-
90	N.D.	-

N.D. = Not Detected

Figure 9.12

Time Course for the Degradation Products of ANP

Inc.Time	Peak Area $x10^{-3}$				
(min)	1	2	3	4	5
2	51.5	48.9	-	-	0.4
5	47.6	43.6	5.16	25.2	18.7
10	53.2	41.3	15.8	34.3	34.3
20	66.1	36.6	19.7	36.1	24.3
40	99.7	66.9	53.5	30.3	17.1
90	129	67.7	52.9	1.5	3.3
%ACN	19.2	22.8	35.0	43.5	45

Figure 9.13

The Effect of Various Protease Inhibitors on [^{125}I]-ANP Degradation by a Soluble Fraction from Rat Lung

Inhibitor	[M]	% Maximum Degradation	No.	p<
Phosphoramidon	10^{-5}	96.3±11.6	3	NS
PMSF	$5x10^{-4}$	98.5±2.4	4	NS
Aprotinin	10^{-6}	100.8±1.2	3	NS
Amastatin	10^{-6}	95.5±2.5	3	NS
E-64	10^{-5}	105.2±5.5	3	NS
1,10 Phenanthroline	10^{-5}	35.1±8.0	3	0.02
Bacitracin	1mg/ml	20.4±3.9	3	0.01
EDTA	10^{-3}	101.5±3.8	2	NS
PCMB	10^{-6}	88.9±4.3	3	NS

Figure 9.14

The Effect of Various Protease Inhibitors on [^{125}I]-ANP Degradation by a Soluble Fraction from Rat Kidney Cortex

Inhibitor	[M]	% Maximum Degradation	No.	p<
Phosphoramidon	10^{-5}	98.7±6.1	4	NS
PMSF	$5x10^{-4}$	93.3±1.9	5	0.01
Aprotinin	10^{-6}	99.5±1.3	3	NS
Amastatin	10^{-6}	101.5±10.2	4	NS
E-64	10^{-5}	95.1±7.2	5	NS
1,10 Phenanthroline	10^{-5}	29.7±3.2	4	0.001
Bacitracin	1mg/ml	25.4±1.9	3	0.001
EDTA	10^{-3}	71.3±6.4	4	0.05
PCMB	10^{-6}	92.0±6.2	3	NS

Figure 9.15

The Effect of Various Protease Inhibitors on [^{125}I]-ANP Degradation by a Soluble Fraction from Rat Kidney Medulla

Inhibitor	[M]	% Maximum Degradation	No.	p<
Phosphoramidon	10^{-5}	83.8±4.7	3	NS
PMSF	$5x10^{-4}$	93.9±3.4	4	NS
Aprotinin	10^{-6}	99.5±0.9	3	NS
Amastatin	10^{-6}	96.6±9.9	3	NS
E-64	10^{-5}	102.1±1.7	3	NS
1,10 Phenanthroline	10^{-5}	18.8±4.6	3	0.01
Bacitracin	1mg/ml	16.2±8.2	3	0.01
EDTA	10^{-3}	72.6±10.7	2	NS
PCMB	10^{-6}	79.7±4.1	3	0.05

Figure 9.16

Dose Response Curves for the Inhibition of [^{125}I]-ANP Degradation by ANP, Glucagon, and Bradykinin

Conc (M)	ANP	Glucagon	Bradykinin
10^{-9}	98.9	-	-
$3x10^{-9}$	-	97.2±1.0	-
10^{-8}	100±2.1	-	-
$3x10^{-8}$	-	97.9±4.2	-
10^{-7}	81.9±3.6	-	-
$3x10^{-7}$	65.4±0.0	79.5±4.1	-
10^{-6}	45.6±1.0	-	97.6±0.8
$3x10^{-6}$	27.1±5.4	58.3±9.0	80.4±5.7
10^{-5}	10.6±2.1	-	67.6±2.0
$2x10^{-5}$	-	-	52.6±0.8
$3x10^{-5}$	-	32.5±5.0-	
$5x10^{-5}$	-	40.2±1.4	
10^{-4}	-	-	32.5±2.0

Figure 9.17

Dose Response Curves for the Inhibition of [^{125}I]-ANP Degradation by ANP, Glucagon, and Bradykinin

Conc (M)	ANP	Glucagon	Bradykinin
10^{-9}	104.2	-	-
$3x10^{-9}$	-	106.7±2.3	-
10^{-8}	103±2.0	-	-
$3x10^{-8}$	-	98.3±3.6	-
10^{-7}	93.6±1.1	-	-
$3x10^{-7}$	78.7±4.3	90.6±5.6	-
10^{-6}	56.6±4.2	-	93.7±2.1
$3x10^{-6}$	42.7±4.8	81.0±4.7	94.3±1.1
10^{-5}	19.5±7.0	-	77.5±2.6
$2x10^{-5}$	-	-	64.6±3.6
$3x10^{-5}$	-	39.6±6.2	-
$5x10^{-5}$	-	-	55.1±4.7
10^{-4}	-	-	47.1±8.3

Figure 9.18

Dose Response Curves for the Inhibition of [^{125}I]-ANP Degradation by ANP, Glucagon, and Bradykinin

Conc (M)	ANP	Glucagon	Bradykinin
10^{-9}	95.9	-	-
$3x10^{-9}$	-	97.7±1.8	-
10^{-8}	97.5±18	-	-
$3x10^{-8}$	-	100.6±2.3	-
10^{-7}	85.1±1.1	-	-
$3x10^{-7}$	56.9±3.5	95.1±2.3	-
10^{-6}	36.0±2.8	-	97.1±0.2
$3x10^{-6}$	19.9±4.4	81.1±4.3	87.9±3.9
10^{-5}	9.6±2.0	-	72.9±2.9
$2x10^{-5}$	-	-	54.8±0.8
$3x10^{-5}$	-	40.9±6.3	-
$5x10^{-5}$	-	-	36.0±1.1
10^{-4}	-	-	23.6±3.6